Steroid Signalling Via Nuclear Hormone Receptors

A thesis submitted for the degree of
Doctor of Philosophy, Imperial College London

Isabel Fernandes Freitas

2019

Section of Endocrinology and Investigative Medicine
Division of Diabetes, Endocrinology and Metabolism
Department of Medicine
Imperial College London

Abstract

Hormone-sensing in the brain is essential for reproduction and consequent survival of species. In females, estrogen must exert simultaneous positive- and negative-feedback on the anteroventral periventricular nucleus (AVPV) and the arcuate Nucleus (ARC) of the hypothalamus, respectively, to maintain fertility. However, even though the positive effects of estrogen in the hypothalamus have been extensively investigated, the mechanistic basis for the opposing feedback of estrogen in the arcuate nucleus has, for decades, remained elusive. In order to understand what is driving the differential effects of estrogen in the ARC and AVPV, we analysed and compared the expression of estrogen target genes and coregulatory proteins in these two female hypothalamic nuclei under basal and estrogen-treated conditions. We found that the arcuate nucleus and anteroventral periventricular nucleus respond differently to estrogen. And that, the nuclear receptor Dax1, which acts as a region-specific ligand-dependant repressor of estrogen-receptor (ERα) activity, is, by far, the most enriched gene in the arcuate nucleus.

Here, we show for the first time that the negative-feedback in the ARC is mediated by the nuclear receptor Dax1. It couples gonadotropin release to the developmental stage of the oocyte, and mice lacking this mechanism have abnormal estrogen-stimulated gonadotropin secretion and fail to cycle normally. As such, the interaction between Dax1 and ERα in the female hypothalamus explains the paradoxical observation of estrogen negative-feedback, and is shown here to be essential for normal fertility.

Further to this, we show that the C57BL/6J background is highly sensitive to male-to-female sex-reversal in the absence of the nuclear receptor Dax1, and that a minority of sex-reversed XY (Dax1-/Y) mice have markers of fertility and can produce live offspring without any assisted fertility treatment. As such, our observations in sex-reversed XY (Dax1-/Y) mice support the notion that XY sex-reversal is not formally incompatible with reproduction. However, our data also suggest that the inter-individual milieu of mechanical and development complications caused by the presence of the Y-chromosome makes successful reproduction highly unlikely.

Declaration of Contributors

The majority of the work presented in this thesis was performed by the author. All collaboration and assistance are described below.

Chapter 4:

Dr Alexandra Milona helped with the immunofluorescence data and Mr Steven Rothery (Imperial College FILM Facility) helped with imaging.

Chapter 5:

Experiments were performed with the help of Dr Bryn Owen.

Acknowledgments

I would like to express my utmost gratitude to my supervisor Dr Bryn Owen for accepting me into his laboratory and for the mentorship, guidance and endless support he has provided me throughout my PhD. His endless drive, patience and enthusiasm have been a source of inspiration and motivation during this period. Many thanks to my second supervisor Professor Waljit Dhillo for his advice and deadlines that have guided my work.

I am incredibly grateful to Dr Alexandra Milona for the guidance and critical discussions she has provided me with throughout the project.

I would like to specially acknowledge Mariana Norton's contributions and help during the past four years. We started this journey together and her help has been invaluable for the completion of this thesis.

I am incredibly grateful to Markus for his belief in me, support, patience, humor, positivity and, sometimes annoying, interest in my work; and to some of my closest friends Delisha, Natacha and Maria for their constant support, without them this would not have been possible.

Above all I would like to thank my mother, Rita Fernandes, for her undevoted belief in me and in my abilities, even when, I, myself, doubted my own abilities. She has passed onto me a resilience and strength that I will, forever, be grateful for and that has helped me throughout my whole life. If proven successful, this victory is as much hers as it is mine.

Finally, the time spent during my PhD has thought me many things from perseverance, to fighting spirit, ability to continuously challenge myself and a never give up attitude that I will forever take with me. And as I listened to the press conference announcing the first ever image captured of a black hole one of the scientists in the panel quoted Stephen Hawking, a quote that perfectly resonated with me and describes to perfection the experiences and feelings I have lived throughout my PhD.

"Black holes ain't as black as they are painted. They are not the eternal prisons they were once thought. Things can get out of a black hole both on the outside and possibly to another universe. So if you feel you are in a black hole, don't give up – there's a way out." – Stephen Hawking

Table of Contents

List of Figures

List of Tables

List of Abbreviations

AF-1	Activating function-1
AF-2	Activating function-2
ARC	Arcuate nucleus
AVPV	Anteroventricular araventricular nucleus
AHC	Adrenal hypoplasia congenita
BCA	Biocinchonicic acid
BSA	Bovine serum albumin
Ca2+	calcium
CNS	Central nervous system
cDNA	Complementary deoxyribonucleic acid
CTD	Carboxyl-terminal domain
Dax1+/+	Control (wild type) female mice
Dax1+/Y	Control (wild type) male mice
Dax1-/Y	Sex-reversed XY mice
DNA	Deoxyribonucleic acid
DAPI	4',6-diamidoino-2-phenylindole
DMSO	Dimethyl sulfoxide
DBD	DNA-binding domain
DMEM	Dulbecco's modified eagle medium
Dax1	Dosage sensitive sex-reversal (DSS), adrenal hypoplasia congenita (AHC), on chromosome X, gene 1
DSS	Dosage sensitive sex-reversal
estrogen	17β-estradiol
ER	Estrogen receptor
ERα	Estrogen receptor alpha
ERβ	Estrogen receptor beta
ERE	Estrogen response element
FBS	Fetal bovine serum
FITC	Fluorescein isothiocyanate
FSH	Follicle-stimulating hormone
GnRH	Gonadotropin-releasing hormone
GPCR	G-protein couple receptor

HPAG	Hypothalamic-pituitary adrenal gonadal axis
HPG	Hypothalamic-pituitary gonadal axis
HH	Hypogonadotropic hypogonadism
IP3	Inositol-(1,4,5)-triphosphate
icv	Intracerebroventricular
IHH	Idiopathic hypogonadotropic hypogonadism
ISH	*In situ* hybridization
kb	Kilobases
kDa	Kilodaltons
Kiss1	Kisspeptin gene
Kiss1r	Kisspeptin receptor
KO	Knock-out
LH	Luteinizing hormone
LBD	Ligand binding domain
LxxLL	Short leucine motif
MIS	Müllerian-inhibiting substance
mRNA	Messenger ribonucleic acid
mPOA	Medial preoptic area
Nr0b	Nuclear receptor subfamily 0 group B
Nr0b1	Nuclear receptor subfamily 0 group B member 1
Nr0b2	Nuclear receptor subfamily 0 group B member 2
NR-Box	Nuclear receptor box
NTD	Amino-terminal domain
OVX	Ovariectomised
PBS	Phosphate buffered saline
RT-qPCR	Reverse transcriptase polymerase chain reaction
RNA	Ribonucleic acid
SEM	Standard error of the mean
Sf1	Steroidogenic factor 1
SFRE	Steroidogenic factor response element
Shp	Small heterodimer protein

Sry	Sex-determining gene
TBS-T	Tris-buffered saline with Tween
XY	Male genotype
WT	Wild type
WT1	Wilm's tumour 1

Introduction

1 Introduction

1.1 The Female Reproductive System

1.1.1 The Hypothalamic-Pituitary-Ovarian (HPO) Axis

Reproductive function is essential for the survival of species. In females, reproduction is controlled and maintained by a series of complex and intricate interactions and feedback loops between the hypothalamus, anterior pituitary and the ovaries this pathway is denominated as the Hypothalamic-Pituitary-Ovarian (HPO) axis (Yen, 1977)(Figure 1).

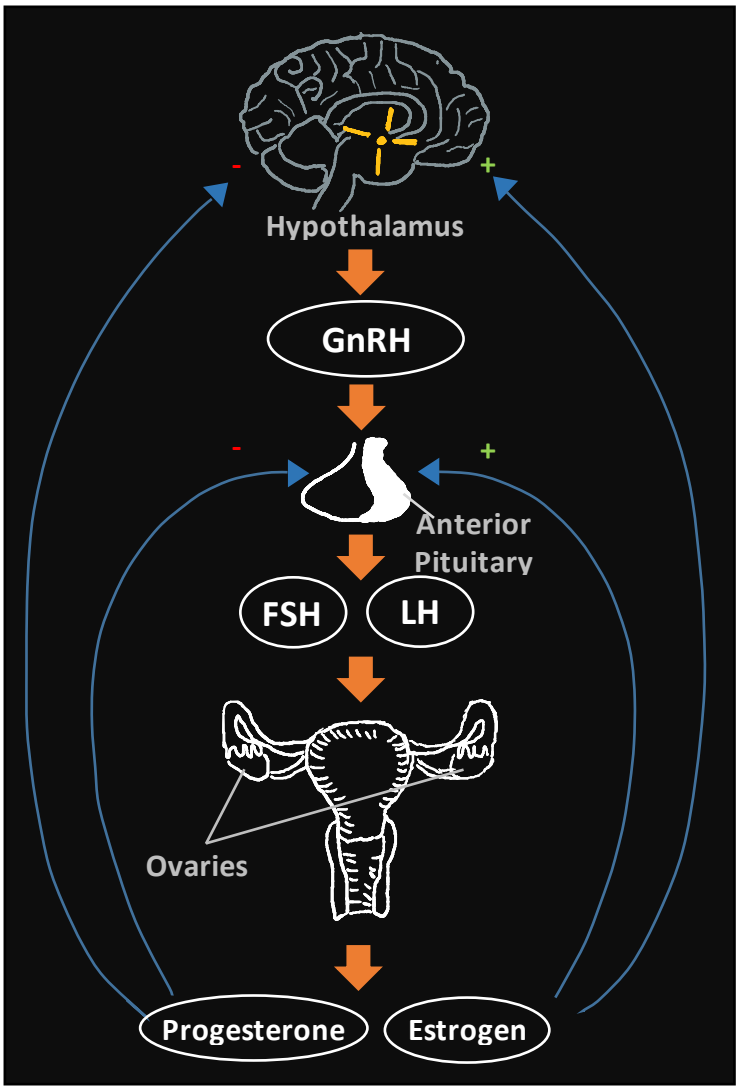

Figure 1: The hypoothalamic-pituitary-ovarian (HPO) axis.

Adapted from Pinilla et al.*, 2012.*

Traditionally, it has been viewed that at the top of the hypothalamic-pituitary-ovarian axis are the gonadotropin releasing hormone (GnRH) neurons, located in the medial preoptic area (mPOA) of the hypothalamus (Yen, 1977; Coss, 2018). Upon puberty, gonadotropin releasing hormone neurons start releasing gonadotropin releasing hormone in a pulsatile manner (Yen, 1977; Coss, 2018; Kaprara & Huhtaniemi, 2018; Schally *et al.*, 1971). GnRH reaches the anterior pituitary gland through the hypophyseal capillaries where it binds to its G-protein coupled receptor (GPCR), gonadotropin releasing hormone receptor (GnRHR), on the surface of gonadotropes to stimulate these cells to synthesise and release gonadotropin hormones, follicle stimulating hormone (FSH) and luteinising hormone (LH) (Yen, 1977; Coss, 2018; Stamatiades & Kaiser, 2018; Schally *et al.*, 1971). In females, these hormones are exocytotically secreted into the systemic circulation and have as target the ovaries, where, through their interaction with G-protein coupled receptors (GPCRs) present on ovarian cells, follicle stimulating hormone stimulates production of estrogen and ensures maturation of immature follicles and luteinising hormone promotes synthesis of androgen precursors, induction of ovulation of mature follicles and sustainability of the corpus luteum (Coss, 2018; Yen, 1977). The estrogen produced by the ovaries is then release into the systemic circulation and acts at the level of the hypothalamus to regulate both gonadotropin releasing hormone and gonadotropin release through both negative and positive feedback loops (Channing & Tsafriri, 1977; Richards, 1980; Pinilla *et al.*, 2012).

1.1.1.1 GnRH-Mediated Differential Regulation of Luteinising Hormone and Follicle Stimulating Hormone Synthesis and Release

Follicle stimulating hormone and luteinising hormone are important hormones for reproductive fitness. Luteinising hormone is required for pubertal development and gonadal function, in humans and mice, lack of luteinising hormone results in hypogonadotropic hypogonadism (HH, a condition characterised by low levels of gonadotropins, and sex steroids, and gonadal function) and infertility (Ma *et al.*, 2004; Huhtaniemi, 2006; Kaprara & Huhtaniemi, 2018). Absence of follicle stimulating hormone also leads to reproductive phenotypes: absent or incomplete pubertal development in humans while female mice are infertile (due to a block in folliculogenesis) (Kumar *et al.*, 1997; Lamminen *et al.*, 2005). Regulation of these hormones is, therefore, important to ensure follicullogenesis, steroidogenesis (via induction of steroidogenic enzymes in theca cells of the ovary) and ovulation (Coss, 2018; Voliotis *et al.*, 2018; Kaprara & Huhtaniemi, 2018; Stamatiades & Kaiser, 2018; Kumar *et al.*, 1997; Lamminen *et al.*, 2005). LH and FSH are synthesised by the

same anterior pituitary cells (gonadotropes) but their concentrations fluctuate throughout the estrous cycle (Coss, 2018). The mechanisms that regulate the differential regulation of these gonadotropins has been an area of interest. It is known that pulsatile release of gonadotropin releasing hormone is essential for reproduction and that the pulse frequency determines the effects of GnRH on target cells. In this way, it is hypothesised that the differential concentration of gonadotropins is determined by the frequency and amplitude of GnRH pulses, with LH being released, preferentially, as a result of high GnRH pulse frequencies (e.g. GnRH has been shown, in mice, to exhibit high pulse frequency in proestrous (Harris & Levine, 2003; Levine *et al.*, 1985)) and follicle stimulating hormone, on the other hand, being preferentially secreted when low GnRH pulse frequency are detected (i.e. tonic) (Coss, 2018; Voliotis *et al.*, 2018; Stamatiades & Kaiser, 2018).

1.1.1.2 Regulation of Gonadotropin Releasing Hormone Neurons of the Hypothalamus

The gonadotropin releasing hormone neuronal population, in mice, originates outside the central nervous system (CNS), on the medial olfactory placode (Kaprara & Huhtaniemi, 2018). During development these neurons migrate across the nasal septum into the septal-preoptic area and the anterior hypothalamus. In the adult mouse, even though GnRH is synthesised and found in peripheral tissues such as the gonads, placenta and mammary glands, its primary localisation is in the anterior hypothalamus, where neuronal process extend into the median eminence to allow for the pulsatile release of gonadotropin releasing hormone into the hypophysial circulation (Kaprara & Huhtaniemi, 2018; Schally *et al.*, 1971). The mechanisms that control the hypothalamic-pituitary-ovarian axis are of extreme importance and GnRH is an important hormone in the regulation of reproductive fitness and thus survival of species. However, until a decade ago, the mechanisms underlying gonadotropin releasing hormone pulsatile release were unknown, and thus the interest in this area of research grew. Over the years, several different neuronal populations have been found to directly regulate GnRH synthesis and release from the hypothalamus. The contribution of the neuropeptide kisspeptin is the main focus of this thesis and thus will be the one discussed in great detail.

1.2 Kisspeptin

Kisspeptin was originally discovered, in 1966, where it was found to restrict growth of secondary tumours by suppressing metastisis, and as a consequence, it was named metastin (Dungan, Clifton & Steiner, 2006; Tng, 2015; Lee *et al.*, 1996). It was only later, in 2003, following work done, independently, by *Seminara et al.* and by *de Roux et al.* that kisspeptin emerged as a potential regulator of GnRH neuronal activity and thus a key neuropeptide hormone in the regulation of reproductive function and fertility (Dungan, Clifton & Steiner, 2006; Seminara *et al.*, 2004; de Roux *et al.*, 2003). During their studies a relatively high incidence of hypogonadotropic hypogonadism (HH) in consanguineous families was observed. Affected individual possessed homozygous mutations in the *GPR54* gene. *GPR54* was found to be the receptor for kisspeptin (de Roux *et al.*, 2003; Seminara *et al.*, 2004; Dungan, Clifton & Steiner, 2006; Gottsch *et al.*, 2011; Popa, Clifton & Steiner, 2008; Kotani *et al.*, 2001; Lee *et al.*, 1999b). Hypogonadotropic hypogonadism is a condition characterised by low levels of gonadotropins (follicle stimulating hormone and luteinising hormone) and sex steroids, underdeveloped gonads (smaller testes and partial breast development) and infertility (de Roux *et al.*, 2003; Seminara *et al.*, 2004). With these findings, *Seminara et al.* and by *de Roux et al.* were the first to establish a link between *GPR54*/kisspeptin and reproductive function.

This link and observations were further strengthened by the animal studies that followed. The data obtained using *Gpr54* knockout (KO) mice (*Gpr54*$^{-/-}$) was in line with the phenotype observed in humans. Animals presented with decreased levels of luteinising hormone, follicle stimulating hormone, and sex steroids and as a consequence their gonads were poorly developed (e.g. small testes and underdeveloped ovaries). Furthermore, animals failed to mate and female presented with estrous cycle disturbances (Seminara *et al.*, 2004; Funes *et al.*, 2003; Colledge, 2009). Further to this, mice with mutations in the *Kiss1* gene mimicked the phenotype observed in *Gpr54*$^{-/-}$ mice (Popa, Clifton & Steiner, 2008; d'Anglemont de Tassigny *et al.*, 2007). In both species, humans and mice, anterior pituitary function was found to be normal and that exogenous administration of GnRH restored the reproductive phenotype, thus highlighting the importance of *Gpr54* and kisspeptin signalling in reproduction.

1.2.1 Kisspeptin Synthesis and Expression

The kisspeptins refer to a family of peptides encoded by the *Kiss1* gene, which is located on the long arm of human chromosome 1 at the 1q32 locus and contains 4 exons (West *et al.*, 1998). The *Kiss1* gene encodes the kisspeptin precursor, made of 145 amino acids (aa) that is enzymatically cleaved into a 54 amino acid peptide, known as kisspeptin-54 (kp54) or metastin. Kisspeptin-54 can be further truncated into 14, 13 or 10 amino acid peptides (kisspetin-14, -13 and -10, respectively), collectively these peptides are known as the kisspeptins (Dungan, Clifton & Steiner, 2006; Kotani *et al.*, 2001) (Figure 2).

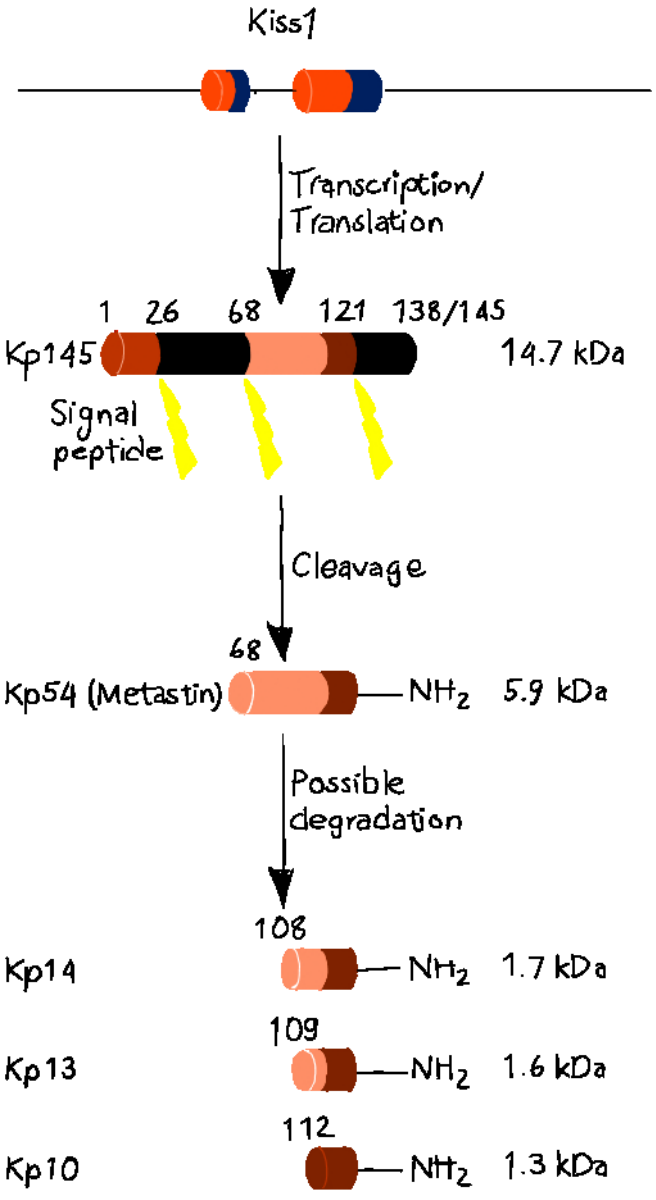

Figure 2: Generation of kisspeptins from the Kiss1 gene.

Adapted from d'Anglemont de Tassigny & Colledge, 2010.

Kisspeptin is a highly conserved peptide found in the brain and peripheral tissues of non-mammalian and mammalian vertebrates. In the mouse, kisspeptins are expressed in the gonads, placenta, and pancreas, however it is in the hypothalamus that the majority of kisspeptin neurons are located (Tng, 2015; Dungan, Clifton & Steiner, 2006; Kotani *et al.*, 2001; Ohtaki *et al.*, 2001). Immunohistochemistry (IHC) and *in situ* hybridisation (ISH) data show that kisspeptin cells are located in two nuclei of the hypothalamus that are important in the regulation of reproductive function: the arcuate (ARC) nucleus, equivalent to the infundibular nucleus in primates, and in the anteroventral periventricular (AVPV) nucleus, equivalent to the preoptic area (POA) (Tng, 2015; Dungan, Clifton & Steiner, 2006; Clarkson *et al.*, 2009; Clarkson & Herbison, 2006). Kisspeptin expression is sexually dimorphic in the anteroventral periventricular nucleus but not in the arcuate nucleus, with females having a much higher density of kisspeptin neurons in the anteroventral periventricular nucleus than males (Popa, Clifton & Steiner, 2008; Oakley, Clifton & Steiner, 2009; Clarkson & Herbison, 2006; Kauffman *et al.*, 2007).

1.2.2 The Kisspeptin Receptor

The kisspeptin receptor (*Kiss1r*), *Gpr54*, maps to chromosome 19p13.3 and was initially identified as an orphan G-protein coupled receptor (GPCR) of unknown function (Lee *et al.*, 1999b). *Gpr54* mRNA is expressed in the brain, including the hypothalamus and in other tissues such as the pituitary gland, testis, ovaries, placenta, pancreas and kidney (Popa, Clifton & Steiner, 2008; Lee *et al.*, 1999a; Kotani *et al.*, 2001; Ohtaki *et al.*, 2001). It was only later on that scientists discovered that *Gpr54* had a high affinity to kisspeptin. The first piece of evidence that showed that kisspeptins activate *Gpr54* come from studies using cells that express *Gpr54*, Chinese hamster ovary (CHO)-K1. Placenta extracts was shown to increase intracellular Ca^{2+}, investigators then isolated kisspeptins from human placenta and found that all kisspeptins (kisspeptin-54, -14, -13 and -10) bind and activate the *Gpr54* receptor, present on CHO cells, with the same affinity (Dungan, Clifton & Steiner, 2006; Popa, Clifton & Steiner, 2008; Rhie, 2013; Ohtaki *et al.*, 2001; Kotani *et al.*, 2001).

1.2.3 Role of Kisspeptin in Reproduction

The importance of kisspeptin in reproduction was first highlighted with the finding that homozygous mutations in the kisspeptin receptor, *GPR54*, caused individuals to develop classical symptoms of idiopathic hypogonadotropic hypogonadism (IHH) (de Roux *et al.*, 2003; Seminara *et al.*, 2004). As previously mentioned, these findings were corroborated with the generation of transgenic mouse lines where either the *Gpr54* gene or the *Kiss1* gene was mutated. As in humans, mice, were also, reproductively impaired (i.e. infertile) they presented with low levels of gonadotropic hormones (both luteinising hormone and follicle stimulating hormone) and sex steroids. They also presented with impaired pubertal development (de Roux *et al.*, 2003; Seminara *et al.*, 2004). Subsequent studies showed that *Kiss1* mutant animals retained the ability to secrete gonadotropin in response to kisspeptin administration and that and *Grp54* mutant mice retained normal pituitary response to GnRH administration (de Roux *et al.*, 2003; Seminara *et al.*, 2004; Tng, 2015), thus suggesting that at the basis of the reproductive phenotype observed in idiopathic hypogonadotropic hypogonadism is a primary defect in the GnRH pulse generator due to deficient signalling of an essential upstream regulator, kisspeptin.

1.2.3.1 Kisspeptin Stimulates GnRH Secretion

The presence of kisspeptin and its receptor in the posterior part of the arcuate nucleus, (thought to be the putative GnRH pulse generator, in primates) and in the pituitary, and the significance of these structures during puberty and reproduction highlights the importance of kisspeptin for reproduction (Ramaswamy et al., 2008). Indeed, central administration of kissppetin antagonists to the posterior part of the arcuate nucleus suppresses GnRH pulsatility in animals and thus suggests that kisspeptin neurons form the GnRH pulse generator, and thus suggesting that kisspeptin is a key regulator of the hypothalamic-pituitary-gonadal axis (Roseweir et al., 2009; Li et al., 2009). Kisspeptins stimulate GnRH secretion by acting directly on GnRH neurons through *Gpr54* (Tng, 2015; Herbison *et al.*, 2010; Irwig *et al.*, 2004). The mechanism is thought to be as follow; kisspeptin binds to the *Kiss1r* on GnRH neurons, coupled to the G protein subunit, $G_{q/11}\alpha$, ligand binding causes an intracellular signalling cascade that results in depolarisation of GnRH neurons which culminates in the release of GnRH and consequent modulation of follicle stimulating hormone and luteinising hormone secretion from the anterior pituitary (Tng, 2015).

Many lines of evidence corroborate the above mechanism; *Gpr54* is expressed within the preoptic area (POA), which colocalises with approximately 60% to 90% of GnRH neurons

(Herbison *et al.*, 2010; Irwig *et al.*, 2004). Studies also show that the majority, about 75%, of GnRH neurons express the kisspeptin receptor (Irwig *et al.*, 2004; Popa, Clifton & Steiner, 2008; Oakley, Clifton & Steiner, 2009). Furthermore, *Kiss1* and *Gpr54* knockout mice present with significantly lower FSH and LH levels when compared to wildtype mice (Seminara *et al.*, 2004; Funes *et al.*, 2003; Messager *et al.*, 2005). *Irwig et al.* (2004) demonstrated, in rats, that central administration of kisspeptin-10 increased C-fos expression in GnRH neurons, indicating neuronal activation (Irwig *et al.*, 2004). Central (via intracerebroventricular injection) and peripheral administration of kisspeptin has been shown to stimulate dose-dependent rise in serum levels of LH and FSH in many species (e.g. mice, rats, humans) (Matsui *et al.*, 2004; Thomson *et al.*, 2004; Messager *et al.*, 2005; Dhillo *et al.*, 2005, 2007). Further to this, kisspeptin administration has no effect on gonadotropin release in mice lacking a functional *Gpr54* gene (Messager *et al.*, 2005), and administration of GnRH antagonists abolishes the expected rise in follicle stimulating hormone and luteinising hormone following kisspeptin administration (Navarro *et al.*, 2005; Matsui *et al.*, 2004; Gottsch *et al.*, 2004). The data above are only some of the findings that demonstrate that kisspetin acts through its *Gpr54* receptor to regulate GnRH and gonadotropin release, and in turn ensures reproductive function.

1.2.3.2 Kisspeptin and the Onset of Puberty

The onset of puberty is triggered by the resurgence of GnRH secretion at a specific and appropriate stage during development (Shahab *et al.*, 2005). Considering the amount of compelling evidence that demonstrates that kisspeptin acts centrally on GnRH neurons to induce GnRH secretion and subsequent gonadotropin release in order to regulate reproduction (e.g. mice with mutations in the *Kiss1* gene and *Gpr54* gene fail to reach puberty) (Matsui *et al.*, 2004; Thomson *et al.*, 2004; Messager *et al.*, 2005; Dhillo *et al.*, 2005, 2007). It was questioned whether kisspeptin and *Gpr54* signalling could be at the basis of the mechanisms that lead to and sustain the onset of puberty. Indeed, data and observations from several different laboratories seems to corroborate the idea that kisspeptin-*Gpr54* signalling might play an important role in the onset of puberty. *Navarro et al.*, in 2004, reported that pre-pubertal animals exposed to both chronic and central administration of kisspeptin went through the onset of puberty earlier (in mice vaginal opening is the external indicator of onset of puberty) (Navarro *et al.*, 2004c). *Teles et al.*, in 2008, reported similar findings, central and peripheral administration of kisspeptin induced precocious puberty in rodents. Further to this, the GnRH secretion pattern following kisspeptin administration resembled the GnRH

secretion pattern observed during puberty (Teles *et al.*, 2008). Moreover, increased *Kiss1* and *Gpr54* gene expression, in the arcuate nucleus and anteroventral periventricular nucleus, is observed during pubertal development (Navarro *et al.*, 2004a; Shahab *et al.*, 2005). It is known that central administration of kisspeptin stimulates the release of gonadotropin hormones through its effects on gonadotropin releasing hormone neurons (Matsui *et al.*, 2004; Thomson *et al.*, 2004; Messager *et al.*, 2005; Dhillo *et al.*, 2005, 2007). While the evidence presented here appears to show that kisspeptin-*Gpr54* signalling plays role in the onset of puberty, it is likely that more than one factors regulates the mechanisms that trigger puberty.

1.2.4 Link Between Reproduction and Metabolism

Fertility and the hypothalamic-pituitary-gonadal axis are closely linked to nutritional status, this is because reproduction is an energetically demanding process and, as such, species have developed mechanisms by which energy levels and the nutritional state of the animal are detected (Quennell *et al.*, 2011). In animals, a negative energy balance due to, for example starvation and excessive exercise, inhibits the hypothalamic-pituitary-gonadal axis (Quennell *et al.*, 2011). Nutritional status is relayed to the brain by circulating metabolic fuels (such as glucose) and by hormones produced in peripheral tissues (e.g. leptin and insulin)(Quennell *et al.*, 2011). Leptin is a metabolic hormone secreted from fat cells, its main role is to regulate energy intake and expenditure. However, animals with abnormal leptin signalling also present with reproductive impairments. Indeed leptin replacement can overcome fasting-induced suppression of luteinising hormone pulses in rodents and primates. Leptin acts centrally to affect the reproductive axis, however *Quennell et al.* (2011) showed that leptin does not interact directly with GnRH neurons, therefore an intermediary mechanism must exist linking metabolic status and reproductive function. Recently, kisspetin joined the list of neuropeptides that may act as the neuropeptide link between leptin receptors and GnRH neurons. Several lines of evidence support this potential role of kisspeptin, for example leptin-deficient mice (*ob/ob*) are infertile and present with low levels of gonadotropin hormones and sex steroids. *Smith et al.* (2006) showed that approximately 40% of *Kiss1* neurons, in the arcuate nucleus, express the active form of the leptin receptor, *Ob-Rb* (Smith *et al.*, 2006a; Quennell *et al.*, 2011). Furthermore, food restriction, fasting and lactation (three states of negative energy balance) all culminated in decreased hypothalamic levels of *Kiss1* mRNA (Quennell *et al.*, 2011). These results provide evidence for the complex mechanisms that surround reproduction and establishes a potential link between kisspeptin-*Gpr54*

signalling, reproduction, and metabolism (Popa, Clifton & Steiner, 2008; Tng, 2015; Dungan, Clifton & Steiner, 2006).

1.3 Estrogen

1.3.1 Estrogen Synthesis and Expression

Estrogens are a group of steroidal hormone that are involved in and regulate many physiological process, including reproduction, sexual development, normal cell growth, energy homeostasis and tissue-specific gene regulation in the reproductive tract, central nervous system and skeletal system (Hillier, 2001; Gruber *et al.*, 2002). Estrogen also influences the pathological mechanisms of hormone-dependent diseases, such as cancer, namely breast, endometrial and ovarian, as well as osteoporosis (Matthews & Gustafsson, 2003; Gruber *et al.*, 2002). Three forms of estrogen are found within the body: estriol, estrone and estradiol, which has two further subforms, 17α-estradiol and 17β-estradiol. 17β-estradiol is by far the most potent and predominant estrogen produced in the body. On the other, is 17α-estradiol is not present in the systemic circulation, its expression and production is restricted to the brain, as evidenced by observations that levels of 17α-estradiol remain constant following ovariectomy, adrenaolectomy and castration. Furthermore, the metabolites, estrone and estriol, previously thought to be inactive, are now known to have tissue-specific roles (Gruber *et al.*, 2002; Matthews & Gustafsson, 2003).

The primary source of systemic estradiol is the ovary, it is here that estrogen biosynthesis takes place. According to the two-cell theory of estrogen synthesis, theca cells of the ovary produce the C-19 androgen precursors, androstenedione and testosterone, from which all estrogens are derived. Following androgen synthesis, theca cells release the precursors which diffuse into granulosa cells of the ovary. Here, aromatase cytochrome p450, an enzyme belonging to the p450 superfamily, catalyses the conversion of androgens to estrogens (Gruber *et al.*, 2002; Matthews & Gustafsson, 2003; Millier, Whitelaw & Smyth, 1994). The main site of estrone and estriol synthesis is the liver, where these two metabolites are formed from estradiol (Gruber *et al.*, 2002; Matthews & Gustafsson, 2003). Other tissues and cells such as osteoblasts and chondrocyte, adipose tissue, are also known to produce much lower levels of estrogen (Gruber *et al.*, 2002).

1.3.2 Estrogen Receptor

The biological actions of estrogen are mediated by three estrogen receptors (ER), estrogen receptor alpha (ERα), estrogen receptor beta (ERβ) and the G-protein coupled receptor 30 (Gpr30). The first two are nuclear and the latter is a membrane-bound receptor. Estrogen receptors belong to the nuclear receptor (NR) superfamily, a family of ligand-regulated transcription factors that are thought to be evolutionary conserved. Analysis of receptors has led to their subdivision into six different families: class I, II, III, IV, V and VI (Aranda & Pascual, 2001; Arnal *et al.*, 2017; Yaşar *et al.*, 2017; Laudet, 1997). Steroid receptors fall within the third family and, like most other members of this superfamily, with a few exceptions, ERα and ERβ are composed of six evolutionarily conserved functional and structural domains (A-F) (Aranda & Pascual, 2001; Yaşar *et al.*, 2017; Arnal *et al.*, 2017; Laudet, 1997; Kumar *et al.*, 1987) (Figure 3). The central and most conserved domain is the DNA binding domain (DBD) (C domain), which is involved in DNA recognition and binding. Binding of the ligand to the receptor occurs at the ligand binding domain (LBD) (domain E) in the COOH-terminal. The DBD and LBD are connected by the hinge region (D region). Transcriptional activation is ensured by two activation functions (AF), the first, AF-1, is constitutively active and resides in the A/B domain which is located in the N-terminal of the receptor. On the other hand, AF-2, is ligand-dependent and is found in the LBD. Both AF domains interact with factors that make-up the transcriptional machinery and are responsible for recruiting coregulatory proteins to the DNA bound receptor (Heldring *et al.*, 2007; Matthews & Gustafsson, 2003; Arnal *et al.*, 2017; Aranda & Pascual, 2001; Yaşar *et al.*, 2017; Kumar *et al.*, 1987).

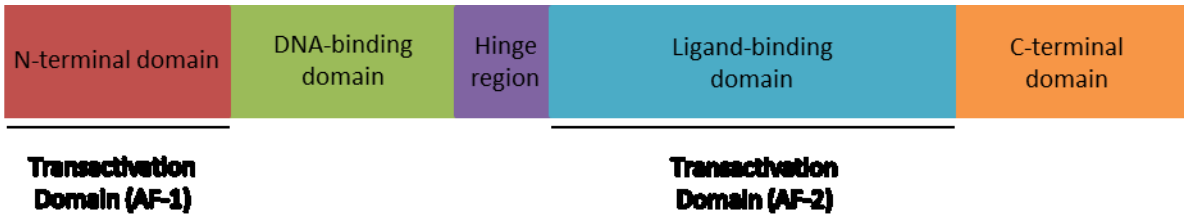

Figure 3: Schematic of estrogen receptors (ERs) structural regions.

The NH_2-terminal region (A/B) contains the ligand-independent transactivation domain 1 (AF-1). The DNA binding domain (C region) recognises specific DNA sequences. The hinge region (D) connects the DNA-binding domain and the ligand binding domain. The ligand binding domain (E region) contains the ligand-dependent transactivation domain 2 (AF-2) Adapted from Aranda & Pascual, 2001.

1.3.2.1 Estrogen Receptor Structure

1.3.2.1.1 NH_2-Terminal Region - A/B Domain

The N-terminal domain is highly variable, in both length and sequence, but in most nuclear receptors, like estrogen receptor, this region contains the constitutively active transactivation function (AF-1) (Heldring *et al.*, 2007; Matthews & Gustafsson, 2003; Arnal *et al.*, 2017; Aranda & Pascual, 2001; Yaşar *et al.*, 2017; Kumar *et al.*, 1987).

1.3.2.1.2 DNA Binding Domain (DBD) – C Domain

The DNA binding domain is by far the most conserved region among nuclear receptors (90% homology) and between species, and it is therefore considered the phylogenetic signature of NRs. The DNA binding domain is responsible for the recognition and specific binding to DNA sequences in target genes, known as estrogen response elements (EREs). The DBD contains conserved components that are required for affinity upon binding to EREs, such as cysteines. It is made of two zinc binding motifs (also known as "zinc fingers") which are formed by a zinc ion (Zn) interacting with four cysteines. The two zinc fingers fold together to form a compact structure. The amino acids required for discrimination and identification of EREs are present in the P box (on the first zinc finger). As it can be seen bellow (Figure 4), the second zinc finger contains the D box, composed by amino acids involved in receptor dimerization (Aranda & Pascual, 2001; Yaşar *et al.*, 2017; Arnal *et al.*, 2017).

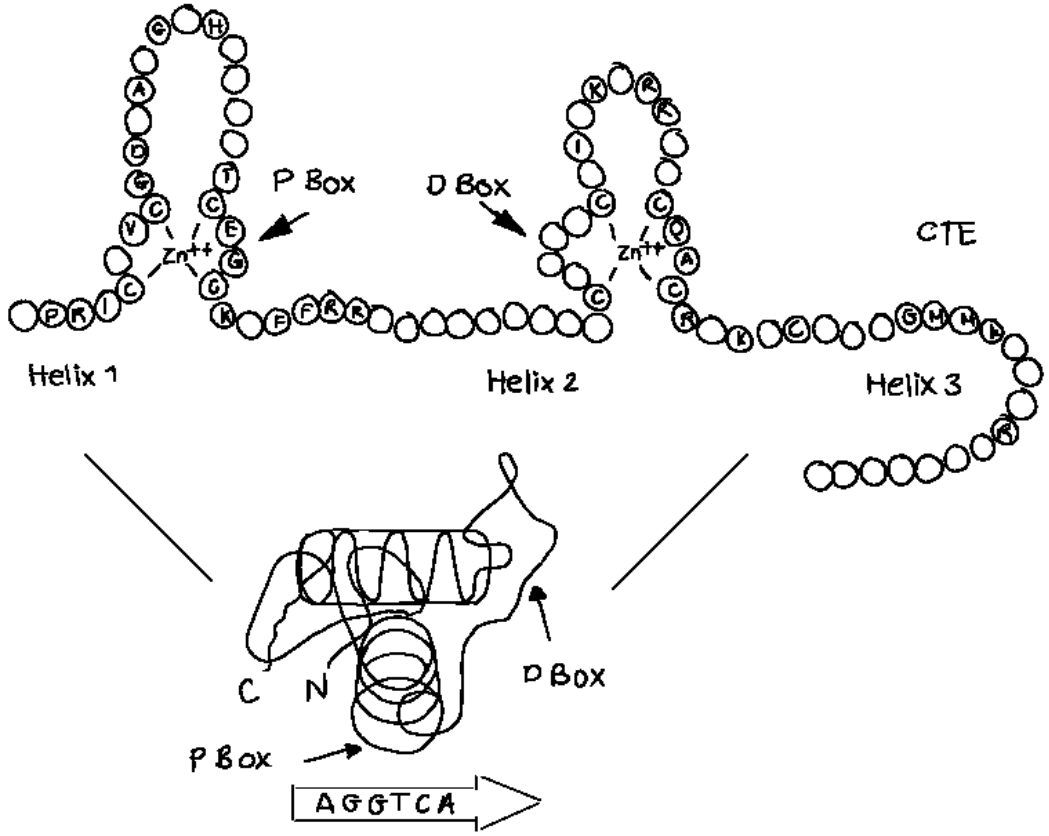

Figure 4: DNA binding domain of estrogen receptors.

Above: A diagram of the two zinc finger motifs, each zinc ion is surrounded by four cysteine residues. The P-box, located in the first zinc motif, determines the DNA binding specificity and it important for sequence discrimination and binding to estrogen response elements. The D-box, located in the second zinc finger, is involved in discrimination of half-site spacing. Below: A diagram of the tertiary structure of estrogen receptors. Adapted from Aranda & Pascual, 2001.

1.3.2.1.3 Hinge Region – D Domain

The region is weakly conserved and its size is variable among the nuclear hormone receptors. As the name specifies, the D domain serves as a hinge between the DNA binding domain and the ligand binding domain (Krust *et al.*, 1986). This structure allows for conformational changes upon estrogen and DNA binding, and also during protein to protein interactions. The hinge region also harbours nuclear localisation signals (NLS) which are important for nuclear translocation of the receptor (Ylikomi *et al.*, 1992). Further to this, the hinge region contains residues that are important for interaction with nuclear receptor coregulatory proteins. Mutations in these residues leads to failure in interactions with corepressors (Aranda & Pascual, 2001; Yaşar *et al.*, 2017; Arnal *et al.*, 2017; La Rosa & Acconcia, 2011)

1.3.2.1.4 Ligand Binding Domain (LBD) – E Domain

The E domain is a relatively large and complex, both in structure and function, component of the estrogen receptor (Figure 5). It composed of two well-conserved regions, the signature motif and the COOH-terminal AF-2 motif which is responsible for ligand transcriptional activation. It is structurally composed of 12 conserved α-helices numbered from H1 to H12, a conserved β-turn is situated between H5 and H6 (Brzozowski *et al.*, 1997; Wurtz *et al.*, 1996) (Figure 5). The ligand binding domain is organised into three layers, there is a core layer made up by three helices which is packed between two additional layers of helices which creates a hydrophobic cavity to which the ligand can bind, the ligand-binding pocket. This highly organised structure undergoes conformational remodelling upon ligand binding in order to give rise to a more compact structure. For example, in the absence of ligand the LBD is in a more open conformation with H12 being located away from the body of the receptor, however when the ligand binds to the ligand-binding domain the new conformation means that H12 is now positioned on the exit/entry route for ligands and thus traps the ligand at the ligand-binding pocket (Aranda & Pascual, 2001; Yaşar *et al.*, 2017; Arnal *et al.*, 2017).

The LBD not only mediates binding of the ligand to the estrogen receptor, but it is, also, the main dimerisation interface of the receptor, mediating both homodimerisation and hetereodimerisation, further to these functions it is here that chaperone proteins attach during inactivation of the receptor and maintain their nuclear localisation (Aranda & Pascual, 2001; Yaşar *et al.*, 2017; Arnal *et al.*, 2017).

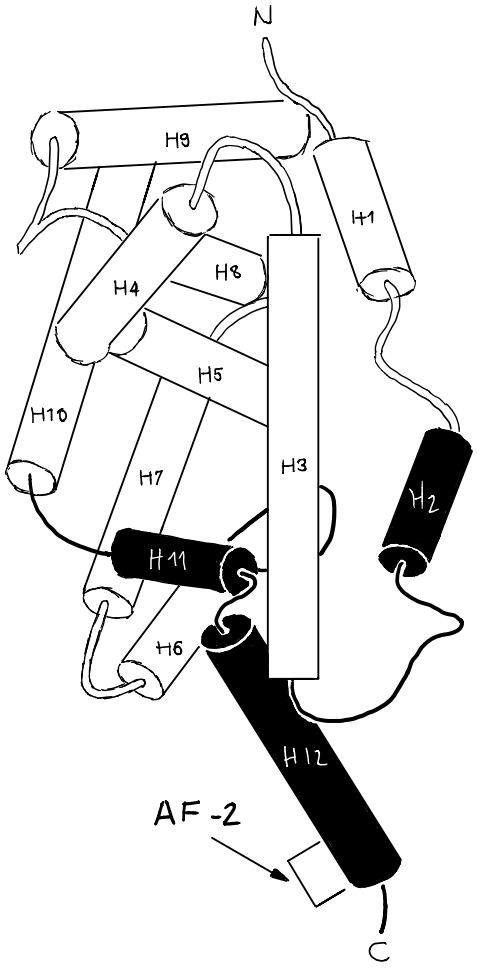

Figure 5: Drawing of the ligand binding domain (LBD).

Cylinders represent the alpha helices 12 conserved α-helices numbered from H1 to H12. Adapted from (Aranda & Pascual, 2001).

1.3.2.1.5 F Domain

The F domain is the least conserved of all the components that make up the estrogen receptor, some nuclear receptors do not have a clearly defined/structured F domain. The F domain of ERα is thought to be involved with modulation of the transcriptional activity, stability of the receptor, interactions with coregulatory proteins and dimerisation (Aranda & Pascual, 2001; Yaşar *et al.*, 2017; Arnal *et al.*, 2017).

1.3.2.2 Estrogen Receptor Alpha and Estrogen Receptor Beta

ERα and *ERβ* are encoded by genes on different chromosomes, the gene for the first receptor was mapped to the long arm of chromosome 6 (Ponglikitmongkol, Green & Chambon, 1988; Sand *et al.*, 2002), while the gene coding for *ERβ* is located on chromosome 14 q22-24 (Enmark *et al.*, 1997). Despite the homology seen at the level of the DNA binding domains (90% homology), the overall degree of homology between the receptors is low, with the A/B, D and F regions sharing 17%, 36% and 18% amino acid identity between the estrogen receptors (Yaşar *et al.*, 2017). Further to this, only 55-56% of the amino acid sequence that makes-up the ligand binding domain is identical between the receptors (Gruber *et al.*, 2002; Heldring *et al.*, 2007; Yaşar *et al.*, 2017) (Figure 6). As a consequence, *ERα* and *ERβ* have been found to have similar but unique roles within the body as well as distinct, and at times, overlapping expression patterns. Estrogen receptors are co-expressed in a number of tissues including the bones, thyroid, adrenal, brain, certain regions of the brain, etc. ERα is uniquely expressed in the uterus, kidney and heart, whereas ERβ is distinctively seen in the ovary, prostrate, lung, central nervous system and other (Heldring *et al.*, 2007; Gruber *et al.*, 2002; Yaşar *et al.*, 2017).

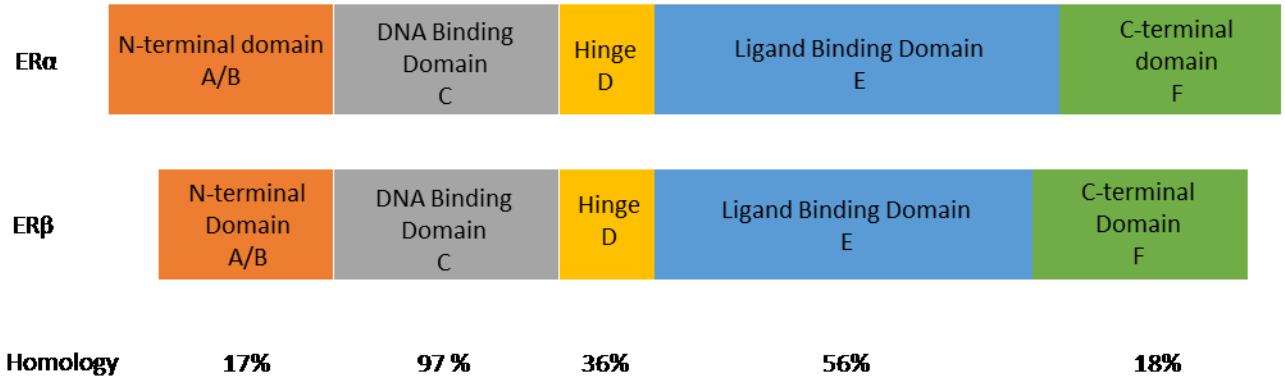

Figure 6: Schematics of the estrogen receptor alpha and estrogen receptor beta structural regions and their homology.

Adapted from Yaşar et al.*, 2017.*

1.3.3 Molecular Actions of Estrogens and Estrogen Receptors

The biological actions of estrogens are mediated by binding of estrogens to its receptors. However, the specific molecular actions of estrogens following ligand-binding are influenced by several factors such as characteristics of the target gene promoter, the balance of coactivators and corepressors, the structure of the hormone (Gruber *et al.*, 2002). Emerging evidence suggests that estrogens and estrogen receptors can act through several mechanisms to regulate its biological functions (Heldring *et al.*, 2007) (Figure 7).

In the classical pathway, estrogen moves freely into the cytoplasm where estrogen receptor is kept inactive through the action of heat shock proteins (hsp), acting as chaperones. Binding of the ligand causes the receptor to change its conformation that results in dissociation of heat shock proteins from estrogen receptor, which leads to dimerisation of two estrogen receptors, steroid receptors almost exclusively act as homodimers on estrogen response elements. (Monroe *et al.*, 2006; Aranda & Pascual, 2001). Following homodimersation, the estrogen receptor moves into the nucleus where it is able to bind to palindromic sequences on estrogen response elements, located in the regulatory (promoter) region of specific target genes (Nilsson *et al.*, 2019; Aranda & Pascual, 2001; Monroe *et al.*, 2006; Gruber *et al.*, 2002; Heldring *et al.*, 2007). The estrogen receptor-ligand recruits and interacts with coregulatory proteins (coregulators) which, subsequently, regulate recruitment of other transcription factors to form the RNA polymerase II (RNAP II) transcriptional machinery, or the preinitiation complex, which modulates gene expression (Monroe *et al.*, 2006).

For several years, it was thought that the only way through which estrogen affected the transcription of estrogen target genes was by direct binding of activated estrogen receptors to estrogen response elements. This theory become invalidated with the discovery that some estrogen-sensitive genes do not contain estrogen response elements or ERE-like sequences (McDevitt *et al.*, 2009; O'Lone *et al.*, 2004) and with the realisation that several actions of estrogen, such as rapid activation of growth-factor-related signalling pathways in neuronal cells and short-term vasodilation of coronary arteries, are simply too rapid and therefore cannot be explained and achieved by the traditional estrogen-signalling nuclear actions, which typically take minutes or even hours to alter target gene transcription and subsequent protein synthesis (McDevitt *et al.*, 2009; O'Lone *et al.*, 2004).

It is, now, known that estrogen receptor actions on signalling pathways can be described into classical, described above, and non-classical. There are three types of non-classical estrogen receptor actions: ERE-independent genomic actions, non-genomic actions and ligand-independent genomic actions. In the first mechanism, the estrogen-ER complex influences

the transcription of genes that do not harbour estrogen response elements in their promoter regions (Gruber *et al.*, 2002; Heldring *et al.*, 2007; Matthews & Gustafsson, 2003; Monroe *et al.*, 2006; Vrtačnik *et al.*, 2014; Kushner *et al.*, 2000; Gaub *et al.*, 1990). In this case, estrogen binds and activates the estrogen receptor which instead of binding to DNA directly it establishes protein-protein interactions with other classes of transcription factors (TF) at their response elements, which results in activation or repression of target genes. It is known that ER establishes protein-protein interactions with trans-acting transcription factors such as SP1 and AP-1 (consisting of fos-jun dimers), which are bound to their respective cognate DNA-binding elements (Gruber *et al.*, 2002; Heldring *et al.*, 2007; Matthews & Gustafsson, 2003; Monroe *et al.*, 2006; Vrtačnik *et al.*, 2014; Kushner *et al.*, 2000; Gaub *et al.*, 1990).

The second mechanism, also known as non-genomic, is poorly understood but has been seen in many tissues, and explains the rapid actions of estrogen. Briefly, estrogen binds to cell-membrane estrogen receptors (Gpr30) which are located in the invaginations of the cell membrane, known as caveolae. Binding of estrogen to estrogen receptor activates a signalling cascade involving secondary messengers (SM) that can affect ion fluxes across membranes, increase nitric oxide levels in the cytoplasm and activate kinases and phosphatases, all of these effects lead to rapid physiological responses that do not involve gene regulation (Zárate & Seilicovich, 2010; Gruber *et al.*, 2002; Matthews & Gustafsson, 2003; Heldring *et al.*, 2007; Vrtačnik *et al.*, 2014).

The final mechanism, ligand-independent, relies on the fact that estrogen receptor is a phosphoprotein, which means that its action can be influenced by phosphorylation, in the absence of the normal ligand. In this pathway, activators of protein kinases, such as growth factors (GF), activate protein-kinase cascades that phosphorylate and activate nuclear estrogen receptors at estrogen response elements. Like in the classical pathway, activation of the receptor results in interaction with coregulatory proteins and in the formation of the preinitiation complex at ERE of target genes which results in regulations of target gene expression (Gruber *et al.*, 2002; Heldring *et al.*, 2007; Matthews & Gustafsson, 2003; Bjornstrom & Sjoberg, 2005).

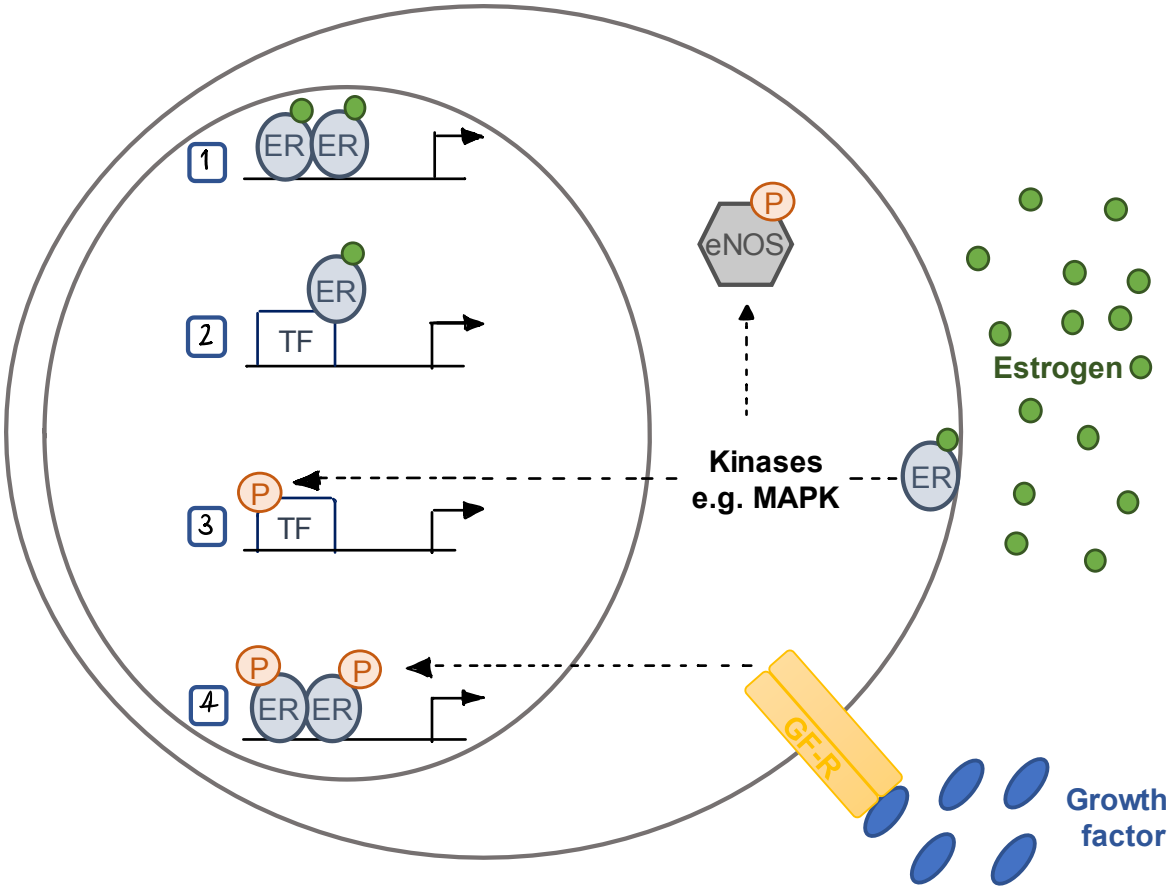

Figure 7: Estrogen receptor alpha signalling pathways.

(1) *Classical pathway: liganded estrogen receptor binds to estrogen response elements on target genes.* ***(2)*** *Estrogen response element-independent, in which liganded estrogen receptor binds and interacts with other transcription factors (TF) bound to their response elements and modulates gene expression.* ***(3)*** *Membrane initiated: membrane associated estrogen receptor (Gpr30) acts through kinases to phosphorylate other transcription factors.* ***(4)*** *Ligand independent: estrogen receptor is activated by phosphorylation. Pathways 2 to 4 are known as non-classical. From McDevitt* et al.*, 2009.*

1.3.4 Role of Estrogen in Reproduction

As mentioned previously, kisspeptin/*Gpr54* signalling on GnRH neurons leads to GnRH release into the median eminence, close to the pituitary portal vessels. GnRH stimulates synthesis and secretion of pituitary gonadotropin hormones (luteinising hormone and follicle stimulating hormone) which act on the gonads to activate steroidogenesis and gametogenesis. Estrogen then act centrally to regulate both GnRH secretion and the pituitary response to GnRH (Moenter *et al.*, 2003; Wintermantel *et al.*, 2006; Herbison & Pape, 2001). The effect of estradiol on the reproductive axis is of particular interest, this is because this steroidal hormone has both negative and positive effects on GnRH secretion. Throughout most of the estrous cycle, estrogen exerts a negative feedback, marked by suppression of GnRH pulse amplitude and frequency, on GnRH neurons resulting in restrained LH secretion. However, during the period prior to ovulation in females, proestrous (in rodents) and late stage of the follicular phase (in humans), estrogen levels rises as a consequence of the growing ovarian follicle, the effects of estrogen become stimulatory ("positive feedback") evoking a surge in GnRH secretion and, consequently, of LH, known as the GnRH/LH surge, a pre-requisite for ovulation in most species (Moenter *et al.*, 2003; Wintermantel *et al.*, 2006; Herbison & Pape, 2001). While the crucial roles of estrogen during reproduction are known, the underlying signalling mechanisms that contribute to estrogen positive and negative feedback remain poorly understood (McDevitt *et al.*, 2009). In the field, the general view is that estrogen feedback is, primarily, mediated by ERα.

1.3.4.1 Estrogen-Mediated Regulation of GnRH Neurons

Estrogens are important regulators of GnRH neuronal activity and thus of the hypothalamic-pituitary-gonadal axis (Herbison & Pape, 2001). However, the mechanisms by which estrogens influence GnRH secretion remains unclear.

Studies using mice with inactivating *ERα* or *ERβ* mutations (*ERα*KO and *ERβ*KO, respectively) have demonstrated that the effects of estrogen on GnRH are mediated via estrogen receptor alpha, alone, and not via *ERβ* (Wintermantel *et al.*, 2006). They found that the estrogen positive feedback, required for the pre-ovulatory LH surge, was normal in *ERβ* knockout mice. In contrast animals with inactivating *ERα* mutations did not present with normal estrogen positive feedback (as evidenced by inability to induce pre-ovulatory LH surge) (Wintermantel *et al.*, 2006).

However, several immunohistochemical studies, conducted on a variety of species, failed to detect the presence of *ERα* in GnRH neurons (Herbison & Pape, 2001). Further to this, dual *in situ hybridisation*/immunocytochemical studies also did not manage to detect *ERα* mRNA or protein in GnRH neurons (Herbison & Pape, 2001). These findings led to the hypothesis that the effect of estrogens may be transmitted to GnRH in an indirect manner by *ERα*-expressing neurons, glia or endothelial cells (Wintermantel *et al.*, 2006). *Wintermantel et al.* in 2006 identified *ERα*-expressing neurons, and not any other types of cells, as the key cells involved in relaying the effects of sex steroids on GnRH neurons.

1.3.4.1.1 Estrogen Mediates its Effects on GnRH through Kisspeptin Neurons

1.3.4.1.1.1 Estrogen-Mediated Differential Regulation of *Kiss1* in the Arcuate Nucleus and Anteroventral Periventricular Nucleus

The hypothalamic kisspeptin population is a key target of estrogen and has emerged as a potential intermediary neuronal network mediating the effects of estrogen on gonadotropin releasing hormone neurons.

The role of sex steroids on kisspeptin neurons was first documented in Navarro *et al.*, 2004, where gonadectomy of female and male rats increased *Kiss1* mRNA expression in the hypothalamus, and sex steroid replacement reversed this effect (Navarro *et al.*, 2004b). The studies that followed highlighted differential estrogen regulation of *Kiss1* gene expression in the two female hypothalamic nuclei, the arcuate nucleus and the anteroventral periventricular nucleus (Kauffman *et al.*, 2007; Smith *et al.*, 2005b, 2005a; Kauffman, Clifton & Steiner, 2007; Smith *et al.*, 2006b). Gonadectomy, in mice, caused an increase in *Kiss1* mRNA expression in the arcuate nucleus. While, in the anteroventral periventricular nucleus, lack of sex steroids (gonadectomy) repressed *Kiss1* mRNA expression. These changes were reversed with sex steroid replacement (Kauffman *et al.*, 2007; Smith *et al.*, 2005b, 2005a; Kauffman, Clifton & Steiner, 2007; Smith *et al.*, 2006b). Studies in which the levels of *Kiss1* were examined across the rat ovarian cycle further supported the findings described above. In the arcuate nucleus, *Kiss1* levels were increased in diestrous, when estrogen levels are low, and decreased during proestrous, when estrogen levels are at their highest. On the contrary, in the anteroventral periventricular nucleus, *Kiss1* mRNA expression is at its highest during proestrous, when estrogen is at peak levels (Castellano *et al.*, 2006). These studies demonstrate, that kisspeptin neurons in the arcuate nucleus mediate the negative effects of estrogen in the gonadotropin releasing hormone neurons. While, kisspeptin neurons in the

anteroventral periventricular nucleus, mediate the positive effects of estrogen on the gonadotropin axis.

Multiple lines of evidence shows that estrogen acts through estrogen receptor alpha (ERα) to mediate both the positive and negative regulation of *Kiss1* gene expression. In females, the vast majority of kisspeptin neurons in the arcuate nucleus and anteroventral periventricular nucleus express estrogen receptor alpha (90% and 70%, respectively). While only 25% to 40% of these neurons express the estrogen receptor beta (ERβ) (Kumar *et al.*, 2015; Smith *et al.*, 2005a). Studies using female mice with inactivating *ERα* or *ERβ* mutations (*ERα*KO and *ERβ*KO, respectively), show that *Kiss1* expression in the anteroventral periventricular nucleus and arcuate nucleus is intact in *ERβ*KO but not in *ERα*KO (Smith *et al.*, 2005a). These findings were further confirmed by experiments where ERα was selective blocked in free-cycling females. ERα selective blockade completely abolished LH responses to kisspeptin, eliminating the endogenous preovulatory rise of luteinising hormone, and hence blocking ovulation (Roa *et al.*, 2008). Thus these results suggest that the estrogen-driven positive feedback on *Kiss1* gene expression, in the anteroventral periventricular nucleus of hypothalamus, drives the preovulatory surge in luteinising hormone responsible for ovulation (Popa, Clifton & Steiner, 2008; Oakley, Clifton & Steiner, 2009; Roa *et al.*, 2008). Further to this, administration of the ERα agonist 4,4',4''-(4-Propyl-[1H]-pyrazole-1,3,5-triyl) trisphenol (PPT) mimicked *Kiss1* gene expression, in the arcuate nucleus, in response to estrogen (i.e. repressed *Kiss1* gene expression). On the other hand, administration of the ERβ specific agonist 2,3-bis(4-Hydroxyphenyl)-propionitrile (DPN) did not mirror the effects of *Kiss1* expression in the arcuate nucleus (Bateman & Patisaul, 2008). These results indicate that estrogen acts through ERα to mediate both the negative and positive effects of estrogen in *Kiss1* expression in the female hypothalamic nuclei, arcuate nucleus and anteroventral periventricular nucleus, respectively (Figure 8).

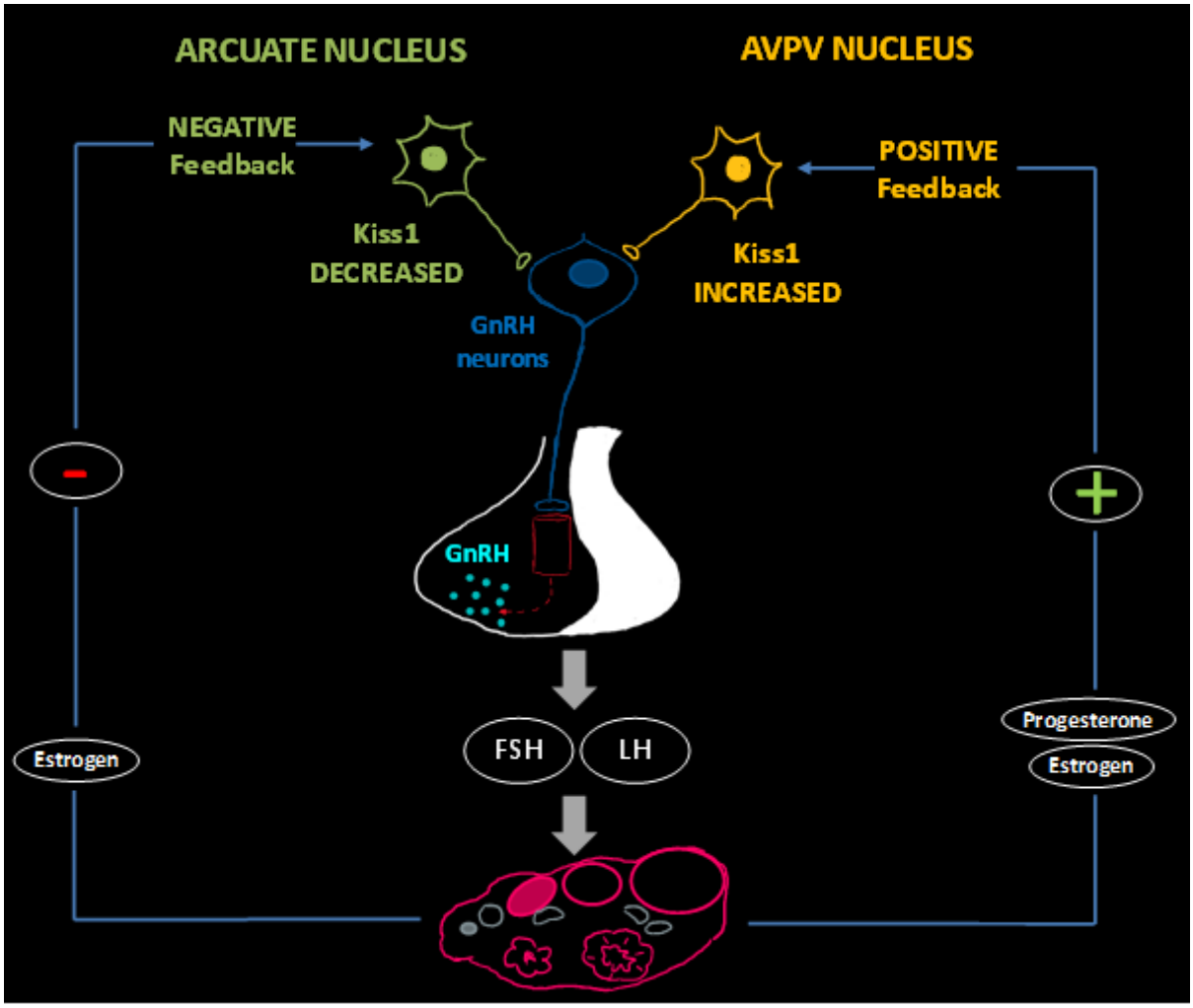

Figure 8: Model of differential estrogen-driven regulation of Kiss1 expression in female hypothalamic nuclei.

Kisspeptin has an important role in mediating the effects of sex steroids onto hypothalamic gonadotropin releasing hormone neurons. Kiss1 activates Kiss1 receptors (Gpr54) on gonadotropin releasing hormone neurons, resulting in gonadotropin releasing hormone secretion, which in turn acts at the pituitary to stimulate luteinising hormone and follicle stimulating hormone synthesis and secretion, and subsequent production of sex steroids from the gonads. Estrogen then feedbacks to the hypothalamus where, in the arcuate nucleus, downregulates Kiss1 expression. Conversely, estrogen upregulates Kiss1 expression in kisspetin cells of the anteroventral periventricular nucleus of the hypothalamus, which drives the LH surge. In this way, the hypothalamic kisspeptin neuronal population provides a mechanism whereby estrogen can exert both negative and positive feedback effects on the estrous cycle. Adapted from Kauffman, Clifton & Steiner, 2007.

It is interesting to note that the vast majority of kisspeptin neurons in the arcuate nucleus co-express neurokinin B (NKB) and dynorphin A (DYN) and are collectively known as the KNDy neurons (Goodman *et al.*, 2007). Co-expression of these neuropeptides in kisspeptin neurons may be physiologically relevant considering that NKB and DYN have been shown to inhibit LH secretion in rodents, further to this there is an association between kisspeptin/NKB neurons with GnRH fibres in the median eminence (d'Anglemont de Tassigny & Colledge, 2010). KNDy neurons form connections between themselves and it has been suggested that signalling between these neuropeptides may coordinate the release of kisspeptin in order to generate pulsatile GnRH release. Interesting, both neurokinin B and dynorphin A also express estrogen receptor alpha, and, as it is the case with kisspeptin, in the presence of estrogen their expression is also negatively regulated (d'Anglemont de Tassigny & Colledge, 2010). Therefore, while not well understood, it is possible to hypothesise that the interplay of these neuropeptides in response to estrogen is important for the mechanisms that drive reproduction (d'Anglemont de Tassigny & Colledge, 2010).

1.3.4.2 Coregulators are Involved in Estrogen Receptor Alpha Activity

The estrogen receptor alpha is a ligand-inducible transcription factors that specifically regulates the expression of target genes in response to sex steroid, estrogen. Estrogen receptor alpha transcriptional regulation of their target genes results from close and essential interplay between the receptor (ERα), the ligand (estrogen), DNA estrogen-response elements and coregulatory proteins (Girault, Bièche & Lidereau, 2006).

Coregulators play a central role in mediating transcriptional regulation of estrogen receptor target genes. Coregulators are proteins that participate in the complex that is recruited to the genome by DNA-binding transcription factors and through this recruitment the complex regulates the rate of transcription of estrogen receptor target genes (Millard *et al.*, 2013). Coregulators can be divided into coactivators and corepressors, the first are factors that interact with estrogen receptors and enhance transactivation of target genes (e.g. SRC1). Conversely, corepressors, are factors that interact with estrogen receptor alpha and repression transcription of estrogen receptor target genes (e.g. N-CoR and SMRT). (Mckenna, Lanz & O'Malley, 1999; Aranda & Pascual, 2001).

Coactivators and corepressors are able to interact with the hydrophobic groove of the ligand-binding domain of estrogen receptor through conserved regions, LxxLL (the nuclear receptor box, where L is leucine and x is any amino acid) and LxxH/IIxxxI/L (the CoRNR box), respectively (Millard *et al.*, 2013; Heery *et al.*, 1997; Hu & Lazar, 1999; Nagy *et al.*, 1999).

1.3.4.2.1 Coregulator Composition and their Relative Expression Determines Tissue-Specific Actions of Selective Estrogen Receptor Modulators (SERMs)

Selective estrogen receptor modulators are receptor ligands that exhibit agonistic or antagonistic effects in tissue-, cell-, and gene context-dependent manner (Arnal *et al.*, 2017). The prototypical selective estrogen receptor modulator is tamoxifen, which acts as an antagonist (i.e. opposes the effects of estrogens and inhibits estrogen receptor action) on breast tissue, and thus has been primarily used as an agent to treat and prevent breast cancer (Girault, Bièche & Lidereau, 2006; Turner *et al.*, 2009). On the other hand, in the skeleton and in the uterus, tamoxifen acts as an agonist (i.e. has estrogen-like activity) (Girault, Bièche & Lidereau, 2006; Turner *et al.*, 2009). The differential actions of tamoxifen has been thought to be due to its partial agonist/antagonist activity. Even before coregulators were identified, it was hypothesised that tissue-specific factors could account for the antagonistic/agonistic activity of selective estrogen receptor modulators (Katzenellenbogen, O'Malley & Katzenellenbogen, 1996). It is now known that coregulators play an important role in the tissue-specific actions of selective estrogen receptor modulators. The relative expression of coactivators and corepressors was envisioned as the main mechanism controlling the estrogen-like and anti-estrogen actions of selective estrogen receptor modulators. This is because selective estrogen receptor modulators induce characteristic alterations in the ligand-binding domain of the estrogen receptor which influences its ability to interact with coregulators. Therefore, differences in the relative expression of coactivators and corepressors accounts for the tissue-specific antagonistic versus agonistic actions of selective estrogen receptor modulators (Arnal *et al.*, 2017; Smith & O'Malley, 2004; Smith, Nawaz & O'Malley, 1997).

Binding of agonists to the ligand binding domain of estrogen receptor alpha causes conformational changes, with helix 12 (C-terminal helix) packing against helices 3, 5/6, and 11 and forming the coactivator binding groove (active state) (Heery *et al.*, 1997). The agonist-induced ligand binding domain confirmation is favourable to coactivator binding. Coactivators bind to the ligand binding domain of estrogen receptor alpha through the nuclear receptor box motif (LxxLL) (Heery *et al.*, 1997). On the other hand, while the mechanisms behind binding of antagonists to the estrogen receptor alpha are less clear, it is known that it involves conformational changes in the ligand-binding domain of estrogen receptor alpha, involving helix 3, 5 and 12 (Huang, Norris & McDonnell, 2002). Binding of antagonistic changes the position of helix 12, which hides the coactivator binding pocket, which renders interaction with coactivators and formation of the preinitiation complex

impossible (inactive state) (Huang, Norris & McDonnell, 2002; Smith & O'Malley, 2004). Most importantly, this new conformation favours recruitment and interaction with corepressors via CoRNR box, resulting in the loss of transcriptional activity. In the presence of selective estrogen receptor modulators, estrogen receptor alpha adopts an intermediary conformation between the active and inactive state, allowing for interactions with either corepressors or coactivators which dictates antagonist or agonist actions of selective estrogen receptor modulators (Smith & O'Malley, 2004; White & Parker, 1998; Arnal *et al.*, 2017). Therefore, tissue-specific activity of estrogen receptor bound to selective estrogen receptor modulators depends on the relative and absolute changes in coactivators and corepressors expression (Smith & O'Malley, 2004) (Figure 9).

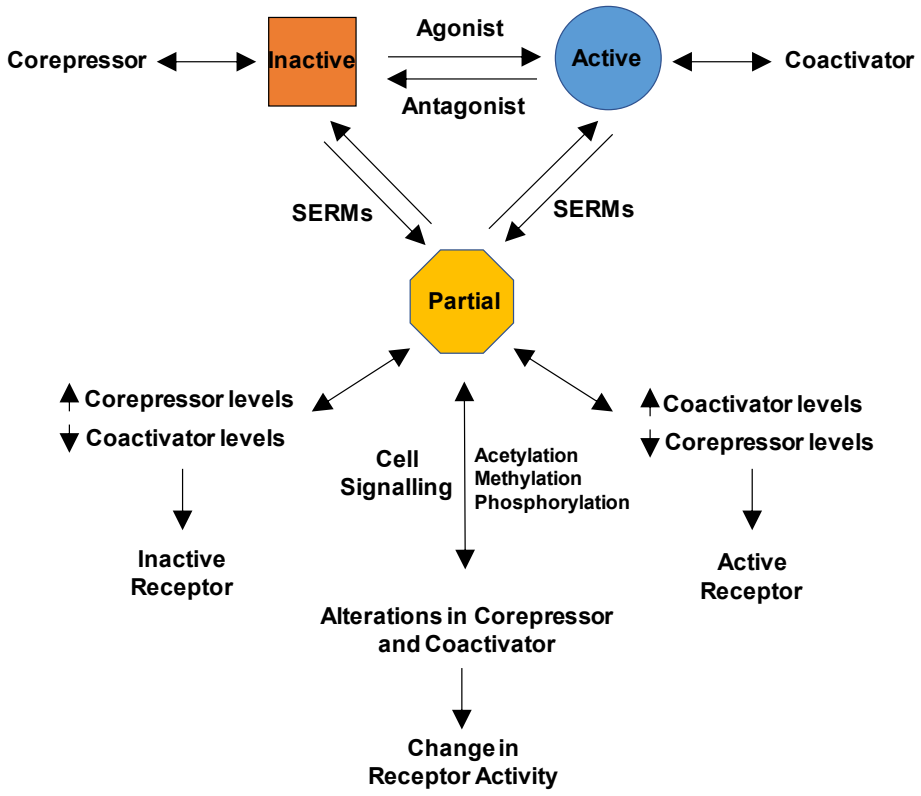

Figure 9: Model of the contribution of coregulators to relative selective estrogen receptor modulators agonist and antagonist activity.

In the presence of an agonist, estrogen receptor adopts an active conformation which allows for interaction with coactivators and is transcriptionally active. In the presence of an antagonist, estrogen receptor adopts an inactive conformation and interacts, preferentially, with corepressors and thus repressing estrogen receptor target gene transcription. When a selective estrogen receptor modulator is present, estrogen receptor adopts an intermediate conformation, between the active and inactive states, and therefore has the potential to exert partial activity. The activity of the SERM-bound estrogen receptor is determine by the relative expression of corepressors and coactivators in cells and tissues. From Smith & O'Malley, 2004.

1.3.4.2.2 Mechanisms of Coregulator Actions

In cells, DNA is packed and organised into chromatin structures which give rise to histones that make up chromosomes. Coregulators regulate transcription of target genes due to their ability to recruit enzymes that bring about post-translational modifications of histone tails that influence and modify accessibility of the transcriptional machinery (preinitiation complex) to target genes (Gronemeyer, Gustafsson & Laudet, 2004; Aranda & Pascual, 2001; Mckenna, Lanz & O'Malley, 1999; Martin & Cardoso, 2010). Coregulators can, therefore, enhance or inhibit estrogen receptor action by modifying histones. Histone acetylation, methylation, phosphorylation and ubiquitylation are some of the best-known modifications mediated by coregulators (Millard *et al.*, 2013). Only some of these modifications will be explored here. One such modification is histone acetylation and deacetylation, which is the process by which acetyl groups are added or removed, respectively, to lysine residues on histones. Histone acetylation plays an important role in the regulation of target gene regulation (Xhemalce, Dawson & Bannister, 2011). These reactions are catalysed by enzymes with histone acetyltransferases (HATs) and histone deacetylases (HDACs) activity (Martin & Cardoso, 2010; Millard *et al.*, 2013; Xhemalce, Dawson & Bannister, 2011). Histone acetyltransferases add acetyl groups to histone which changes the conformation of the chromatin, from a closed to an open structure, thus enabling interactions of DNA binding proteins with exposed sites, on target genes, and in this way activating gene expression (Martin & Cardoso, 2010; Millard *et al.*, 2013; Xhemalce, Dawson & Bannister, 2011). Conversely, histone deacetylases mediate removal of acetyl groups from histones which leads to chromatin compaction. The transcriptional machinery is unable to bind to promoter sequences on target genes and therefore gene expression is repressed (Figure 10) (Verdin & Ott, 2015; Xhemalce, Dawson & Bannister, 2011). Indeed, once bound to the ligand-binding domain of estrogen receptor alpha, coactivators recruit enzymes with histone acetyltransferase activity to enhance transcription of target genes. Whereas, corepressors recruit histone deacetylases to repress gene expression (Martin & Cardoso, 2010; Millard *et al.*, 2013).

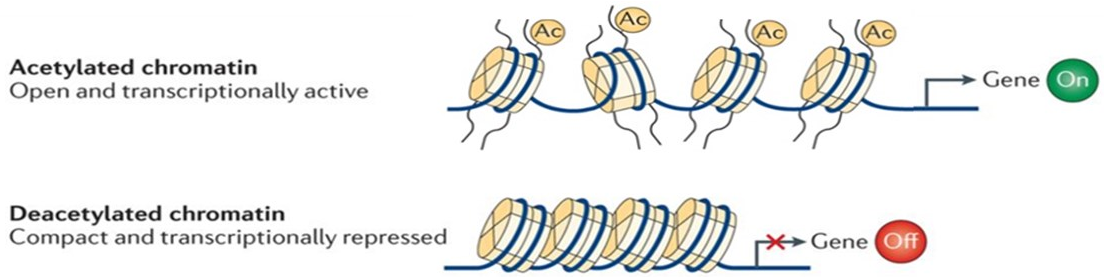

Figure 10: Histone acetylation, chromatin condensation and target gene expression.

In the top figure acetylation of lysine residues in histone proteins occur, leading to chromatin decondensation which allows access of transcription factors and other coactivators which drive expression. In the bottom figure, the absence of acetyl groups in histone tails leads enables folding of the nucleosome into secondary and tertiary chromatin structures. This compact conformation prevents interaction with transcriptional machinery but also promotes further recruitment of corepressors, repressing target gene expression. Adapted from Verdin & Ott, 2015.

Coregulators can also recruit other enzymes or secondary coregulators with histone methyltransferase (HMTs) or histone demethylase activity, which respectively, adds or removes methyl groups to specific lysine and arginine residues. Histone methylation also plays an important role in gene transcription, however the exact mechanisms by which this modification regulates gene transcription remains poorly understood (Millard *et al.*, 2013). What is known, is that the addition/removal of methyl groups to specific residues determines whether there is a positive or negative effect on target gene transcription. Coactivator-associated arginine methyltransferase 1 (CARM1) is one of the best characterized examples of histone methyltransferases, it plays an important role in mediating estrogen receptor function. CARM1 induces methylation of arginine 2, 17 and 26 of histone H3 which are associated with transcriptional activation (Bauer *et al.*, 2002; Chen *et al.*, 1999; Ma *et al.*, 2011; Wu & Zhang, 2009). It is important to mention that CARM1 is a secondary coactivator of estrogen receptor and only functions when p160 coactivators are present (Chen *et al.*, 1999). The importance of CARM1 actions in estrogen receptor-dependent transcription is seen in CARM1 null fibroblasts which exhibit abnormal expression of estrogen-responsive genes (Yadav *et al.*, 2003). Further, addition of estradiol to the breast cancer cell line (MCF-7) leads to activation of estrogen-responsive genes which coincides with CARM1 recruitment (Bauer *et al.*, 2002). It is therefore visible, that coactivators and corepressors alter the local chromatin environment, in part, by recruiting enzymes or secondary coregulators with chromatin-modifying activities that either promote or inhibit accessibility of the

transcriptional machinery to target genes, and thus either activate or repress transcription of target genes, respectively.

1.3.4.3 Tissue-Specific Coregulator Composition and their Relative Expression Might Determine Estrogen-Mediated Differential *Kiss1* Expression in the Anteroventral Periventricular Nucleus and Arcuate Nucleus

The demonstration that changes in coactivator and corepressor composition as well as their relative expression levels modulates the tissue-specific actions of selective estrogen receptor modulators raised the question whether this could also account for the tissue-specific responses to estrogen. This has become a topic of interest and some have addressed this question, there is some suggestions that this might be the case. However, more research is required so that a clear picture of the tissue-specific expression profile of corepressors and coactivators is acquired. The hypothesis that follows is that tissue-specific coregulator composition and their relative expression might determine the estrogen-mediated differences in *Kiss1* gene expression between the arcuate nucleus and anteroventral periventricular nucleus. The hypothesis is that in the anteroventral periventricular nucleus the expression of coactivators is more abundant than that of corepressors. The higher presence of coactivators in this nucleus facilitates interaction with coactivators that recruit enzymes and secondary coactivators with histone modification properties, and in this way positively modulate *Kiss1* gene transcription. On the other hand, in the arcuate nucleus, there is a greater expression of corepressors which facilitates interaction with corepressors. Corepressors changes the conformation of the ligand-binding domain thus preventing interaction with coactivators. It also promotes recruitment of enzymes and secondary corepressors that act on histones to repress *Kiss1* gene expression (Heldring *et al.*, 2007; Gronemeyer, Gustafsson & Laudet, 2004).

1.4 Dax1 (Dosage-sensitive sex reversal (DSS), adrenal hypoplasia critical region (AHC), on chromosome X, gene 1)

The nuclear receptor *Dax1*, also known as *Nr0b1*, encodes the Dax1 protein which stands for dosage sensitive sex-reversal (DSS), adrenal hypoplasia congenita (AHC), on chromosome X, gene 1. *Dax1* is expressed in the adrenal and in all regions of the hypothalamic-pituitary-gonadal axis during development and in the adult. Its expression in the developing gonad decreases as testicular differentiation in the developing gonad it decreases as testicular differentiation increases but continues in the case of ovarian differentiation. Multiple lines of evidence suggest that Dax1 plays a key role in sexual development, reproduction and steroidogenesis. Its name derives from two syndromes caused by genetic alterations the *NR0B1* gene in humans: adrenal hypoplasia congenita (AHC) and dosage-sensitive sex reversal. Adrenal hypoplasia congenita (AHC) is a disorder characterised by underdevelopment of the adrenal cortex (McCabe, 2001). It is estimated to occur at a frequency of 1:12,500 live births (Sikl, 1948; Jadhav, Harris & Jameson, 2011; Iyer & McCabe, 2004; Mitchell & Rhaney, 1959; Petersen *et al.*, 1982). Histologically, adrenal hypoplasia congenita presents in two forms: the miniature adult and the cytomegalic form. Patients with the adult miniature version have a permanent zone that is much smaller than normal, with minimal or absent fetal cortex (Iyer & McCabe, 2004; Niakan & McCabe, 2005; Jadhav, Harris & Jameson, 2011). In the cytomegalic form of adrenal hypoplasia congenita, the permanent zone of the cortex is mostly absent or absent, the rest of the adrenal tissue is structurally disorganised. This form of the disease is associated with *NR0B1* mutations, it is inherited in an X-linked manner and as such affects mainly males (McCabe, 2001). Clinical symptoms include the characteristic features of adrenal insufficiency: hypotension, hypoglycaemia, decreased reduced cortisol, among others. If left untreated, without mineralocorticoid and glucocorticoid replacement, adrenal hypoplasia congenita can be lethal (Iyer & McCabe, 2004; Niakan & McCabe, 2005; Jadhav, Harris & Jameson, 2011). Further to this, patients with adrenal hypoplasia congenita, display variable onset of puberty, due to hypogonadotropic hypogonadism (HH) (Petersen *et al.*, 1982; Prader, Zachmann & Illig, 1975; Jadhav, Harris & Jameson, 2011). Most commonly boys fail to enter puberty and gonadotropin levels are low and unresponsive to gonadotropin releasing hormone. This results from variable deficiency of gonadotropin releasing hormone secretion and/or deficiency pituitary response to gonadotropin releasing hormone (Jadhav, Harris & Jameson, 2011)j. Hypogonadotropic hypogonadism is a distinctive characteristic of adrenal hypoplasia congenita.

X-linked adrenal congenita hypoplasia was initially mapped to Xp21.3-p21.2 and to the *NR0B1* gene. Subsequently, identification of mutations in *NR0B1* confirmed that *Dax1* is the causative gene for adrenal hypoplasia congenita and associated hypogonadotropic hypogonadism (Muscatelli *et al.*, 1994; Zanaria *et al.*, 1994; Iyer & McCabe, 2004; Niakan & McCabe, 2005; Jadhav, Harris & Jameson, 2011; Habiby *et al.*, 1996). The importance of *NR0B1* in sex determination and gonadal development emerged with the finding that duplications of *NR0B1* led to male to female sex reversal in XY individuals. In this way *Nr0b1* positions itself as the dosage sensitive sex reversal gene (DSS) (Iyer & McCabe, 2004).

1.4.1 Structure of the *Nr0b1* Gene and of its Protein, Dax1

Nr0b1 has a very simple genomic structure, it is composed of two exons separated by one 3.4Kb intron. Exon 1 is 1168 base pairs (bp) long, exon 2 is much shorter (245 base pairs in length). Exon 1 contains the majority of the gene's coding sequence, it encodes the DNA binding domain (DBD) and a part of the ligand binding domain (LBD), while exon two encodes the remaining part of the ligand binding domain (Burris, Guo & McCabe, 1996; McCabe, 2001).

Dax1 has been classified as an atypical, orphan member of the nuclear receptor family. It is an orphan receptor, because, thus far, no natural ligand has been identified for Dax1. Members of the nuclear receptor superfamily share, with a few exceptions, a characteristic domain structure consisting of domains A-F (Aranda & Pascual, 2001; Arnal *et al.*, 2017; Yaşar *et al.*, 2017). The A/B is the least conserved domain, it contains the hormone independent transactivation domain (Activation Function 1 or AF-1). The DNA binding domain is by far the most conserved region (C domain). Through its zinc fingers it recognises and binds to hormone response elements in the promoter sequences of target genes. The hinge region allows for conformational changes in the receptor upon ligand binding (D region), it connects the DNA binding domain to the ligand binding domain, it is also a docking site for coregulators. The second most conserved region is the ligand binding domain (E domain), as the name suggests, it mediates ligand binding to the receptor, dimerisation and nuclear localisation. It is formed of 12 helices and contains a hormone-dependent transactivation domain (AF-2) (Iyer & McCabe, 2004; Aranda & Pascual, 2001; Arnal *et al.*, 2017; Yaşar *et al.*, 2017; Kumar *et al.*, 1987; Krust *et al.*, 1986; Ylikomi *et al.*, 1992; La Rosa & Acconcia, 2011; Brzozowski *et al.*, 1997; Wurtz *et al.*, 1996).

Unlike most nuclear receptors, *Nr0b1* encodes a nuclear receptor that lacks some of these characteristic conserved domains: the DNA binding domain, the hinged region and the ligand-

independent transactivation 1 (AF-1) domain and the hinge region (Niakan & McCabe, 2005; McCabe, 2001). Instead, Dax1 has two main structures: (i) the carboxyl-terminal domain (CTD) which is homologous to the ligand binding domain of nuclear receptor with a ligand-dependent transactivation domain (AF-2), (ii) in the amino-terminal domain (NTD), a novel and unique structure is found. It consists of three complete and one incomplete alanine-glycine rich repeats motifs of (65-67 amino acids long each), each repeat also contains a short leucine motif, LxxLL (usually found in coactivators) (Figure 11) (Niakan & McCabe, 2005; Iyer & McCabe, 2004; McCabe, 2001).

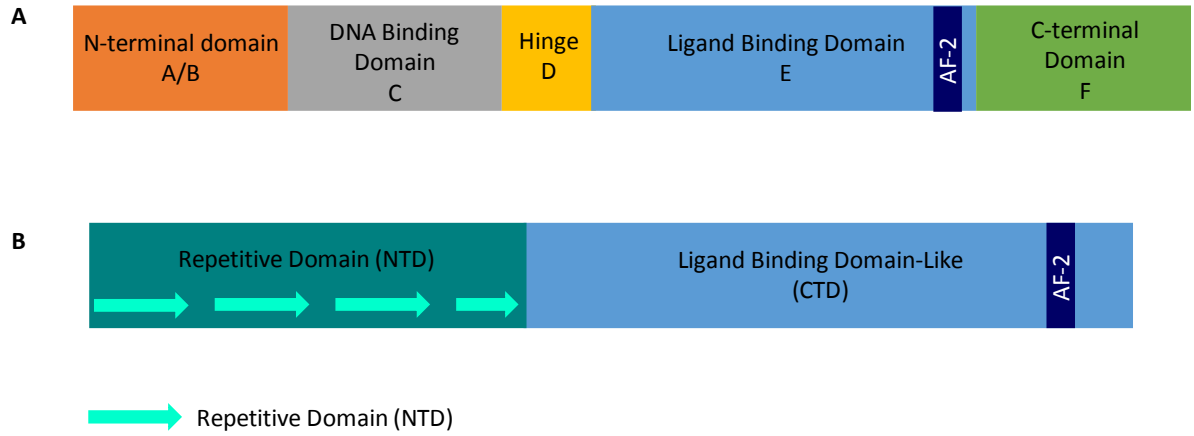

Figure 11: Functional domain structure in members of the nuclear receptor superfamily (A) and in Dax1 (B).

Adapted from Iyer & McCabe, 2004

1.4.2 Dax1 is a LxxLL-Corepressor of Nuclear Hormone Receptors

Nuclear receptors are transcription factors that regulate networks of genes important for sex development, reproduction and homeostasis in response to various signals (extracellular or intracellular). These signals, nuclear receptor ligands, bind to the ligand binding domain of the nuclear receptor and activate them (Zhang *et al.*, 2000). Ligand binding induces conformational changes, specific to the status of the ligand (agonist, antagonist, partial) in the nuclear receptor allowing them to interact with coregulatory proteins, which possess enzymatic properties and are able to recruit complexes that collectively work on hormone response elements to either positively (coactivators) or negatively (corepressors) regulate target gene expression (Heery *et al.*, 1997; Hu & Lazar, 1999; Nagy *et al.*, 1999). It is known, that these coregulatory proteins interact with the ligand binding domain via short leucine motifs (LxxLL, coactivators) or NR-Box (corepressors) (Heery *et al.*, 1997; Hu & Lazar, 1999; Nagy *et al.*, 1999).

Dax1 and its closest relative of the small heterodimer protein (Shp), which is encoded by *Nr0b2*, belong to the nuclear receptor subfamily 0 group B (*Nr0b*) which encodes for unique nuclear receptors, as they bind to other activated nuclear receptors to regulate their activity. Dax1 is now known to repress the transcriptional activity of other nuclear receptors such as steroidogenic factor 1 (SF1) and estrogen receptor (Crawford *et al.*, 1998; Zhang *et al.*, 2000). Transcriptional activity repression of nuclear receptors is as follows: Dax1, interacts with the coactivator binding surface, on the ligand binding domain of activated nuclear receptor, via the short leucine motif (LxxLL), and in this way competes with and displaces coactivators. Transcriptional repression is then achieved by both Dax1's potent silencing functions (harboured in its C-terminal ligand binding domain-like structure) as well as Dax1-mediated recruitment of corepressors to DNA-bound nuclear receptors (e.g. Alien and N-CoR) (Figure 12) (Crawford *et al.*, 1998; Zhang *et al.*, 2000).

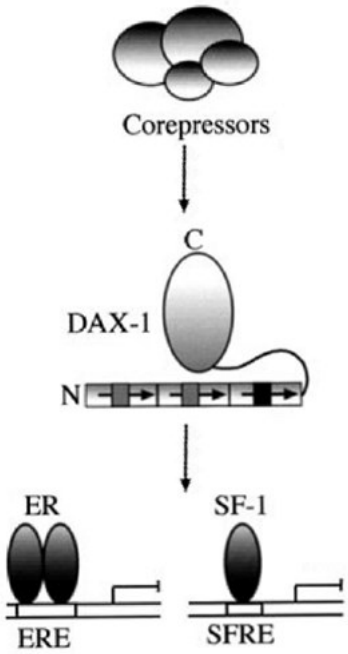

Figure 12: Mechanisms of Dax1-mediated repression of estrogen receptor and steroidogenic factor 1.

Adapted from Zhang et al., 2000.

1.4.2.1 Dax1 Regulates Transcriptional Activity of Steroidogenic Factor 1 (SF1)

The expression profile of Dax1 during development and in the adult is similar to the expression of *Sf1* (*Nr5a1*), an orphan nuclear receptor that regulates differentiation of the hypothalamic pituitary adrenal and gonadal (HPAG) axis and hormone synthesis (Parker, 2004). SF1 disruption causes a similar phenotype to that seen in adrenal hypoplasia congenita patients (i.e. the adrenals and gonads fail to develop/function normally, pituitary

and hypothalamic defects) (Parker, 2004). Dax1 is a transcriptional repressor of Sf1, and acts to inhibit regulation of Sf1 target genes (genes involved in steroid hormone synthesis throughout the HPGA axis) (Ito, Yu & Jameson, 1997) (mechanism described above). It is, therefore, postulated that a fine balance between Sf1 and Dax1 is required for proper adrenal development. Dax1 represses steroidogenic gene expression in order to allow cells of the adrenal to proliferate and differentiate into the different zones of the adrenal (glomerulosa, fasciculata, and reticularis). Absence of Dax1 and inability to regulate steroidogenic gene expression is most likely at the origin of adrenal hypoplasia congenita (Lalli & Sassone-Corsi, 2003).

1.4.2.2 Dax1 is a Corepressor of Estrogen Receptor Transcriptional Activity

The idea that Dax1 might interact with estrogen receptor and modulate its transcription activity emerged with the expression of profile of Dax1. Dax1 has been found to be expressed in several estrogen target tissues such as adrenal, ovary, testis hypothalamus, and pituitary, with coexpression in the ovary and testis during development (Bae *et al.*, 1996).

Indeed, Dax1 has been found to repress the transcriptional transactivation of estrogen receptor. Dax1 does not interfere with estrogen receptor dimerization or even its ability to bind to estrogen response elements, instead Dax1 competes for and binds to the, via the leucine short motif (LxxLL), coactivator binding sequence on the ligand binding domain (AF-2) of ligand-bound nuclear receptors, preventing interactions with coactivators (Zhang *et al.*, 2000). Dax1 subsequently recruits other corepressors to further exacerbate the repressive effects on the transcriptional activity of estrogen receptor. The interaction of Dax1 with estrogen receptors raises several possibilities, which remains unaddressed, it is conceivable that Dax1 is involved in the control of the physiological response to estrogen or may be important in mediating tissue-specific actions of estrogen receptor signalling or even repress estrogen receptor target genes at critical times (i.e. development, reproductive cycle) (Zhang *et al.*, 2000).

1.4.3 Role of Dax1

1.4.3.1 Role of Dax1 Sex Determination

Over the years there has been an interest in understanding the tissue- and pathology-specific actions of Dax1 and how its actions affects reproduction and sexual development. Some progress has achieved in the field and we can now explain some of the mechanisms that were previously unknown. For example, increased expression of Dax1 (genetic duplications) causes dosage-sensitive sex reversal. Dax1 has been shown to repress expression of Müllerian-inhibiting substance (MIS) by antagonising the interaction of Sf1 with GATA-4 and Wilm's Tumour 1 (WT1) (Nachtigal *et al.*, 1998; Iyer & McCabe, 2004; Tremblay & Viger, 2005). In males, Müllerian-inhibiting substance is activated in sertoli cells to inhibit the development of the female reproductive tract, or Müllerian ducts. In dosage sensitive sex reversal, Dax1 is thought to repress the expression of Müllerian-inhibiting substance, causing XY animals to develop and present phenotypically as females (Nachtigal *et al.*, 1998; Iyer & McCabe, 2004).

1.4.3.2 The Role of Dax1 in Hypothalamic and Pituitary Function and Associated Pathogenesis of Hypogonadotropic Hypogonadism

The role of Dax1 in the hypothalamus and pituitary has not been investigated in detail, it is known that mutations in the Dax1 gene leads to the development of hypogonadotropic hypogonadism, which is associated with adrenal hypoplasia congenita. It appears that the phenotype is due deficient hypothalamic and pituitary function (Iyer & McCabe, 2004). Dax1 is thought to be important for the development of these organs, nonetheless the exact mechanism behind this phenotype remains elusive (Iyer & McCabe, 2004).

1.4.3.3 The role of Dax1 in Testicular and Ovarian Development and Function

If we consider the role of Dax1 in sex development, initially, with the finding that duplications in *NR0B1* (high Dax1) was at the origin of male to female sex reversal led to a suspicion towards Dax1 acting as an ovary-determining gene or anti-testis factor influencing gonadal development (Jadhav, Harris & Jameson, 2011). This theory was tested using homozygous Dax1-deficient mice (Cre-mediated deletion of exon 2) (Yu, Ito & Jameson, 2014). Contrary to the initial hypothesis, ovarian development was normal and instead testis development was affected. Male animals presented with hypogonadotropic hypogonadism and were infertile (Yu, Ito & Jameson, 2014). This phenotype could not be explained by a hormonal defect, as gonadotropin releasing hormone, follicle stimulating hormone and testosterone levels were

normal. But instead there were testicular defects due to disorganised testis cord formation possible due to impaired differentiation of peripubertal myoid and sertoli cells (Bouma, 2005; Yu, Ito & Jameson, 2014; Jadhav, Harris & Jameson, 2011). However, female mice were mostly normal and fertile, with only a slight follicular defect (Yu, Ito & Jameson, 2014). These findings oppose the initial concept and, it is now known, that Dax1 is necessary for proper testicular development and function (Yu *et al.*, 1998; Iyer & McCabe, 2004; Eddy *et al.*, 1996). However, Dax1 might have several other roles, for example the role of Dax1 in the adult female has not been properly investigated.

1.5 Hypothesis and Aims

Hypothesis

The mechanisms that regulate the differential effects of estrogen in *Kiss1* gene expression in the arcuate nucleus and anteroventral periventricular nucleus of hypothalamus and that mediates and regulates reproduction and fertility is analogous to the mechanisms that regulate tissue-specific actions of selective estrogen receptor modulators.

We hypothesise that nuclear receptor coregulators modulate hypothalamic estrogen receptor signalling and therefore female fertility.

Aim

- The aim of this project is to understand estrogen signalling in the arcuate nucleus and anteroventral periventricular nucleus of the hypothalamus under physiological conditions.

- Identification of coregulators that might mediate the differential effects of estrogen signalling in the female hypothalamic nuclei.

- The physiological role of estrogen receptor alpha coregulators will be established by generating *Kiss1*-specific knockout mice.

Materials and Methods

2 Methods and Materials

2.1 Materials

All solvents and chemicals were of analytical grade and purchased from Abcam (Cambridge, UK), Ambion (Abingdon, UK), Amersham Biosciences (Amersham, UK), Applied Biosystems (Cheshire, UK), Becton & Dickinson (New Jersey, USA), Bio-Rad (Hemel Hempstead, UK), BOC (Guilford, UK), Cell Signalling Technology (Danvers, USA), Corning (New York, USA), Enzo Life Sciences (Exeter, UK), Fisher Scientific (Loughborough, UK), GeneCopoeia (Rockville, USA), Invitrogen (Paisley, UK), Kapa Biosystems (Wilmington, USA), MyBioSource (California, USA), National Diagnostics (Georgia, USA), Pierce (Illinois, USA), Promega (Southampton, UK), QIAGEN (Crawley, UK), Roche (Lewes, UK), SHANDON (Sigma-Aldrich (Poole, UK), Thermo Fisher Scientific (Fife, UK), Tocris Bioscience (Bristol, UK), Vector Laboratories (Peterborough, UK), VWR (Lutterworth, UK) and Zeiss (Oberkochen, Germany).

2.1.1 Chemicals, Reagents and Solvents

1Kb DNA Ladder	Invitrogen
4',6-Diamidin-2-Phenylindole,Dihydrchloride (DAPI)	Thermo Fisher Scientific
17α-Estradiol	Merck
17β-Estradiol	Merck
17β-Estradiol	Tocris Bioscience
20% Sodium Dodecyl Sulfate (SDS) Solution	National Diognostics
30% Hydrogen peroxide (H_2O_2)	VWR
37% HCL	WVR
40% Acrylamide	Bio-Rad
Absolute Alcohol	VWR
Agarose	Merck
Ampicillin	Merck
β-Mercaptoethanol	Merck
Bovine Serum Albumin (BSA)	Merck
Carbogen (95% O_2/5% CO_2)	BOC
Chloroform	Merck
Complete Protease Inhibitor	Promega
DEPC-Treated Water	Ambion
Dextrose	Merck
Dimethyl Sulfoxide (DMSO)	Merck

ECL Plus Western Blotting Detection System	GE Healthcare
Ethidium Bromide	Invitrogen
Ethylenediaminetetraacetic Acid (EDTA)	Merck
Fugene 6 Transfection Reagent	Roche
HEPS	Merck
Isopropanol	Thermo Fisher Scientific
KCl	Merck
LC-MS grade water	Thermo Fisher Scientific
Methanol	VWR
$MgCl_2$	Merck
$MgSO_4$	VWR
NaCl	Merck
$NaHCO_3$	VWR
NaH_2PO_4	VWR
NaOH	Merck
Normal Donkey Serum (NDS)	Merck
Phosphate Buffered Saline	Merck
Ponceau S Solution	Merck
Precision Plus Protein Dual Colour Standards	Bio-Rad
Protease Inhibitor Cocktail	Promega
Skimmed Milk Powder	Merck
S.O.C. media	Invitrogen
TEMED	Bio-Rad
Tris Base	Merck
Tris HCL	Merck
Triton X-100	Merck
Tween 20	Bio-Rad

2.1.2 Antibodies

Anti-Mouse Alexa Fluor 488	A-21121 – Goat	Thermo Fisher Scientific
Anti-Mouse Alexa Fluor 568	A-21124 – Goat	Thermo Fisher Scientific
DAX-1	39983 – Mouse	Active Motif
DAX1, Clone 2F4	MABD398 – Mouse	Merck
Estrogen Receptor Alpha – E115	Ab32063 – Rabbit	Abcam
ERα (MC-20) X	sc-542 – Rabbit	Santa Cruz Technology
GAPDH (14C10)	2118S – Rabbit	Cell Signalling Technology
GFP Tag	A-6455 – Rabbit	Thermo Fisher Scientific
HRP anti-Rabbit IgG	15015 – Goat	Active Motif
HRP anti-Rabbit IgG	PI1000 – Goat	Vector
HRP anti-Mouse IgG	15014 – Goat	Active Motif
HRP anti-Mouse Kappa Light Chain	ab99617 – Rat	Abcam
LH-Beta Monoclonal Ab	518B7 – Bovine	UC Davis (Lillian E Sibley)
LH Polyclonal Ab	AFP240580Rb – Rabbit	AF Parlow Mouse RIA kit
Progesterone	ab63605 – Rabbit	Abcam

2.1.3 Enzymes

DNase 1	Bio-Rad
HotStart DNA Taq Polymerase	QIAGEN

2.1.4 Plasmids

GAPDH-PG04-*Luciferase*	GeneCopoeia
CS-MPRM26651-PG04-01-*Luciferase*	GeneCopoeia
NEG-PG04-*Luciferase*	GeneCopoeia
Mouse Estrogen Receptor 1 Alpha (Esr1)	GeneCopoeia
Mouse Nr0b1	GeneCopoeia

2.1.5 Assay Kits

BCA Protein Assay Kit	Pierce
SensiFast cDNA Synthesis Kit	Bioline
SensiFast SYBR Hi-ROX Kit	Bioline

Estradiol 17-Beta Human ELISA kit	Abcam
iQ SYBR Green Supermix	Bio-Rad
iScript cDNA Synthesis Kit	Bio-Rad
Secrete-Pair Dual Luminescence Luciferase Assay Kit	GeneCopoeia
PureLink RNA Mini Kit	Ambion
Progesterone ELISA Kit	Enzo Life Sciences
Mouse Follicle Stimulating Hormone ELISA Kit	MyBioSource
QIAprep Spin Miniprep Kit	QIAGEN
QIAprep Plasmid Maxi Kit	QIAGEN
RNeasy Plus Micro Kit	QIAGEN
KAPA HS Mouse Genotyping	Kapa Biosystems

2.1.6 Cell Lines

Female Mouse Hypothalamic-A50 (mHypoA-50)

Female Mouse Hypothalamic-A55 (mHypoA-55)

Human Embryonic Kidney cells 293 (HEK293T)

Chinese Hamster Ovary (CHO)

2.1.7 Cell Culture Materials

Charcoal Stripped Fetal Bovine Serum (FBS)	Thermo Fisher Scientific
Dulbecco's Modified Eagle Medium (DMEM)	Merck
Fetal Bovine Serum	Invitrogen
Opti-MEM I Reduced Serum Medium	Thermo Fisher Scientific
Penicillin (100U/mL)	Merck
Phenol Red Free Dulbecco's Modified Eagle Medium	Thermo Fisher Scientific
Streptomycin (50µg/mL)	Merck
Trypsin	Merck

2.1.8 Buffers, Solution and Gels

Immunostaining Permeabilisation Buffer	PBS 1X, 0.5% Triton X-100
Immunostaining Blocking Buffer	PBS 1X, 0.3% Triton X-100, 10% Normal Donkey Serum
Immunostaining Antibody Incubation Buffer	PBS 1X, 0.5% Triton X-100, 1% Normal Donkey Serum
Immunostaining Washing Buffer	PBS 1X, 0.3% Triton X-100
Western Blot SDS Running Buffer	0.2M Tris Base, 2M Glycine, 0.03M SDS
Western Blot SDS Transfer Buffer	25mM Tris Base, 190mM Glycine
Western Blot Blocking Buffer	2.5% Bovine Serum Albumin (BSA), 2.5% Skim Milk Powder, 0.01% Tween-20, TBS 1X
Western Blot Tris-Buffered Saline (TBS)	0.4M Tris Base, 2.8M NaCL
Western Blot Tween-20	0.4M Tris Base, 2.8M NaCL, 0.01% Tween-20
Western Blot Stripping Buffer	100mM ⍰-Mercaptoethanol, 2% (w/v) SDS, 62.5mM Tris HCl pH 6.7
Lammeli Buffer (2x)	4% (w/v) Acrylamide, 20% (v/v) Glycerol, 10% (v/v) β mercaptoethanol, 0.005%

	(w/v) Tris-HCl pH 6.8
12% SDS Running Gel	1M Tris-HCl pH 8.8, 12% SDS, 40% Acrylamide, Water, 10% APs, TEMED
12% SDS Stacking Gel	1M Tris-HCl pH 8.8, 10% SDS, 40% Acrylamide, Water, 10% APs, TEMED
Protein Loading Buffer (2x)	10% (w/v) SDS, 20% (v/v) Glycerol, 250mM Tris-HCl pH6.8, 0.7M Mercaptoethanol, 0.02% (w/v) Bromophenol Blue (Stored at -20˚C)
Phosphate Buffer Saline (PBS)	140mM NaCl, 2.5mM KCl, 1.5mM KH_2PO_4 pH7.2, 10mM Na_2HPO_4 pH7.2
RIPA Lysis Buffer	150mM NaCl, 1% NP-40, 0.5% Deoxycholic acid, 0.1% SDS, 50mM Tris pH 8.0, Promega Complete Protease Inhibitor (1x)
Artificial Cerebral Spinal Fluid	126mM NaCl, 3.5mM KCl, 1.25mM NaH_2PO_4, 10mM Dextrose, 2mM $CaCl_2$, 1mM $MgSO_4$
LH ELISA Blood Collection Buffer	0.05% Tween-20, PBS 1X

LH ELISA Coating Buffer	0.015M Na_2CO_3, 0.035M $NaHCO_3$, ddH_20, pH 9.6
LH ELISA Washing Buffer	0.05% Tween-20, 0.25% BSA, PBS 1X
LH ELISA Blocking Buffer	0.05% Tween-20, 0.25% BSA, 5% Skim Milk Powder, PBS 1X

2.1.9 Software Packages

Adobe Suite	Adobe Inc., San Jose, California, USA
GraphPad Prism 7	GraphPad Software, San Diego, California, USA
ImageJ	National Institutes of Health and the Laboratory for Optical and Computational Instrumentation, University of Wisconsin, Wisconsin, USA
Microsoft Office Software Suite	Microsoft Corporation, Redmond, Washington, USA

2.2 Methods

2.2.1 Manipulation of mice

2.2.1.1 General Maintenance

Wild-type animals were B57BL/6 and purchased from Charles River (UK). All animals used in this thesis were bred and maintained at the animal facilities in Imperial College London. Maintenance and animal studies were conducted in accordance with 'The Animals (Scientific Procedures) Act 1986'. Animals were housed under standard conditions on a 12-hour daylight cycle and had free access to water and standard diet (ERD).

2.2.1.2 Dax1 null mice

In order to obtain mice with conditional knockout of Dax1 in *Kiss1* neurons (Dax1$^{tm(Kiss1)}$), *BeEi*-Dax1^{flox} mice were purchased from Jackson Laboratory (Bar Harbor, USA, (stock #007006) and crossed to homogosity. They were then crossed with *Kiss1-CreGFP* animals (Jackson Laboratory, stock #017701) to excise the LoxP site and intercrossed to generate wild type (Dax1^{tm}) and knockout (Dax1$^{tm(Kiss1)}$) mice.

2.2.1.2.1 Genotyping Strategy

2.2.1.2.1.1 Genomic DNA preparation from ear notches

DNA was extracted from ear samples using the KAPA Mouse Genotyping Kit (KAPA Biosystems). Individual ear notches (approximately 2mm) were digested in a 20 µL reaction containing KAPA Express Extract Enzyme (1U/µL) and KAPA Express Extract Buffer (10X). Tissue lysis followed, 75°C for 10 minutes, and the enzyme was subsequently inactivated with a 95°C incubation for 5minutes. Genomic DNA was diluted ten-fold in 10mM Tris-HCl (pH 8.5).

2.2.1.2.1.2 Genotyping

A 10µL reaction containing $MgCl_2$ (1.5mM), dNTPs (0.2mM), and 10µM of each primer, LC-MS grade water, Fast DNA polymerase and 1µL of genomic DNA was set up. DNA was initially denatured by heating the solution to 95°C for 3 minutes which was followed by a protocol consisting of 35 cycles of: 95°C for 1 minute, 60°C for 15 seconds, and 72°C for 15 seconds. Followed by a final extension of 72°C for 3 minutes. The PCR products were then analysed by gel electrophoresis. Three primer sets were used to genotyped Dax1 knockout mice; a Dax1 common primer, wild type primer and a mutant reverse primer. Used in combination it is possible to distinguish between the three possible genotypes: wild type (Dax1 WT band

only), heterozygote (a Dax1 WT band and a Dax1 null band) and (knockout Dax1 null band). For primer sequences see Appendix 1.

2.2.1.2.1.3 DNA agarose gel electrophoresis

Agarose powder was mixed with fresh 1X TAE in order to make a 2% (w/v) agarose gel. The solution was heated up in a microwave until the boiling point was reached, it was then left to cool to approximately 60°C, and 0.2µg/mL ethidium bromide was then added and mixed thoroughly. The solution was poured into a gel mould, and once it had set it was placed into a gel tank and submerged in fresh 1X TAE. 5 µL of 1Kb plus DNA maker (Thermo Fisher) and of each of the DNA samples, loading dye is already included in the KAPA2G Fast Genotyping Mix, were loaded onto the gel and the current was set at 50V until the DNA fragments were resolved (approximately 45 minutes). The DNA fragments were visualised using a long wave UV light box and photographed, their sizes were compared to the known sizes in the DNA marker.

2.2.1.2.2 Estrous Cycle Experiments

2.2.1.2.2.1 Phenotyping of Mice with Conditional Knockout of Dax1 in Kisspeptin Cells

At the weaning age (13 days after birth), pups were removed from the parent cage, immediately genotyped and allocated into two groups $Dax1^{tm}$ and $Dax1^{tm(Kiss1)}$, according to their genotype. Female animals were subsequently single housed and they were followed for a total of 16 weeks. During this time several different phenotypic aspects were analysed (described below).

2.2.1.2.2.1.1 Reproductive phenotype

2.2.1.2.2.1.1.1 Determining the Age and Weight at the Onset of Puberty

The onset of puberty, in mice, was visually determined by vaginal opening (VO), an apoptosis-driven event that occurred as a consequence of increased levels of circulating estradiol. The vulva of single caged mice was examined daily to assert the day of vaginal opening. In brief, mice were removed from their home cages by the tail and placed on the Animal Transfer Station (AllenTown Inc). The animal was then held by the tail, towards the base of the tail, and was subsequently lifted in order to gain visual access to the vulva. The openness and the redness of the vulva was assessed and the day of opening was documented for every animal. Further to this, the body weight at the onset of puberty was also examined. A balance was set up and tarred with a 500mL plastic beaker (VWR), after assessment of the vulva was completed, the animals were placed into the beaker by the tail and their body weight was recorded. Recordings were taken daily until the day of vaginal opening was detected.

2.2.1.2.2.1.1.2 Estrous Cycle Measurement

In mice, assessment of the reproductive cycle was commonly achieved by vaginal smear cytology. This method enabled determination of the estrous cycle phases according to the proportion of three specific types of cells present in the smear: cornified cells, epithelial cells and leukocytes. The estrous cycle of mice is approximately 4-6 days long and it is comprised of four stages. The first one is the proestrous which is mainly characterised by nucleated epithelial cells, these can appear in clusters or individually, some cornified cells might also be visible in the smear. The presence of clusters of anucleated cornified squamous epithelial cells is a distinctive characteristic of the next stage of the cycle, estrous. A mixture of cells (i.e. nucleated epithelial cells, anucleated cornified squamous epithelial and leukocytes, by far the most visible) defines the metestrus. Finally, the vaginal smear collected from animals in diestrous is marked by the presence of leukocytes (Caligioni, 2009).

Vaginal smears were taken daily for the duration of the study at approximately 1300 hours. Mice were removed from the cages and placed on the Animal Transfer Station, the tail of the mouse was lifted at the base in order to expose the vulva. A transfer pipette (ThermoFisher Scientific) containing sterile 1X phosphate buffer saline (PBS) was gently inserted into the vagina, it is important not to insert the pipette too deep into the vagina as this can lead to pseudo-pregnancies. The vagina was gently flushed three to five times with the PBS, the final flush is collected in the pipette tip and vaginal smears were placed on glass slides (VWR), covered with a cover slide (VWR). Cellular contents were analysed under a light microscope

(Motic SFC-100 FLED Monocular Cordless Microscope, Thermo Fisher Scientific), 10X objective. Cycle length and regularity of each cycle was determined by the sequence of smears. A full cycle, in this study, was defined as observing at least three stages of the cycle in the right order, with estrous and diestrous being two of those stages. The number of days to that took to fulfil this criteria defined the length of the estrous cycle.

2.2.1.3 Follicle Stimulating Hormone Suppression and Luteinising Hormone Surge Assay

2.2.1.3.1 Subcutaneous Administration of 17β-Estradiol

The day before ovariectomy experiment two different silastic capsules were prepared, one containing 17β-estradiol (Merk) that was thoroughly mixed in sesame oil (0.1mg/kg), and the other one was filled with sesame oil only (vehicle). Silastic implants are commonly used in mice to deliver controlled concentrations of hormones over a prolonged period of time.

One centimetre of silastic tube (Silastic tube, 508-005, Dow Corning) was cut, another silastic tube with smaller diameter (Silastic tube, 508-003, Dow Corning) was inserted into the previously cut tube with bigger diameter, one end of the smaller tube was sealed with Gorilla Glue, the glue was allowed to dry. Using a syringe and needle the smaller tube was filled with either 17β-estradiol in sesame oil or with sesame oil alone, the tube was then completely sealed off with glue. Capsules were stored at overnight at 4˚C in either17β-estradiol and sesame oil solution or sesame oil only, according to the capsules' content.

2.2.1.3.2 Ovariectomy Surgery

Age matched (6-8 weeks old) female Dax1^{tm} and Dax1$^{tm(Kiss1)}$ mice were anesthetised using 1.5% isoflurane (3% for induction) in an oxygen/nitrous oxide 30%/70% mixture. The animals were placed in the prone position in a heating pad and their lower back was shaved, liquid iodine was then applied to the shaved area and lacrillube was placed on the eyes of the animals to prevent them from drying out. Subsequently, 4 mg/kg of carprofen (Rimadyl) and 0.12 mg/kg of buprenorpherrine (Temgesic) were administered intra-scruff, while the antibiotics Flucloxacillin and Amoxicillin (mixed in a 1:1 ratio with a final dose of 25 mg/kg) were administered intraperitoneally (IP). A 3 centimetre midline back incision was performed using a blunt forceps, the fascia underneath the skin was then separated from the skin and two incisions were made into the peritoneal cavity on both flanks. Using blunt tweezers, the adipose tissue was removed from the cavity in order to aid in the localisation of the ovaries, vessels and uterine horns were ligated and the ovary was removed. The

remaining tissue was placed back into the abdominal cavity. This procedure was repeated for the other ovary.

The silastic capsule containing either vehicle or 17β-estradiol were wiped and inserted subcutaneously. The wound was then closed using two to three wound staples and the animals were allowed to recover from anaesthesia in a heated box (25˚C to 27˚C) for one hour. The animals were housed according to the treatment that they received and allowed to recover from surgery for one week.

2.2.1.3.3 Injections

After recovery, mice were injected at 09:00 with either vehicle (sesame oil) or estradiol benzoate (0.05 mg/kg).Three groups were created: (i) control – mice that were implanted with silastic capsule containing sesame oil, and injected with sesame oil (vehicle), (ii) low estrogen – mice implanted with silastic capsule containing 17β-estradiol in sesame oil and injected with sesame oil; and (iii) high estrogen - mice implanted with silastic capsule containing 17β-estradiol in sesame oil and injected with estradiol benzoate.

2.2.1.3.4 Plasma and Tissue Collection

The following day, at 14:00, mice were decapitated using sharp scissors (World Precision Instruments), blood was collected using microvettes 500 coated with EDTA K3 (Sarstedt), the blood was placed on ice. The brain was, subsequently, carefully removed from the skull, placed in a 7 mL sterelin (WVR) and snap frozen in liquid nitrogen. Blood was centrifuged (Eppendorf, 5417R) at 4000 rpm, for 15 minutes at 4˚C in order to separate the plasma from white and red blood cells. After centrifugation plasma was removed and placed into a labelled 1.5 mL tube (Eppendorf). Brain and plasma samples were subsequently stored at -80˚C. Between five to six mice were used per group.

2.2.1.4 Organotypic Brain Slice Cultures

2.2.1.4.1 Artificial Cerebrospinal Fluid preparation

Three litres of artificial cerebrospinal fluid (ACSF) were prepared the night before the experiment, two of those litres were stored at 4˚C while the remaining litre was placed at 37˚C, overnight. In the morning of the experiment, the artificial cerebrospinal fluid was bubbled through with carbogen (95% O_2/5% CO_2) for about 10 minutes, and only after ACFS oxygenation was the 2mM $CaCl_2$. A 20 mL syringe was filled with ice cold artificial cerebrospinal fluid and attached to a 21G blunt microfine needle (Becton & Dickinson).

2.2.1.4.2 Experimental Set-Up

On the day of the experiment, three containers were filled with 400mL of warm and oxygenated artificial cerebrospinal fluid, one of these will be used for recovery of the brain slices (artificial cerebrospinal fluid only) and the other two for treatments: vehicle and 10nM 17β-estradiol (artificial cerebrospinal fluid with either 100% ethanol or 10nM 17β-estradiol, respectively). The containers were placed in a water bath set at 37˚C, PVC tubes connected to the carbogen gas tank were attached to each container in order to continuously oxygenate the treatment solutions.

The vibratome 1500 (The Vibratome Company, Missouri, USA) tank was filled with cold ACSF and ice was added to the tank when required in order to keep the artificial cerebrospinal fluid cold throughout the duration of the experiment. The thickness of the vibratome was set to 800μm, the amplitude to 10 and the speed to 5, while the blade angle was kept at 0˚. Furthermore, a PVC tube connected to the carbogen tank was also attached to the inside of the vibratome tank in order to ensure oxygenation of the brain throughout the slicing process.

2.2.1.4.3 Cardiac Perfusion using Artificial Cerebrospinal Fluid

Wild-type B57BL/6 female mice (6-8 weeks old) were terminally anesthetised intraperitoneally with sodium pentobarbital (50-90 mg/kg) (Nembutal). Once the animal reached a surgical plane of anaesthesia, determined by the toe pinch-reflex, an incision beneath the rib cage and through the abdominal cavity was made using blunt scissors, vertical cuts through the ribs and up to the collarbone were done on either side, creating a flap. The connective tissue linking the rib cage to the body was subsequently, and carefully, cut in order to expose the pleural cavity by lifting the sternum which was clamped with a hemostat and placed over the animal's head in order to obtain a better view of the heart. The

right atrium was snipped and the needle and syringe containing the artificial cerebrospinal fluid was inserted into the left ventricle, reaching the ascending aorta. The animal was then perfused with artificial cerebrospinal fluid at a slow and steady rate.

2.2.1.4.4 Brain dissection

The animal's head was removed using a pair of scissors, the skin was subsequently removed too in order to expose the skull, and leftover connective tissue was also removed. Sharp scissors were inserted into the foramen magnum of the skull and the skull and bones all around the brain until the eye socket were cut, this was repeated for the opposite side. A final cut through the midline of the eyes was performed, thus allowing detachment of the skull and brain from the rest of the head. A cut through the midline of the skull was performed which enabled removal of the frontal bone of the skull and partial exposure of the brain. The brain was scooped out with blunt forceps and placed immediately on oxygenated ice cold artificial cerebrospinal fluid.

2.2.1.4.5 Preparation and treatment of organotypic slices

The dissected brain was rapidly superglued onto the chuck of the vibratome, the brain was left to set for 2-3 seconds and was subsequently placed inside the vibratome container, previously filled with artificial cerebrospinal fluid, the cold liquid helps to further solidify the glue as well as hold the brain in place. The entirety of the entire anteroventral periventricular nucleus and arcuate nucleus were subsequently cut into equal parts, the slices of the first nuclei were of 200 μm, while the thickness of the slices cut for the latter nuclei were of 800 μm each. The slices were transferred to a 100 μm cell strainer (Corning) and covered with parafilm (VWR), each cell strainer contained a slice of AVPV and one of ARC. The cell strainers containing the organotypic slices were initially placed in the recovery chamber for 30 minutes, and were then treated for six hours in either vehicle or 10nM 17β-estradiol.

At the end of the treatment, each slice, one at the time, was placed on ice cold artificial cerebrospinal fluid and the AVPV or the ARC was dissected using forceps and magnifying glasses. The brain nuclei were placed in previously labelled 2mL eppendorfs, snap frozen in liquid nitrogen and stored at -80˚C until needed.

2.2.2 Cell Culture

2.2.2.1 Maintenance of cells

Cells were cultured in a humidified atmosphere at 37˚C and 5% (v/v) CO_2 as a monolayer in 175 cm^2 tissue culture flasks. Cells were maintained in DMEM supplemented with 1% (v/v) penicillin/streptomycin and 10% (v/v) fetal bovine serum (FBS). Cells cultures were divided twice a week, in short, the medium was removed and the cells were washed with 15 mL of warm PBS 1X, the cells were then detached from the flask using 2 mL of pre-warmed trypsin, cells were incubated at 37˚C for 2 minutes. To further aid the detachment of cells, flasks were tapped gently until most of the cells dislodge from the flask. The cells were re-suspended in 10 mL of pre-warmed DMEM (supplemented with 10% (v/v) FBS and 1% (v/v) penicillin/streptomycin), which acts to neutralise the trypsin. The cell suspension was transferred to a 50 mL sterile falcon (VWR) and centrifuged at 600 rpm in a bench top centrifuge for 5 minutes. The supernatant was removed and the cell pellet was gently re-suspended in fresh, warm DMEM; and the cells were cultured in fresh DMEM at a suitable dilution.

2.2.2.2 Cryopreservation of cells

80%-90% confluent cultures were trypsinised and pelleted as described previously, the cells were then re-suspended in 6 mL of pre-warmed DMEM supplemented with 10% (v/v) FBS and containing 10% (v/v) DMSO. The cell suspension was aliquoted into cryo-vials, placed on a cryogenic freezing container for 24 hours and were then transferred into a liquid nitrogen tank for long-term storage.

Recovery of cells stored in liquid nitrogen was done by thawing cells at room temperature, once the cell suspension reached a sluggish texture they were then transferred into a 25 cm^2 tissue culture flask containing 5 mL of pre-warmed DMEM supplemented with 10% (v/v) FBS and 1% (v/v) penicillin/streptomycin. The cells were then allowed to attach to the flask, for about 6 to 8 hours, the DMEM was removed so to eliminate the DMSO and any dead cells, the cells were washed with PBS 1X and fresh, pre-warmed growth medium.

2.2.3 Transient Transfection

Temporary introduction of genomic DNA into cells was done through transient transfection. Several methods were tested in order to determine the best and most efficient transfection method.

2.2.3.1 Transfection in 6-well plate using the Lipofectamine 2000 protocol

Following ThermoFisher's protocol lipofectamine 2000, cells were seeded at a density so that a confluency of 70-90% was achieved at the time of transfection (the following day), by diluting the necessary number of cells in DMEM supplemented with 1% (v/v) penicillin/streptomycin and 10% (v/v) FBS. Briefly, two master mixes were prepared, one containing all common DNA plasmids (4 µL of DNA/ well) and half the amount of total Opti-MEM required for the experiment, and the other containing 10 µl of lipofectamine per well as well as the other half of the total volume of lipofectamine. The two master mixes were then incubated at room temperature for 5 minutes, after this incubation period the two solutions were gently and thoroughly mixed together and then incubated at room temperature for 30 minutes. The appropriate volume (500 µL) of the final DNA-Opti-MEM solution was to the cells, each was done in triplicate, and the volume was then made up to a final volume of 3 mL with Opti-MEM. Cells were then incubated at 37˚C and 5% (v/v) CO_2 for 48 hours, during the incubation the growth medium was changed twice once at 6 hours post transfection when the Opti-MEM-DNA-Lipofectamine solution was gently removed and replaced with pre-warmed DMEM supplemented with 1% (v/v) penicillin/streptomycin and 10% (v/v) FBS, and at 24 hours DMEM was replaced with fresh and warm DMEM.

2.2.3.2 Transfection in 96-well plate using the Lipofectamine 2000 protocol

The protocol performed was very similar to the above described with the only changes being the amount of DNA used (0.32 µg) as well as the volume of lipofectamine and Opti-MEM used, 0.48 µL/well and 83.2 µL/well respectively. Each well had a total volume of 170µL which was made up with pre-warmed Opti-MEM.

2.2.3.3 Transfection in 96-well plate using the Cell Line Nucleofector Kit V protocol

Following Lonza's nucleofection protocol, cells were seeded in 175cm^2 tissue culture flask at a density so that a confluency of 70-90% was achieved the following day. Cultures were trypsinised and pelleted as described previously, trypan blue and the LUNA-II Automated Cell Counter were used to calculate the number of cells in e ach flask. A volume of cell suspension

containing the required number of cells (a million cells were used per nucleofection reaction) was added to a 15 mL falcon containing 5 mL of pre-warmed DMEM supplemented with 1% (v/v) penicillin/streptomycin and 10% (v/v) FBS. The cells were centrifuged at 1600 rpm and RT for 5 minutes, the supernatant was subsequently removed and the cells were pelleted in 100µL of nucleofection buffer. The cell suspension was placed onto a previously labelled 2 mL tube, here the required amount of DNA (3 µg of DNA) was added to the cells and mixed thoroughly by pipetting up and down. The cell suspension was then transferred into a sterile nucleofection cuvette using a fine plastic Pasteur pipette, the cuvette was subsequently place onto the Lonza nucleofection machine, and the Mouse Hypothalamus 0003 programme was used. After the programme finished, the cuvette was removed from the machine and 500 µL of pre-warmed DMEM supplemented with 1% (v/v) penicillin/streptomycin and 10% (v/v) fetal bovine serum (FBS). The cells were either added to 6-well plates containing 3 mL of pre-warmed DMEM or the cell suspension was divided into a 96-well plate. The latter was achieved by transferring the nucleofected cells into a 50 mL falcon containing 15 mL of pre-warmed DMEM and mixing it well, 100µL of cells were added to each of the well in a 96-well plate. The cells were allowed to attach and after 4 to 6 and 24 hours post transfection the growth medium was changed and replaced with fresh, pre-warmed DMEM supplemented with 1% (v/v) penicillin/streptomycin and 10% (v/v) fetal bovine serum (FBS).

2.2.3.4 Reporter assays for 96-well plate transfection

The cells were assayed using the Secrete-Pair Dual Luminescence Assay Kit (GeneCopoeia), this assay relies on cells being transfected with plasmids that contain in their sequence *Gausia* Luciferase (GLuc) and Secreted Alkaline Phosphatase (SEAP), reporter proteins situated downstream of the promoter of interest. These reporter proteins are secreted into the medium upon and during promoter activation, due to the nature of the assay, it is possible to assay the same sample multiple times and exposing them to different conditions. Briefly, 24 hours after transient transfection of cells 50µL of culture medium was removed from each well, using a multipipette, and transferred to a 96-well PCR plate (ThermoFisher Scientific). 10µL of each these were placed into a white 96-well MICROLITE plate (Dynex), while another 10 µL of each of the medium samples were transferred to a different 96-well PCR plate, these last samples were incubated at 65˚C for a period of 10 minutes, and where subsequently transferred to the same white 96-well MICROLITE plate. At the same time, two different buffers were prepared: GL-S and AP, both were incubated at room temperature and protected from light however the incubation time differed, the first buffer was incubated for 25 minutes

while the later was incubated for only 10 minutes. Subsequently, 100 µL of AP buffer was added to the culture media that had previously been incubated at 65˚C, while 100µL of GL-S buffer were added to the other samples. The samples were incubated at room temperature for 5 minutes and the SpectraMax i3 (Molecular Devices) was used to measure luminescence.

2.2.4 Bacteria

2.2.4.1 Storage of bacteria

The one Shot TOP10 competent *Escherichia coli* were used to propagate all plasmids. The plasmids used throughout this thesis carry either the kanamycin (Kan^r) or the ampicillin (Amp^r) resistant genes. Transformed bacteria were grown in Luria Broth (LB) or in LB agar plates containing either 100 µg/mL ampicillin or 50 µg/mL kanamycin, according to the resistant gene in each plasmid. Bacteria transformants were then stored in LB containing 50% (v/v) glycerol at -80˚C.

2.2.4.2 Transformation of competent bacteria by heat shock

Here 50 µL of competent bacteria were used for the transformation of pre-chilled plasmids. Competent cells were initially thawed on dry ice and subsequently on wet ice, the required amount of cells (50 µL) were transferred to a 2 mL tube to which 1µL of 2-mercaptoethanol was added, the solution was then incubated on ice for 10 minutes, the solution was gently mixed every 2 minutes. 0.1-50 ng of DNA was added and incubated on ice for 30 minutes, the solution was again gently mixed every 2 minutes. The samples were then placed at 42˚C for 30 seconds, followed by a further incubation on ice for 2 minutes. 250 µL of pre-warmed LB was added to the competent cells and incubated at 37˚C with rotation for 1 hour. Finally, 200 µL of solution was streaked onto a LB agar plate containing either 100 µg/mL ampicillin or 50 µg/mL kanamycin, the plates were inverted and placed overnight in an incubator at 37˚C.

2.2.5 DNA manipulation and cloning

2.2.5.1 Preparation of plasmid DNA

Based on the quantity of plasmid required, the DNA was either prepared by either small or large-scale methods.

2.2.5.2 Small scale preparation of plasmids (Miniprep)

The QIAGEN miniprep kit was used to prepare up to 20 µg of high-copy plasmid DNA. A single bacterial colony was used to inoculate 5 mL of LB containing either 50 µg/mL kanamycin or 100 µg/mL ampicillin and incubated overnight at 37˚C with vigorous shaking. The following day the bacterial cultures were harvested through centrifugation at 8000 rpm for 5 minutes at 4˚C. The DNA plasmid was subsequently prepared by following the manufacturer's instructions. The protocol consists of three basic steps, preparation and clearing of bacterial lysate, absorption of DNA onto the QIAprep membrane, and washing and elution of plasmid DNA. In short, the protocol involved lysing bacteria under alkaline solutions, the lysate was subsequently neutralised and altered to high-salt binding conditions. The solution was passed through a silica-membrane which allowed for absorption of plasmid DNA in a high salt buffer and elution is low salt buffer. The membrane and salts used ensure that ensure that only plasmid DNA is bound however a few washes were performed to ensure that endonucleases and salts are removed from the membrane. Plasmid DNA was then eluted with 50 µL of water, the eluted, purified DNA was then ready to be used.

2.2.5.3 Large scale preparation of plasmids (Maxiprep)

The QIAGEN maxiprep kit was used to prepare up to 1 mg of high-copy plasmid DNA. Plasmid DNA prepared through this method were used for transient transfection and *in vitro* transcription. A single bacterial colony was used to inoculate 5mL of LB containing either 50 µg/mL kanamycin or 100 µg/mL ampicillin and incubated during the day for about 8 hours at 37˚C with vigorous shaking. The 5 mL culture grown during the day was then added to a 2 L baffled culture flask containing 500 mL LB supplemented with 50 µg/mL kanamycin or 100 µg/mL ampicillin, the culture was harvested the following day by centrifuging it at 6000 x g for 15 minutes at 4˚C. The bacteria pellet was processed according to the manufacturer's instructions. As the previous one, this protocol is also based on a modified alkaline lysis method, and uses NaOH-SDS with RNaseA to harvest plasmid DNA inside bacterial cells. The high salt solution caused SDS to precipitate with denatured proteins, cellular debris, and chromosomal DNA trapped in high-salt complexes. The plasmid DNA which is smaller and

covalently closed is re-natured and remained in the solution. Bacterial lysates were then cleared by centrifugation at high-speed, with the plasmid DNA remaining in the supernatant. The supernatant was subsequently transferred into a pre-equilibrated anion-exchange column that works through gravity under low salt and pH conditions. A wash buffer was then used to remove RNA, proteins and other low molecular weight impurities. Plasmid DNA was eluted from the column using a high-salt buffer and then concentrated and desalted by isopropanol precipitation and subsequent 70% ethanol wash. Purified DNA was air-dried and re-suspended in 10nM Tris-HCL pH 8.5. DNA purity and concentration were assessed through measurement of the OD_{260} and OD_{280} using a spectrophotometer.

2.2.6 RNA Manipulation

2.2.6.1 Isolation of RNA from cells and tissues using the TRIzol® method

Throughout this protocol RNase-free plastic ware and RNase-free water were used to prepare solutions. TRIzol® reagent was used to extract total RNA from both tissues and cells, samples were processed according to the manufacturer's protocol. TRIzol® reagent is a monophasic solution of phenol and guanidine isothiocyanate that disrupts the cells and tissues during sample homogenisation while maintaining the integrity of the RNA due to the highly effective inhibition of RNase activity. Tissues and cells were placed in 2 mL eppendorfs containing TRIzol® reagent and stainless-steel beads (QIAGEN, 69989), samples were homogenised for one minute at a frequency of 30000 using the TissueLyser II (QIAGEN). Following homogenisation, 200 µL of chloroform was added to the samples, which were then centrifuged at 10,000 rpm for 10 minutes at 4˚C, centrifugation separates the solution into an aqueous phase and an organic phase. The RNA remains exclusively on the aqueous, clear phase, which was then transferred to a 1.5 mL tube. RNA was precipitated from the aqueous phase through the addition of 500 µL isopropanol (stored at -20˚C), samples were vortexed to mix. Samples were then placed at -20˚C for 10 minutes, and the centrifuged at 14000 rpm for 10 minutes at 4˚C and the supernatant discarded. The RNA precipitates forming a pellet on the bottom and side of the tube, the pellet was washed with 500 µL of 70% ethanol (stored at -20˚C) and centrifuged at 14000 rpm for 5 minutes at 4˚C. The ethanol was discarded and the purified RNA pellet was air-dried and re-dissolved in RNase-free water. The NanoDrop Lite Spectrophotometer was used to measure RNA concentration as well as purity through the 260/280 ratio, OD260/ OD280 ratio of around 2 indicates good quality RNA. Finally, the samples were stored at -80˚C.

2.2.6.2 Isolation of RNA from cells and tissues using the PureLink® RNA Mini Kit

Throughout this protocol RNase-free plastic ware and RNase-free water were used. The PureLink® RNA Mini Kit is a simple and rapid column-based method for isolating and purifying up to 1 mg of total RNA from cells and tissues. This method has the advantage of using non-hazardous chemicals by combining non-toxic guanidine-isothiocyanate lysis with silica-membrane purification. Samples were processed according to manufacturer's instructions. Briefly, tissues and/or cells were placed in 2 mL eppendorfs containing lysis buffer supplemented with β-Mercaptoethanol and stainless-steel beads, samples were homogenised for one minute at a frequency of 30000 using a TissueLyser. Following homogenisation, samples were centrifuged at 14000 for 5 minutes at 4˚C. The supernatant was removed, discarding any cell/tissue debris, and placed on a 1.5 mL tube with 600 µL of 70% ethanol, to precipitate the RNA, the solution was mixed well by vortexing. The solution was then added to the spin cartridges with collection and centrifuged for 15 seconds, the supernatant was discarded. The RNA now retained in the spin column was washed and purified once with wash buffer 1 (700 µL) and twice with wash buffer 2 (500 µL/wash). Every wash required the columns to be centrifuged at 14000 rpm for 15 seconds at RT, the supernatant was subsequently removed. Finally the columns were dried by centrifugation (14000 rpm for 2 minutes at RT) and columns were placed on a 1.5 mL tube, RNA was eluted with RNase-free water (10-50 µL, volume can be adjusted according to the size of the tissue/number of cells). As before, the RNA concentration and quality was determined by measuring the OD260 and OD280 on a spectrophotometer, a value of 2 for the OD260/OD280 ratio indicates good quality RNA. Finally, the samples were stored at -80˚C.

2.2.7 cDNA synthesis

2.2.7.1 DNase treatment

Total RNA preparations may contain small amounts of genomic DNA that need to be removed to prevent it from being amplified along with the target mRNA. 1 µg of total RNA was digested with 1µL of ezDNase (Thermo Fisher Scientific) and 1x ezDNase buffer in a total volume of 10µL, the reaction was incubated at 37˚C for 2 minutes and then placed on ice. The whole of the reaction is then used for first strand cDNA synthesis.

2.2.7.2 First strand DNA synthesis

DNase-treated RNA (10µL) was reverse transcribed, following the manufacturer's instructions, using the SuperScript IV VILO Master Mix synthesis system for Real Time QPCR (RT-QPCR) (Thermo Fisher Scientific). In brief, it consists of a three-step protocol, the first step involves incubating the reaction at 25˚C for 10 minutes to allow for primers to anneal to the RNA strand, in the second the temperature was increased to 50˚C, to enable reverse transcriptase to work, and the solution was incubated for a further 10 minutes. In the last step, the reaction was incubated at 85˚C for 5 minutes to inactive the enzyme. Finally, cDNA was diluted 1:5 with LC-MS grade water and stored at -20˚C.

2.2.8 Gene expression analysis using Real-Time PCR

2.2.8.1 Amplification of target cDNA (principal)

Following cDNA synthesis target cDNA was amplified using specific primer pairs by RT-QPCR, this was done using the CFX384 Real Time System C1000 Thermal cycler (BioRad). Briefly, this technique enables real time quantification of DNA present in each sample through the binding of fluorescent DNA-binding molecules, in this case sensiFAST SYBR Hi-ROX, to double stranded DNA (dsDNA). In its free form, SYBR green I, has undetectable fluorescence but emits fluorescence when bound to dsDNA. This technique allows for DNA quantification by detecting and measuring accumulation of amplified products as the PCR reaction progresses. Each gene has a pre-defined fluorescent signal threshold, set within the linear phase of the reaction, which is constant between multiple samples. During RT-QPCR, cycle threshold (Ct) value is determined for each sample, which corresponds to the number of PCR cycles required to reach the pre-defined fluorescent signal. The fluorescence signal is directly proportional to the amount of DNA, the greater the target cDNA present the lower the Ct value. Gene expression is then calculated relative to that of a 'housekeeper' gene, which controls, mainly, for differences in cDNA amplification efficiency. Fold changes can then be

calculated from the relative expression of control and treated samples. The software used can detect changes, from baseline, in intensity (ΔRn) at each time point throughout the reaction. Based on these readings, the software constructs amplification plots of ΔRn vs cycle number. The threshold value (Ct value) is calculated as the point at which the fluorescence exceeds the pre-determined threshold limit.

2.2.8.2 Amplification of target cDNA

Genes of interest were amplified using the sensiFAST SYBR Hi-ROX master mix, the reactions were set-up in a 384-well plate. Each reaction was run in triplicates and contained 5 µL of sensiFAST SYBR Hi-ROX (2x), 0.625µL of 10 µM forward primer, 0.625µL of 10 µM reverse primer, 1.25µL of cDNA template, and finally 2.5µL of LC-MS grade water. The samples were then centrifuged at 10000 rpm at RT for 1 minutes to mix all the components, it was then placed on the CFX384 Real Time System C1000 Thermal cycler (Bio Rad) and the following real-time PCR conditions were applied. There was an initial polymerase activation step of 2 minutes at 95˚C, then a set of 40 cycles were applied which consisted of a 5 second denaturation step at 95˚C, followed by annealing of primers for 10 seconds at 60˚C, a final extension step was performed (20 seconds at 72˚C).

2.2.8.3 RT-PCR primer design

Primers were designed within a short sequence of cDNA to give a product of approximately 100 base pairs. Sequences were obtained from relevant papers and were compared and matched to the mouse genome using the Ensembl mouse genome database (https://www.ensembl.org/Mus_musculus/Info/Index). The sequences were then applied to OligoArchitect™ Online (Sigma-Aldrich). On arrival primers were dissolved in LC-MS grade water to a final concentration of 100 µmol/µL, this was then further diluted to a working concentration of 10µmol/µL. For primer sequences see Appendix 1.

2.2.8.4 Relative Quantification

The comparative Ct method was used to quantify gene expression, this method uses arithmetic manipulations to calculate the relative expression of a gene of interest (ΔCt) compared to that of a known 'housekeeper' gene (*Cyclophilin*) and of control samples (untreated). The method relies on the idea that the difference in the threshold cycles (ΔCt) between the gene of interest and the internal control gene, ΔCt = Ct (gene of interest) – Ct (*Cyclophilin*), is proportional to the level of expression of the gene of interest. ΔΔCt was then calculated by subtracting the ΔCt of each sample from a single, randomly chosen cDNA ΔCt (calibrator). The following equation: $2^{-\Delta\Delta Ct}$ where ΔΔCt = ΔCt (sample) - ΔCt (calibrator) gives the amount of gene of interest normalised against and relative to the calibrator. Relative expression and standard error of the mean (SEM) were then calculate using the mean ΔΔCt values of each sample of a treated group relative to the mean ΔΔCt values for samples of the control group.

2.2.9 Histological Analysis and Microscopy

2.2.9.1 Protein Labelling in Mouse Tissue by Immunofluorescense

2.2.9.1.1 Tissue Processing

Animals were terminally anesthetised intraperitoneally (IP) with sodium pentobarbital (50-90 mg/Kg) (Nembutal). Once the animal reached a surgical plane of anaesthesia, determined by the toe pinch-reflex, an incision beneath the rib cage and through the abdominal cavity was made using blunt scissors, vertical cuts through the ribs and up to the collarbone were done on either side, creating a flap. The connective tissue linking the rib cage to the body was subsequently, and carefully, cut in order to expose the pleural cavity by lifting the sternum which was clamped with a hemostat and placed over the animal's head in order to obtain a better view of the heart. The right atrium was snipped and a needle attached to a syringe was inserted into the left ventricle, reaching the ascending aorta. The animal was then flushed at a slow and steady with 15mL of Heparin Sodium (100 I.U./mL) dissolved in PBS 1X, which is an anticoagulant and was used to prevent blood clot formation. The animal was subsequently perfused with 4% Formaldehyde Solution in PBS 1X (PFA 4%).

To access the brain first detach the animal's head from the rest of the body using a pair of scissors, in order to expose the skull all the skin and connective tissue around the head was removed. Sharp scissors were inserted into the foramen magnum of the skull and the skull and bones all around the brain until the eye socket were cut, this was repeated for the opposite side. A final cut through the midline between the eyes was performed, thus allowing detachment of the skull and brain from the rest of the head. A cut through the midline of the skull was performed which enabled removal of the frontal bone of the skull and partial exposure of the brain. Blunt forceps were used to scoop out the brain that was immediately placed on a 7mL bijou container with 5mL of PFA 4%, to be further fixed overnight at 4°C. After overnight fixation, the brain was washed three times in PBS 1X for 1 hour at room temperature with gentle rotation. Neuronal tissue was cryopreserved by incubating the brain in 5mL of 30% sucrose in PBS 1X at 4°C until the brain sunk to the bottom of the 7mL bijou container.

The SHANDON AS200 Base Sledge Microtome (SHANDON) was used to slice the neuronal tissue, the brain was allowed to reach a temperature of -15°C before slicing started. Regions of interest were sliced in their entirety at a thickness of 40µm, and the slices were placed straight away on Polysine coated adhesion slides (VWR) with the help of a fine paint brush. The samples were left to air dry at room temperature for 1 hour following slicing and were then stored at -20°C until needed.

2.2.9.1.2 Immunofluorescence Protocol

Brain samples were removed from the -20°C freezer and were allowed to defrost and dry at room temperature for 1 hour before starting the staining process, that was carried out at all times in a pre-prepared humidified chamber, to prevent sample dehydration during the protocol. Further to the humidified chamber, pieces of parafilm were also pre-prepare and cut to the size of the Polysine coated adhesion slides, these were place on top of the slides throughout all the protocol in order to further prevent dehydration of samples. Samples were initially incubated with 250 µL of Immunosatining permeabilisation buffer (0.5% Triton X-100 in PBS 1X) for 30 minutes at 4°C. Subsequently, 250µL of Immunostaining blocking buffer (0.3% Triton X-100 in PBS 1X with 10% Normal Donkey Serum) were used to block the samples at room temperature for 1 hour. The next step involved incubating the samples with 250µL of primary antibody in Immunostaining blocking buffer (0.3% Triton X-100 in PBS 1X with 10% Normal Donkey Serum) overnight at 4°C. The optimal antibody concentration was determined during optimisation protocols, when several different concentrations were tested and analysed in order to determine which one yielded the optimal staining pattern. In this project, a concentration of 1:200 in Immunostaining blocking buffer was used for the Anti-DAX1, clone 2F4 antibody (Merck, MABD398), while the GFP Polyclonal Antibody, Alexa Fluor 488 (ThermoFisher Scientific, A-21311) was diluted in Immunostaining blocking buffer at a concentration 1:250. A negative control was also added, where blocking buffer was used instead of primary antibody. The samples underwent a washing step, which consisted of three washes with 250 µL of Immunostaining washing buffer (0.3% Triton X-100 in PBS 1X) each lasting at least 1 hour. Samples were then incubated with secondary antibody against the primary antibody in Immunostaining blocking buffer (1:250) for at least 2 hours at room temperature. The next step in the protocol was a set of another three washes with 250µL of Immunostaining washing buffer (0.3% Triton X-100 in PBS 1X) each lasting at least 1 hour. Samples were then stained with DAPI (ThermoFisher Scientific, D1306) at a concentration of 1:1000 diluted in PBS 1X for minutes at RT. The final wash was performed using 250µL of PBS 1X for 10 minutes at RT. The slides were then dried and mounted with VECTASHIELD Mounting Medium for Fluorescence (Vector Laboratories, H-1000), a rectangular cover glass (22x50mm, VWR) was applied to each slide that was sealed with transparent nail varnish and allowed to air dry before being stored at 4°C until imaging.

2.2.9.1.3 Imaging and Analysis of Immunofluorescence Data

The Zeiss LSM-780 Inverted Confocal Microscope (Zeiss) was used to image and take pictures all the immunofluorescence samples. The data was then analysed using ImageJ software.

2.2.9.2 Haematoxylin & Eosin (H&E) Staining

2.2.9.2.1 Tissue Preparation, Embedding of Tissues and Paraffin Sectioning

Animals were terminally anesthetised intraperitoneally with sodium pentobarbital (50-90mg/kg) (Nembutal). Once the animal reached the surgical plane of anaesthesia the ovaries were harvested and placed in 5% neutral buffered formalin solution overnight at room temperature. Tissues were then dehydrated in 75% ethanol for 48 hours, followed by another 2 hours of dehydration using in this case 100% ethanol. Samples were subsequently 'cleared' in histoclear (VWR) reagent for 4 hours, which is essential for the removal of lipids in the tissue. Samples were then placed in melted paraffin for 2 hours prior to embedding. The samples were encase in moulds filled with hot paraffin wax, which was then allowed to solidify. Prior to sectioning, embedded blocks were cooled on ice for 10 minutes. The Leica microtome was used to cut 5µm thick sections, which were placed in a clean 40°C water bath using forceps, they were subsequently recovered onto polysine coated adhesion slides and incubated overnight in a drying oven at 37°C. Once dried samples were used for H&E staining.

2.2.9.2.2 H&E Staining Protocol

Haematoxylin and Eosin staining was performed according to standard protocols. In brief, samples were de-waxed in histoclear and rehydrated through a serious of ethanol washes with descending concentrations of ethanol (prepared with distilled water) with the final wash being distilled water only. Samples were immersed in each solution, Haematoxylin and Eosin, for 5 minutes at RT, with a wash with distilled water before the latter was applied. Samples were then dehydrated using solutions with increasing concentrations of ethanol to 100% and placed in histoclear. Finally, slides were cover slip mounted using nail varnish.

2.2.10 Hormone Measurement

2.2.10.1 Plasma Collection

Given the substantial volume of blood required for the hormone measurement experiments decapitation from live using sharp operating scissors (World Precision Instruments, 501231-G) was deemed the most appropriate method to humanely end the animals. Blood was collected into EDTA-coated microvette (Sarstedt, NC9990563), placed on ice. Blood was centrifuged (Eppendorf, 5417R) at 4000 rpm, for 15 minutes at 4˚C in order to separate the plasma from white and red blood cells. After centrifugation plasma was removed and placed into a labelled 1.5 mL tube (Eppendorf), the samples were stored at -80˚C.

2.2.10.2 Mouse Follicle Stimulating Hormone ELISA Kit

The Mouse Follicle Stimulating Hormone ELISA Kit (MyBioSource, MBS727159) is a highly specific and sensitive assay used for the detection and measurement of FSH in mouse's plasma samples. This kit is a ready-to-use microwell, strip plate enzyme-linked immunosorbent ass assay (ELISA) which relays on FSH antibody and FSH antigen interactions, together with HRP colorimetric detection system to quantify FSH levels in samples. The assay was performed according to the manufacturer's instructions. In summary, plasma samples were prepared as detailed above. An initially test run experiment was performed, as recommended, using neat samples (undiluted), samples diluted 1:2 and 1:4 (in PBS 1X) in order to assess optimal sample concentration. The results obtained for the neat samples fell within the standard curve and therefore all FSH measurements were performed using undiluted plasma. Samples and reagents were equilibrated to room temperature prior to the start of the protocol. 50 µL of each standard, blank control (PBS 1X) and samples were added to the appropriate wells (the plate layout was previously determined). 5µL of Balance Solution was added to the wells containing plasma samples only while 100µL of Conjugate was added to all the wells expect the blank control well. The plate was mixed well for 1 minute at RT in an orbital micro-plate shaker (VWR). The plate was then incubated at 37˚C for 1 hour. The plate was manually washed, by disposing of the incubation mixture into an appropriate waste container and adding 350µL of washing solution into each well, which was then disposed. Repeat this procedure so that the wells are washed for a total of five times. Subsequently, 50µL of Substrate A and 50µL of Substrate B were added to all the wells (standard, blank control and sample) and the plate was incubated at 37˚C for 15 minutes, protected from light. After incubation 50µL of Stop Solution was added to all the wells and

optical density (O.D.) was measured, immediately, at 450 nm using a microplate reader (Molecular Devices, SpectraMax i3).

2.2.10.3 17-β Estradiol ELISA Kit

Estradiol (17-β Estradiol) is the most predominant form of the sex hormone, estrogen, in female animals. Plasma estradiol levels are a reflection of ovarian estrogen production. The 17-β Estradiol competitive ELISA Kit (Abcam, ab108667) was used to accurately quantify 17-β Estradiol in plasma samples. The assay was performed according to the manufacturer's instructions. Briefly, all reagents, samples and controls were prepared and equilibrated to room temperature prior to use. 25µL of standards, control and undiluted plasma samples were added to the pre-coated, with anti-Estradiol IgG, 96-well plate (following pre-determined plate layout). 200µL of 17-β Estradiol-HRP Conjugate was added to each of the wells, including the blank control. Estradiol in the sample competes with the added Estradiol-HRP for antibody binding. The plate was then protected from light with the foil supplied in the kit and incubated for 2 hours at 37˚C. Once the incubation was finished, the contents were aspirated and three washes were performed using the pre-prepared washing solution (300 µL). 100µL of TMB Substrate Solution was then added to all the wells and the plate was incubated for exactly 30 minutes at room temperature protected from light. The reaction was terminated by the addition of Stop solution (100µL) to all the wells, which prevents further colour development and produces a colour change from blue to yellow. The plate was shaken using an orbital micro-plate shaker and absorbance of the samples was measured at 450 nm. The intensity of the signal is inversely proportional to the amount of 17-β Estradiol in the sample. The cross reaction of the antibody calculated at 50% is: 100% estradiol, 2.0% estrone and 0.39% estriol.

2.2.10.4 Progesterone ELISA Kit

Progesterone is the major female sex hormone, it is responsible for regulating several reproductive-related activities such as cell cycle progression. Progesterone is largely secreted by the corpus luteum and the levels of this hormone can be detected in the plasma by enzyme immunoassays. The competitive Progesterone ELISA Kit by Enzo Life Sciences (ADI-900-011) was chosen to quantify progesterone levels in plasma samples. The assay was performed according to the manufacturer's instructions. As recommended an initial pre-run experiment was carried out in which a total of six different sample concentrations were tested: 1:10, 1:30, 1:90, 1:270, 1:810 and 1:2430. The optimal sample dilution was found to

be 1:180. All the reagents and samples were prepared prior to the experiment and were allowed to equilibrate to RT. The standards, controls and samples were added to the plate as detailed in the Assay Layout Sheet, and all the solutions were added as per instructed in the protocol. Once all the solutions were added to the respective wells, the plate was gently mixed and incubated at room temperature on an orbital microplate shaker for 2 hours at 500 rpm. At the end of the incubation, the contents of the wells were emptied and the wells were washed by adding 400 µL of Wash Solution to every well, a total of three washes were performed. After the final wash, the contents of the wells were aspirated and the plate was firm tapped on a lint free paper towel to remove any remaining washing buffer. 200 µL of pNpp Substrate solution was added to every well and the plate was incubated at RT for 45 minutes without shaking. 50 µL of Stop Solution was added to every well, this stopped the reaction and the absorbance was immediately read, at 405 nm, using microplate reader.

2.2.10.5 Luteinising Hormone ELISA Assay

Luteinising Hormone (LH) is a hormone which is made up two subunits – alpha and beta. The first in 92 amino acids (aa) long, while the β-subunit is longer, 121 amino acids, and it is the latter subunit that is responsible for the hormone's biological activity. LH is produced by gonadotrophic cells in the anterior pituitary gland, an acute rise of LH during the estrous cycle, LH surge, triggers ovulation and development of the corpus luteum in females. A custom made LH ELISA assay, as described in Cimino (2016), was used to measure quantify Luteinising Hormone levels in blood samples. Briefly, 5 µL of blood were diluted in 195 µL of PBS-Tween 0.05%. A 96-well high-affinity binding microplate (Corning, 9018) was coated with 50 µL capture antibody (Bovine Anti-LH Beta Subunit Monoclonal Antibody, University of California, 518B7) at a final concentration of 1:1000 (in PBS 1X, 9 g of NaCl, 0.32 g of NaH_2PO_4 (anhydrous) and, 1.09 g of Na_2HPO_4 (anhydrous) in 1000 mL of distilled water) and incubated overnight at 4˚C. The following day, the solution in the wells was discarded and the wells were incubated with 200 µL of blocking buffer (5% (w/v) skim milk powder in 1 PBS-T (PBS 1X with 0.05% Tween 20) for 2 hours at RT. The standard curve was obtained by generating a twofold serial dilution of mLH (reference preparation, AFP-5306A, National Institute of Diabetes and Digestive and Kidney Diseases–National Hormone and Pituitary Program (NIDDK-NHPP)) in 0.2% (w/v) bovine serum albumin in PBS-T. Blood and LH standards were then incubated with 50 µL of detection antibody (Rabbit LH antiserum, polyclonal antibody, AFP240580Rb; NIDDK-NHPP) at a final dilution of 1:10000 for 1 hour and 30 minutes at room temperature. Each well containing bound substrate was incubated

with 50 µL of horseradish peroxidase-conjugated antibody (Goat Polyclonal Anti-Rabbit Antibody, Vector, PI1000) at a final concentration of 1:10000 for 1 hour and 30 minutes, 100 µL of o-phenylenediamine (Invitrogen, 002003) substrate, containing 0.1% H_2O_2, was added to each well and left at room temperature for 30 minutes. The reaction was stopped by the addition of 50 µL of 3M HCl to each well, and absorbance was measured at a wavelength of 490 nm using microplate reader.

2.2.10.6 Pulsatile Luteinising Hormone Measurement

Female mice were habituated with daily handling for three to four weeks in order to reduce stress levels during the experimental period, as this negatively impacts LH levels. Blood samples (5µL) were taken from the tail every 10 minutes for a period of 2 hours, between 12:00 and 15:00). The blood samples were placed on pre-labelled 0.2 mL tube strips (ThermoFisher Scientific, AB0849) each containing 195 µL of PBS-Tween 0.05% and frozen immediately. These samples were then used to perform the Luteinising Hormone ELISA Assay protocol as described above (2.2.11.5).

2.2.11 Pathway-Focused Array Profiling

The RT^2 Profiler™ PCR Arrays (QIAGEN) enable quick, reliable and effective analysis of pathway-focused gene expression levels. This is because these assays take advantage of a combination of real-time RT-PCR, which is a highly reliable and sensitive method for quantifying gene expression levels, and microarrays which enables identification and analysis of a panel of genes that relate to a specific disease, signal transduction or biological process. The vast range of arrays available enables quick and simple gene expression analysis of more than 170 different biological pathways.

2.2.11.1 Tissue Collection

Mice were terminally anesthetised intraperitoneally with sodium pentobarbital (50-90 mg/Kg) (Nembutal). Once the animal reached a surgical plane of anaesthesia, determined by the toe pinch-reflex, the animal's head was removed using a pair of scissors, the skin was subsequently removed too in order to expose the skull, and any leftover connective tissue was removed. Sharp scissors were inserted into the foramen magnum of the skull and the skull and bones all around the brain until the eye socket were cut, this was repeated for the opposite side. A final cut through the midline of the eyes was performed, thus allowing detachment of the skull and brain from the rest of the head. A cut through the midline of the

skull was performed which enabled removal of the frontal bone of the skull and partial exposure of the brain. The brain was scooped out with a blunt pair of forceps, placed in a 7 mL bijou container and snap frozen in liquid nitrogen. The Arcuate Nucleus (ARC) and the Anteroventral Periventricular Nucleus (AVPV) were then manually extracted while the tissue was frozen and stored in 2 mL tubes with stainless-steel beads, samples were stored at -80˚C until needed.

2.2.11.2 RNA extraction, Quantification and Quality Control

High-quality RNA is essential for obtaining good real-time PCR results, the PureLink® RNA Mini Kit was used to extract up to 1 mg of RNA from samples collected previously. Samples were processed according to manufacturer's instructions. Briefly, tissues and/or cells were placed in 2 mL eppendorfs containing lysis buffer supplemented with β-Mercaptoethanol and stainless-steel beads, samples were homogenised for one minute at a frequency of 30000 using a TissueLyser. Following homogenisation, samples were centrifuged at 14000 rpm for 5 minutes at 4°C. The supernatant was removed, discarding any cell/tissue debris, and placed on a 1.5 mL tube with 600 µL of 70% ethanol, to precipitate the RNA, the solution was mixed well by vortexing. The solution was then added to the spin cartridges with collection and centrifuged for 15 seconds, the supernatant was discarded. The RNA now retained in the spin column was washed and purified once with wash buffer 1 (700 µL) and twice with wash buffer 2 (500 µL/wash). Every wash required the columns to be centrifuged at 14000 for 15 seconds at RT, the supernatant was subsequently removed. Finally the columns were dried by centrifugation (14000 rpm for 2 minutes at RT) and columns were placed on a 1.5 mL tube, RNA was eluted with RNase-free water (50 µL). RNA concentration and quality was determined using a spectrophotometer; regarding the RNA quality the A_{260}:A_{230} ratio should be greater than 1.7 while the A_{260}:A_{280} ratio should be between 1.8 and 2.0.

2.2.11.3 cDNA Synthesis and Amplification Using the RT^2 First Strand Kit

Following the manufacturer's instructions 1 µg of total RNA was reverse transcribed using the RT^2 First Strand Kit (QIAGEN, PAMM-056Y). Briefly, the reagents of the RT^2 First Strand Kit were thawed and centrifuged for 15 seconds. 10 µL of genomic DNA elimination mix was prepared for each DNA sample, this was added to the samples by pipetting up and down and by centrifugation, which was then incubated for 5 minutes at 42˚C and subsequently placed on ice for 1 minute. 10 µL per DNA sample of reverse-transcription mix was prepared and added to each tube containing 10 µL of genomic DNA elimination mix and DNA, this was

mixed up and down. The solution was incubated at 42˚C incubated for 15 minutes, the reaction was then immediately stopped by incubating for 5 minutes at 95˚C.

2.2.11.4 Real-Time PCR for RT^2 Profiler PCR Arrays

The amplified cDNA was then diluted with 91 µL of RNase-free water and used to prepare the PCR mix composed of 2x RT^2 SYBR Green Mastermix, cDNA synthesis reaction and RNase-free water (QIAGEN, 330529). 25 µL of the experimental mix was added to each well of the RT2 Profiler PCR Array plate according to the plate layout. The plate was tightly sealed with an optical adhesive film and was centrifuged at room temperature for 1 minute at 1000 g. Real-Time PCR was performed on the CFX384 Real Time System C1000 Thermal cycler (BioRad) and using the SYBR green detection filter with the following PCR cycling program: the first step was a single cycle incubation at 95˚C for 10 minutes (activation of HotStart *Taq Polymerase*), followed by a step of 40 cycles composed of incubation at 95˚C for 15 seconds and 60˚C incubation for 1 minute (fluorescent data collection).

2.2.11.5 Analysis of Real-time PCR Array Data

Each array contained 5 different housekeeping genes (*LDHA*. *RPL13A*, *ACTB*, *RPLP1* and *HPRT*) and a panel of proprietary controls to monitor genomic DNA contamination (GDC) as well as the first strand synthesis (RTC) and real-time PCR efficiency (PPC). The use of these controls enabled normalisation of the data to the housekeeping gene (HKG). Once the PCR was completed, C_T values were exported to an Excel file so to create a table with all the C_T values, this table was then uploaded onto the data analysis web portal (http://www.qiagen.com/geneglobe). Samples were assigned to either control or test groups and the data was analysed. The Data analysis web portal calculates fold change using the $\Delta\Delta C_T$ method, in which ΔC_T is calculated for each gene of interest (GOI) and an average of the housekeeping genes (HKG) (C_T value for the GOI – C_T value for the HKG). $\Delta\Delta C_T$ was then calculated at such (ΔC_T (Test Group) - ΔC_T (Control Group)), fold change was then calculated using $2^{(-\Delta\Delta CT)}$. Based on these values the data analysis web portal was able to produce scatter plots, volcano plots, heat maps and clustergram for each data set.

2.2.11.6 Effect of Estrogen Treatment on Pathway-Focused Array Profiling of the Arcuate and Anteroventral Periventricular Nuclei of the Hypothalamus

The effect of varying concentrations of estrogen in the expression of genes involved Estrogen Receptor Signalling were investigated using the RT^2 Profiler™ PCR Array Mouse Breast Cancer (QIAGEN, PAMM-131Z), RT^2 Profiler™ PCR Array Mouse Female Infertility (QIAGEN, PAMM-164Z) and RT^2 Profiler™ PCR Array Mouse Estrogen Receptor Signalling (QIAGEN, PAMM-005Z). In this experiment age matched (6-8 weeks old) female mice were ovariectomised as described in 2.2.1.3.2 and implanted with either a silastic capsule containing 17β-estradiol (Merk) in sesame oil (0.1 mg/mL) or with silastic capsule containing only sesame oil only (vehicle) (Sigma-Aldrich) (2.2.1.3.1). As detailed in 2.2.1.3.3, following recovery, mice were injected at 09:00 with either vehicle (sesame oil) or estradiol benzoate (0.05 mg/kg), thus creating three groups: (i) control – mice that were implanted with silastic capsule containing sesame oil, and injected with sesame oil (vehicle), (ii) low estrogen – mice implanted with silastic capsule containing 17β-estradiol in sesame oil and injected with sesame oil; and (iii) high estrogen - mice implanted with silastic capsule containing 17β-estradiol in sesame oil and injected with estradiol benzoate. Brain tissue was collected as outlined in 2.2.12.1 and the samples underwent the steps described from 2.2.12.2 to 2.2.12.5. A total of 24 animals (8 animals per group and 3 groups) were used for this study as each sample was made up of two pooled samples of AVPV or ARC, respectively.

2.2.11.7 Pathway-Focused Array Profiling of the Arcuate and Anteroventral Periventricular Nuclei of the Hypothalamus

Considering that the Arcuate Nucleus (ARC) and the Anteroventral Periventricular Nucleus (AVPV) are key nuclei in the regulation of female fertility, the comparative analysis of gene expression profiles between them could provide crucial insight into how this essential function is regulated and maintained. For this purpose, the RT^2 Profiler™ PCR Array Mouse Nuclear Receptors & Coregulators (QIAGEN, PAMM-056Y) was used. In this study 96 genes were profiled on 8 samples, 4 AVPV and 4 ARC samples, a total of 16 animals were used for this study, as each sample was made up of two pooled samples of AVPV or ARC, respectively. The protocol described above was followed (2.2.12.1 to 2.2.12.5).

2.2.12 Statistical Analysis

All values are expressed as mean +/- standard error of the mean (SEM) for biological replicates. GraphPad Prism was used to identify outliers and calculate statistical significance. Data were analysed using two-tailed student's t-test. P-values representing statistical significance between groups are indicated.

Results: Chapter 1 - Exploring Estrogen Signalling in the Hypothalamus

3 Exploring Estrogen Signalling in the Hypothalamus

3.1 Introduction

Estrogen is responsible for regulating gonadotropin releasing hormone and gonadotropin secretion via feedback loops that act within the hypothalamic-pituitary-gonadal (HPG) axis. Estrogen plays a pivotal role in reproductive mechanisms such as sexual differentiation and sexual behaviour (Morris, Jordan & Breedlove, 2004). There are three forms of estrogen: estriol, estrone and estradiol, which has two further subforms, 17α-estradiol and 17β-estradiol, which is by far the most potent and common. Estrogen receptors mediate the biological actions of estrogen on target tissues and cells. In the absence of estrogen, estrogen receptor alpha (ERα) is kept inactive through the action of chaperone proteins (heat shock proteins (hsp)) (Monroe *et al.*, 2006; Aranda & Pascual, 2001). In the classical pathway, binding of estrogen to intracellular estrogen receptor alpha leads to conformational changes that allow for dissociation of heat shock proteins, activation of the receptor, consequent dimerisation and binding of dimers to estrogen response elements (EREs) on estrogen-target genes (Nilsson *et al.*, 2019; Aranda & Pascual, 2001; Monroe *et al.*, 2006; Gruber *et al.*, 2002; Heldring *et al.*, 2007).

As mentioned previously, estrogen is essential for reproduction. Estrogen released from the ovaries enters the peripheral circulation and acts on the gonadotropin releasing hormone (GnRH) neurons of the hypothalamus to regulate GnRH and gonadotropin hormones release. Gonadotropin releasing hormone is an essential component of the hypothalamic-pituitary-gonadal axis. Adequate pulsatile GnRH secretion is essential to maintain normal cycling and reproduction (Yen, 1977). Although the importance of gonadotropin releasing hormone neuronal network in the control of reproduction has been known for decades, the upstream mechanisms controlling GnRH release remained elusive.

Studies using mice with inactivating *ERα* mutations (*ERα*KO) showed that the effects of estrogen on gonadotropin releasing hormone neurons are mediated by estrogen receptor alpha (ERα) alone (Wintermantel *et al.*, 2006). However, immunohistochemical, and *in situ* hybridisation studies, on a variety of species, failed to detect presence and expression of *ERα* in gonadotropin releasing hormone neurons (Herbison & Pape, 2001). These findings led to the hypothesis that the effects of estrogen might be mediated by an intermediary *ERα*-expressing network of neurons (Wintermantel *et al.*, 2006).

It was only in 2003, following work by *Seminara et al.* and by *de Roux et al.*, that the kisspeptin neuronal network emerged as a potential regulator of GnRH neuronal activity and, consequently, a key neuropeptide hormone in the regulation of reproductive function and fertility (Dungan, Clifton & Steiner, 2006; Seminara *et al.*, 2004; de Roux *et al.*, 2003). *Seminara et al.* and by *de Roux et al.* found that homozygous mutations in the kisspeptin receptor, *GPR54,* led individuals to develop classical symptoms of idiopathic hypogonadotropic hypogonadism (IHH) (a condition characterised by low levels of gonadotropin hormones and sex steroids, and underdeveloped gonads) (de Roux *et al.*, 2003; Seminara *et al.*, 2004). The findings in humans were corroborated by studies using transgenic mouse lines where either the *Gpr54* gene or the *Kiss1* gene was mutated. As in humans, mice, were also, reproductively impaired (i.e. infertile) they presented with low levels of gonadotropin hormones (both luteinising hormone and follicle stimulating hormone) and sex steroids. Further to this, these animals also presented with impaired pubertal development (de Roux *et al.*, 2003; Seminara *et al.*, 2004). Subsequent studies showed that *Kiss1* mutant mice retained the ability to secrete gonadotropin hormones in response to kisspeptin administration. *Grp54* mutant mice demonstrated normal pituitary response to GnRH administration (de Roux *et al.*, 2003; Seminara *et al.*, 2004; Tng, 2015). Thus suggesting that at the basis of the reproductive phenotype, observed in idiopathic hypogonadotropic hypogonadism, is a primary defect in the GnRH pulse generator due to deficient signalling of an essential upstream regulator, kisspeptin.

Kisspeptins are a highly conserved familiy of peptides encoded by the *Kiss1* gene, they bind to the G-prtein coupled receptor 54 (Gpr54) (Tng, 2015; Dungan, Clifton & Steiner, 2006; Lee *et al.*, 1999b). They are expressed in the gonads, placenta, pancreas, and in the brain: in the anterodorsal preoptic area, and throughout the hypothalamus. It is in the arcuate (ARC) nucleus (equivalent to the infundibular nucleus in primates) and anteroventral periventricular (AVPV) nucleus (preoptic area (POA) in primates) of the hypothalamus that the majority of kisspeptin cells are found (Tng, 2015; Dungan, Clifton & Steiner, 2006).

Multiple lines of evidence show that *Kiss1* is an estrogen-target gene. In females, the vast majority of kisspeptin neurons in the arcuate nucleus and anteroventral periventricular nucleus express estrogen receptor alpha (90% and 70%, respectively) (Kumar *et al.*, 2015; Smith *et al.*, 2005a). Further to this, gonadectomy of female rats increased *Kiss1* mRNA expression in the hypothalamus, and sex steroid replacement reversed this effect (Navarro

et al., 2004b). Studies using female mice with inactivating *ERα* mutations (*ERα*KO), showed absent *Kiss1* gene expression in the hypothalamus (Smith *et al.*, 2005a).

The studies that followed demonstrated that estrogen-mediated *Kiss1* expression is different in the arcuate nucleus and anteroventral periventricular nucleus of the hypothalamus. In the arcuate nucleus *Kiss1* expression is inhibited by estrogen, whereas, in the anteroventral periventricular nucleus, estrogen increases *Kiss1* expression (Smith *et al.*, 2005a). Gonadectomy, in mice, caused an increase in *Kiss1* mRNA expression in the arcuate nucleus. While, in the anteroventral periventricular nucleus, lack of sex steroids (gonadectomy) repressed *Kiss1* mRNA expression. These changes were reversed with sex steroid replacement (Clarkson *et al.*, 2009). Studies in which the levels of *Kiss1* were examined across the rat ovarian cycle further supported the findings above descried. In the arcuate nucleus, *Kiss1* levels were increased in diestrous, when estrogen levels are low, and decreased during proestrous, when estrogen levels are at their highest. On the contrary, in the anteroventral periventricular nucleus, *Kiss1* mRNA expression is at its highest during proestrous, when estrogen concentration is high (Tomikawa *et al.*, 2012; Dubois *et al.*, 2015; Uenoyama *et al.*, 2016). These results indicate that kisspeptin might act as the intermediary neuronal network that relays the effects of estrogen onto GnRH neurons.

Several studies have corroborated the above hypothesis. *Gpr54* is expressed within the preoptic area (POA), which colocalises with approximately 60% to 90% of GnRH neurons (Herbison *et al.*, 2010; Irwig *et al.*, 2004). Studies also show that the majority, about 75%, of GnRH neurons express the kisspeptin receptor (Irwig *et al.*, 2004; Popa, Clifton & Steiner, 2008; Oakley, Clifton & Steiner, 2009). Furthermore, *Kiss1* and *Gpr54* knockout mice present with significantly lower follicle stimulating hormone and luteinising hormone levels when compared to wildtype mice (Seminara *et al.*, 2004; Funes *et al.*, 2003; Messager *et al.*, 2005). *Irwig et al.* (2004) demonstrated, in rats, that central administration of kisspeptin-10 increased C-fos expression in GnRH neurons, indicating neuronal activation (Irwig *et al.*, 2004). Central (via intracerebroventricular injection) and peripheral administration of kisspeptin has been shown to stimulate dose-dependent rise in serum levels of LH and FSH in many species (e.g. mice, rats, humans) (Matsui *et al.*, 2004; Thomson *et al.*, 2004; Messager *et al.*, 2005; Dhillo *et al.*, 2005, 2007). Further to this, kisspeptin administration has no effect on gonadotropin release in mice lacking a functional *Gpr54* gene (Messager *et al.*, 2005), and administration of GnRH antagonists abolishes the expected rise in follicle stimulating hormone and luteinising hormone following kisspeptin administration (Navarro *et al.*, 2005;

Matsui *et al.*, 2004; Gottsch *et al.*, 2004). After years of research, it is now clear that kisspeptins and, its receptor, G-prtein coupled receptor 54 are essential regulators of the hypothalamic-pituitary-gondal axis, playing a key role in reproductive development and function.

Nevertheless there are still some unanswered questions regarding regulation of the hypothalamic-pituitary-gonadal axis. For example, it is known that estrogen differentially regulates *Kiss1* gene expression in the arcuate nucleus and the anteroventral periventricular nucleus of the hypothalamus (Smith *et al.*, 2005a). In the anteroventral periventricular nucleus, estrogen-driven positive feedback on *Kiss1* gene expression is responsible for the preovulatory surge in GnRH and luteinising hormone responsible for ovulation (Popa, Clifton & Steiner, 2008; Oakley, Clifton & Steiner, 2009; Roa *et al.*, 2008; Wiegand *et al.*, 2008; Ma, Kelly & Ronneklei, 1990). Whereas, in the arcuate nucleus, estrogen feedback represses *Kiss1* gene expression. Much less is known about the estrogen-driven negative feedback loop in the arcuate nucleus. It is, however, hypthesised that it regulates secretion of follicle stimulating hormone via its action on GnRH neurons (Navarro *et al.*, 2011). However, while important, the mechanisms underlying tissue-specific actions of estrogen are not entirely understood. For this reason we decided to explore estrogen signalling in the arcuate nucleus and anteroventral periventricular nucleus of the hypothalamus, two areas known to respond differently to estrogen and that regulate reproduction and fertility.

3.2 Results

Gene expression was used to explore and determine the effects of estrogen in the arcuate and anteroventral periventricular nuclei of the hypothalamus, two areas of the brain known to respond to estrogen. In order to facilitate analysis, the RT^2 Profiler PCR Array Mouse Estrogen Receptor Signalling (QIAGEN, PAMM-005Z) was used. For this experiment, adult female mice (6 to 8 weeks old) were ovariectomised. A silastic capsule containing either vehicle (sesame oil) or 17β-estradiol was inserted subcutaneously. Animals were left to recover for one week. After recovery animals were subdivided into two groups: (i) control group - mice that were implanted with a vehicle silastic capsule were injected with vehicle (sesame oil) and (ii) estrogen exposed group – mice that were implanted with a silastic capsule containing 17β-estradiol were given an intraperitoneal injection of estradiol benzoate (0.05 mg/kg). Twenty-four hours after, mice were humanly killed, their brains were removed and snap frozen in liquid nitrogen. Bilateral tissue samples of the arcuate nucleus and anteroventral periventricular nucleus were subsequently collected and prepared for gene expression analysis (RNA extraction, cDNA synthesis) using the RT^2 Profiler™ PCR Array.

3.2.1 Estrogen Differentially Regulates *Kiss1* Gene Expression in the Female Hypothalamic Nuclei

We started this project by trying to replicate the differential effects of estrogen in *Kiss1* gene expression in the arcuate nucleus and anteroventral periventricular nucleus of the hypothalamus (Figure 13). Wild type female mice were ovariectomised and we implanted with a silastic capsule containing 17β-estradiol. After recovery, mice either received an intraperitoneal injection of vehicle (sesame oil) or were injected with estradiol benzoate (0.05 mg/kg). Thus creating two groups: (i) low estrogen (ii) high estrogen. The following day, mice were humanly killed and brains were snap frozen and bilateral samples of the arcuate nucleus were collected and *Kiss1* gene expression, relative to the housekeeping gene cyclophilin, was assessed in the arcuate nucleus of the hypothalamus.

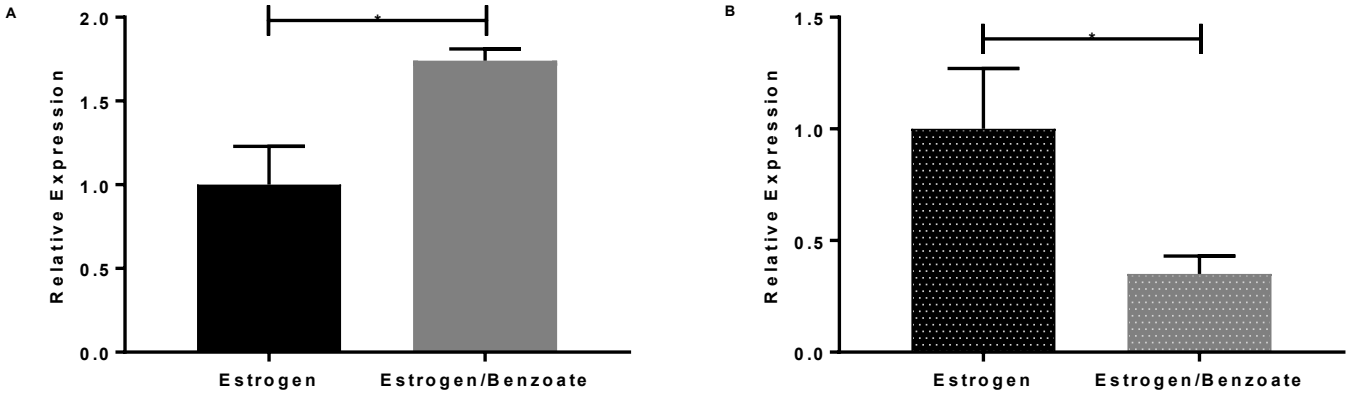

Figure 13: **Kiss1** ***expression in the female hypothalamic nuclei of wild female animals following estrogen treatment.***

Legend: Estrogen – *low estrogen (to resemble the estrogen levels observed during the follicular stage of the cycle) (black bars).* ***Estrogen/Benzoate*** *– high estrogen (to resemble the estrogen levels during the late afternoon of the proestrous) (grey bars).* ***A:*** Kiss1 *mRNA expression in the anteroventral periventricular nucleus of wild type female animals exposed to different concentrations of estrogen (black and grey solid bars).* ***B:*** Kiss1 *mRNA expression in the arcuate nucleus of wild type female animals exposed to different concentrations of estrogen (black and grey dotted bars). Data is expressed as relative expression ± SEM, Student's t-test was the statistical method used, n=6.*

It is well established that estrogen signalling differentially regulates *Kiss1* gene expression in the female hypothalamic nuclei. Estrogen increases *Kiss1* gene expression in the anteroventral nucleus and represses it in the arcuate nucleus. Here, we were able to replicate the already established effects of estrogen on *Kiss1* mRNA expression in the arcuate nucleus and anteroventral periventricular nucleus. In this way, exposure of female wild type mice to estrogen levels that resemble those seen in the late afternoon of proestrous (high concentration of estrogen) (grey solid bar) significantly increased *Kiss1* gene expression in the anteroventral periventricular nucleus by 74% (p=0.012) when compared to animals exposed to follicular levels of estrogen (low levels of estrogen) (black solid bar) (Figure 13A). On the other hand, exposure of female wild type animals to high levels of estrogen (resembling the levels of estrogen during proestrous) (grey dotted bar) significantly repressed *Kiss1* mRNA expression in the arcuate nucleus when compared to control animals (low estrogen - resembling follicular levels of estrogen) (by 65%, p=0.031) (black dotted bar) (Figure 13B).

3.2.2 Only Modest Differences were Observed Between the Arcuate Nucleus and the Anteroventral Paraventricular Nucleus in the Absence of Estrogen

The first experiment conducted looked at the gene expression profile of estrogen target genes in the arcuate nucleus and the anteroventral paraventricular nucleus in the absence of estrogen (Figure 14). The purpose of this comparison was to determine whether there were significant differences in estrogen receptor target-genes between these two estrogen-responsive tissues, under basal conditions. In according to advice from the manufacturer (Qiagen), statistical t-tests were performed without a multiple-test correction because of our interest in global patterns of gene expression. We considered it preferable to obtain few false-positive findings, rather than to eliminate true positives from the conclusions.

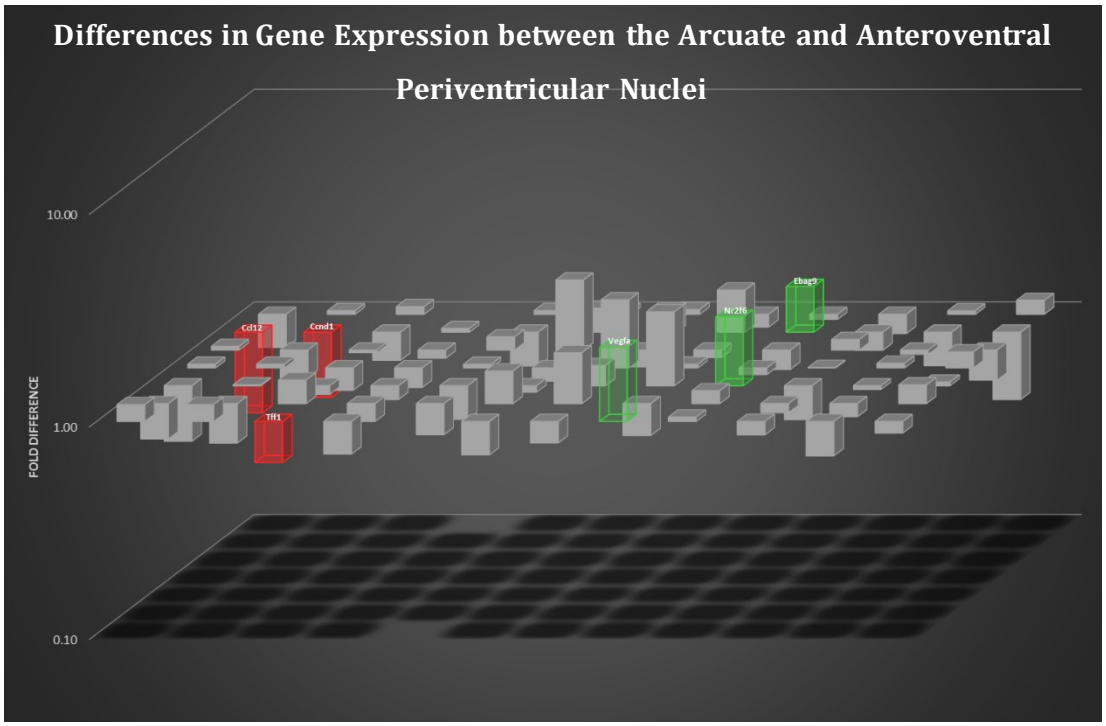

Figure 14: 3D graphical representation of differences in gene expression of estrogen target genes between the arcuate nucleus and anteroventral periventricular nucleus.

Gene expression data is presented as fold change relative to anteroventral periventricular (set as the control sample for this experiment). ***Legend: Grey bars:*** *Genes that were not statistically differently expressed between the arcuate and anteroventral periventricular nuclei.* ***Red bars:*** *Genes, which expression, was statistically lower in the arcuate nucleus when compared to the anteroventral nucleus.* ***Green bars:*** *Represents genes that were statistically more expressed in the arcuate nucleus than in anteroventral periventricular nucleus. Data is expressed as fold change relative to gene expression in the anteroventral periventricular nucleus, Student's t-test was the statistical method used, $p \leq 0.05$ $n=4$, with each 'n-number' representing RNA pooled from four individual mice.*

Gene	Higher or Lower in the Arcuate relative to the AVPV	Fold Change Higher or Lower	p-value
Ccl12	Lower	-2.40	0.014007
Ccnd1	Lower	-2.03	0.021854
Tff1	Lower	-1.56	0.042350
Ebag9	Higher	1.64	0.048615
Nr2f6	Higher	2.11	0.049841
Vegfa	Higher	2.23	0.023941

Table 1: List of genes, which expression, was either signifcantly lower (red) or higher (green) in the arcuate nuclues comparatively to its expression in the anteroventral periventriclar nucleus.

As it can be seen, the expression of the expression levels of the majority of the estrogen-target genes analysed were not significantly different when the two female hypothalamic regions were compared (78 out of 84 genes) (grey bars). Only 6 genes had expression levels that were significantly different upon comparison, with the expression levels of three of those, Ccl2, Ccnd1 and Tff1, being significantly lower in the arcuate nucleus when compared to the anteroventral periventricular nucleus. Conversely, the expression levels of Ebag9, Nr2f6 and Vegfa was significantly higher in the arcuate when compared to their expression in the anteroventral periventricular nucleus.

Therefore, these results show that, in the absence of estrogen, the arcuate nucleus and anteroventral periventricular nucleus display surprisingly similar profiles of known estrogen responsive genes.

3.2.3 The Effect of Estrogen in Female Hypothalamic Nuclei

3.2.3.1 Estrogen Almost Exclusively Upregulates Gene Expression in the Arcuate Nucleus

The next step was to investigate the effect of estrogen on known estrogen receptor target genes in each of the female hypothalamic regions. Figure 15 is a graphical representation of gene expression profile following estrogen treatment.

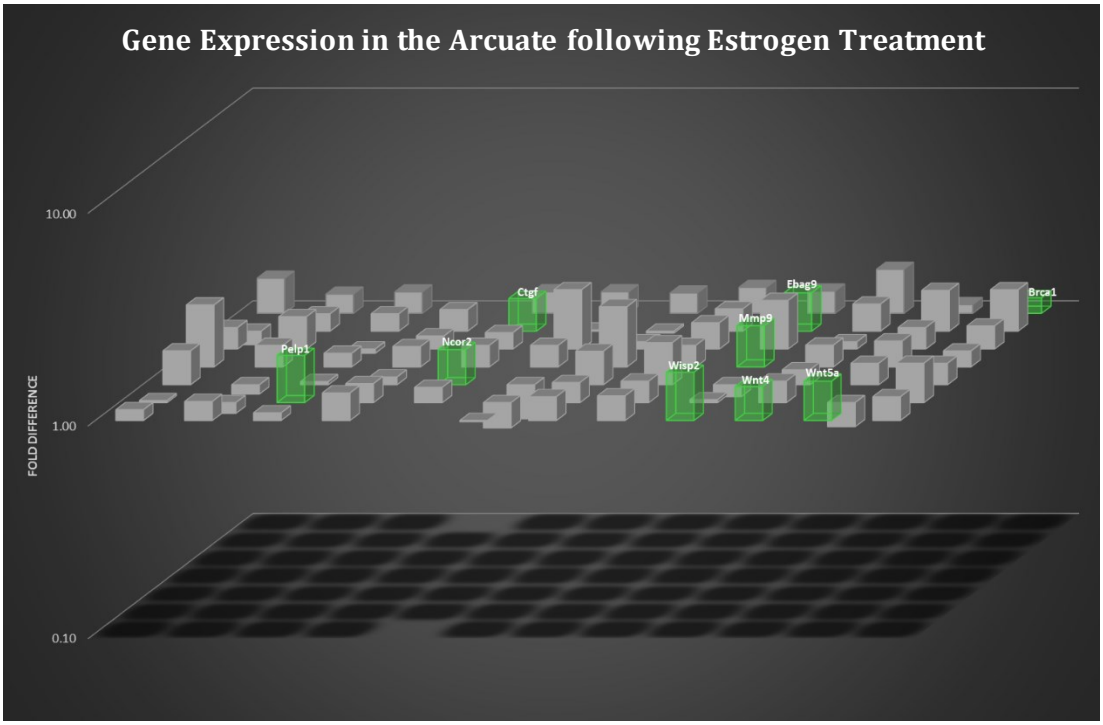

Figure 15: Gene expression profile in the arcuate nucleus following estrogen treatment.

Gene expression data is presented as fold change relative to expression of genes in the vehicle group (set as the control sample for this experiment). ***Legend: Grey bars:*** *Genes that were not statistically differently expressed following exposure to estrogen.* ***Red bars:*** *Genes, which expression, was statistically lower in the estrogen group when compared to the vehicle group.* ***Green bars:*** *Represents genes that were statistically more expressed in the following treatment with estrogen. Data is expressed as fold change relative to gene expression in vehicle group, Student's t-test was the statistical method used, $p \leq 0.05$, $n=4$, with each 'n-number' representing RNA pooled from four individual mice.*

Gene	Up or down	Fold Up- or Down-Regulation	p-value
Brca1	Up	1.61	0.028184
Ctgf	Up	1.43	0.043996
Ebag9	Up	1.51	0.042529
Mmp9	Up	1.56	0.031727
Ncor2	Up	1.46	0.045838
Pelp1	Up	1.67	0.016904
Wisp2	Up	1.69	0.012876
Wnt4	Up	1.44	0.042583
Wnt5a	Up	1.53	0.045630

Table 2: List of genes that were either signifcantly upregulated (green) or downregulated (red) in the arcuate nucleus, following estrogen tretament.

As it can be seen in Figure 15, there is a moderate effect on gene expression following exposure to estrogen, with a trend towards increased gene expression across the majority of the array. Even though, following estrogen treatment, there is a trend towards higher gene expression levels for the vast majority of the genes analysed (84 genes), this difference was only significantly different for 9 of those genes (listed in Table 2), with the fold change for all of these genes being bellow 2. This is likely due to the limited statistical power associated with our small sample size (n=4). It is interesting to note that, in the arcuate nucleus, exposure to estrogen did not cause significant downregulation of any of the estrogen target genes analysed. Analysis, therefore, demonstrates only a moderate effect of estrogen on gene expression, with this effect being mostly up-regulatory.

3.2.3.2 Gene Expression in The Anteroventral Periventricular Nucleus is Mostly Unaffected Following Estrogen Treatment

The effect of estrogen in the anteroventral nucleus was then assessed. Figure 16 is a graphical representation of gene expression profile in the anteroventral periventricular nucleus following estrogen treatment.

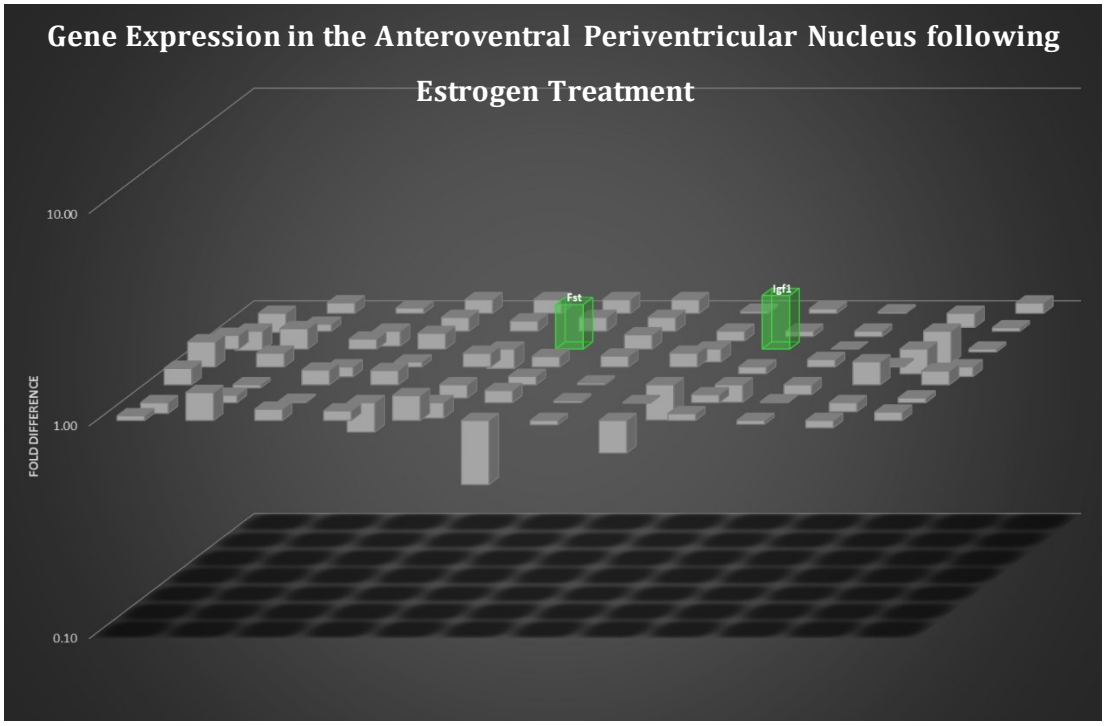

Figure 16: Gene expression profile in the anteroventral periventricular nucleus following estrogen treatment.

Gene expression data is presented as fold change relative to expression of genes in the vehicle group (set as the control sample for this experiment). ***Legend: Grey bars:*** *Genes that were not statistically differently expressed following exposure to estrogen.* ***Red bars:*** *Genes, which expression, was statistically lower in the estrogen group when compared to the vehicle group.* ***Green bars:*** *Represents genes that were statistically more expressed in the following treatment with estrogen. Data is expressed as fold change relative to gene expression in vehicle group, Student's t-test was the statistical method used, p≤0.05, n=4, with each 'n-number' representing RNA pooled from four individual mice.*

Gene	Up or down	Fold Up- or Down-Regulation	p-value
Fst	Up	1.62	0.024193
Igf1	Up	1.79	0.007021

Table 3: List of genes that were either signifcantly upregulated (green) or downregulated (red) in the anteroventral periventricular nucleus, following estrogen tretament.

Estrogen had a modest effect on the expression of genes in the anteroventral periventricular nucleus of the hypothalamus. The expression levels of the vast majority of genes did not significantly change following estrogen treatment, some remained unchanged, while others trended towards lower or higher expression. But the ones that significantly changed, Fst and Igf1, were upregulated following estrogen exposure.

3.2.3.3 Estrogen Exposes Differences Between the Arcuate and Anteroventral Periventricular Nuclei

We have shown only modest differences in expression of known estrogen receptor target-genes between the arcuate and anteroventral periventricular hypothalamic nuclei under basal conditions (Figure 14). However, the arcuate nucleus appears to be more responsive to estrogen than the anteroventral periventricular nucleus (Figure 15 and Figure 16). For example the *Nr0B2* gene is the most striking. Under basal conditions (i.e. vehicle) the expression of *Nr0B2* gene was 2 fold higher in the arcuate nucleus when compared to its expression in the anteroventral periventricular nucleus. However, following estrogen treatment, its *Nr0B2* gene expression in the arcuate nucleus was 5 fold higher than in the anteroventral periventricular nucleus (Figure 18). This suggests that estrogen treatment exacerbates differences in target-gene expression between these two nuclei. In order to investigate this, we compared target-gene expression between the arcuate nucleus and the anteroventral periventricular nucleus of the hypothalamus under estrogen-treatment (Figure 17 and Figure 18).

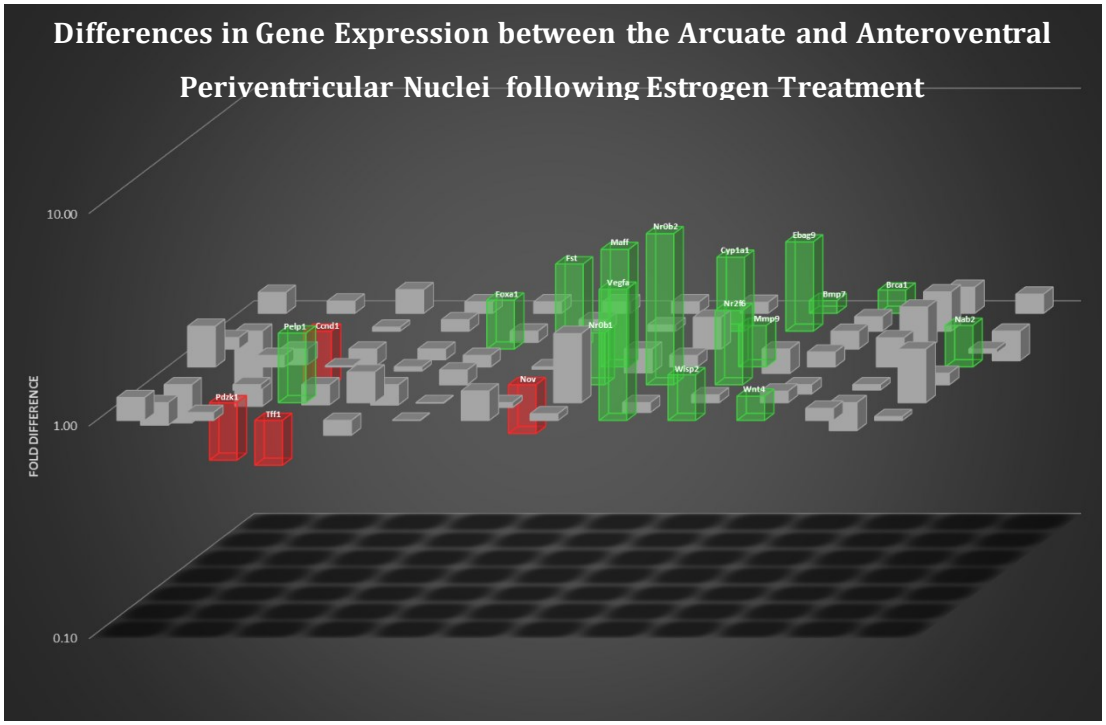

Figure 17: Representation of differences in gene expression between the arcuate nucleus and anteroventral periventricular nucleus following estrogen treatment.

Gene expression data is presented as fold change relative to anteroventral periventricular (set as the control sample for this experiment) following estrogen treatment. ***Legend: Grey bars:*** *Genes that were not statistically differently expressed between the arcuate and anteroventral periventricular nuclei.* ***Red bars:*** *Genes, which expression, was statistically lower in the arcuate nucleus when compared to the anteroventral nucleus.* ***Green bars:*** *Represents genes that were statistically more expressed in the arcuate nucleus than in anteroventral nucleus. Data is expressed as fold change relative to gene expression in the anteroventral periventricular nucleus, Student's t-test was the statistical method used, $p \leq 0.05$, $n=4$, with each 'n-number' representing RNA pooled from four individual mice.*

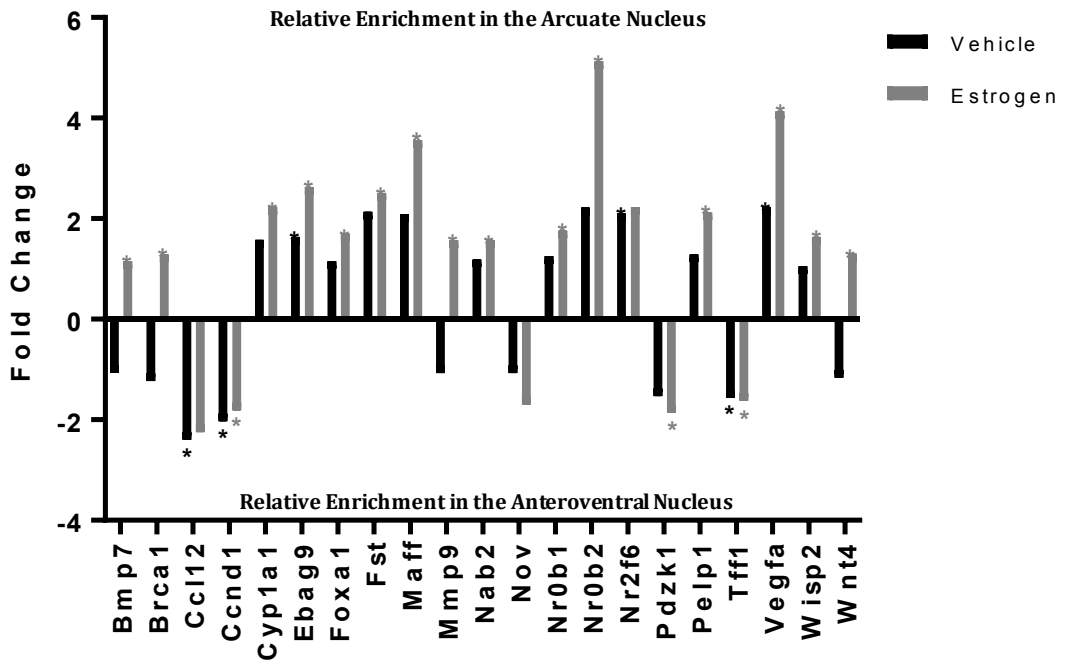

Figure 18: Differential regulation of estrogen-responsive genes in the ARC and AVPV.

The relative magnitude of fold change for each of the genes, whose expression levels was significantly different between the two female hypothalamic nuclei, following vehicle (black bars) and estrogen treatment (grey bars) is illustrated above. Data is expressed as fold change relative to the anteroventral periventricular nucleus following vehicle and estrogen treatment. Fold changes above the axis shows genes enriched in the arcuate nucleus. Fold changes below the x axis represents genes that are enriched in the anteroventral periventricular nucleus.

The data above highlights that estrogen treatment accentuates the differences in gene expression between the anteroventral periventricular nucleus and the arcuate nucleus. Estrogen treatment increased the number of genes which expression was significantly different in the arcuate relative to the anteroventral periventricular nucleus, from 6 genes to 21 genes (Figure 17). Estrogen also increased the magnitude of changes (fold change) as it can be easily seen in Figure 18.

Therefore, it can be seen that the arcuate nucleus and anteroventral periventricular nucleus are differentially regulated by estrogen.

3.2.4 Nuclear Hormone Receptor and Coregulator Differences between the Arcuate Nucleus and Anteroventral Periventricular Nucleus of the Hypothalamus

As mentioned previously, the arcuate nucleus and anteroventral periventricular nucleus are differentially regulated by estrogen. We hypothesise that tissue-specific actions of estrogen are mediated by coregulatory proteins, therefore the expression of genes encoding nuclear receptors and their coregulators, in the arcuate nucleus and anteroventral periventricular, was analysed using the RT^2 Profiler™ PCR Array Mouse Nuclear Receptors & Coregulators (PAMM-056Y).

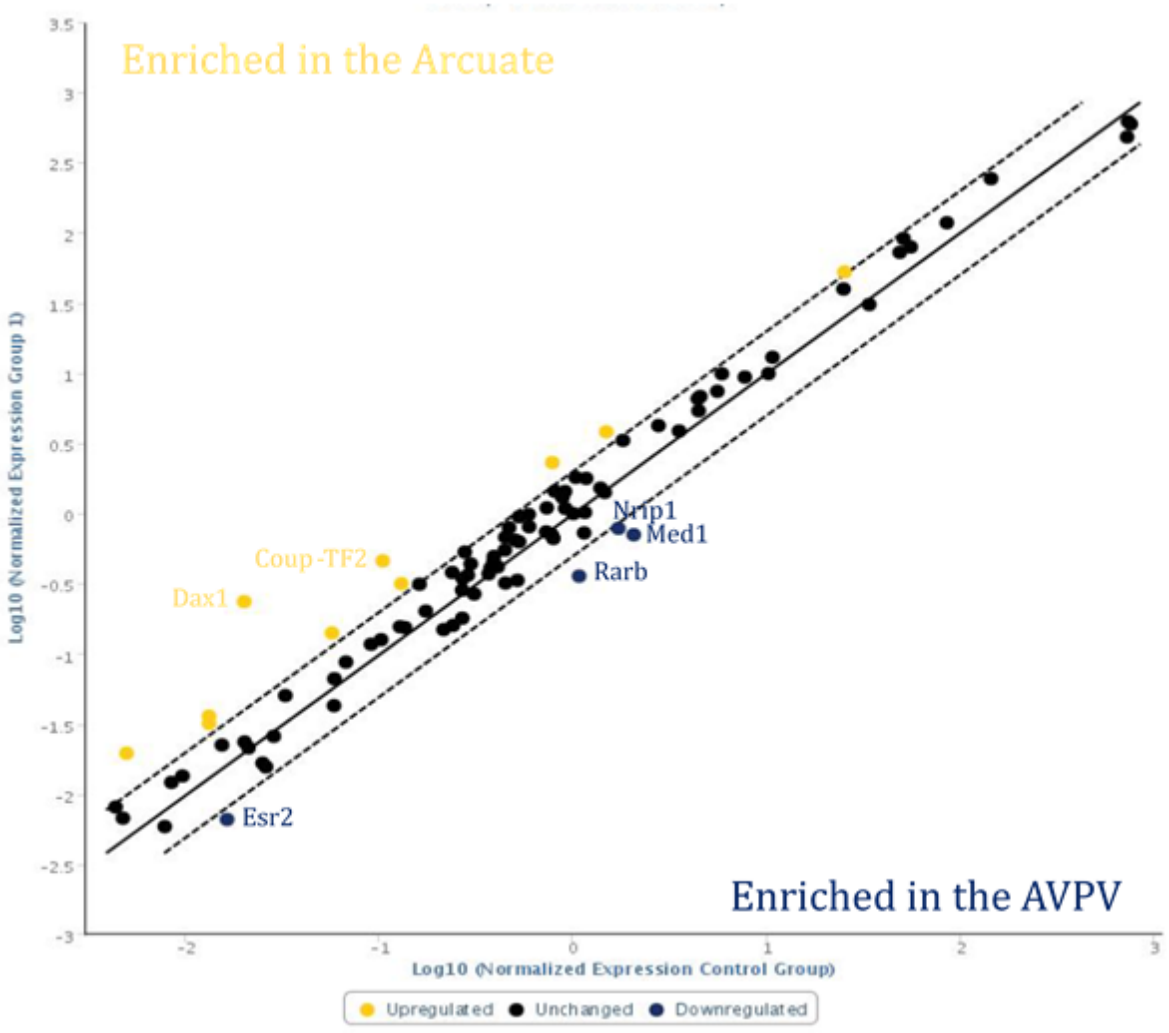

Figure 19: Differences in nuclear receptor and coregulator gene expression between the arcuate nucleus and anteroventral periventricular nucleus.

Gene expression data is presented as fold change relative to anteroventral periventricular. Expression of genes in yellow (above the black dotted lines) is significantly higher in the arcuate nucleus compared to the anteroventral periventricular nucleus. While the expression of those in blue (below the black dotted lines) are significantly reduced in the arcuate nucleus when compared to the anteroventral periventricular nucleus (i.e. enriched in the anteroventral periventricular nucleus). ***Legend: Black solid line:*** *Indicates a fold change of 1.* ***Black dotted lines:*** *Indicates a fold change of 2 (set by the software arbitrarily). Data is expressed as fold change relative to gene expression in the anteroventral periventricular nucleus, Student's t-test was the statistical method used, p≤0.05, n=4, with each 'n-number' representing RNA pooled from four individual mice.*

Gene	Higher or Lower in the Arcuate relative to the AVPV	Fold Change Higher or Lower
Rarb	Lower	-2.99
Med1	Lower	-2.91
Esr2	Lower	-2.47
Nrip1	Lower	-2.18
Nr0b1	Higher	11.81
Nr2f2	Higher	4.42
Nr2f1	Higher	2.96
Nr5a1	Higher	2.73
Psmc5	Higher	2.58
Ppard	Higher	2.48
Nr6a1	Higher	2.44
Vdr	Higher	2.43
Ncoa4	Higher	2.09

Table 4: List of genes whose expression was eitther signifcantly lower (red) or higher (green) in the arcuate nucleus relative to their expression in the antereoventral periventricular nucleus.

Analysis of genes that code for nuclear receptors and their coregulators revealed (Figure 19) that the levels of expression for the vast majority of these genes is similar in the anteroventral periventricular nucleus and in the arcuate nucleus (with the fold change falling below 2 for 71 out 84 genes). Nr0b1 was, by far, the gene which showed the highest difference in expression levels between the two areas. Nr0b1 expression in the arcuate nucleus was 11.81 fold higher than in the anteroventral periventricular nucleus (p=0.02621). Another 8 other genes also were also enriched in the arcuate nucleus but to a lesser extent than Nr0b1 (also

known as Dax1). On the other hand, only 4 were significantly enriched in the anteroventral periventricular nucleus (Rarb, Med1, Esr2, and Nrip1).

The above data clearly highlights differences in the expression of genes that code for nuclear receptors and coregulators between the arcuate nucleus and the anteroventral periventricular nucleus of the hypothalamus, which could explain the differential effects of estrogen, on gene expression, in these two female hypothalamic nuclei.

3.2.5 Dax1 is Highly Enriched in the Arcuate Nucleus of Female Mice

3.2.5.1 Confirmation of Dax1 Enrichment by RT-qPCR

The Nuclear Receptors & Coregulators PCR array (Figure 19 and Table 4) highlight differences in gene expression between the arcuate and anteroventral periventricular nuclei of the hypothalamus. Most of the genes which expression was different between the two nuclei were genes involved in transcriptional regulation. Dax1 was by far the most significantly changed gene, its expression in the arcuate nucleus was 11.88 higher than its levels in the anteroventral periventricular nucleus. Dax1 is an orphan nuclear receptor mainly expressed in adrenal, ovary, hypothalamus and pituitary. Dax1 is known to interact with both estrogen receptor alpha in order to repress activity of liganded estrogen receptors. Multiple lines of evidence suggests key roles for Dax1 in sex development, reproduction and steroidogenesis. While Dax1 gene inactivation in male mice causes infertility due to developmental defects in testes-formation, little is known about the female specific roles of Dax1 in adult mice (Zhang *et al.*, 2000). We therefore became interested in Dax1 and started exploring Dax1 and its functions. To do so, Dax1 gene expression levels, relative to the housekeeping gene cyclophilin, was assessed in the arcuate nucleus and anteroventral periventricular nucleus of the hypothalamus (Figure 20). Wild-type B57BL/6 female mice (6-8 weeks old) were terminally anesthetised intraperitoneally with sodium pentobarbital and their brains were removed and snap frozen in liquid nitrogen. Bilateral arcuate snap frozen arcuate nucleus and anteroventral periventricular nucleus tissue samples were dissected and prepared for RT-qPCR.

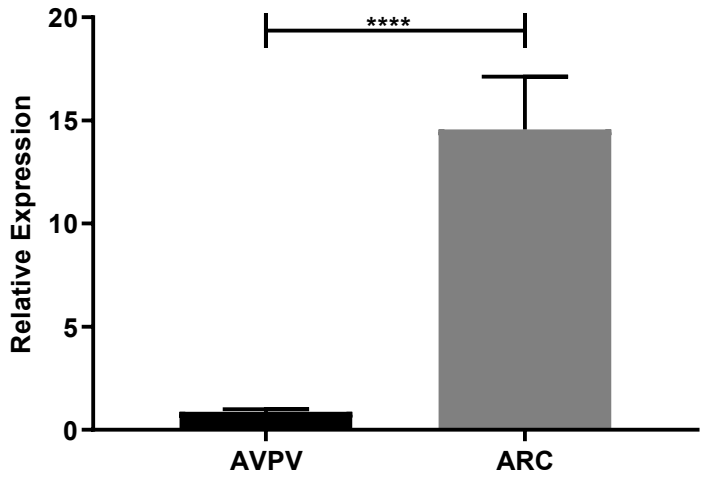

Figure 20: Dax1 expression in female hypothalamic nuclei.

Data is expressed as relative expression ± SEM, Student's t-test was the statistical method used, n=18.

RT-qPCR data confirms the results obtained when the RT^2 Profiler™ PCR Array Mouse Nuclear Receptors & Coregulators (PAMM-056Y) was used. Dax1 expression is differently expressed in female hypothalamic nuclei, with its expression being significantly higher, by 16.71 fold, in the arcuate nucleus than in the anteroventral periventricular nucleus of the hypothalamus ($p<0.0001$).

3.2.5.2 Confirmation of Dax1 Enrichment by Immunofluorescence

Dax1 expression at the protein level was then analysed by immunofluorescence. Anteroventral periventricular nucleus and arcuate nucleus sections (40µm thick) were collected from wild-type B57BL/6 female mice (6-8 weeks old) and prepared for immunofluorescence. The samples were incubated with the Anti-DAX1, clone 2F4 antibody (Merck, MABD398) (1:100), used to detect Dax1 in and with nuclear stain (DAPI) (Figure 21).

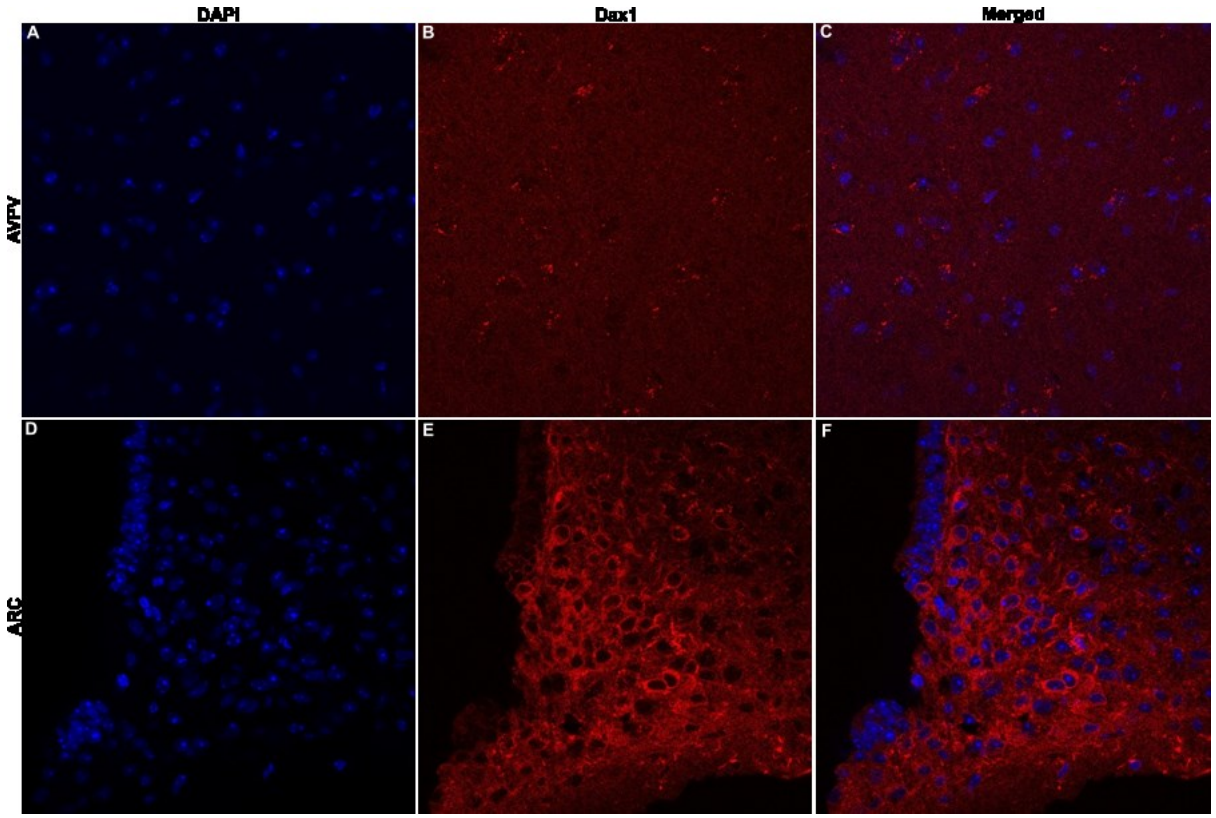

Figure 21: Representative image of Dax1 expression in the anteroventral periventricular nucleus (AVPV) and arcuate nucleus (ARC) of the hypothalamus.

A - C: *Dax1 protein expression in the anteroventral periventricular nucleus of wild type mice. n=3.* ***D - F:*** *Dax1 protein expression in the arcuate nucleus of wild type mice. n=3.* ***A and D:*** *Pictures of the nuclear counter stain DAPI (1:1000) in the anteroventral periventricular nucleus (**A**) and in the arcuate nucleus (**B**).* ***B and E:*** *Dax1 staining in AVPV samples (**B**) and in ARC samples (**E**) can be seen in red (the anti-DAX1, clone 2F4 antibody (1:100) was used).* ***C and F:*** *Nuclear (blue) and Dax1 (red) staining in anteroventral periventricular samples (**C**) and in arcuate samples (**F**) were merged together to facilitate localisation of expression. Images were acquired using the Zeiss LSM-780 Inverted Confocal Microscope (Zeiss), 20x magnification, z-stack. Image processing was performed using the ImageJ (Fiji) software.*

Figure 21 clearly shows that the reduced levels of mRNA in anteroventral periventricular nucleus also correlate with a decrease in Dax1 protein expression. Figure 21E show a very strong Dax1 staining for Dax1, which is mainly cytoplasmic with some cells displaying nuclear localisation too (not shown). The Dax1 staining observed for the arcuate panel contrast with that observed for the anteroventral nucleus, with barely any staining being visible (Figure 21E and Figure 21B).

3.2.6 Dax1 Expression is Enriched in the Female Hypothalamus

We then explored whether expression of genes coding for nuclear receptors and their coregulators in the arcuate nucleus was sexually dimorphic. Here to the RT^2 Profiler™ PCR Array Mouse Nuclear Receptors & Coregulators (PAMM-056Y) was used to analyse expression of these genes in arcuate samples collected from wild-type B57BL/6 female and male mice (6-8 weeks old).

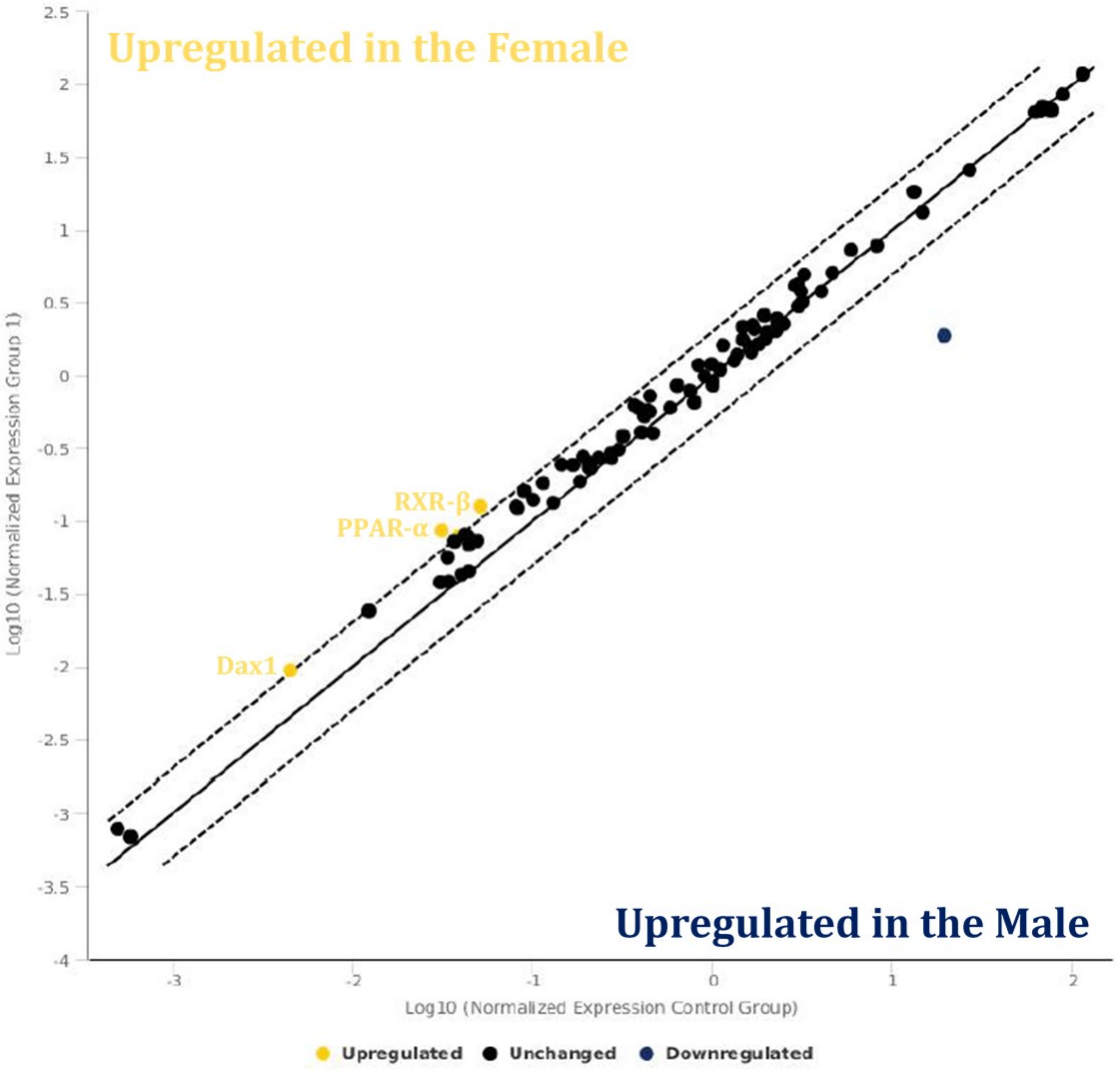

Figure 22: Differences in nuclear receptor and coregulator gene expression in the arcuate nucleus of female and male mice.

Gene expression data is presented as fold change relative to the male arcuate nucleus. Expression of genes in yellow is significantly higher in the female arcuate nucleus when compared to the male nucleus. While the expression of those in blue and below the black dotted lines are significantly reduced in the arcuate nucleus when compared to the anteroventral periventricular nucleus (i.e. enriched in the anteroventral periventricular nucleus). ***Legend: Black solid line:*** *Indicates a fold change of 1.* ***Black dotted lines:*** *Indicates a fold change of 2 (set by the software arbitrarily). Data is expressed as fold change relative to gene expression in the male arcuate nucleus, Student's t-test was the statistical method used, p<0.05, n=4, with each 'n-number' representing RNA pooled from four individual mice.*

Gene	Higher or Lower in the Female Arcuate relative to the Male Arcuate	Fold Change Higher or Lower
Hdac2	Lower	-10.31
Pparα	Higher	2.73
Rxrb	Higher	2.46
Nr2e3	Higher	2.08
Nr0b1	Higher	2.02

Table 5: List of genes whose expression was eitther signifcantly lower (red) or higher (green) in the female arcuate nucleus relative to their expression in the male arcuate nucleus.

The expression of genes that code for nuclear receptors and their coregulators is very similar in the arcuate nucleus of female and male animals. Nevertheless, 5 genes were statistically differently expressed in the two genders. The expression of Pparα, Rxrb, Nr2e3 and Nr0b1 was significantly higher in the female arcuate nucleus than in the male (2.73, 2.46, 2.08 and 2.02, respectively). On the contrary, only Hdac2 was enriched in the male arcuate nucleus (10.31 fold). This gene is a histone deacetylase, and its role in the male arcuate nucleus warrants further investigation but is beyond the scope of the current project.

As it can be seen Dax1 expression is sexually dimorphic, with is expression being higher in the female hypothalamus (Figure 22). These results were then confirmed by RT-qPCR (Figure 23), and again Dax1 expression was significantly higher in the female arcuate nucleus when compared to the male arcuate nucleus (2.21 fold change, p=0.005).

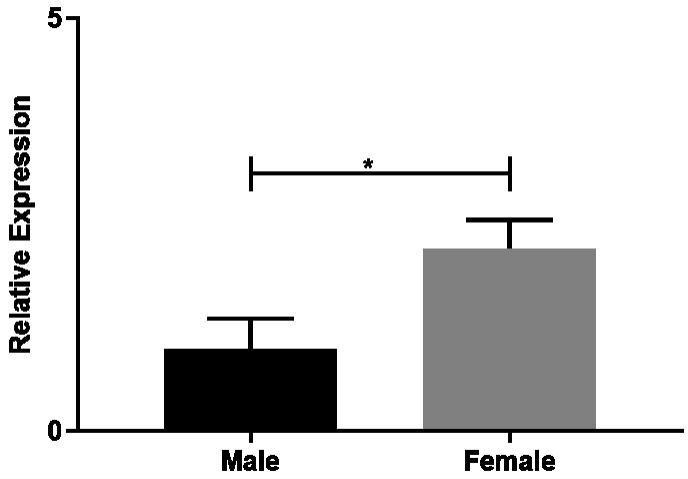

Figure 23: Dax1 expression in the female and male arcuate nucleus.

Data is expressed as relative expression ± SEM, Student's t-test was the statistical method used, n=18.

Together, these data raise the possibility that Dax1 may play a role in modulating estrogen-responsive gene expression in female hypothalamic nuclei. In particular, given its known role as a ligand-dependent repressor of gene expression, and its presence in the arcuate hypothalamic nucleus, it may be involved in the repression of the *Kiss1* gene by estrogen in this location. As such, we decided to quantify Dax1 expression in Kiss1-cells of the female arcuate nucleus (Figure 24).

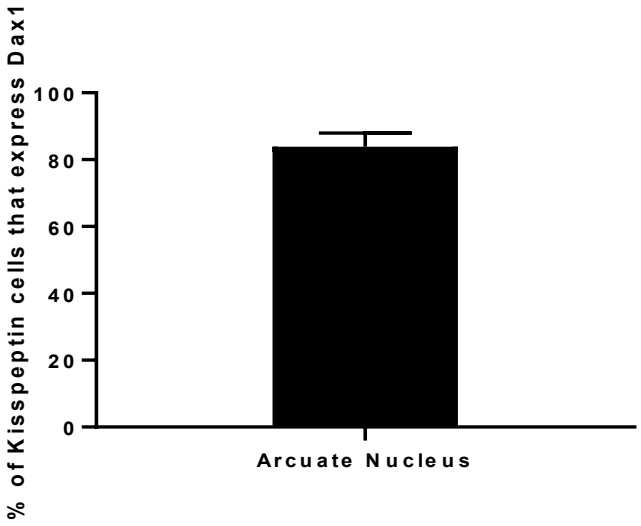

Figure 24: Percentage of kisspeptin cells that express Dax1 in the arcuate nucleus wild type mice.

Kisspeptin cells across the arcuate nucleus of wild type female animals were analysed in order to quantify the percentage kisspepin cells that colocalise with Dax1. Data is expressed as percentage ± SEM, Student's t-test was the statistical method used, n=3.

While there was some variability in the percentage of kisspeptin cells that express Dax1 between the animals analysed (values varied from 72.7% to 96.7%), Figure 24 demonstrates that the majority of kisspeptin cells in the arcuate nucleus of wild type female express Dax1 (84%).

3.2.7 Understanding the Mechanisms of Dax1 Action

3.2.7.1 *In-vitro* Assay to Understand Mechanisms of Dax1 Action are not Informative

It is well known that estrogen plays an important role in the mechanisms that control reproduction and the hypothalamic-pituitary-gonadal axis. Estrogen acts on the hypothalamus to regulate the expression of *Kiss1*. *Kiss1* is important in the regulation of pulsatile secretion of gonadotropin releasing hormone release from the hypothalamus, which is necessary for the maintenance of reproduction. *Kiss1* is expressed in two main areas of the hypothalamus, the anteroventral periventricular nucleus and the arcuate nucleus. These two areas are the main targets of estrogen action where it has differential effects. *Kiss1* expression in the arcuate nucleus is repressed by estrogen, whereas in the anteroventral periventricular nucleus *Kiss1* expression is upregulated by estrogen. These opposite effects of estrogen are crucial for reproduction, however the mechanisms behind this differential regulation are not well understood. It is thought that the tissue-specific actions of estrogen might be due to differences in coregulator composition. Considering that Dax1 is highly enriched in the arcuate nucleus when compared to its expression in the anteroventral periventricular nucleus. We decided to explore the actions of Dax1 and whether this differential expression of Dax1 can explain the differential effects of estrogen in *Kiss1* expression in the two female hypothalamic nuclei.

To do so, the mHypoA-50 and mHypoA-55 cell lines were purchased. These cell lines were generated by the Belsham Lab, they are reported to express well known markers of anteroventral periventricular and arcuate nuclei, respectively. In addition, these markers behave like the anteroventral periventricular nucleus and arcuate nucleus, respectively, in response to estrogen (Treen *et al.*, 2016).

Therefore, the mHypoA-50 and mHypoA-55 cell lines were treated with 10nM of estrogen for 24 and 4 hours, respectively, and then Kiss1 mRNA expression was determined by RT-qPCR (Figure 25).

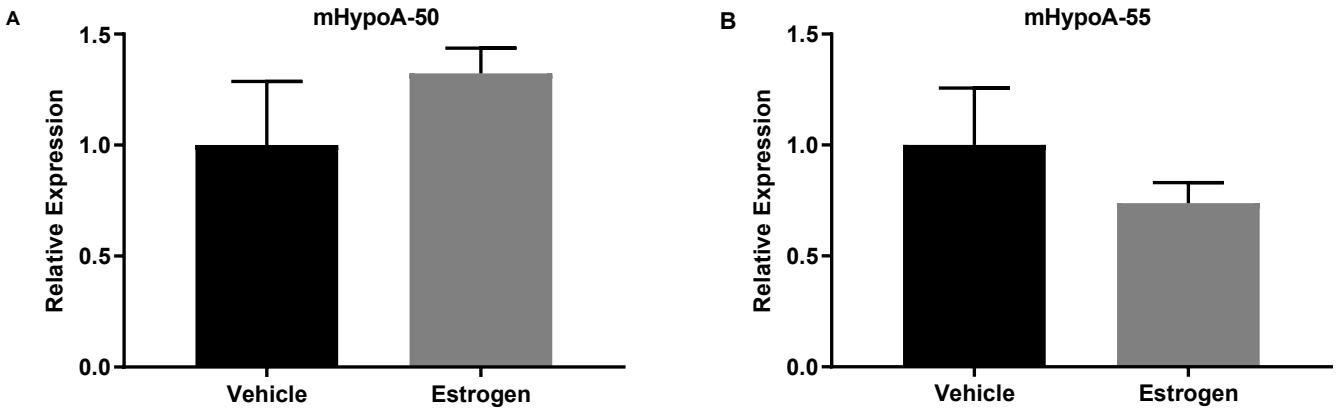

Figure 25: Effect of estrogen treatment on Kiss1 mRNA expression in the mHypoA-50 and mHypoA-55 cell lines.

Cells were treated with vehicle or 10nM estrogen. mRNA from mHypoA-50 was harvested at 4 hours, and mHypoA-55 mRNA was harvested at 24 hours. Changes in Kiss1 expression were measured using RT-qPCR. mRNA levels were normalised to cyclophilin control. ***A:*** *Kiss1 mRNA expression in mHypoA-50. p=0.3187.* ***B:*** *Kiss1 mRNA expression in mHypoA-55. p=0.3588. Data is expressed as relative expression ± SEM, Student's t-test was the statistical method used, n=3-12 independent experiments.*

In the anteroventral periventricular cell model, mHypoA-50, there was a trend towards increased *Kiss1* gene expression at 24 hours with 10nM estrogen (vehicle 1 ± 0.2870 vs estrogen 1.324 ± 0.1130, p=0.3187) (Figure 25A). On the contrary, in the arcuate cell model, mHypoA-55, there was a trend towards decreased *Kiss1* gene expression following estrogen treatment (10nM) (vehicle 1 ± 0.2564 vs estrogen 0.7377 ± 0.093, p=0.3588) (Figure 25B). While the first experiments yielded results that trended towards the expected effect on *Kiss1* expression following estrogen treatment in the two cell lines. With estrogen increasing *Kiss1* expression in the anteroventral periventricular cell line (mHypoA-50) and decreasing its expression in the arcuate nucleus cell line (mHypoA-55) (Figure 25B). This difference was not significantly different. And in the experiments that followed produced results in which estrogen induced the expected effects on *Kiss1* gene expression (Figure 26A) or it led to the complete opposite effects (Figure 26B).

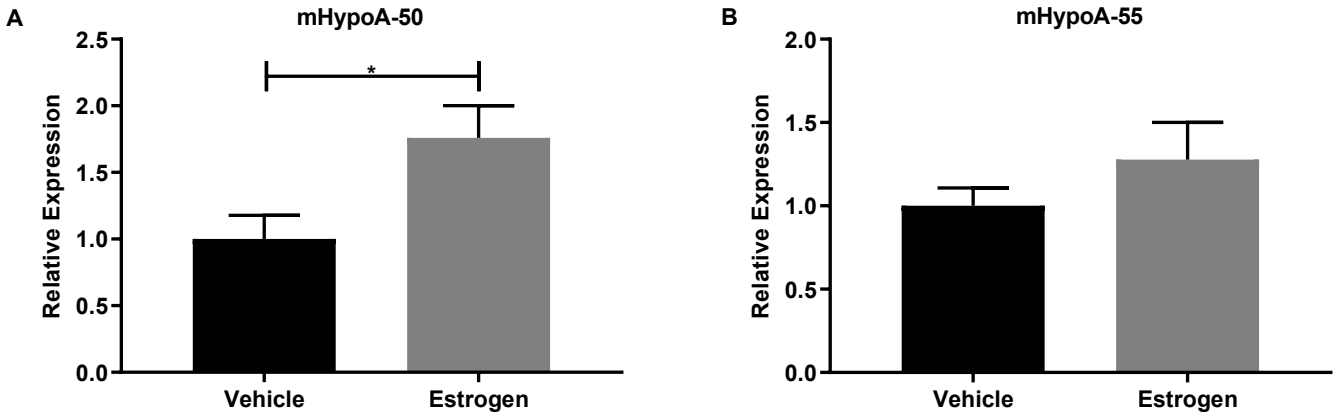

Figure 26: Repeat experiment looking at the effects of estrogen treatment on Kiss1 mRNA expression in the mHypoA-50 and mHypoA-55 cell lines.

Cells were treated with vehicle or 10nM estrogen. mRNA from mHypoA-50 was harvested at 4 hours, and mHypoA-55 mRNA was harvested at 24 hours. Changes in Kiss1 expression were measured using RT-qPCR. mRNA levels were normalised to cyclophilin control. ***A:*** *Kiss1 mRNA expression in mHypoA-50. p=0.0305.* ***B:*** *Kiss1 mRNA expression in mHypoA-55. p=0.2888. Data is expressed as relative expression ± SEM, Student's t-test was the statistical method used, n=3-12 independent experiments.*

As expected, estrogen treatment yield the desired effects in the anteroventral periventricular cell model, mHypoA-50. *Kiss1* gene expression at 24 hours was significantly higher with 10nM estrogen (vehicle 1 ± 0.1775 vs estrogen 1.324 ± 0.1130, p=0.0305) (Figure 26A). On the contrary, in the arcuate cell model, mHypoA-55, estrogen treatment instead of repressing *Kiss1* gene expression, as expected, it actually upregulated *Kiss1* gene expression (vehicle 1 ± 0.1082 vs estrogen 1.278 ± 0.2233, p=0.2888) (Figure 26B).

We were unable to consistently obtain the expected results as the mHypoA-50 and mHypoA-55 cell lines failed to respond to estrogen treatment as reported in Treen *et al.*, 2016. In addition, these cell lines express very low levels of both Dax1 (Ct 38) and Kiss1 (Ct 35). Therefore, we conclude that these cell lines are not suitable models to study the endogenous regulation of *Kiss1* by both estrogen or Dax1.

3.2.7.1.1 Functional Consequences of the Dax1 Interactions with Estrogen Receptor Alpha

To investigate the functional consequences of interactions of Dax1 in *Kiss1* gene expression, the mHypoA-50 and mHypoA-55 cell lines were transiently transfected with a combination of different constructs (as it can be seen in Figure 28): (i) no promoter (negative control), (ii) GAPDH (positive control), (iii) Kiss1, (iv) ERα and (v) Dax1. The no promoter control, GAPDH and Kiss1 constructs were designed in a way that a heterologous reporter gene, the luciferase gene, was fused downstream of the promoter for the gene of interest (Figure 27). Under the regulation of the gene of interest, the luciferase gene encodes expression of a 61 kDa enzyme that oxidises D-luciferin in the presence of ATP and oxygen, yielding a fluorescent product that can be quantifying by measuring released light. In this way the reporter's fluorescence within a transfected cell population is approximately proportional to the genes of interest mRNA levels. We therefore transfected the female hypothalamic nuclei, mHypoA-50 and mHypoA-55, which are reported to behave like the anteroventral periventricular nucleus and the arcuate nucleus with the constructs mentioned above to assess the effect of Dax1 in *Kiss1* mRNA expression in the arcuate (data not shown) and anteroventral periventricular nucleus (Figure 28).

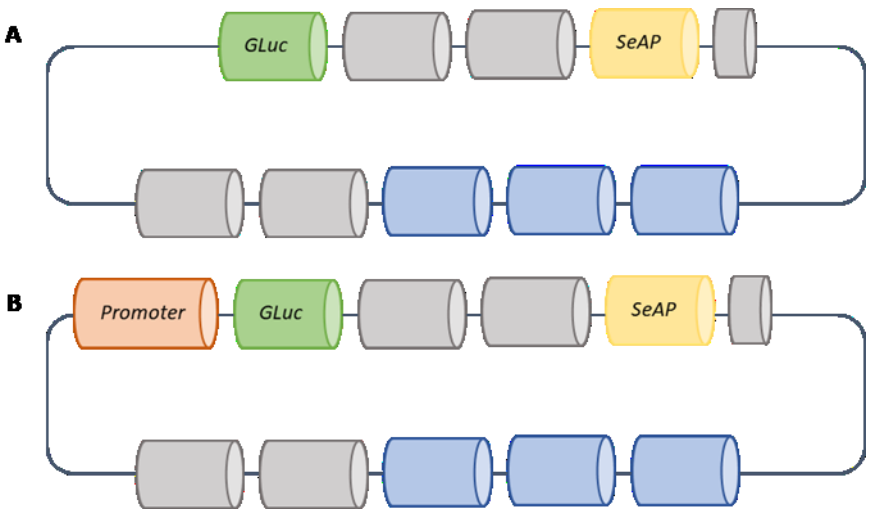

Figure 27: Graphical representation of the luciferase constructs used for these experiments.
A: *No promoter (negative control).* ***B:*** *Construct used for the gene of interest (e.g. Kiss1).*

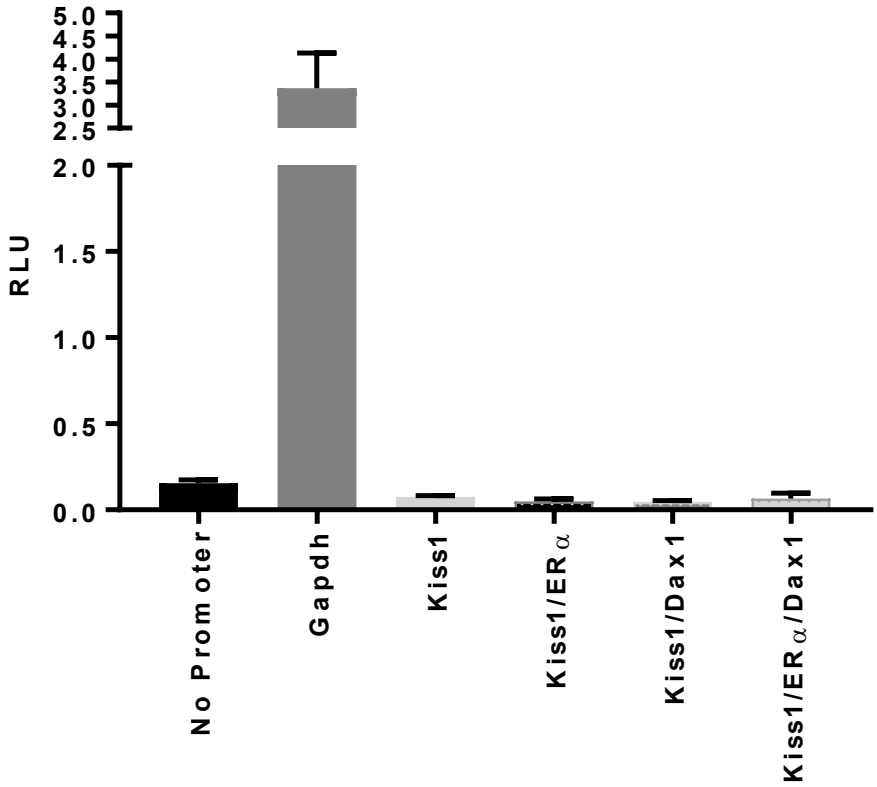

Figure 28: Luciferase reporter assay demonstrating unresponsiveness of the Kiss1 promoter in the mHypoA-50 cell line.

While cells transfected with control constructs (i.e. no promoter and Gapdh) behaved as expected with the expression of the no promoter being low, and luciferase expression being high in cells transfected with Gapdh, transient transfection of cells with the other construct combinations (Kiss1 alone, Kiss1 with ERα, Kiss1 with Dax1, Kiss1 with ERα and Dax1) did not yield any significant results.

In summary, the data shows that the mHypoA-50 and mhypoA-55 cannot respond to estrogen either endogenously (Figure 25, 26), or in transfection-based luciferase assays (Figure 28) under the conditions reported here. The reason for this is are not currently known (discussed below). This is likely because they have lost the necessary machinery to drive *Kiss1* gene expression, but it could also be to the fact that there is a generalised lack of knowledge in the field regarding the exact location of *Kiss1* gene promoter in hypothalamic tissue (discuused in 3.3.5).

3.2.7.2 *Ex-vivo* Mechanisms Used to Understand Mechanisms of Dax1 Action

The cell lines available for the study of differential estrogen-mediation *Kiss1* expression consistently failed to respond to estrogen treatment in the expected manner. For this reason we tried to establish an *ex-vivo* system in which brain cultures from the arcuate nucleus and anteroventral periventricular nucleus were prepared and treated with estrogen. The effect of estrogen in *Kiss1* gene expression was then assessed. In this experiment, B57BL/6 female mice (6-8 weeks old) were transcardially perfused with cold artificial cerebrospinal fluid (ACSF). The brain was the carefully extracted and placed on cold artificial cerebrospinal fluid. Two 900µm and 800µm thick sections were then cut from the anteroventral periventricular nucleus and placed into an oxygenated chamber at 37°C for recovery. The brains samples were subsequently treated for 6 hours with either vehicle (100% ethanol) or with different concentrations of estrogen (2nM, 10nM and 20nM) (Figure 29).

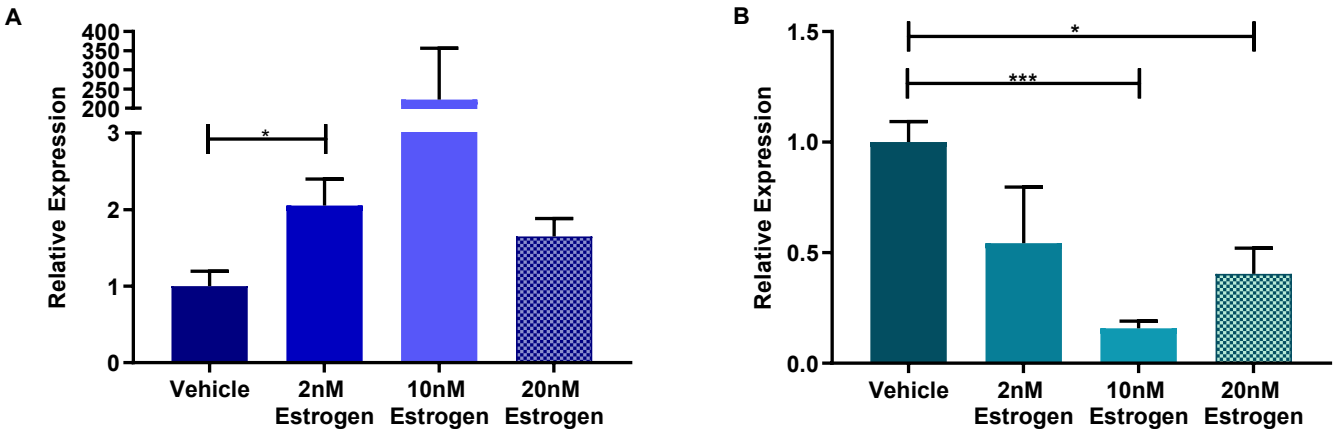

Figure 29: Effect of estrogen treatment on Kiss1 mRNA expression on organotypic slices of the anteroventral periventricular nueleus (A) and arcuate nucleus (B).

An estrogen dose study (2nM, 10nM and 20nM) was performed. Organotypic brain slices were treated with either vehicle or estrogen for 6 hours. After which mRNA was collected from the anteroventral periventricular nucleus and arcuate nucleus were collected and changes in Kiss1 expression was measured using RT-qPCR. mRNA levels were normalised to cyclophilin control. ***A:*** *Kiss1 mRNA expression in anteroventral periventricular nucleus.* ***B:*** *Kiss1 mRNA expression in arcuate nucleus.*

Data is expressed as relative expression ± SEM, Student's t-test was the statistical method used, each treatment: n=6.

In the anteroventral periventricular nucleus, estrogen treatment had the expected effects, it increased *Kiss1* expression at all concentrations of estrogen (2nM, 10nM and 20nM) (Figure 29A). Treatment with 2nM of estrogen was the only concentration that statistically increased *Kiss1* expression (vehicle 1 ± 0.1939 vs 2nM estrogen 2.0536 ± 0.0.3468, p=0.0264). In the arcuate nucleus, estrogen also had the predicted effects, all the concentration of estrogen repressed *Kiss1* expression. Treatment with 10nM and 20nM of estrogen significantly repressed *Kiss1* gene expression (10nM – vehicle 1 ± 0.1939 vs 10nM 0.1587 ± 0.0317, p=0.0001; 20nM – vehicle 1 ± 0.1939 vs 20nM 0.4041 ± 0.1164, p=0.0040) (Figure 29B). The estrogen dose study (2nM, 10nM and 20nM) also demonstrated that 10nM is the concentration that induced higher changes in *Kiss1* expression and therefore all future experiments were performed using 10nM of estrogen (Figure 29B).

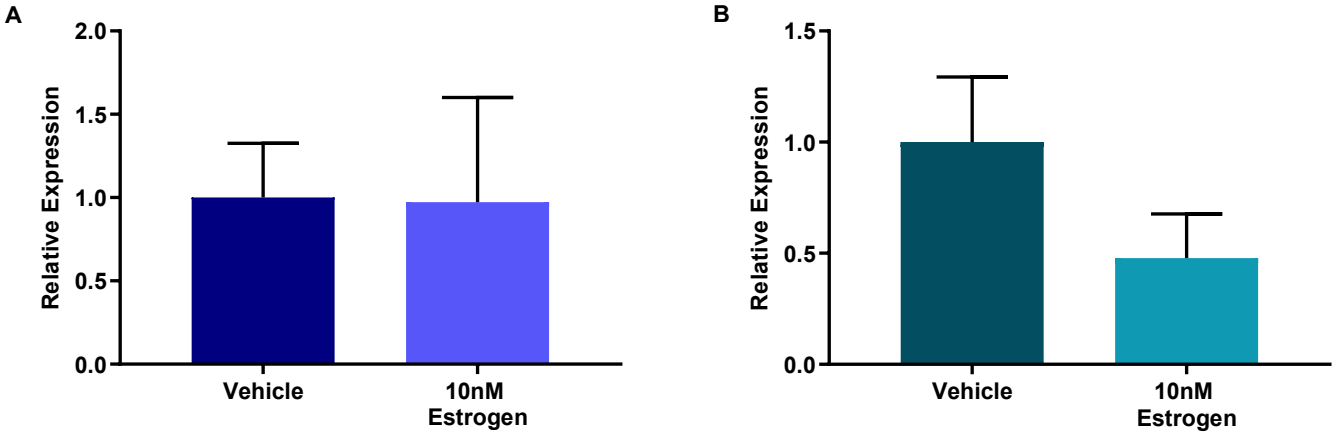

Figure 30: Repeat experiment looking at the effects of estrogen treatment on Kiss1 mRNA expression on organotypic slices of the anteroventral periventricular nueleus (A) and arcuate nucleus (B).

Organotypic brain slices were treated with either vehicle or estrogen 10nM for 6 hours. After which mRNA was collected from the anteroventral periventricular nucleus and arcuate nucleus were collected and changes in Kiss1 expression was measured using RT-qPCR. mRNA levels were normalised to cyclophilin control. ***A:*** *Kiss1 mRNA expression in anteroventral periventricular nucleus.* ***B:*** *Kiss1 mRNA expression in arcuate nucleus.Data is expressed as relative expression ± SEM, Student's t-test was the*

While the initial experiment (Figure 29) presented promising results, with estrogen having the desired effects on *Kiss1* expression, estrogen in the anteroventral periventricular nucleus significantly increased *Kiss1* expression (2nM) and in the arcuate nucleus estrogen significantly decreased *Kiss1* gene expression (10nM and 20nM). The experiments that followed (Figure 30) did not produced to the same extent the desired results and therefore

this method was ruled as inconsistent and unreliable, and therefore it wasn't used to understand the mechanisms of Dax1. For this reason, the mice with conditional knockout of Dax1 in kisspetin cells were generated to assess the function and mechanisms of Dax1 action.

3.3 Discussion

3.3.1 Estrogen Receptor Signalling

Estrogen regulates fertility and reproduction through its effect on *Kiss1* gene expression the female hypothalamic nuclei, the arcuate nucleus and the anteroventral periventricular nucleus. Estrogen expression in the arcuate nucleus represses *Kiss1* gene expression, whereas in the anteroventral periventricular, estrogen stimulates *Kiss1* gene expression. The mechanisms underlying differential estrogen signalling in these two hypothalamic areas remain elusive.

To address this mystery a detailed comparative analysis of the genes involved in estrogen receptor activation and response in these two nuclei was performed under basal conditions and following estrogen treatment. The Student's t-test was the statistical test used here, however, considering that this study was conducted in order to gain a broad picture of the expression levels of estrogen-target genes in the arcuate nucleus and anteroventral periventricular nucleus, multiple comparison tests were not performed. We accept the risk of, potentially, including into our analysis false-positive results in detriment of, potentially, not identifying an important estrogen-target gene (false-negative).

Here we found that the actions of estrogen in estrogen-target genes are almost exclusively up-regulatory. In both the arcuate nucleus and in the anteroventral periventricular nucleus all the genes that displayed significant changes in their expression levels were upregulated following estrogen treatment.

The arcuate nucleus of the hypothalamus is more sensitive to estrogen receptor signalling than the anteroventral periventricular nucleus. Estrogen treatment significantly increased the expression of nine estrogen-target genes in the arcuate nucleus as opposed to only two genes in the anteroventral periventricular nucleus. Even though the majority of estrogen-target genes in the arcuate nucleus displayed an overall trend towards increased gene expression, following estrogen treatment, only nine were significantly different. This is most likely due to the number of biological samples used. Here, an n number of four was used, which was based on previous experiments as well as the hypothesised n number required to achieve results that were biologically relevant. In hindsight, however, a bigger sample size would have, potentially, allowed for a better understanding of the effects of estrogen on the expression of estrogen-target genes in these two areas of the hypothalamus. This estrogen signalling receptor array highlights the differential effects of estrogen in the arcuate nucleus and anteroventral periventricular nucleus, with estrogen having different target genes in these two female hypothalamic nuclei.

Furthermore, it is possible to determine that, under basal conditions, there are not many differences, as determined by the expression of estrogen target genes, between the arcuate nucleus and anteroventral periventricular nucleus of the hypothalamus, with the majority of estrogen-target genes being equally expressed in these two female hypothalamic nuclei. However, estrogen treatment exacerbates differences between the arcuate nucleus and anteroventral periventricular nucleus. Following estrogen treatment, the vast majority of estrogen target genes were enriched in the arcuate nucleus with only a few genes being expressed to a higher level in the anteroventral periventricular nucleus.

Estrogen treatment caused significant upregulation of a variety of different estrogen-target genes in the arcuate nucleus and anteroventral periventricular nucleus, from genes involved in female and male sexual differentiations (e.g. *Wnt4*, *Vegfa*, *Fst*) to genes involved in development (e.g. *Nr2f6*, *Nab2*, *Fox1a*). It is interesting to note that a significant proportion of these genes code for coregulatory proteins (corepressors and coactivators) (e.g. *Nr0b1*, *Nr0b2*, *Igf1*). These findings supported the hypothesis that the tissue-specific actions of estrogen are analogous to selective estrogen receptor modulators (SERMs). Selective estrogen receptor modulators are ligands that exhibit agonistic or antagonistic effects in tissue-, cell-, and gene context-dependent manner. The tissue- and cell-specific coregulator composition as well as the relative expression of coactivators and corepressors accounts for the tissue-specific antagonistic versus agonistic action of selective estrogen receptor modulators (Arnal *et al.*, 2017; Smith & O'Malley, 2004; Smith, Nawaz & O'Malley, 1997).
To explore this hypothesis we compared the expression of genes encoding for nuclear receptors and their coregulators, in the arcuate nucleus and anteroventral periventricular, under basal conditions. As hypothesised, the coregulator composition and relative expression of coregulators diverged when the two female hypothalamic nuclei were compared, with the majority of genes encoding for nuclear receptors and their coregulators being enriched in the arcuate nucleus. Dax1 (a product of *Nr0b1* gene), a known estrogen receptor corepressor, was, by far, the mostly differentially expressed gene between the arcuate nucleus and anteroventral periventricular nucleus. Dax1 was found to be highly enriched in the arcuate nucleus when compared to the anteroventral periventricular nucleus. The expression profile of Dax1 in the arcuate nucleus, its well-characterised role as a corepressor of estrogen receptor transcriptional transactivation together with its documented roles in reproduction led to the hypothesis that Dax1 might mediate the

differential effects of estrogen signalling in *Kiss1* gene expression in the arcuate nucleus (repressive) and anteroventral periventricular nucleus (positive).

Indeed it is known that Dax1 interacts with estrogen receptor alpha (the receptor through which estrogen acts in the female hypothalamic nuclei (Crawford *et al.*, 1998; Zhang *et al.*, 2000)). Further to this, epigenetic modification of genomic DNA and histones are tightly linked to chromatin organisation and transcriptional regulation. Coregulatory proteins (i.e. coactivators and corepressors) recruit enzymes with ability to alter chromatin structure and organisation in order to mediate their effects on estrogen-target gene expression (Castellano *et al.*, 2014; Zhang *et al.*, 2000; Crawford *et al.*, 1998). Indeed it has been shown, that estrogen, in the anteroventral periventricular nucleus, increases histone H3 acetylation in the *Kiss1* promoter which coincides with estrogen-mediated transcriptional activation of the *Kiss1* gene (Tomikawa *et al.*, 2012; Uenoyama *et al.*, 2016). Indeed, Tomikawa *et al.*, 2012 found that histone H3 acetylation in the *Kiss1* promoter region of the anteroventral periventricular nucleus was much higher in proestrous (i.e. high levels of circulating estrogen) than in diestrous (i.e. low levels of circulating estrogen). In contrast, estrogen, in the arcuate nucleus, decreased the levels of histone acetylation at the *Kiss1* promoter (Tomikawa *et al.*, 2012; Uenoyama *et al.*, 2016). Therefore, the enrichment of Dax1, a corepressor, with transcriptional repressive properties and the ability to recruit other proteins that repress estrogen target gene trasncription (e.g. histone deacetylases), in the arcuate nucleus, could be mediating the differential effects of estrogen in the female hypothalamic nuclei.

3.3.2 Estrogen-Mediated Kiss1 Expression in the Arcuate Nucleus is Unique

It is interesting to note that, in the arcuate nucleus, estrogen treatment had almost exclusively upregulatory effects on the expression levels of the majority of the estrogen-target genes analysed using the RT^2 Profiler PCR Array Mouse Estrogen Receptor Signalling (QIAGEN, PAMM-005Z). However it is known, and we have demonstrated it here, that exposure to estrogen leads to *Kiss1* gene repression in the arcuate nucleus of the hypothalamus (not analysed in this array). Therefore, the *Kiss1* gene presents itself as a unique gene. Even though, it is known that estrogen-mediated *Kiss1* repression in the arcuate nucleus is importantfor the mechanisms that maintain reproduction and fertility, we are still not able to understand what drives differential transcription regulation of estrogen-target genes in the arcuate nucleus following estrogen treatment.

3.3.3 Dax1 Expression in the Arcuate Nucleus is Sexually Dimorphic

Mammals, including humans, exhibit enormous difference in anatomical, behavioural and psychological traits. It is well known that some species present with anatomical differences in the brain of males and females. For example, if we take into consideration the hypothalamic nuclei, the arcuate nucleus and the anteroventral periventricular nucleus. The female anteroventral periventricular nucleus is much larger and has a higher number of kisspeptin neurons than the male (Kauffman, 2013; d'Anglemont de Tassigny & Colledge, 2010). In contrast, the arcuate nucleus of rodents does not display sexually dimorphism regarding kisspeptin neuronal density or distribution. Therefore, we were surprised to find that Dax1 is enriched in the arcuate nucleus of female animals when compared to males (Kauffman, 2013; d'Anglemont de Tassigny & Colledge, 2010). This, most likely, highlights the importance of Dax1 in regulating the negative effects of estrogen in this hypothalamic nucleus which is essential for female fertility. While in males testosterone signalling in the arcuate nucleus is not thought to be an important factor for male fertility in the female estrogen-negative feedback is crucial for reproduction and fertility and therefore highlights as a potential important regulator of the estrogen-mediated transcriptional repression of *Kiss1* gene expression (Kauffman, 2013; d'Anglemont de Tassigny & Colledge, 2010).

3.3.4 The *In Vitro and Ex Vivo* Methods Currently Available to Explore the Mechanisms Underlying the Differential Effects of Estrogen in the Arcuate Nucleus and Anteroventral Periventricular Nucleus of the Hypothalamus Have Proved Unreliable and Inconsistent

In order to understand the mechanisms that regulate fertility (i.e. differential effects of estrogen on *Kiss1* expression) two female hypothalamic kisspeptin cell lines were generated from microdissected anteroventral periventricular nucleus (mHypoA-50) and arcuate nucleus (mHypoA-55) (Treen *et al.*, 2016). These cell lines were reported to present with, following immortalisation, relevant reproductive neuropeptides (e.g. Kiss1, ERα, ERβ, etc.) (Treen *et al.*, 2016). Further to this, studies using estrogen treatment, demonstrated that these cells respond to estrogen exactly as the female hypothalamic nuclei i.e. estrogen in the arcuate nucleus cell line (mHypoA-55) has repressive effects on *Kiss1* gene expression, whereas in the anteroventral periventricular nucleus estrogen exposure drives *Kiss1* gene expression. These cell lines, therefore, presented themselves as an ideal *in vitro* method to understand the mechanisms controlling estrogen signalling in the arcuate nucleus and anteroventral periventricular nucleus. However, our results show that these cells do not

represent a reliable method to investigate estrogen-mediated *Kiss1*-gene expression in the female hypothalamic nuclei. This is because over several months and a multitude of experiments we failed to consistently and reliably replicate the expected *Kiss1* gene expression levels in the arcuate nucleus and anteroventral periventricular nucleus following estrogen treatment. While some experiments yielded results that were consistent with the reported effects of estrogen in *Kiss1* gene expression in the anteroventral periventricular nucleus and the arcuate nucleus, the vast majority of experiments failed to do so and some even showed the polar opposite effects than those expected and published (i.e. estrogen increased *Kiss1* gene expression in the arcuate nucleus) (Treen *et al.*, 2016).
Several factors could account for this inability to consistently replicate the expected findings: (i) experimental set-up appears to be crucial, any slight change affected the ability of the cell lines to respond to estrogen treatment and regulate *Kiss1* gene expression in the expected manner, (ii) it is possible that the cell lines do not possess all the required components to drive estrogen-mediated regulation of the *Kiss1* gene, it is hypothesised that coregulators play an important role in the differential effects of estrogen, however so far it is not possible to ascertain which ones are the most important and if all of these are present in the immortalised cell lines, (iii) as the cells get older (through several number of passages) they might start to, gradually, loose some of the regulatory components necessary to drive *Kiss1* gene expression; (iv) even though a concentration study was performed to determine the appropriate estrogen dose to be applied to the kisspeptin cell lines, the amount of estrogen applied to the cells *in vitro* might differ from the estrogen concentration in the hypothalamus during the estrous cycle of a free-cycling animal and in this way we might not be replicating, with accuracy, the normal estrogen environment, (v) further to this it is possible to reason that even if the female hypothalamic cell lines preserved all of their gene-regulatory characteristics they might still behave differently as a result of the immortalisation process.

In order to address this issue we tried to develop an improved method, in this way we prepared organotypic brain slice cultures which were treated with estrogen. This was hypothesised to be an improved system to the so-known cell lines. The advantage of this system is that the tissue suffers minimal handling and therefore their composition (interactions) do not suffer any alterations. While the initial results were positive(i.e. with the tissues responding to estrogen in the predicted manner) the experiments that followed also rendered this method inconsistent and unreliable for studying Kiss gene expression, as there are technical challenges that might hinder the potential of this method. For example, it

is crucial that the time spent between the cardiac perfusion and placing the dissected brain on the microtome is as short as possible, because during this period the brain is not being oxygenated and therefore some cellular death is unavoidable. While we aimed to be as quick and effective as possible some animal variability might have led to more time being spent in this part of the protocol, causing cellular death and thus affecting our results.

Further to this, even though the concentration of estrogen used here was based on previous studies (Treen *et al.*, 2016) this concentration might differ significantly from the levels of estrogen present in the brain during the estrous cycle and therefore we might not be replicating the environment in the brain accurately, which might have hindered the arcuate nucleus and anteroventral periventricular response to estrogen.

It is also important to note that the organotypic brain slices used in these experiments were 800μm to 1000μm thick, the thickness of the samples combined with a lack of a blood system irrigating the tissues (as it happens in the free-living animal) could have affected the penetration of the estrogen treatment onto tissues and thus affecting the overall results.

3.3.5 The *Kiss1* Promoter

While the importance and role of kisspeptin in the control of reproduction and fertility is well understood and studied, much less is known about the transcriptional control of the *Kiss1* gene in the hypothalamus in general (Castellano *et al.*, 2014). In order to understand the mechanisms controlling *Kiss1* regulation within the brain it is important that the exact location of the promoter for the *Kiss1* gene is identified. In the mouse, the *Kiss1* promoter has been estimated using public databases depicting the beginning of exon 1 and from the alignment of transcript sequences, instead of specific detection methods (Castellano *et al.*, 2014).

The luciferase reporter assay is a common tool used to assess gene expression at the transcriptional level. Here, we tried to understand the mechanisms underlying *Kiss1* gene expression in the arcuate nucleus and anteroventral periventricular nucleus of the hypothalamus. For this purpose the mHypoA-50 and mHypoA-55 cell lines (anteroventral periventricular and arcuate nucleus, respectively) were transfected with a *Kiss1* reporter construct (1kb upstream and 200 base pairs bellow the *Kiss1* transcription start sites (TSSs)), in which the luciferase gene was fused downstream of the *Kiss1* promoter. In this experiment reporter's fluorescence within a transfected cell population is approximately proportional to the genes of interest mRNA levels. The idea here was to establish a method to investigate transcriptional regulation of the *Kiss1* and to test the role of Dax1, by far the most differently

expressed coregulator protein between the arcuate and anteroventral periventricular nuclei of the hypothalamus, on *Kiss1* gene expression. We consistently failed to detect any effects on *Kiss1* gene expression, regardless of the construct combinations used.

As showed previously, the mHypoA-50 and mhypoA-55 cell lines consistently failed to respond to estrogen treatment as expected and described in Treen *et al.*, 2016. Therefore it is feasible that failure to detect *Kiss1* gene could be due to the fact that these cells do not possess the necessary machinery to drive *Kiss1* gene expression. For this reason, we conducted the same experiments using different cell lines such as Hek293T (data not shown). However the results did not differ, no *Kiss1* transcriptional activity was detected following transfection with the various constructs. This could be because there is a generalised lack of knowledge in the field regarding the exact location of *Kiss1* gene promoter (d'Anglemont de Tassigny & Colledge, 2010). The *Kiss1* is located in close proximity to the *Golt1a* (golgi transport 1 homolog A) gene in most species. In humans and mice, the *Kiss1* gene consists of two coding exons downstream at least one noncoding exon. While the human *KISS1* promoter has been mapped immediately upstream of the noncoding exon (Huijbregts & De Roux, 2010; West *et al.*, 1998), the exact location of the *Kiss1* promoter in the mouse remains poorly understood and its regulation seems to be more complex than initial thought (d'Anglemont de Tassigny & Colledge, 2010).

While some groups report to have identified the mouse hypothalamic *Kiss1* promoter using the luciferase reporter assay, and have performed experiments at the level of *Kiss1* transcriptional regulation (Tomikawa *et al.*, 2012; Castellano *et al.*, 2014), the ensembl genome browser characterises the *Kiss1* gene as alternative spliced transcript of the *Golt1a* gene, indeed several alternatively spliced *Kiss1* transcripts have been identified containing sequences from the first exon of the *Golt1a* gene. Therefore, it is possible that, in the hypothalamus of rodents, *Kiss1* transcripts can be generated from *Kiss1* promoters and from *Golt1a* promoters (d'Anglemont de Tassigny & Colledge, 2010, personnal communication). While we did conduct luciferase reporter assay experiments using the *Golt1a* construct these were performed using the mHypoA-50 and mhypoA-55 cell lines and therefore this could explain the lack of *Kiss1* regulation (data not shown). Therefore further experiments are needed to pinpoint the exact *Kiss1* promoter in the mouse genome. Successful localisation of the *Kiss1* gene promoter in the mouse/rat, the two most commonly used model organisms in *Kiss1* research, is important as it would allow not only for an understanding of sex steroid-mediated regulation of *Kiss1* expression and understanding the subtleties of *Kiss1* gene expression but would also enable the generation of tissue-specific *Kiss1* knock out animals.

Nevertheless, alternative methods, for example *Kiss1* and *Grp54* knock out mice, have been used and have increased our understanding of *Kiss1*/*Grp54* signalling over the years and will continue to be used in order to enhance our understanding of this pathway.

3.4 Summary of Findings

- The female hypothalamic nuclei, arcuate nucleus and anteroventral periventricular nucleus, respond differently to estrogen.

- The corepressor Dax1, potentially, mediates estrogen differential regulation of *Kiss1* in the arcuate nucleus and anteroventral periventricular nucleus.

- The *in vitro* and *ex-vivo* methods available to study *Kiss1* gene expression are unreliable and inconsistent.

Results: Chapter 2 – Development and Characterisation of the *Kiss1*-Specififc Dax1 Knockout Mouse

4 Development and Characterisation of the *Kiss1*-Specific Dax1 Knockout Mouse

4.1 Introduction

Dax1, is an orphan member of the nuclear hormone receptor superfamily. It is expressed in the adrenal and in all the regions of the hypothalamic pituitary gonadal axis during development and in the adult animal. Dax1 is thought to play an important role in sexual development, reproduction and steroidogenesis (Jadhav, Harris & Jameson, 2011). Dax1 is encoded by *Nr0b1*, which a very simple genomic structure and can be found the X-chromosome. *Nr0b1* is composed by two exons: exon 1 and exon 2, which are 1168 and 245 base pairs (bp) long, respectively, separated by one intron (Burris, Guo & McCabe, 1996; McCabe, 2001). Dax1 is classified as an atypical member of the nuclear receptor family because it lacks some of the characteristic, conserved, domains present in the vast majority of nuclear hormone receptors (Aranda & Pascual, 2001; Arnal *et al.*, 2017; Yaşar *et al.*, 2017. Structurally, Dax1 does not have a DNA binding domain, the ligand-independent transactivation 1 (AF-1) domain and a hinge region (Niakan & McCabe, 2005). Instead, Dax1 is composed by two main structures: (i) a carboxyl-terminal domain (CTD) which is homologous to the ligand binding domain of nuclear receptor with a ligand-dependent transactivation domain (AF-2), and (ii) an amino-terminal domain (NTD) which is a unique structure. It consists of three complete and one incomplete alanine-glycine rich repeats motifs of (65-67 amino acids long each), each repeat also contains a short leucine motif, LxxLL (Iyer & McCabe, 2004; Aranda & Pascual, 2001; Arnal *et al.*, 2017; Yaşar *et al.*, 2017; Kumar *et al.*, 1987; Krust *et al.*, 1986; Ylikomi *et al.*, 1992; La Rosa & Acconcia, 2011; Brzozowski *et al.*, 1997; Wurtz *et al.*, 1996) (Niakan & McCabe, 2005; Iyer & McCabe, 2004) .

Nuclear receptors are transcription factors that regulate expression of genes in response to both extracellular and intracellular signals (i.e. ligands) (Zhang *et al.*, 2000). Ligand binding to the receptor leads specific conformational changes that activate the receptor enabling dimerisation and consequent interaction with hormone response elements on target genes. Nuclear receptors recruit and interact with coregulators to regulate target gene expression (Millard *et al.*, 2013). Coregulatory proteins (coregulators) are important regulators of target gene expression. They can be divided into coactivators and corepressors depending on their overall effect on gene expression. The first are factors that interact with nuclear receptors and enhance transactivation of target genes. Whereas, corepressors are proteins that interact with nuclear receptors and inhibit target gene transcription. Coactivators and corepressors interact with the hydrophobic groove of the ligand binding domain of nuclear receptors

through conserved regions, LxxLL (the nuclear receptor box, where L is leucine and x is any amino acid) and LxxH/IIxxxI/L (the CoRNR box), respectively (Millard *et al.*, 2013; Heery *et al.*, 1997; Hu & Lazar, 1999; Nagy *et al.*, 1999). They bring about their effects on target gene expression through the recruitment of enzymes that carry-out post-translational modifications of histone tails, thus modifying the accessibility of the transcriptional machinery to the response elements on target genes (Gronemeyer, Gustafsson & Laudet, 2004; Aranda & Pascual, 2001; Mckenna, Lanz & O'Malley, 1999; Martin & Cardoso, 2010). Histone acetylation, phosphorylation, methylation and ubiquitination are the best-known histone modifications regulated by coregulators (Millard *et al.*, 2013). Acetylation/deacetylation of histone tails is the best-described mechanism. This is the process by which acetyl groups are added/removed to lysine residues on histone tails (Xhemalce, Dawson & Bannister, 2011). These reactions are catalysed, respectively, by histone acetyltransferases (HATs) and histone deacetylases (HDACs) (Martin & Cardoso, 2010; Millard *et al.*, 2013; Xhemalce, Dawson & Bannister, 2011). Addition of acetyl groups is mediated by histone acetyltransferases (HATs), which alters the conformation of the chromatin from a compact to an open and transcriptionally active structure. In this new conformation the response elements are exposed and the transcriptional machinery can bind and drive gene expression (Martin & Cardoso, 2010; Millard *et al.*, 2013; Xhemalce, Dawson & Bannister, 2011). Histone acetylation is associated with coactivators. Conversely, corepressors recruits histone deacetylases (HDACs) to remove acetyl groups from lysine residues leading to a compact and transcriptionally inactive chromatin (Martin & Cardoso, 2010; Millard *et al.*, 2013; Verdin & Ott, 2015; Xhemalce, Dawson & Bannister, 2011).

Dax1 is an unique nuclear receptor because it binds and interacts with other, activated, nuclear receptors to regulate their transcriptional activity and it this way regulate expression of their target genes (Crawford *et al.*, 1998; Zhang *et al.*, 2000). Dax1 is a potent corepressor of nuclear hormone receptors. The principal mechanism by which Dax1 mediates its transcriptional repression action on nuclear receptors is as follows: Dax1 interacts with the transactivation domain 2 (AF-2), on the ligand-binding domain of the activated nuclear receptors, via the short leucine rich motif (LxxLL, found in coactivators). Dax1 competes with coactivators for the coactivator binding groove, displacing them, and antagonising the protein-protein interactions driving gene expression. Transcriptional repression is achieved by Dax1's potent silencing functions (harboured in its C-terminal ligand binding domain-like structure) as well as Dax1-mediated recruitment of corepressors and proteins with

transcriptional repressive activities to DNA-bound nuclear receptors (e.g. Alien, N-CoR, and many others) (Crawford *et al.*, 1998; Zhang *et al.*, 2000).

Dax1 expression has been mapped to the ovary, testis, hypothalamus, pituitary and adrenal, which are all estrogen responsive genes. Further to this Dax1 and estrogen receptor alpha expression overlaps, in the ovaries and testis, during development. These observations raised questions about Dax1's ability to interact with estrogen receptors and modulate its transcriptional activity and consequently expression of its target genes (Bae *et al.*, 1996). Indeed, Dax1, via the short leucine motif (LxxLL), binds to the coactivator binding groove preventing interaction between the estrogen receptor and its coactivators. Dax1 then recruits other corepressors in order to exacerbate its repressive effects on the transcriptional activity of estrogen receptor (Zhang *et al.*, 2000). Considering that estrogen is a key steroid in the regulation of fertility and reproduction, the repressive effects of Dax1 on the transcriptional activity of estrogen receptor highlights Dax1 as an important regulator of reproduction.

Many of the animals studies performed, using Dax1-deficient mice, focused on the male, which presented with hypogonadotropic hypogonadism and were infertile (Yu, Ito & Jameson, 2014). The findings have defined Dax1 as a testis-determining gene, essential for testis development and function but not for ovarian development (Bouma, 2005; Yu, Ito & Jameson, 2014; Jadhav, Harris & Jameson, 2011). However, the roles of Dax1 in the adult female has not been properly investigated, and there is suggestion, that Dax1 might have a role as a regulator of steroid synthesis during the estrous cycle, as Dax1-deficient female mice presented with slight follicular defect (Iyer & McCabe, 2004; Yu, Ito & Jameson, 2014). Therefore, the role of Dax1 in reproduction requires further investigation.

4.2 Results

4.2.1 Generation of Animals with Specific Knockout of Dax1 in Kisspeptin Cells

In order to assess the role of Dax1 in female reproduction, Dax1 was deleted specifically from kisspeptin cells, which are mostly expressed in the ARC and AVPV. We therefore generated C57BL/6J mice lacking exon 2 of the Dax1 (*Nr0b1*) gene, essentially as described (Bouma, 2005). Briefly, the Cre/loxP technology was employed, given that Cre recombinase excises any region of DNA that is between two loxP sites (a 34 bp nucleotides that can be genetically inserted around an essential exon in a gene), Dax1 floxed mice (a floxed PGK-neomycin resistance cassette was introduced on either side of exon 2 of the mouse *Nr0b1* locus and a third loxP site was inserted upstream of the splice acceptor signal in exon 2) were purchased from Jackson Laboratory and bred to homozygosity so that both alleles of all cells were floxed (Figure 31). These animals were then crossed with mice expressing Cre recombinase downstream of the Kiss1 promoter (heterozygous), to ensure that Dax1 deletion is limited and specific to kisspeptin expressing cells (*Kiss1-CreGFP* (Jackson Laboratory, stock #017701)) (Gottsch *et al.*, 2011) (Figure 31). In this way, control (Dax1^{tm}) and knockout (Dax1$^{tm(Kiss1)}$) mice were generated.

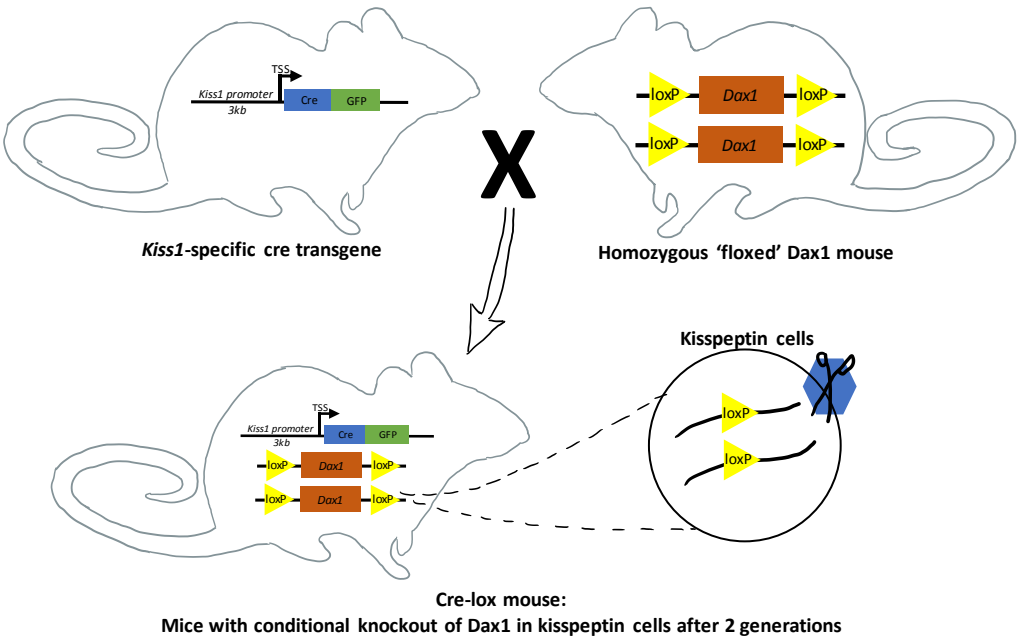

Figure 31: Knockout strategy used to generate mice with conditional knockout of Dax1 in kisspeptin cells.

4.2.1.1 Confirmation of Conditional Knockout of Dax1 in Kisspeptin Cells of the Arcuate Nucleus by RT-qPCR

The microarray and gene expression data obtained and described in Chapter 3 shows that Dax1 is enriched in the arcuate nucleus when compared with the anteroventral periventricular nucleus. Therefore from this moment onwards the arcuate nucleus, unless otherwise stated, will be the main focus of the experiments and results mentioned.

In order to assess if the gene deletion strategy yielded the desired outcomes, *Dax1* gene expression, relative to the housekeeping gene cyclophilin, was assessed in the arcuate nucleus of the hypothalamus. Bilateral arcuate snap frozen tissue samples were dissected from Dax1 control ($Dax1^{tm}$) and knockout ($Dax1^{tm(Kiss1)}$) mice at different stages of the estrous cycle, either at a random stage of the cycle, during estrous and/or during diestrous (Figure 32).

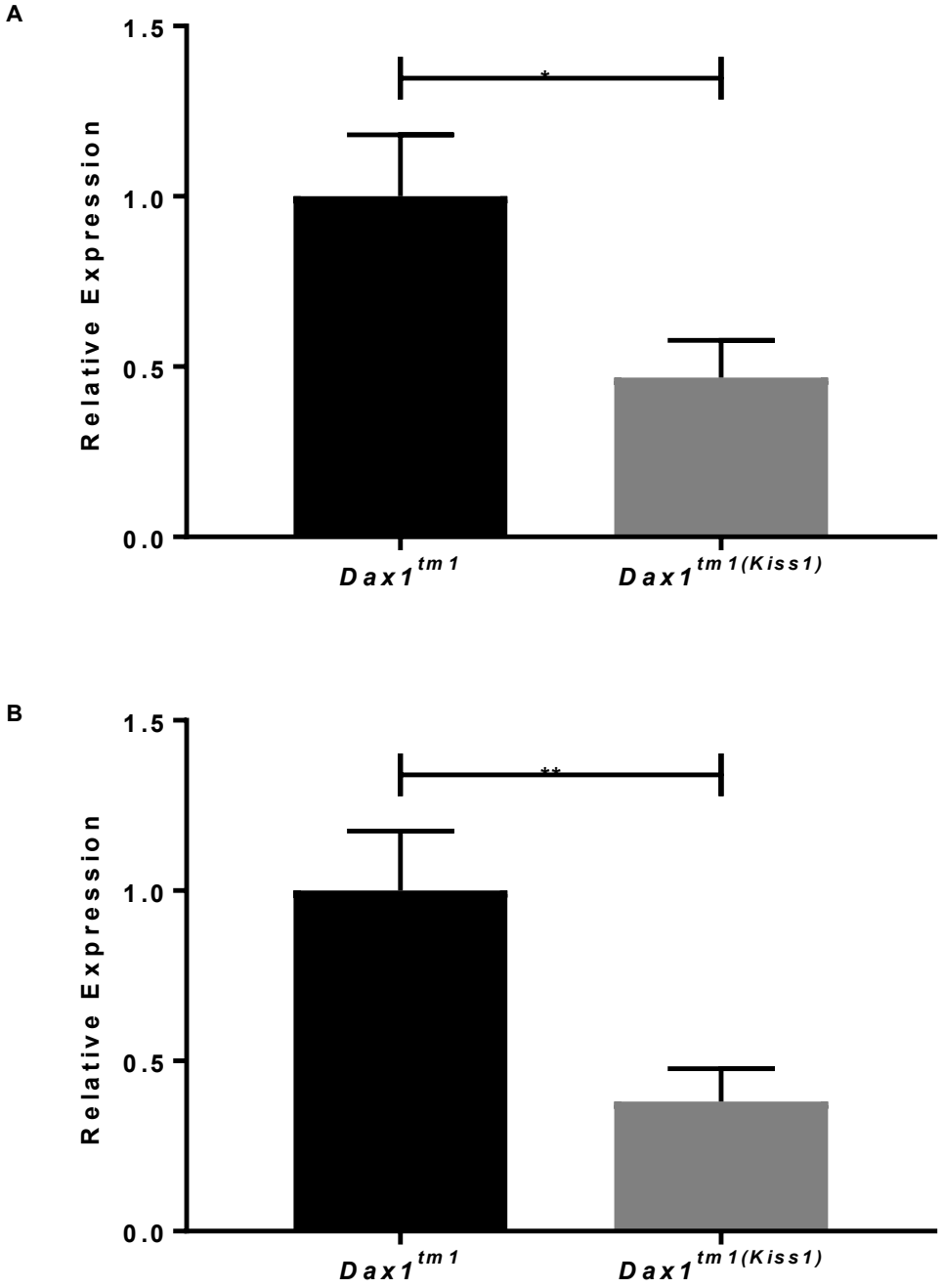

Figure 32: Dax1 expression in the Arcuate nucleus of Dax1^{tm} and Dax1$^{tm(Kiss1)}$ at different stages of the estrous cycle.

A: *Dax1 mRNA expression in the arcuate nucleus of Dax1^{tm} and Dax1$^{tm(Kiss1)}$. Samples for this experiment were collected at a random stage of the estrous cycle. p=0.0169*.* ***B:*** *Dax1 mRNA expression in the arcuate nucleus of Dax1^{tm} and Dax1$^{tm(Kiss1)}$. Samples for this experiment were collected during Diestrous. p=0.005*. Data are expressed as relative expression ± SEM, Student's t-test was the statistical method used,* ***A:*** *n=17,* ***B:*** *n=10-11.*

As it can be seen in Figure 32, Dax1 expression was significantly decreased in mice with conditional knockout of Dax1 in kisspeptin cells ($Dax1^{tm(Kiss1)}$), regardless of the stage of the cycle the animals are in. In diestrous, Dax1 mRNA expression in $Dax1^{tm(Kiss1)}$ mice decreased by 61% (p=0.005) (Figure 32B), while when we analysed the samples collected at a random stage of the estrous cycle, Dax1 mRNA expression in the arcuate nucleus decreased by 53% (p=0.0169) (Figure 32A).

4.2.1.2 Confirmation of Conditional Knockout of Dax1 in Kisspeptin Cells of the Arcuate Nucleus by Immunofluorescence

Figure 32, shows a 61% and 53% significant decrease (depending on the stage of the estrous cycle) in Dax1 expression in mice with conditional knockout of Dax1 in kisspeptin cells ($Dax1^{tm(Kiss1)}$). It is important to take into consideration that these values are a reflection of total *Dax1* expression in the arcuate nucleus. Therefore, in to assess if the gene deletion strategy was successful in kisspeptin cells, immunofluorescence colocalisation experiments were performed. Arcuate nucleus sections (40µm thick) from $Dax1^{tm}$ and $Dax1^{tm(Kiss1)}$ animals were collected and prepared for immunofluorescence. The samples were incubated with two antibodies: the Anti-DAX1, clone 2F4 antibody (Merck, MABD398) (1:100), used to detect Dax1 in the sample and the GFP Polyclonal Antibody, Alexa Fluor 488 (ThermoFisher Scientific, A-21311) (1:100), which was used to target kisspeptin cells, as the Kiss1-CreGFP mouse construct is tagged with enhanced GFP and thus provides an easy way to identify Kiss1 neurons through anti-GFP staining. Samples were also incubated the nuclear stain (DAPI) (Figure 33).

DAPI
Dax1
Kiss1
Merged
Dax1tm1
Dax1tm1(Kiss1)
A
B
C
D
E
F
G
H
B1
D1
F1
H1

Figure 33: Representative image of Dax1 expression in the Arcuate nucleus of Dax1^{tm} and Dax1$^{tm(Kiss1)}$ animals.

A - D: *Dax1 protein expression in the arcuate nucleus of Dax1^{tm} mice. Samples for this experiment were collected at a random stage of the estrous cycle. n=3.* ***E - H:*** *Dax1 protein expression in the arcuate nucleus of Dax1$^{tm(Kiss1)}$ mice. Samples for this experiment were collected at non-specific stage of the estrous cycle. n=3.* ***A and E:*** *Pictures of the nuclear counter stain DAPI in Dax1^{tm} samples (**A**) and in Dax1$^{tm(Kiss1)}$ samples (**B**).* ***B and F:*** *Dax1 staining in Dax1^{tm} samples (**B**) and in Dax1$^{tm(Kiss1)}$ samples (**F**) can be seen in red. The staining is mainly cytoplasmic with some cells displaying nuclear localisation. The Anti-DAX1, clone 2F4 antibody (1:100) was used.* ***C and G:*** *Kiss1 staining in Dax1^{tm} samples (**C**) and in Dax1$^{tm(Kiss1)}$ samples (**G**) can be seen in green. The GFP Polyclonal Antibody, Alexa Fluor 488 (1:100) was used.* ***D and H:*** *Nuclear (blue), Dax1 (red) and Kiss1 (green) staining in Dax1^{tm} samples (**D**) and in Dax1$^{tm(Kiss1)}$ samples (**H**) were merged together to facilitate co-localisation observation of Dax1 and Kiss1. Images were acquired using the Zeiss LSM-780 Inverted Confocal Microscope (Zeiss), 20x magnification, z-stack. Image processing was performed using the ImageJ (Fiji) software.*

Figure 33 is a representative image of the colocalisation experiments carried out, Dax1 is strongly expressed in the control sample (Figure 33B). In this image, Dax1 expression is mainly cytoplasmic (white arrow), but nuclear localisation of Dax1 is also seen in some cells (blue arrow). Figure 33D clearly shows that the vast majority kisspeptin also express Dax1, and therefore colocalisation can be seen.

If we look at Dax1tm$^{(Kiss1)}$ there was an overall decrease in Dax1 expression across the arcuate nucleus (Figure 33G) which correlates with the mRNA results obtained in Figure 32. Not only there was an overall decrease in Dax1 expression, but most of the kisspeptin cells no longer express Dax1 (Figure 33H). Here too, Dax1 is mainly seen in the cytoplasm of cells (white arrow), with some cells displaying nuclear localisation of Dax1 (blue arrows).

4.2.1.2.1 Quantification of Kisspeptin Cells that Expressing Dax1

To confirm knockout of Dax1 in kisspeptin cells, the immunofluorescent data above presented (Figure 33) was quantified. The data was presented as percentage of kisspeptin neurons that express Dax1 in the Dax1^{tm} and Dax1$^{tm(Kiss1)}$ groups (Figure 34). This was done by quantifying the total number of kisspeptin cells across the arcuate nucleus and then determining how many of these expressed Dax1.

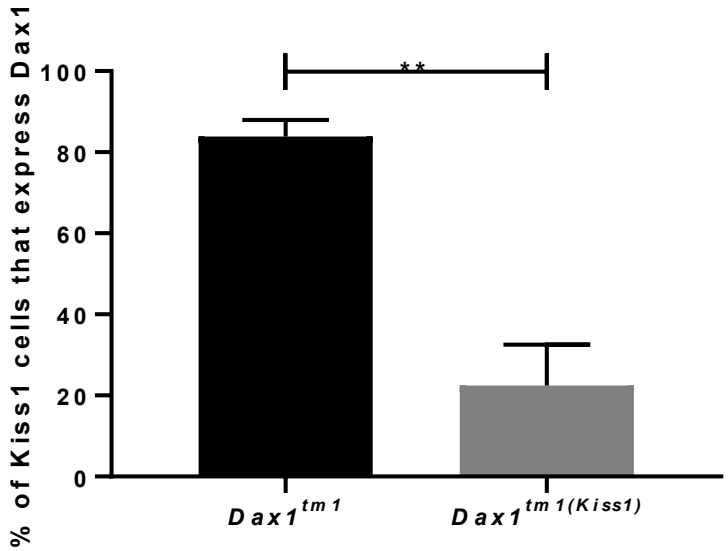

Figure 34: Percentage of kisspeptin cells that express Dax1 in the arcuate nucleus of Dax1^{tm} and Dax1$^{tm(Kiss1)}$ animals.

Kisspeptin cells across the arcuate nucleus of Dax1^{tm} and Dax1$^{tm(Kiss1)}$ animals were analysed and then quantified in order to calculate the percentage of kisspeptin cells that colocalise with Dax1. Data is expressed as percentage ± SEM, Student's t-test was the statistical method used, n=3.

Figure 34 is a graphical representation of the percentage of kisspeptin cells that express Dax1 in the control and knockout group. As it can be seen the majority (84%) of kisspeptin cells in the arcuate nucleus of Dax1^{tm} animals expressed Dax1, this was not the case with kisspeptin neurons in the arcuate nucleus of Dax1$^{tm(Kiss1)}$ with only 22% of these neurons expressing Dax1, with this difference being statistical different p=0.0048. This residual expression of Dax1 could be due to incomplete deletion of Dax1 in kisspeptin cells but it, most likely, reflects the challenging and biased nature of analysing and quantifying these cells, as seen by the range of percentages obtained from the three animals analysed: 27.29%, 34.32% and 3.291%.

Thus the results show that the knocking out strategy employed in this project significantly reduced Dax1 mRNA expression (by 61% in diestrous and 53% in a non-specific stage of the cycle) (Figure 32) but, most importantly, significantly reduced Dax1 expression in the kisspeptin cells of the arcuate nucleus of $Dax1^{tm(Kiss1)}$ animals (by 73.8%) when compared to $Dax1^{tm}$(Figure 34).

4.2.2 Kisspeptin Cells-specific Dax1 Knockout Decreased Kiss1 Gene Expression in the Arcuate Nucleus

Further to looking at the levels of Dax1 mRNA in the $Dax1^{tm}$ and $Dax1^{tm(Kiss1)}$ mice kisspetin mRNA expression was also measured. Kiss1 gene expression, relative to the housekeeping gene cyclophilin, was assessed in the arcuate nucleus of the hypothalamus. Here too, bilateral arcuate snap frozen tissue samples were dissected from Dax1 control ($Dax1^{tm}$) and knockout ($Dax1^{tm(Kiss1)}$) mice at different stages of the estrous cycle, either at a random stage of the cycle, during estrous and/or during diestrous (Figure 35).

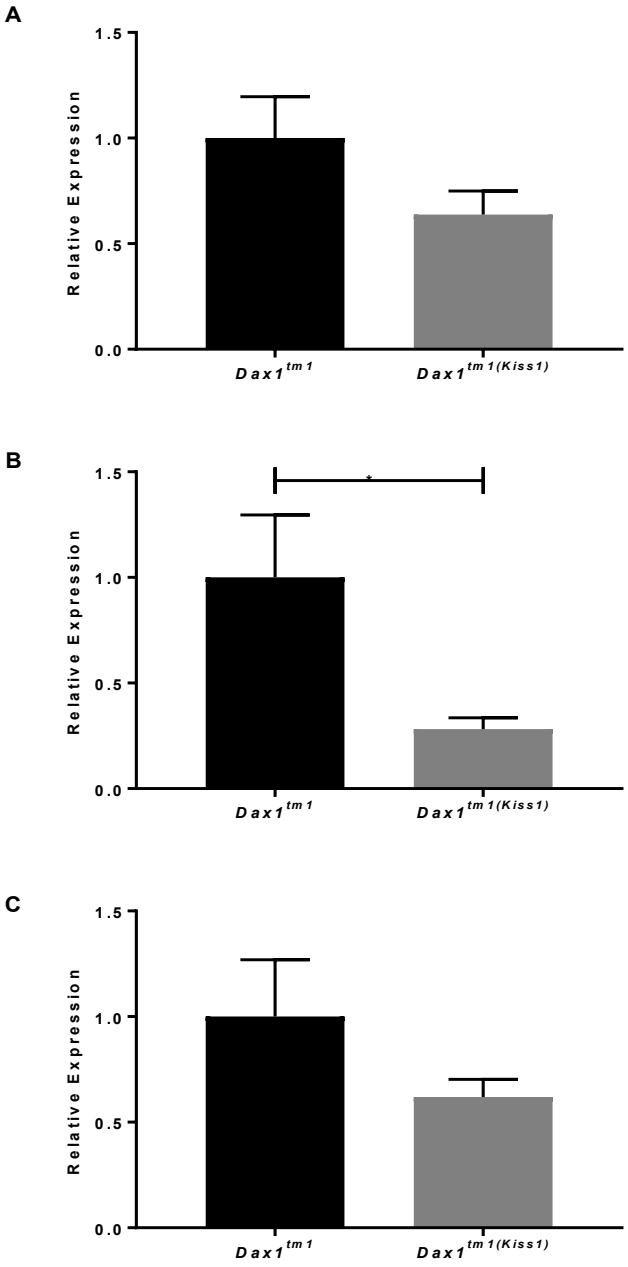

Figure 35: Kiss1 expression in the Arcuate nucleus of Dax1^{tm} and Dax1$^{tm(Kiss1)}$ at different stages of the estrous cycle.

A: *Kiss1 mRNA expression in the arcuate nucleus of Dax1^{tm} and Dax1$^{tm(Kiss1)}$. Samples for this experiment were collected at a random stage of the estrous cycle. p=0.1120.* ***B:*** *Kiss1 mRNA expression in the arcuate nucleus of Dax1^{tm} and Dax1$^{tm(Kiss1)}$. Samples for this experiment were collected during Diestrous. p=0.0484*.* ***C:*** *Kiss1 mRNA expression in the arcuate nucleus of Dax1^{tm} and Dax1$^{tm(Kiss1)}$. Samples for this experiment were collected during the Estrous stage of the cycle. p=0.1988. Data is expressed as relative expression ± SEM, Student's t-test was the statistical method used,* ***A:*** *n=17,* ***B:*** *n=10-11,* ***C:*** *n=8.*

Knocking out Dax1 in kisspeptin cells led to a trend towards decreased *Kiss1* mRNA expression in the arcuate nucleus of *Dax1*$^{tm(Kiss1)}$ when compared to control animals (*Dax1*^{tm}), regardless of the stage of the cycle the animals were in at the time of sample collection (Figure 35A-C). Nevertheless, the decrease in *Kiss1* gene expression between the control and knockout group was only significant when arcuate samples were collected in diestrous ($p=0.0484$), in this stage of the estrous cycle *Kiss1* mRNA levels decreased by 72% in the *Dax1*$^{tm(Kiss1)}$ group (Figure 35B). Even though not significant, *Kiss1* mRNA expression was also decreased in the arcuate samples collected at a non-specific stage of the and during the estrous stage of the cycle by 36% and 38%, respectively (Figure 35A, B).

It is also interesting to note that the biggest decrease in *Dax1* mRNA expression, by 61%, (Figure 32B) also correlates with the biggest decrease in *Kiss1* mRNA expression (72%) (Figure 35B).

4.2.3 Assessing Reproductive Phenotype in Mice with Conditional Knockout of Dax1 in Kisspeptin Cells

Animals used for these experiments were weaned from their parent cage at 13 days after birth, they were immediately genotyped and allocated into two groups Dax1^{tm} and Dax1$^{tm(Kiss1)}$, according to their genotype. The animals were subsequently single housed and they were followed for a total of 16 weeks. During this time several different phenotypic aspects were analysed.

4.2.3.1 Age and Body Weight at Onset of Puberty Was Normal in Mice with Conditional Knockout of Dax1 in Kisspeptin Cells

The age at which animals reached puberty was the first parameter to be measured. In female mice, vaginal opening is used as an external index of puberty onset (Ojeda & Urbanski, 1994). Vaginal opening is an apoptosis-driven event, which results from increased secretion of estradiol, this process can be induced precociously in mice by estradiol injections into immature mice (Rodriguez *et al.*, 1997). In mice, vaginal opening can, but it is often not the case, synonymous of with the day of first ovulation. The first ovulation may occur up to 10 days after vaginal opening (i.e. onset of puberty) (Nelson *et al.*, 1982).

The age of vaginal opening in mice was documented by monitoring mice every morning from the 14 days of age until mice reached puberty. Simple visual examination of the vulva is enough to detect the onset of puberty, in mice vaginal opening occurs at between 26 and 30 days old (Caligioni, 2009).

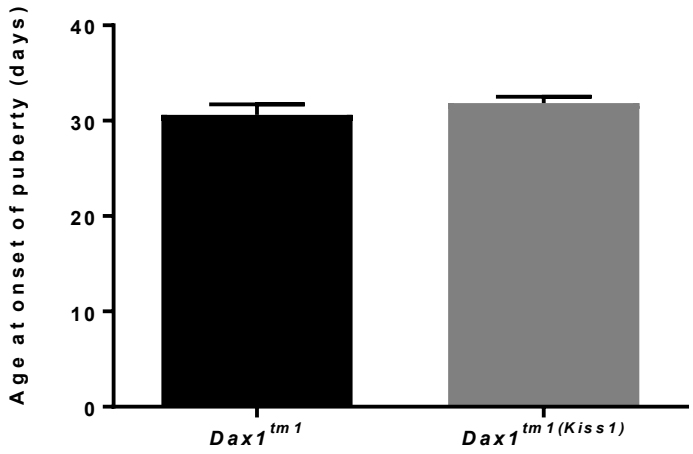

Figure 36: Age at onset of puberty.

Data is expressed in days ± SEM, Student's t-test was the statistical method used, n=5-12.

Analysis of vaginal opening revealed that the two groups, Dax1^{tm} and Dax1$^{tm(Kiss1)}$, went through puberty at a similar age, 31 and 32 days old, respectively (Figure 36). Therefore, knocking out *Dax1* in kisspetin cells did not have a significant effect on the onset of puberty (p=0.3454).

It is thought that body weight can impact timing of onset of puberty for this reason the body weight of these animals, on the day of onset of puberty, was also recorded (Figure 37).

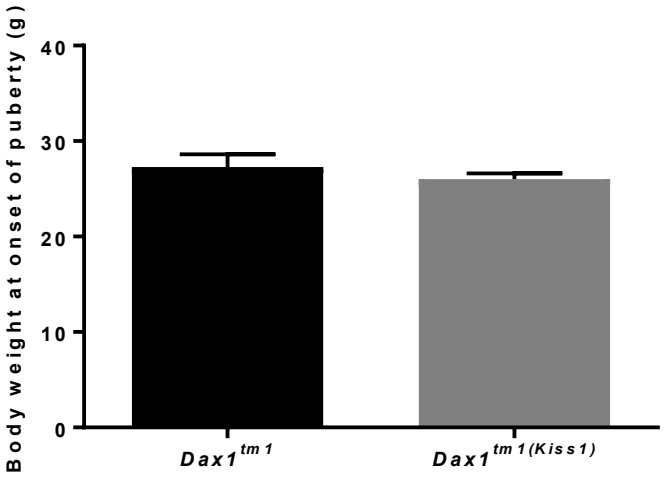

Figure 37: Body weight of Dax1^{tm} and Dax1$^{tm(Kiss1)}$ animals at onset of puberty.

Mean body weight, at the day of onset of puberty, was recorded and compared between the two groups, control animals (Dax1^{tm}) (black bar) and knockout animals (Dax1$^{tm(Kiss1)}$) (grey bar). Data is expressed in grams ± SEM, Student's t-test was the statistical method used, n=5-11.

Body weight, at onset of puberty, was not significantly different between control animals and mice with conditional knockout of Dax1 in kisspeptin cells (p=0.3282) (Figure 37). Dax1$^{tm(Kiss1)}$ animals (grey bar) weighed 27.3g ± 1.3g while Dax1$^{tm(Kiss1)}$ were slight lighter at 26.0g ± 0.6g. The body weight of these animals was monitored every week for the duration of the study (data not shown). There were no significant differences in the body weight of Dax1^{tm} and Dax1$^{tm(Kiss1)}$ animals.

4.2.3.2 Knocking Out Dax1 in Kisspeptin Cells Leads to Estrous Cycle Abnormalities

Following analysis of age at onset of puberty, body weight and reproductive ability, the focus turned onto analysing and comparing the estrous cycle of Dax1^{tm} and Dax1$^{tm(Kiss1)}$ animals.

In mice, estrous cycle analysis involves following the animals for a period of time and collecting daily information regarding the stage of the estrous cycle that the animal is in. Vaginal cytology is used to determine the stage of the estrous cycle, this method enables predicting the stage of the estrous cycle according to the proportion of three types of cells obtained upon a vaginal smear: cornified cells, epithelial cells and leukocytes (Figure 38). Briefly, in proestrous, the pre-ovulatory day, there is a predominance of nucleated epithelial cells (**N**), some cornified cells (**C**) may also appear in the sample (Figure 38a). The estrous stage of the cycle is distinctively characterised by cornified squamous epithelial cells (**C**) which cluster together (Figure 38b). Cornified squamous epithelial cells (**C**) have no visible nucleus, the cytoplasm is granular and their shape is irregular. The following stage of the cycle, the metestrous, is characterised by a mixture of all three types of cells: leukocytes (**L**), cornified (**C**), and nucleated epithelial cells (**N**) but by far the most predominant are the leucocytes (Figure 38c). Vaginal smears collected from the final stage of the estrous cycle, diestrous, is mainly composed of leukocytes (**L**) (Figure 38d) (Caligioni, 2009).

Vaginal smears were obtained by, gently, flushing the vagina three to five times with PBS 1x and collecting the final flush, which was then placed on a slide and analysed under a light microscope using a 10x objective. The proportion of the previously described cells was assessed and thus enabled identification of the stage of the estrous that the animals were in.

Because some stages of the estrous cycle are quite short, vaginal swabs were collected every day at the same time.

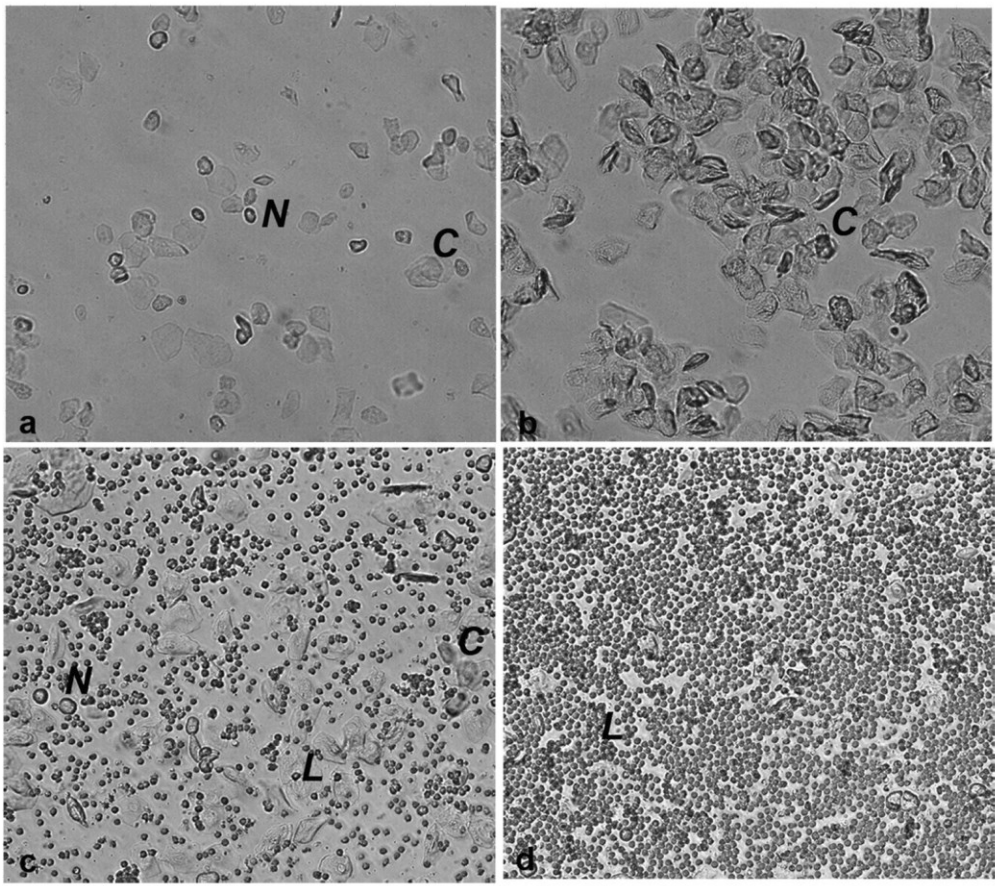

Figure 38: Photomicrographs of vaginal secretions from mice at different stages of the estrous cycle.

a: *Photomicrograph of mice in the Proestrous stage of the estrous cycle. Proestrous is mainly characterised by nucleated epithelial cells (**N**).* ***b:*** *Photomicrograph of mice in the Estrous stage of the estrous cycle. This stage is characterised by anucleated cornified cells (**C**).* ***c:*** *Photomicrograph of mice in the Metestrous stage of the estrous cycle. The Metestrous is characterised by the presence of the three types of cells: leukocytes (**L**), cornified (**C**), and nucleated epithelial cells (**N**).* ***d:*** *Photomicrograph of mice in the Diestrous stage of the estrous cycle. Vaginal smears collected from this stage of the esrous cycle is composed by leucocytes, predominantly.* ***Legend:*** *Nucleated epithilial cells (**N**), leukocytes (**L**) and cornified cells (**C**). Image from Caligioni, 2009.*

4.2.3.2.1 Mice with Conditional Knockout of Dax1 in Kisspeptin Cells Had Longer Estrous Cycles and as a Consequence Went Through Less Rounds of Estrous Cycles

As previously mentioned, daily collection and examination of vaginal smears from Dax1^{tm} and Dax1$^{tm(Kiss1)}$ animals enabled identification of the stage of the estrous that the animals were in. This was done for a total of 16 weeks and the data collected was subsequently analysed. The estrous cycle length of Dax1^{tm} and Dax1$^{tm(Kiss1)}$ animals was the first parameter to be analysed (Figure 39). In mice, the estrous cycle lasts approximately 4 to 6 days (Caligioni, 2009; Yen, 1977). It was important what is meant by a full estrous cycle, in this study, a full cycle was defined as observing at least three stages of the cycle in the right order, with estrous and diestrous being two of those stages. The number of days to that took to fulfil this criteria defined the length of the estrous cycle.

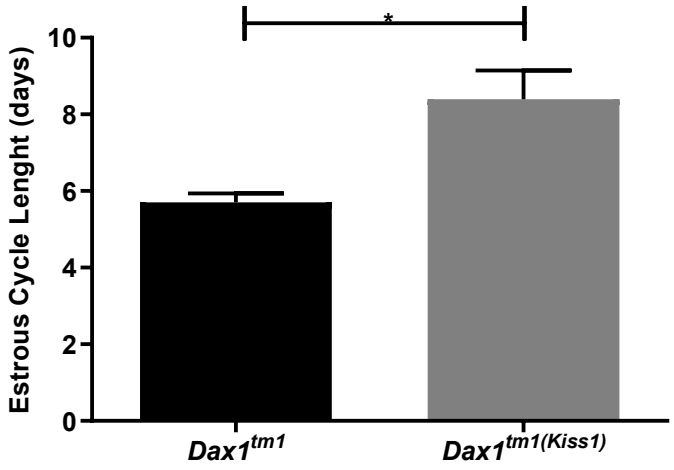

Figure 39: Estrous cycle length of Dax1^{tm} and Dax1$^{tm(Kiss1)}$ animals.

Vaginal cytology was used to determine the stages of the estrous cycle for each of the groups: Dax1^{tm} (black bar) and Dax1$^{tm(Kiss1)}$ (grey bar). In this study, a full cycle was defined as observing at least three stages of the cycle in the right order, with estrous and diestrous being two of those stages. The number of days to that took to fulfil this criteria defined the length of the estrous cycle. Data is expressed in days ± SEM, Student's t-test was the statistical method used, n=5-12.

The estrous cycle of animals with conditional knockout of Dax1 in kisspeptin neurons (Figure 39, black bar) was 8 ± 0.7 days long which is significantly longer (p=0.0393) than the estrous cycle of control animals, which was 6 ± 0.2 days long (Figure 39, grey bar). As a consequence,

the number of full estrous cycles recorded throughout the duration of the study was significantly lower (p=0.0078) in Dax1$^{tm(Kiss1)}$ when compared to those documented for control animals (Dax1^{tm}) (Figure 40). Dax1$^{tm(Kiss1)}$ went through 5 full estrous cycles while data collected for Dax1^{tm} animals show that, in the same period, Dax1^{tm} animals went through two more cycles (7 estrous cycles in total) (Figure 40).

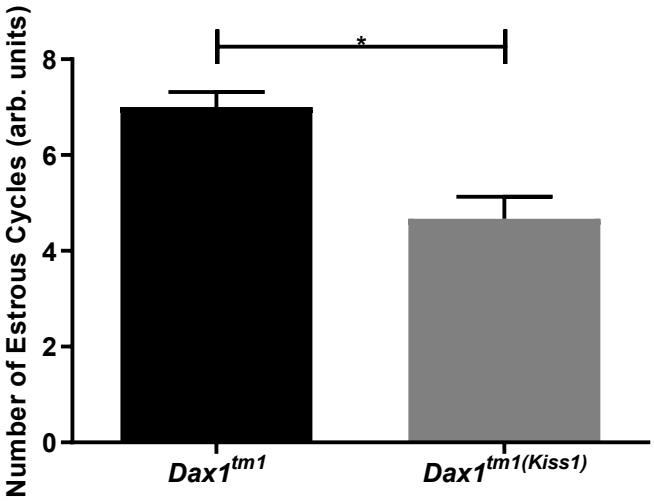

Figure 40: Number of estrous cycles reported in Dax1^{tm} and Dax1$^{tm(Kiss1)}$ animals.

The number of full estrous cycles reported for Dax1^{tm} (black bar) and Dax1$^{tm(Kiss1)}$ (grey bar) animals. Data is expressed as mean number of full estrous cycles in arbitrary units ± SEM, Student's t-test was the statistical method used, n=5-12.

4.2.3.2.1.1 Dax1$^{tm(Kiss1)}$ Animals Spent Significantly More Time in the Estrous Stage of the Reproductive Cycle

Data collected from daily vaginal smears was used to determine, per cycle, the time spent in each stage of the reproductive. The significant difference in estrous cycle length of Dax1^{tm} and Dax1$^{tm(Kiss1)}$ animals can be explained by the fact that mice with conditional knockout of Dax1 spent more days in the estrous stage of the cycle per cycle than control animals, 3 ± 0.3141 and 2 ± 0.2101 days, respectively (p=0.05) (Figure 41A). The mean number of days per cycle spent in the other stages of the estrous cycle was not significantly different between Dax1^{tm} and Dax1$^{tm(Kiss1)}$ animals. Figure 41B, is a graphical representation of the time, in days, spent in diestrous by animals of the two groups. As previously mentioned, this time was not significantly different (p=0.1188) with Dax1^{tm} animals (Figure 41B, black bar) spending one and a half days in diestrous and Dax1$^{tm(Kiss1)}$ animals (Figure 41B, grey bar) spending, on average, 2 days in diestrous.

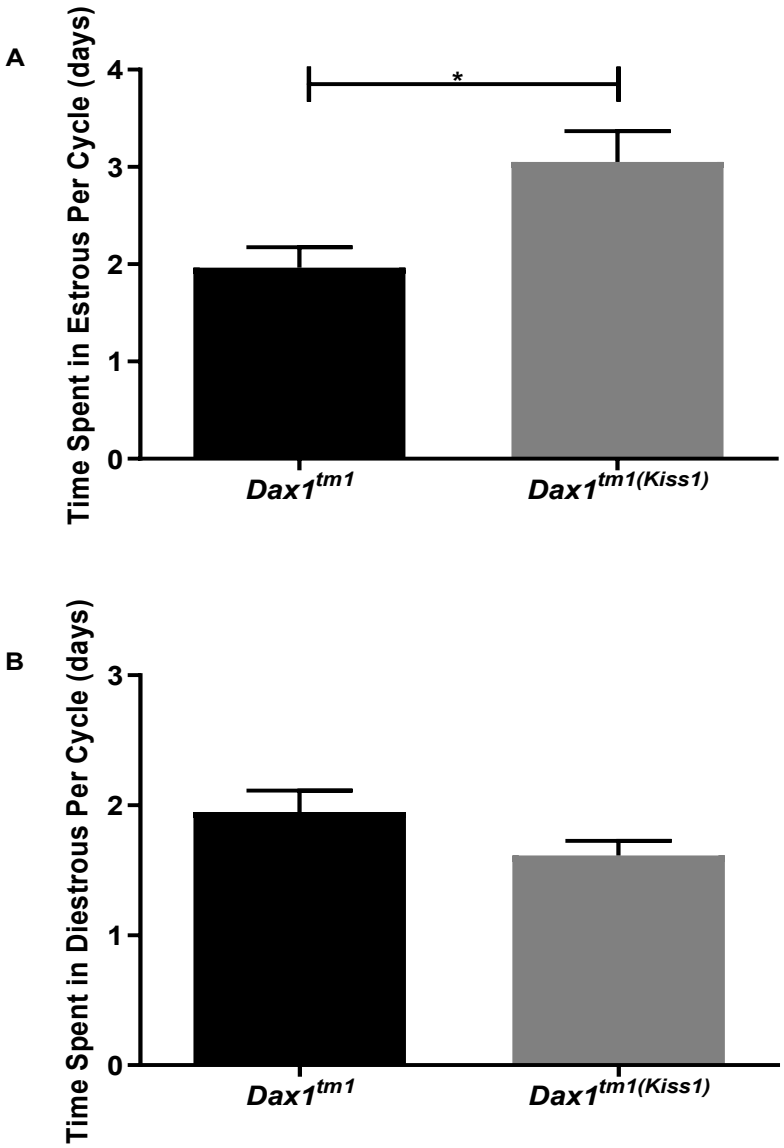

Figure 41: Time spent in different stages of the estrous cycle per cycle.

Data collected from daily analysis of vaginal cytology was used to determine the time spent in each stage of the cycle per cycle. ***A:*** *Number of days spent in estrous per cycle. Mice with conditional knockout of Dax1 in kisspeptin cells spent more time in the estrous stage of the cycle (3 ± 0.3141 days) (grey bar), on average 1 day, than Dax1^{tm} animals (2 ± 0.2101 days) (black bar). p=0.05** ***B:*** *Number of days spent in diestrous per cycle. Dax1^{tm} (black bar) spent one and a half days in diestrous while Dax1$^{tm(Kiss1)}$ (grey bar) spent, on average, two days in diestrous. p=0.1188. Data is expressed as mean number days ± SEM, Student's t-test was the statistical method used,* ***A:*** *n=5-12,* ***B:*** *n=5-11.*

4.2.3.3 Plasma Levels of 17β-Estradiol is Higher in Dax1$^{tm(Kiss1)}$ Animals

Data described in Figures 39, 40 and 42 clearly demonstrates that knocking out Dax1 in kisspeptin cells causes estrous cycle disturbances. In rodents, the reproductive cycle is regulated by estrogen. Therefore the levels of plasma 17β-estradiol in Dax1^{tm} and Dax1$^{tm(Kiss1)}$ animals were measured (Figure 42). For this experiment, blood samples from female adult mice of both genotypes (Dax1^{tm} and Dax1$^{tm(Kiss1)}$) were collected at a non-specific stage of the estrous cycle. The plasma was then separated through centrifugation and the 17β-estradiol competitive ELISA Kit (Abcam, ab108667) was used to accurately quantify 17β-estradiol in plasma samples.

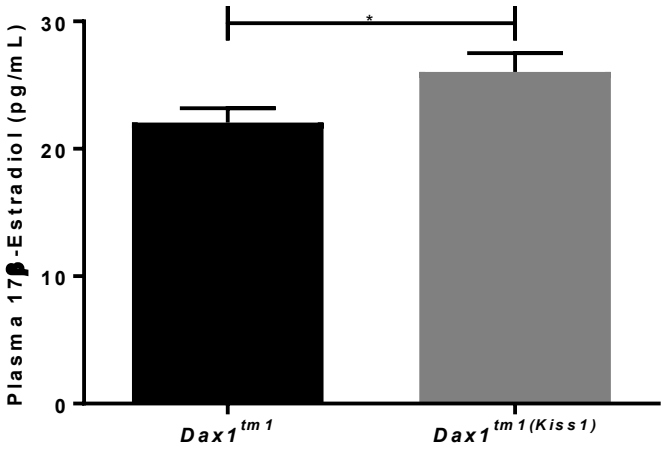

Figure 42: Plasma 17β estradiol levels in Dax1^{tm} and Dax1$^{tm(Kiss1)}$ animals.

Blood samples were collected from adult mice of both genotypes: Dax1^{tm} and Dax1$^{tm(Kiss1)}$. Plasma was then obtained through centrifugation and the17β-Estradiol competitive ELISA Kit (Abcam, ab108667) was used to accurately quantify 17β-estradiol in plasma samples. Data is expressed in pg/mL ± SEM, Student's t-test was the statistical method used, n=26-27.

Dax1$^{tm(Kiss1)}$ animals presented with significantly higher concentrations of 17β-estradiol in their plasma (26.04pg/mL) than control animals (22.07pg/mL) (p=0.0386).

4.2.3.4 There is a Trend Towards More Number of Follicles and Corpora Lutea in Dax1$^{tm(Kiss1)}$ Animals

Ovarian morphology of Dax1^{tm} and Dax1$^{tm(Kiss1)}$ animals was investigated as animals with conditional knockout of Dax1 in kisspeptin cells presented with significantly higher concentrations of 17β-estradiol. Estrogen is produced and synthesised in the in ovarian follicles. To this effect, ovaries from animals of the Dax1^{tm} and Dax1$^{tm(Kiss1)}$ genotype were collected, fixed and stained with hametoxylin and eosin (Figure 43).

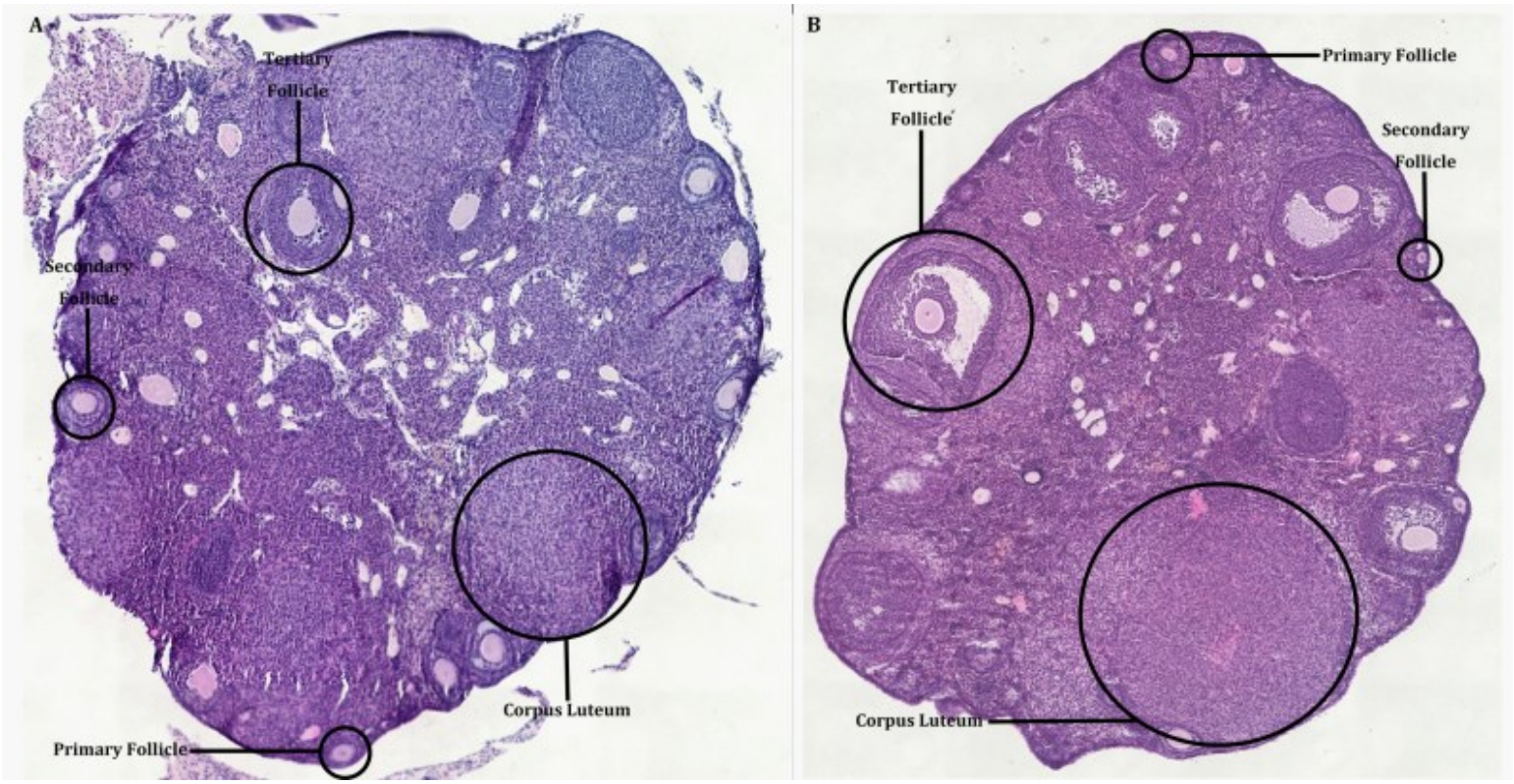

Figure 43: Ovarian morphology of Dax1^{tm} (A) and Dax1$^{tm(Kiss1)}$ animals (B).

The ovaries of control animals and Dax1 knockout animals were removed, fixed, and stained with hametoxylin and eosin stain. Both ovaries presented with varying numbers of normal ovarian structures: primary follicles, secondary follicles, tertiary follicles and corpora lutea. These were circled and labelled for easy identification.

The number of follicles (primary, secondary and tertiary) and of corpora lutea for each of the groups was investigated and compared (Figure 44).

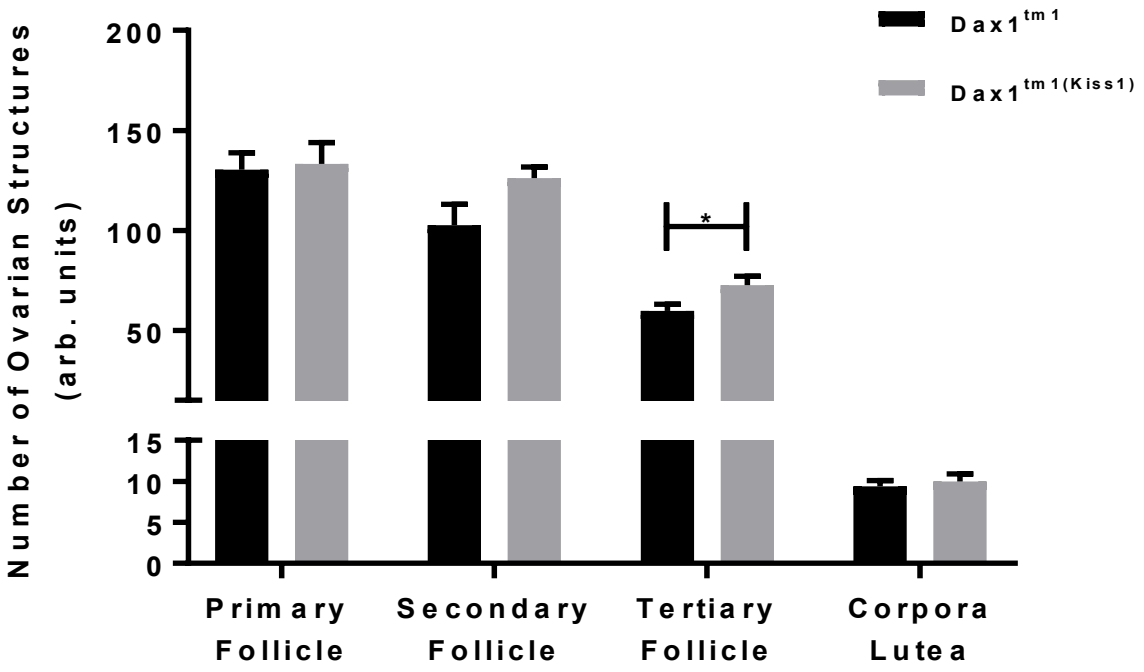

Figure 44: Number of structures present in the ovaries of Dax1^{tm} and Dax1$^{tm(Kiss1)}$ animals.
Ovaries from Dax1^{tm} and Dax1$^{tm(Kiss1)}$ animals were collected and prepared for hametoxylin and eosin staining. Ovarian structures, follicles (primary, secondary and tertiary) and corpora lutea, were quantified in Dax1^{tm} (black bars) and Dax1$^{tm(Kiss1)}$ (greys bars) animals. Data is expressed as mean number of ovarian structures in arbitrary units ± SEM, Student's t-test was the statistical method used, n=5.

Dax1$^{tm(Kiss1)}$ animals presented with more primary, secondary and tertiary follicle, which explains the significantly higher levels in the plasma of these animals. Out of all of these the only significant difference was the number of tertiary follicles (73 tertiary follicles in the Dax1$^{tm(Kiss1)}$ animals compared to 60 in control animals (Dax1$^{tm(Kiss1}$). There was also a trend towards higher number of corpora lutea in the knockout animals but this was not significant. Table 6 (below) facilitates comparison of the data presented in Figure 44.

Structures of the ovary	Mean Number		P-value	Significance
	Dax1^{tm1}	**Dax1$^{tm1(Kiss1)}$**		
Primary Follicles	130	133	0.8425	Not Significant
Secondary Follicles	103	126	0.0817	Not Significant
Tertiary Follicles	60	73	0.0459	*
Corpora Lutea	9	10	0.6075	Not Significant

Table 6: Number of follicles (primary, secondary and tertiary) and corpora lutea in Dax1^{tm} and Dax1$^{tm(Kiss1)}$ animals.

4.2.3.5 Plasma Levels of Follicle Stimulating Hormone Were Significantly Higher in Dax1$^{tm(Kiss1)}$ Animals When Compared With Levels Seen in Dax1^{tm} Animals

The findings above described (significantly higher levels of 17β-estradiol in the knockout animals) opened the question whether there these animals presented with defects in the estrogen negative-feedback system that maintains and regulates the reproductive cycle. Estrogen acts on the hypothalamus in order to mediate the secretion and release of gonadotropic hormone, luteinising hormone and follicle stimulating hormone, via the action of gonadotropin releasing hormone. For this reason, the levels of these two hormones were measured during the late afternoon of proestrous, as this is the point of the estrous when plasma estradiol levels are at their highest level.

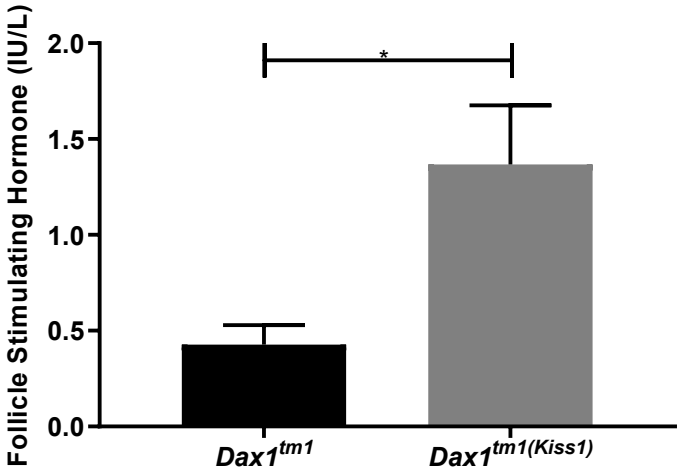

Figure 45: Plasma Follicle Stimulating Hormone levels in Dax1^{tm} and Dax1$^{tm(Kiss1)}$ animals.
Blood samples were collected during the late afternoon of proestrous from adult Dax1^{tm} and Dax1$^{tm(Kiss1)}$ mice, the plasma was extracted following centrifugation and the samples were analysed by the Ligand Hormone Core Facility at the University of Virginia in order to enable accurate determination of plasma levels of follicle stimulating hormone. Data is expressed in IU/L ± SEM, Student's t-test was the statistical method used, n=7-8.

The current study was unable to provide luteinising hormone measurements as the custom made LH ELISA assay, described by (Cimino *et al.*, 2016), selected to measure and quantify this hormone, in blood samples collected from Dax1^{tm} and Dax1$^{tm(Kiss1)}$ animals, proved to lack the sensitivity necessary to measure luteinising hormone in these samples (data not shown). Figure 45 is a graphical representation of the plasma levels of follicle stimulating hormone which in mice with conditional knockout of Dax1 in kisspeptin cells was three fold higher (1.37 IU/L) than those recorded for control animals (0.43 IU/L) (p=0.0170) (Figure 45). This therefore explains the trend towards increased number of follicles in the knockout animals but most importantly it highlights a defect in the negative feedback pathway, mediated by estrogen that regulates the estrous cycle.

4.2.3.6 Dax1$^{tm(Kiss1)}$ Animals Present with Defects in the Estrogen Negative Feedback Pathway that Regulates the Estrous Cycle

The results shown in Figure 45 highlight a potential defect in the estrogen-driven negative feedback mechanism that regulates the events that characterise and drive the estrous cycle. In the estrous cycle, estrogen synthesised and released by the cells of the ovary, acts on kisspeptin cells of the hypothalamus, by binding to estrogen receptor alpha, to either induce or repress (in the anteroventral periventricular nucleus and arcuate nucleus, respectively) kisspeptin expression which regulates gonadotropin releasing hormone from the hypothalamus. Gonadotropin releasing hormone then travels to the anterior pituitary, through the hypophyseal circulation, where it regulates synthesis and release of gonadotropic hormones (luteinising hormone and follicle stimulating hormone).

The differential effect of estrogen in *Kiss1* gene expression, in the arcuate nucleus and anteroventral periventricular nucleus, provided an ideal system to explore the potential defect in the in the estrogen-mediated negative feedback pathway highlighted in 4.2.3.5 (Figure 45). To do so, female mice of both genotypes, Dax1^{tm} and Dax1$^{tm(Kiss1)}$, were ovariectomised and a silastic capsule containing 17β-estradiol was inserted subcutaneously. After recovery, each cohort, Dax1^{tm} and Dax1$^{tm(Kiss1)}$, was subdivided into two groups: mice that were injected with vehicle (sesame oil) and mice that were given an intraperitoneal injection of estradiol benzoate (0.05 mg/kg). Thus creating two groups: (i) low estrogen (which resembles the estrogen levels in the follicular stage) - mice implanted with silastic capsule containing 17β-estradiol in sesame oil and injected with sesame oil and (ii) high estrogen (which resembles the estrogen levels during the late afternoon of the proestrous) - mice implanted with silastic capsule containing 17β-estradiol in sesame oil and injected with estradiol benzoate. The following day, mice were humanly killed and brains were snap frozen and bilateral samples of the arcuate nucleus were collected and *Kiss1* gene expression, relative to the housekeeping gene cyclophilin, was assessed in the arcuate nucleus of the hypothalamus (Figure 46).

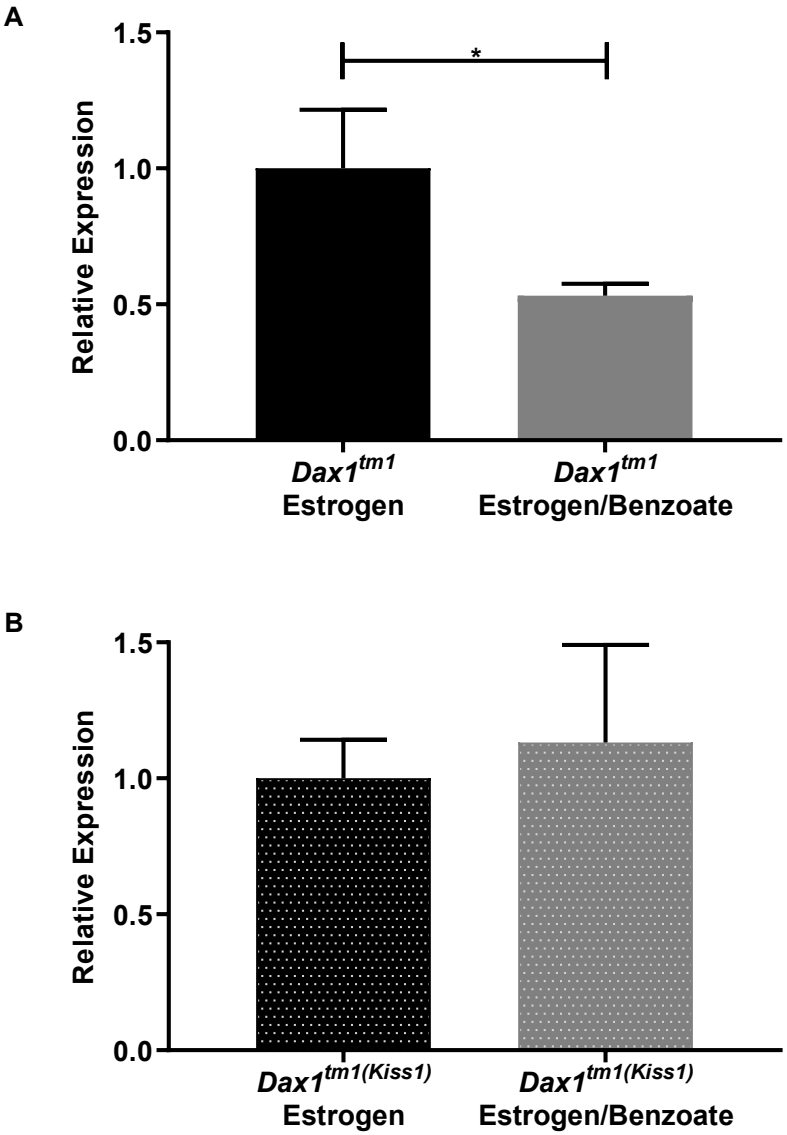

Figure 46: **Kiss1** ***expression in the Arcuate nucleus of Dax1^{tm} and Dax1$^{tm(Kiss1)}$ exposed to different concentrations of estradiol.***

Legend: Estrogen – *low estrogen (to resemble the estrogen levels observed during the follicular stage of the cycle) (black bars).* ***Estrogen/Benzoate*** *– high estrogen (to resemble the estrogen levels during the late afternoon of the proestrous) (grey bars).* ***A:*** Kiss1 *mRNA expression in the arcuate nucleus of Dax1^{tm} animals exposed to different concentrations of estrogen. p=0.0484* (black and grey solid bars).* ***B:*** Kiss1 *mRNA expression in the arcuate nucleus of Dax1$^{tm(Kiss1)}$ animals exposed to different concentrations of estrogen. p=0.7575 (black and grey dotted bars). Data is expressed as relative expression ± SEM, Student's t-test was the statistical method used,* ***A:*** *n=4-5,* ***B:*** *n=5-6.*

It is well established that estrogen signalling, in the arcuate nucleus of the hypothalamus, represses *Kiss1* expression in this nuclei. Figure 46A demonstrates, that in this study, it was possible to replicate the already established effects of estrogen on *Kiss1* mRNA expression in the arcuate nucleus. In this way, exposure of Dax1$^{tm(Kiss1)}$ animals to estrogen levels that resemble those seen in the late afternoon of proestrous (high concentration of estrogen) (grey solid bar) significantly repressed *Kiss1* gene expression in the arcuate by 53% ($p=0.0484$) when compared to animals exposed to follicular levels of estrogen (low levels of estrogen) (black solid bar).

On the other hand, exposure of animals with conditional knockout of Dax1 in kisspeptin cells to high levels of estrogen (resembling the levels of estrogen during proestrous) (grey dotted bar) failed to repress *Kiss1* mRNA expression in the arcuate nucleus when compared to control animals (low estrogen - resembling follicular levels of estrogen) (black dotted bar) (Figure 46B). Thus confirming that Dax1$^{tm(Kiss1)}$ animals present with defects in the estrogen-mediated negative feedback mechanism that regulates the estrous cycle.

4.2.3.7 Estrogen Negative Feedback in the Arcuate Nucleus of the Hypothalamus Regulates Follicle Stimulating Hormone Secretion and Release, that is Impaired in Dax1$^{tm(Kiss1)}$ Animals

Blood samples were also collected from the experiment described in 4.2.3.6, where Dax1^{tm} and Dax1$^{tm(Kiss1)}$ animals were ovariectomised and exposed to different concentrations of estrogen (low and high estrogen: to resemble follicular levels of estrogen and estrogen levels during the late afternoon of proestrous, respectively).

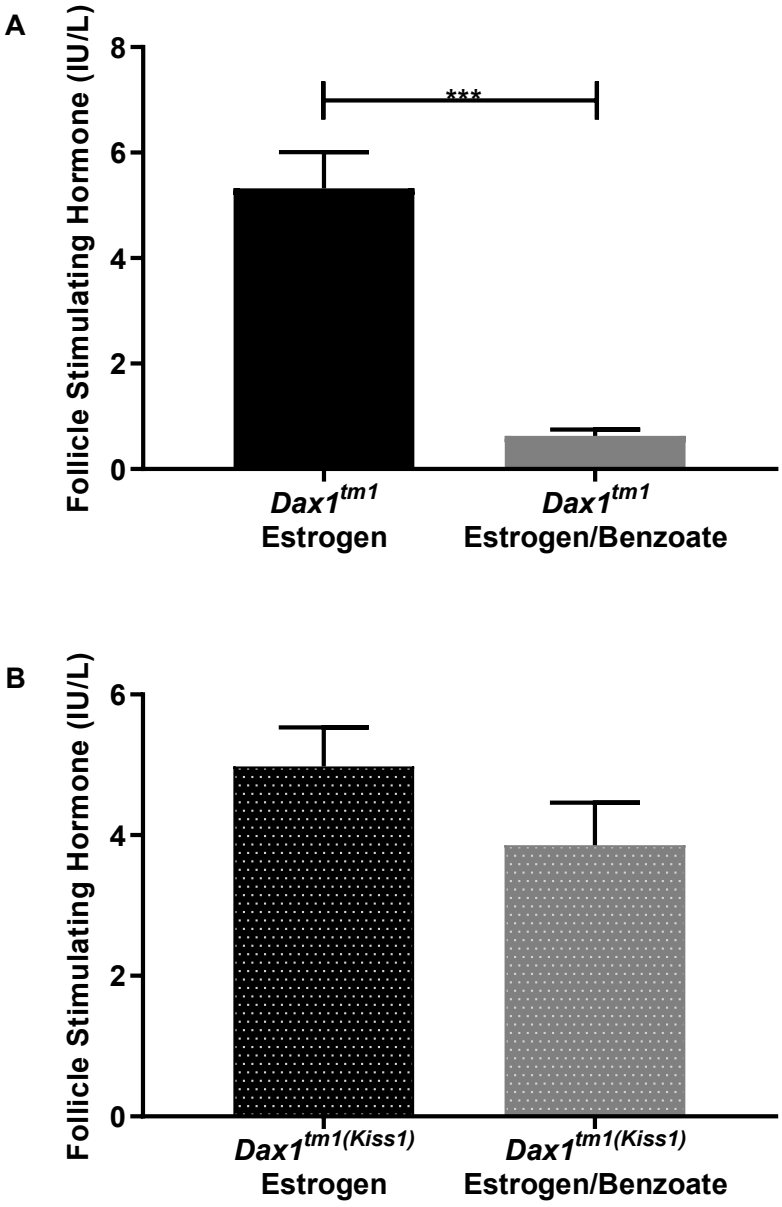

Figure 47: Plasma levels of follicle stimulating hormone in Dax1^{tm} (A) and of Dax1$^{tm(Kiss1)}$ (B) following treatment with different concentrations of estrogen.

Legend: Estrogen – *low estrogen (to resemble the estrogen levels observed during the follicular stage of the cycle) (black bar).* ***Estrogen/Benzoate*** *– high estrogen (to resemble the estrogen levels during the late afternoon of the proestrous) (grey bar).* ***A:*** *Levels of follicle stimulating hormone in plasma samples collected from Dax1^{tm} animals exposed to different concentrations of estrogen. p=0.002***.* ***B:*** *Levels of follicle stimulating hormone in plasma samples collected from Dax1$^{tm(Kiss1)}$ animals exposed to different concentrations of estrogen. p=0.2077. Data is expressed in IU/L ± SEM, Student's t-test was the statistical method used, n=5-6.*

Under normal conditions, as it is the case of Dax1^{tm} animals in Figure 47A, estrogen (grey bar) feedbacks to the arcuate nucleus of the hypothalamus and inhibits synthesis and release of follicle stimulating hormone from gonadtropin cells of anterior pituitary. As it can be seen in Figure 47A, when high concentrations of estrogen (that resemble those seen in the proestrous stage of the cycle) were administered to control animals there was a significant decrease in the plasma levels of follicle stimulation hormone (from 5.322 IU/L to 0.6300 IU/L) (p=0.0002) (Figure 47A).

The repressive effects of estrogen on follicle stimulating hormone is impaired in animals with conditional knockout of Dax1 in kisspeptin cells (Figure 47B). The levels of follicle stimulating hormone measured in Dax1$^{tm(Kiss1)}$, administered with high levels of estrogen, was of 3.858 IU/L (black bar) which was not significantly different (p=0.2077) from the levels seen in Dax1$^{tm(Kiss1)}$ animals that were exposed to lower concentrations of estrogen (4.980 IU/L) (Figure 47B).

Thus, these results (Figure 47) taken together with data analysed in 4.2.3.5 (Figure 45) specifies that the defects in the estrogen-mediated negative feedback mechanism, in the arcuate nucleus of Dax1$^{tm(Kiss1)}$ animals, affects the synthesis and release of follicle stimulating hormone from the anterior pituitary which results in increased plasma levels of follicle stimulating hormone when compared to control animals (Figure 45).

4.3 Discussion

Considering the lack of reliable and consistent methods available to study *Kiss1* gene regulation and their effects on reproduction, knockout mice models have over the years enabled a better understanding of the mechanisms regulating *Kiss1* gene transcription.

Mice with deficient Dax1 expression mouse not only provide an excellent opportunity to understand the role of this corepressor in the estrogen-mediated differential regulation of the *Kiss1* gene in the female hypothalamic nuclei, the anteroventral periventricular nucleus and arcuate nucleus but also enables investigation into the reproductive effects of decreased levels of Dax1 in the adult female mouse. While the effects of deficient Dax1 expression in males have been investigated, with these animals presenting with adrenal insufficiency, fail to undergo puberty and there are hormonal defects at both the hypothalamic and pituitary levels. On the other hand, female animals with heterozygous mutations in the *Nr0b1* gene are normal, however very few studies have looked at the phenotype of female animals carrying homozygous mutations in the *Nr0b1* gene, and even less experiments have looked at the role of Dax1 in the regulation of the estrous cycle.

Here we generated female mice with homozygous mutations in kisspeptin cells ($Dax1^{tm(Kiss1)}$). The Cre/loxP technology was employed here, Dax1 floxed mice (a floxed PGK-neomycin resistance cassette was inserted on either side of exon 2 of the mouse *Nr0b1* locus) were crossed with mice expressing Cre recombinase downstream of the Kiss1 promoter (heterozygous), to ensure that Dax1 deletion is limited and specific to kisspeptin expressing cells. Considering the findings in the estrogen receptor signalling experiments, the focus of this part of the project was on the role of Dax1 in the arcuate nucleus of the hypothalamus.

Using the Cre/loxP technology we, successfully, generated female animals with conditional knockout of Dax1 in kisspeptin cells. Through the immunofluorescence data shown here it was possible to determine that the vast majority of kisspeptin cells, in animals Dax1 homozygous mutations, did not express Dax1. The immunofluorescence and RT-qPCR data collected from these animals also clearly shows that there is a generalised decrease in Dax1 expression throughout the arcuate nucleus and not only in kisspeptin cells. While, we can't ascertain for sure why this is happening, this is most likely due to the fact that Dax1 was knocked out of these animals from birth and caused reproductive defects that might signal to

other parts of the hypothalamus. Therefore the effects of knocking out Dax1 in kisspeptin cells might not only affect these animals at the reproductive level but also at other levels.

We show here too that in the absence of Dax1, these animals are unable to regulate the events that are responsible for fertility. If for example we look at the *Kiss1* gene expression levels in the arcuate nucleus in the control animal we would expect *Kiss1* levels to be high during diestrous (i.e. when estrogen are low) and low during estrous (i.e. when estrogen levels are high). And therefore it is possible to hypothesise that, if Dax1 is mediating the negative feedback effects of estrogen on *Kiss1* gene expression in the arcuate nucleus, then knocking out Dax1 in the arcuate nucleus should result in an inability of estrogen to repress *Kiss1* gene expression when estrogen is high (i.e. estrous). Indeed our data, collected from free-cycling female animals, suggests that animals with conditional knock out of Dax1 in kisspeptin neurons are unable to significantly repress *Kiss1* gene expression in the presence of estrogen (i.e. estrous). Further to this, we also noticed something interesting, the expression of *Kiss1* was significantly repressed in the absence of estrogen (i.e. diestrous) in animals with conditional knockout of Dax1 in kisspeptin neurons. This only highlights that Dax1 is important for the regulation of the reproductive cycle as free-cycling animals with conditional knock out of Dax1 in kisspeptin cells do not respond to estrogen as expected.

Here we show that Dax1 homozygous mutations in kisspeptin cells did not affect the normal development of these mice, they were healthy at birth and developed normally into adulthood. Further to this, deficiency of Dax1 did not affect the age at which these animals went through the onset of puberty. Nevertheless, these animals presented with estrous cycle disturbances. It has been shown that the estrogen-mediated upregulation of the *Kiss1* gene in the anteroventral periventricular is responsible for the luteinising surge required for ovulation but also it regulates both vaginal opening (used as an external indication of the onset of puberty) and the first vaginal estrous (Hu *et al.*, 2015). On the other hand, knocking out kisspeptin in the arcuate nucleus had no effect on the onset of puberty but resulted in abnormal estrous cyclicity (Hu *et al.*, 2015). Therefore, the results obtained using mice with conditional knockout of Dax1 in kisspeptin cells resembles the findings in Hu *et al.*, 2015, where kisspeptin was knocked out in the arcuate nucleus, and highlights Dax1 as an important regulator of *Kiss1* transcription in the arcuate nucleus. The longer estrous cycles observed in animals with conditional knock out of Dax1 in kisspeptin is a direct consequence of the increased time spent in the estrous stage of the estrous cycle. It is interesting that these

animals are spending more time in a stage of the cycle when estrogen is high (i.e. estrous), further highlighting the inability of estrogen to mediate its normal effects on the arcaute nucleus in the absence of Dax1.

While the effects of knocking out Dax1 in kisspepin cells in the estrous cycle, presented here, could be said to be modest this could be due to developmental compensation (Wilkinson, 2019). Knockout models have been used over the years in order to explore and understand the biological significance of a specific gene, and the mechanisms by which it exerts its effects. Conventionally, it is believed that the knocking out strategy (i.e. knocking out a gene in order to render its protein and function inactive) yields more severe biological effects than simply reducing expression of the gene of interest (knockdown). Contrary to what it is believed, the knockout of a gene, often, has less severe biological effects than those seen when the expression of the gene of interest is decreased (El-Brolosy & Stainier, 2017). While the toxic and off-target effects of the chemicals used to induced knockdown of the gene of interest can account for the more severe biological effects when this genetic strategy is used (Kok *et al.*, 2015), this is not always the reason (Rossi *et al.*, 2015). Several authors report the existence of a compensatory molecular mechanism by which knocking out the gene of interest leads to transcriptional activation of genes related to the inactivated gene (El-Brolosy *et al.*, 2019; Ma *et al.*, n.d.). The existence of a developmental compensatory mechanism was first described in the zebrafish where *egfl7* gene knockout led to upregulation of genes that encode proteins related to those encoded by the *egfl7* gene (Rossi *et al.*, 2015). This upregulatory effect was only seen with mutations of the *egfl7* gene and not when the *egfl7* gene was kncoked down (Rossi *et al.*, 2015). This mechanism provides the orgainism with robustness in reponse to mutations that might affect crucial genes (Wilkinson, 2019).

While we can't acertain that knocking out the *Nr0b1* gene initiated the mechanism of developmental compensation and led to transcriptional upregulation of genes coding for related proteins, it is possible that this is the case considereing the reported importnace of Dax1 in reproduction.

In hindsight, adopting a knockdown strategy could have have led to more significant biological effects as the knockout genetic stratey could have potentially masked biological defects. Furthermore, acute knockout of Dax1 by perfoming bilateral injections of adeno-associated virus (AAV) into the arcuate nucleus after puberty could have prevented the potential developmental compensatory mechanisms.

Further to this, analysis of the estrous cycle relies on vaginal cytology which is used to determine the stage of the estrous cycle, this method enables predicting the stage of the estrous cycle according to the proportion of three types of cells obtained upon a vaginal smear: cornified cells, epithelial cells and leukocytes. While its stage is characterised by specific types of cells and their relative abundance, it is true that it is often difficult to distinguish between the stages of the cycle as they can appear, visually, very similar. For this reason, we ensured that vaginal smears were collected every day at the same time and that our analysis of the vaginal smears was as accurate and unbiased as possible. However, it is possible that the difficulty to determine the stage of the cycle might have affected the reported results.

It is well established that the anteroventral periventricular nucleus mediates the positive effects of estrogen in *Kiss1* gene expression that is responsible for inducing the gonadotropin releasing hormone/luteinising hormone surge/peak that is essential for ovulation (Popa, Clifton & Steiner, 2008; Oakley, Clifton & Steiner, 2009; Roa *et al.*, 2008; Wiegand *et al.*, 2008; Ma, Kelly & Ronneklei, 1990). The negative feedback of estrogen on kisspepetin cells of the arcuate nucleus is less understood, but it is hypothesised to regulate the synthesis and release of follicle stimulataing hormone from the anterior pituitary through the action of the the gonadotropin releasing hormone (Navarro *et al.*, 2011).

Here, we confirm this hypothesis and show and identify for the first time an essential protein, Dax1 (encoded by the *Nr0b1* gene) that mediates the negative effects of estrogen on *Kiss1* gene expression. We also demonstrate that the arcuate nucleus is essential for regulating the synthesis and release of follicle stimulating hormone.

Animals with conditional knockout of Dax1 in kisspeptin cells presented with increased plasma estrogen and follicle stimulating hormone levels. The ovaries of these animals differed from those of control animals with a trend towards increased number of follicles. These findings led us to hypothesise that these animals present with a regulatory defect in the estrogen-negative feedback to the arcaute nucleus of the hypothalamus.

We show here for the first time that, Dax1 mediates the estrogen-negative feedback mechanism that regulates the estrous cycle.

We hypothesised that in the absence of Dax1, animals with conditional knockout of Dax1 in kissspeptin cells are unable to regulate *Kiss1* gene expression, in the arcuate nucleus, in response to estrogen signalling. And thus are unable to regulate the plasma levels of follicle stimulating hormone in response to estrogen. In the absence of Dax1, animals with conitional

knockout of Dax1 in kisspeptin cells fail to repress *Kiss1* gene expression in the arcuate nucleus in response to estrogen which culminates in an inability to repress the levels of follicle stimulating hormone. In this way, this hormone continuously acts on the ovary leading to further development of follicles, thus explaining the trend towards higher number of follicles in animals with conditional knockout of Dax1 in kisspetin cells.

4.4 Summary of Findings

- We show for the first time that the negative-feedback of estrogen in Kiss1 in the arcuate nucleus is mediated by the nuclear receptor Dax1.

- Mice with conditional knockout of Dax1 in kisspeptin cells present with the hallmarks of perturbed estrogen-negative feedback.

- Mice with conditional knockout of Dax1 in kisspeptin cells fail to supress *Kiss1* and FSH and fail to cycle normally.

Results: Chapter 3 - Reproductive Function in Sex-Reversed Mice Lacking the Nuclear Receptor Dax1

5 Reproductive Function in Sex-Reversed Mice Lacking the Nuclear Receptor Dax1

5.1 Introduction

Dax1 (dosage sensitive sex-reversal (DSS), adrenal hypoplasia congenita (AHC), on chromosome X, gene 1) is an orphan member of the nuclear hormone receptor superfamily of transcription factors (Mangelsdorf *et al.*, 1995). Its gene, the *Nr0b1*, is found on the X-chromosome and has a fairly simple structure (two exons (1168 and 245 base pairs (bp) long) separated by an intron) (Burris, Guo & McCabe, 1996; McCabe, 2001). *Nr0b1* encodes an unusual orphan nuclear receptor (470 amino acid long), Dax1. Dax1 consists of a carboxyl-terminal domain (CTD) containing a putative ligand-binding domain (homologous to the ligand-binding domain of other nuclear receptors) with a ligand-dependent transactivation domain (AF-2), and an unique amino-terminal domain (NTD), consisting of three complete and one incomplete alanine-glycine rich repeats motifs of (65-67 amino acids long each), each repeat containing a short leucine motif, LxxLL (Niakan & McCabe, 2005; Iyer & McCabe, 2004).

Classically, Dax1 represses the transcriptional-activation function of other nuclear hormone receptors through protein-protein interactions (e.g. interaction with histone acetyltransferases (HATs) and histone deacetylases (HDACs)) (Crawford *et al.*, 2015). However, due to the presence of LxxLL motifs (usually found in coactivators) in its structure, under specific conditions Dax1 has been reported to activate transcription. Dax1's ability to bind directly to DNA confers this nuclear receptor other regulatory functions (Ludbrook & Harley, 2004). Dax1 is expressed throughout the hypothalamic-pituitary-gonadal (HPG) axis in adulthood (Ikeda *et al.*, 2001) and interacts with several steroidogenic receptors including estrogen receptors and testosterone receptor (ERs and TRs, respectively). However, the role of Dax1 in the adult hypothalamic-pituitary-gonadal axis remains largely elusive (Ikeda *et al.*, 2001).

Dax1 is important for sex determination, during development, *Dax1* is a testes-determining gene (Ludbrook & Harley, 2004; Meeks, Weiss & Jameson, 2003). Studies where the role of Dax1 was investigated in male and female animals lacking Dax1 showed that while females were overtly fertile, Dax1-deficient male mice displayed a spectrum of sex-reversal phenotypes (from XY animals to phenotypic females). The phenotypic spectrum obtained has been linked to (i) the background of the strain in which the experiment was conducted (humans with dosage-sensitive sex reversal also present with a phenotypic spectrum) and (ii) with the relative 'strength' of the sex-determining gene, *Sry* (Bouma, 2005).

Nuclear receptors are transcription factors that regulate expression of genes in response to both extracellular and intracellular signals (i.e. ligands) (Zhang *et al.*, 2000). For example, male lacking *Dax1* in a mixed genetic background, and containing a 'weak' *Sry* allele from the *Mus domesticus poschiavinus* Y-Chromosome, present with complete sex-reversal (Meeks, Weiss & Jameson, 2003). Conversely, lack of exon-2 of Dax1 in 129Sv/J male mice results in abnormal testicular development which results in smaller than normal adult testes (Yu *et al.*, 1998).

Lastly, Dax1 plays an essential role during testicular tissue development, in the early stages of development. It is required for the differentiation of somatic cells into sertoli cells. Absence of Dax1 in C57BL/6J mice resulted in complete gonadal sex-reversal (Bouma, 2005). The sex-reversal spectrum presented by animals in which *Dax1* is absent is not thoroughly understood. Nevertheless, it is thought that the *Sry* allele is important. Ovarian development in XY B6 mice lacking *Dax1* can be prevented by the addition of several copies of the *Sry* allele from the 129-strain ('strong' *Sry* allele) (Bouma, 2005). Considering that the expression of *Sry* is also variable between individual animals of the same strain, it possible to hypothesise that there is an associated range of sex-reversal phenotypes within strains, however this has not been investigated.

Here we conducted a reproductive survey of reproductive function in chromosomal-XY C57BL/6J mice lacking exon 2 of the *Dax1* gene, hence forth referred to as *Dax1-/Y* in order to assess intra-strain variability in sex-reversal phenotypes.

5.2 Results

While strain differences have helped explain the differential phenotypes obtained the phenotypic spectrum obtain when *Dax1* is absent in male animals, no studies have been done where intra-strain variability is assessed. Here we generated C57BL/6J mice lacking exon 2 of the *Dax1* gene, referred to as *Dax1-/Y* (described in (Bouma, 2005)). Reproductive studies were conducted in order to determine the reproductive function of *Dax1+/+* (control female animals) and *Dax1-/Y* animals (mice lacking exon 2 of the *Dax1* gene).

5.2.1 Live birth from a Sex-Reversed Chromosomally-Male Mouse Lacking the Dax1 Orphan Nuclear Receptor

An initial experiment to test fertility of sex-reversed XY animals (*Dax1-/Y*) was carried out. 10 *Dax1-/Y* mice were paired with proven wild type (WT) stud-males, otherwise referred as *Dax1+/Y*. Approximately two months after pairing, one *Dax1-/Y* animals gave birth to a single offspring, which was found dead in the its home-cage (data not shown). This finding led us to set up a second fertility study, where the reproductive ability of control female animals (*Dax1+/+*) was compared to that of sex-reversed XY animals (*Dax1-/Y*). Eight Dax1-/Y mice, and four control (*Dax1+/+*) females, each of the animals were paired with *Dax1+/Y* stud-males (Figure 48).

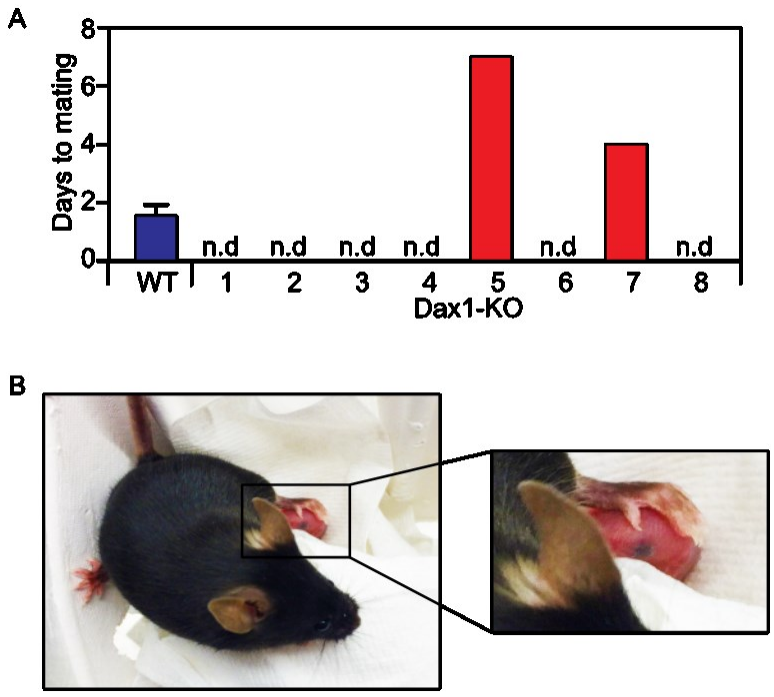

Figure 48: Live-birth in a Dax1-/Y mouse

(A) *Mating success of four WT (Dax1+/+) females presented as average +/-SEM, and eight Dax1-/Y mice with proven stud-males.* ***(B)*** *Photograph of a Dax1-/Y mouse with single live-offspring on post-natal day 1.*

As expected, all of the control female mice (*Dax1+/+*) mated with stud-males, as evidenced by the presence of a vaginal plug in the morning after mating (Figure 48A, blue bar). By contrast, six out of eight sex-reversed XY animals (*Dax1-/Y*) did not mate with the stud-males during the 10-day experimental period ((Figure 48A, n.d.). Nevertheless, an unusual plug was observed in two out of the eight sex-reversed XY animals (*Dax1-/Y*) ((Figure 48A, red bars). One of those animals gave birth to a single offspring, which appeared, at birth, to be healthy (Figure 48B). The pup, however, did not survive beyond postnatal day two, the reason remains undermined to this day. Therefore, we have found that a minority of sex-reversed XY animals (*Dax1-/Y*) are fertile and can give birth to live offspring. However their ability to lactate and support the offspring remains to be determined.

5.2.2 Intra-Strain Variability in Reproductive Phenotype in XY Sex-Reversed Mice

The results obtained from our mating-experiments are suggestive of intra-strain variability in sex-reversed XY animals (*Dax1-/Y*). For this reason, in order to investigate the spectrum of reproductive phenotypes sex-reversed XY animals (*Dax1-/Y*), experiments were conducted in an additional cohort of control female (*Dax1+/+*) animals and eight sex-reversed *Dax1-/Y* mice. The timing of puberty was initially assessed by vaginal opening, an estrogen-mediated event that is considered the first phenotypic evidence of the onset of puberty on female mice (Figure 49).

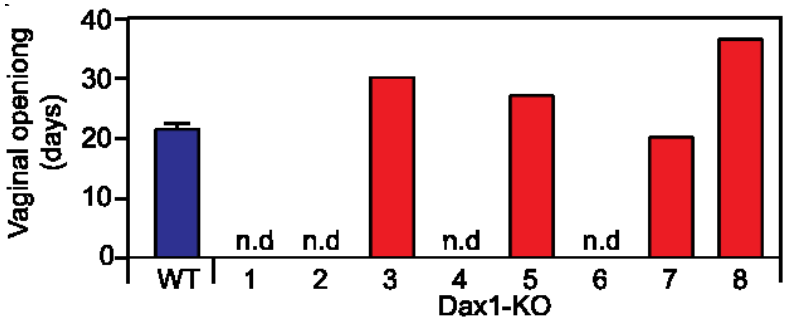

Figure 49: First day of puberty as measured by vaginal opening.
Data for WT (Dax1+/+) is presented as average ± SEM of four animals.

Control (*Dax1+/+*) female animals went through puberty (i.e. underwent vaginal opening) at approximately 21 days of age (Figure 49, blue bar). By contrast, four out of eight sex-reversed XY animals (*Dax1-/Y*) did not undergo vaginal opening at all during the 40-day test-period (Figure 49, n.d.). However, three sex-reversed XY animals (*Dax1-/Y*) underwent delayed vaginal opening (between day 26 and day 35).While one sex-reversed XY (*Dax1-/Y*) mouse underwent vaginal opening on day 20 which was comparable to that observed in control (*Dax1+/+*) females (Figure 49).

We then assessed the estrous cycle by vaginal cytology in our cohort of four control (*Dax1+/+*) females and eight sex-reversed XY (*Dax1-/Y*) animals (Figure 50).

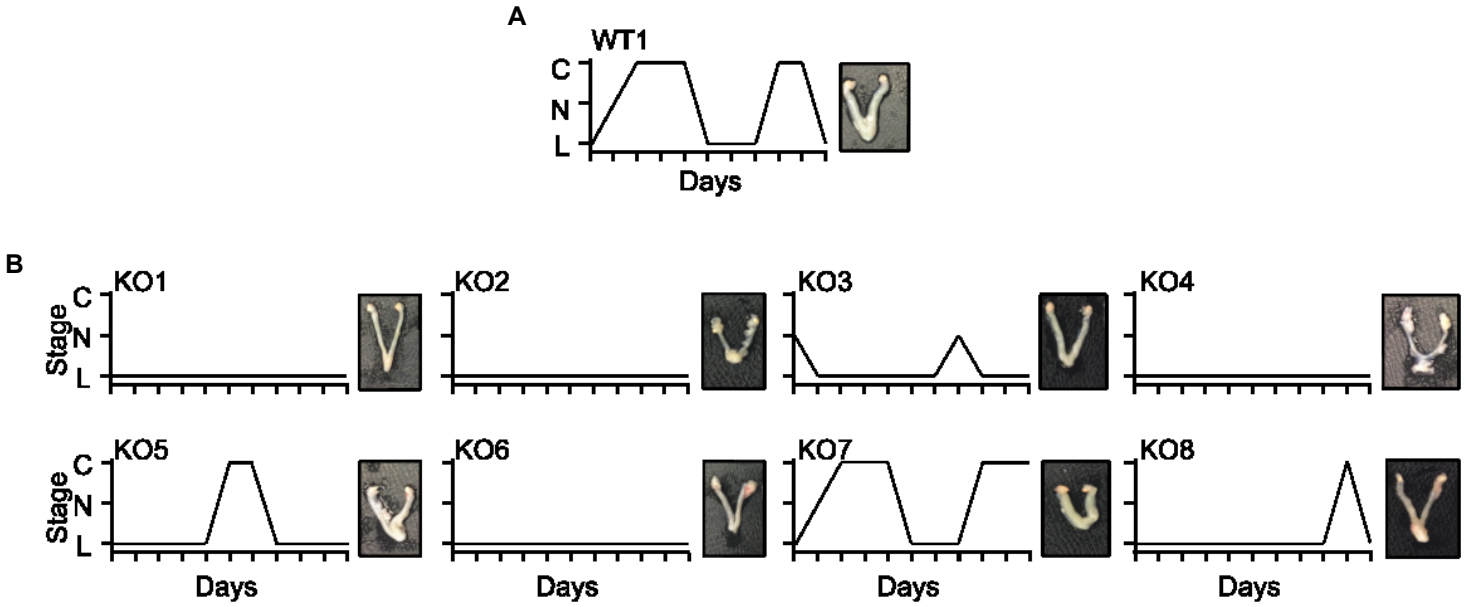

Figure 50: Intra-strain variability in reproductive phenotype of sex-reversed XY (Dax1-/Y) mice.
(A) *Representative estrus cycle and uterus/ovary morphology in a WT (Dax1+/+) female mouse.*
(B) *Individual estrus cycles and uterus/ovary morphology in each Dax1-/Y mouse.*

As expected, the estrous cycle of control Dax1+/+ female mice were 4-6 days, these animals also entered the post-ovulatory estrous-phase twice during the 11-day testing period (Figure 50A). By contrast, over half (five out of eight) sex-reversed XY (*Dax1-/Y*) mice did not enter the ovulatory, estrous, phase of the cycle at all during the testing period (Figure 50B). An additional two sex-reversed XY (*Dax1-/Y*) mice ('KO5' and 'KO8') did enter the estrous phase but did not cycle normally. Nevertheless, one sex-reversed XY (*Dax1-/Y*) mouse ('KO7') appeared to cycle normally, with cycles being similar to those of the control (*Dax1+/+*) females. This mouse, like the control, also entered the estrous phase twice during the test-period. There was a clear connection between the sex-reversed XY (*Dax1-/Y*) individuals that underwent vaginal opening (Figure 49), and those that had evidence of estrous cyclicity (Figure 50B). Additionally, the gross morphology of the uterus and ovaries reflected the vaginal cytology data, with those animals displaying evidence of estrous cyclicity (e.g. 'KO7') having larger uteri and ovaries than those that did not (e.g. 'KO4') (Figure 49 and Figure 50B). Taken together, these data show clear intra-strain variability in the reproductive phenotype of C5BL/6J sex-reversed XY (*Dax1-/Y*) mice. Most of these animals did not go through puberty or fail to cycle normally. However, a minority of sex-reversed XY (*Dax1-/Y*) mice are comparable to control (*Dax1+/+*) females with regards to their onset of puberty and estrous cyclicity.

5.2.3 Sex-Reversed XY (Dax1-/Y) Mice Respond to Ovarian Estrogen Production

In order to gain additional insight into our observations on sex-reversal phenotypes, we conducted post-mortem analysis of plasma hormone levels (Figure 51), ovaries, and hypothalamic neuropeptide gene-expression in our cohort of four control (*Dax1+/+*) and eight sex-reversed XY (*Dax1-/Y*) mice.

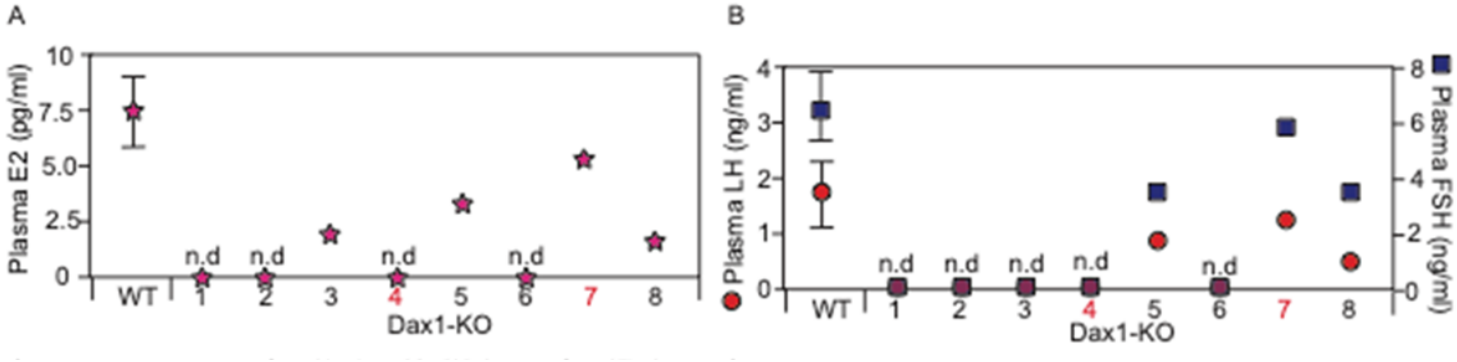

Figure 51: Plasma estradiol (E2) levels (A) and Plasma Luteinising Hormone (LH) and Follicle Stimulating Hormone (FSH) levels.

Plasma estrogen (E2), luteinising hormone (LH), and follicle stimulating hormone (FSH) were all lower in sex-reversed XY (*Dax1-/Y*) mice than in control female (*Dax1+/+*) animals. Indeed, using the assays employed here, these hormone were undetectable in at least half of the sex-reversed XY (*Dax1-/Y*) mice (Figure 51A, B). Nevertheless, estrogen, luteinising hormone and follicle stimulating hormone were detectible in three sex-reversed XY (*Dax1-/Y*) animal and, considering the reported interindividual variability in these hormones, their levels were in a range that may be considered 'normal' (Figure 51A,B).

Examples of ovarian histology and steroidogenic gene-expression from a control (*Dax1+/+*) female, and acyclic *Dax1-/Y* mouse ('KO4'), and a cyclic *Dax1-/Y* mouse ('KO7') are provided in Figure 52.

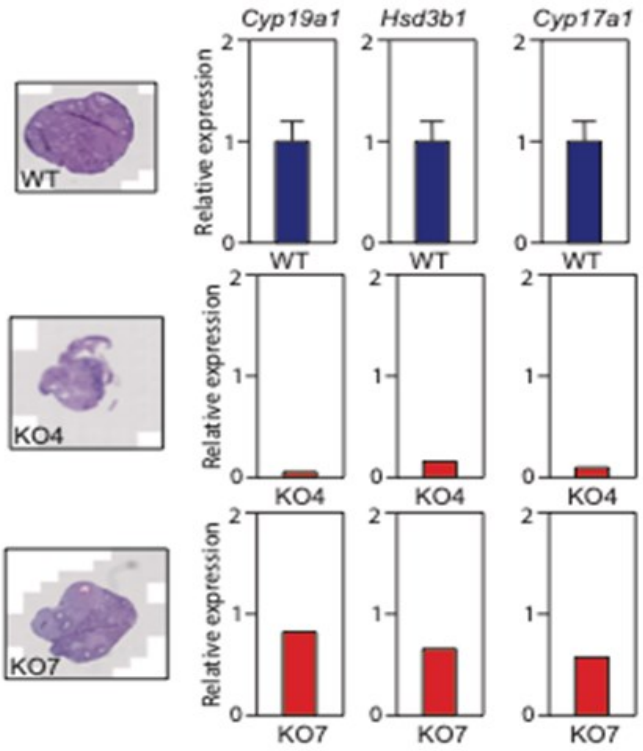

Figure 52: Ovarian histology and steroidogenic gene expression in WT (Dax1 +/+) female mice and sex-reversed XY (Dax1-/Y) mice.

Representative ovarian histology and ovarian steroidogenic gene expression in four control WT (Dax1 +/+) female mice, in an acyclic sex-reversed XY (Dax1-/Y) mouse (KO4), and in a cyclic sex-reversed XY (Dax1-/Y) mouse (KO7).

Examples of ovarian histology and steroidogenic gene expression from a control wild type (*Dax1+/+*) female, and acyclic sex-reversed XY (*Dax1-/Y*) mouse ('KO4'), and a cyclic sex-reversed XY (*Dax1-/Y*) mouse ('KO7') can be seen in Figure 52. The acyclic sex-reversed XY (*Dax1-/Y*) mouse ('KO4') have underdeveloped ovaries with few, if any, mature follicle or corpora lutea (Figure 52). Relative to control wild type (*Dax1+/+*) females, it also presented with dramatically reduced expression of key steroidogenic genes (*Cyp19al* (aromatase), *Hsd3b1*, and *Cyp17a1*) (Figure 52). On the other hand, the cyclic sex-reversed XY (*Dax1-/Y*) mouse ('KO7') had overtly normal ovaries encompassing mature follicle and post-ovulation corpora lutea (Figure 52). When compared to the group-average of control (*Dax1+/+*) female mice the expression of *Cyp19a1*, *Hsd3b1*, and *Cyp17a1* was lower, but comparable (Figure 52).

Kisspeptin (the product of the *Kiss1*-gene) is a neuropeptide that, in the hypothalamus, controls fertility by signalling to gonadotropin releasing hormone (GnRH) neurons. In female mice, plasma gonadotropins (follicle stimulating hormone (FSH) and luteinising hormone (LH)) are controlled by *kiss1*-neurons in the arcuate nucleus (ARC) and anteroventral periventricular nucleus (AVPV), respectively. Hypothalamic *Kiss1* expression was broadly in concordance with plasma gonadotropins (Figure 53 and Figure 51B).

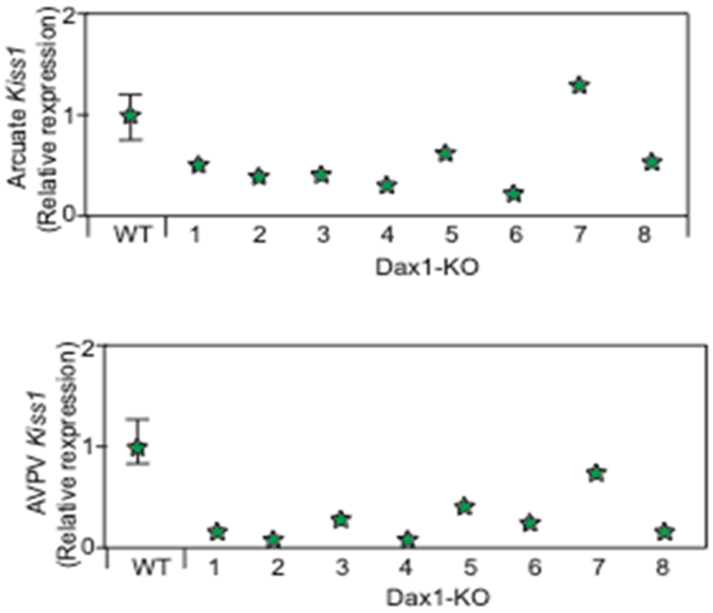

Figure 53: Kiss1 gene-expression in the arcuate and anteroventral periventricular nuclei of the hypothalamus of control (Dax1 +/+) female mice and sex-reversed XY (Dax1-/Y) mice.

Generally, perturbations in *Kiss1*-expression in sex-reversed XY (*Dax1-/Y*) mice were more dramatic in the LH-regulating anteroventral periventricular (AVPV) hypothalamus, than in the FSH-regulating arcuate (ARC) hypothalamus (Figure 53). Furthermore, there is apparent concordance between plasma E2 levels, Plasma LH and FSH levels, and hypothalamic *Kiss1*-expression in sex-reversed XY (*Dax1-/Y*) mice (Figure 51 and Figure 53). This likely suggests that the hypothalamus of sex-reversed XY (*Dax1-/Y*) mice is able to sense, and respond normally, to ovarian sex steroids.

Taken together, these data provide the first evidence of dramatic intra-strain variation in markers of fertility in sex-reversed chromosomally-male mice lacking the nuclear receptor Dax1. They also provide additional evidence that the primary defect in these animals is ovarian, rather than hypothalamic or pituitary. Finally, we show that at the extreme end of the phenotypic-spectrum, a minority of these sex-reversed chromosomally-male mice can undergo puberty, maintain pregnancy, and give birth to live offspring.

5.3 Discussion

Our results confirm that the C57BL/6J background is highly sensitive to male-to-female sex-reversal in the absence of the nuclear receptor Dax1. However, while all sex-reversed XY (*Dax1-/Y*) mice present as phenotypic females, at weaning, and have developed uteri and ovaries, there is marked inter-individual variation in reproductive phenotypes within this strain. While many sex-reversed XY (*Dax1-/Y*) mice fail to enter puberty and are infertile, a minority undergo relatively normal puberty, have markers of fertility that are broadly comparable to control-females (*Dax1+/+*) , and can even become pregnant and give birth to live offspring.

It has been hypotheised that differences in reproductive phenotype amongst different strains of sex-reversed XY (*Dax1-/Y*) mice is due to the relative 'strength' (amount of transcript) of the Sry allele (Meeks, Weiss & Jameson, 2003; Bouma, 2005). Indeed, overexpression of Sry in a strain susceptible to sex-reversal prevented ovary formation in sex-reversed XY (*Dax1-/Y*) mice. However, Sry mRNA has been shown to be variable even within-strain during the early events of testicular development (Bouma, 2005), and therefore provides a logical mechanistic explanation for the intra-strain variation in phenotypes observed here. It is not currently possible, however, to correlate early developmental expression of Sry in the testes to the degree of sex-reversal observed in adult sex-reversed XY (*Dax1-/Y*) mice.

Here, most sex-reversed XY (*Dax1-/Y*) mice presented with apparent hypothalamic hypogonadism (HH); they have low plasma gonadotropins (follicle stimulating hormone and luteinising hormone), and low estradiol levels. However, there was good concordance between plasma estrogen, hypothalamic *Kiss1*-expression, and circulating gonadotropins amongst individual sex-reversed XY (*Dax1-/Y*) mice. This suggests that hypothalamic hypogonadism in these animals is secondary to ovarian dysfunction. In other words, individual sex-reversed XY (*Dax1-/Y*) mice that are able to produce ovarian estrogen (E2) are able to sense this via elevated *Kiss1*-expression and, in turn, elevate luteinising hormone and follicle stimulating hormone levels. Furthermore, the fact that *Kiss1*-expression in the anteroventral periventricular (AVPV) nucleus is more dramatically affected than *Kiss1*-expression in the arcuate nucleus of sex-reversed XY (*Dax1-/Y*) mice is consistent with the hypothesis that the anteroventral periventricular is a female-predominant nucleus which develops under the control of estrogen.

Even though two out of a total of 18 sex-reversed XY (*Dax1-/Y*) mice gave birth, they each produced only one pup, we can only confirm one live-birth, and neither animal survived beyond post-natal day two. As such, although a minority of sex-reversed XY (*Dax1-/Y*) mice have markers of fertility that are generally in line with control females, they are still dramatically sub-fertile. The reasons for this are currently unclear but are probably due to a combination of factors that are likely ultimately a result of abnormal ovarian development. However, the mechanistic presence of a Y chromosome has also been suggested to inhibit meiosis in females (Taketo, 2014; Obata *et al.*, 2008).

This work demonstrates that a minority of sex-reversed XY (*Dax1-/Y*) mice can produce live offspring without any assister fertility treatment. It adds to the small number of reports of live-birth from sex-reversed XY mice (for example (Eicher *et al.*, 1982; Nagy *et al.*, 1999; Kuno *et al.*, n.d.)). These findings begs the questions whether the mechanisms that allow fertility in sex-reversed XY animals are unique to mice? There are reports of fertility in mutant XY sex-reversed wood lemmings (*Myopus shisticolor*) (Liu, Eriksson & Fredga, 1998), and female horses (Sharp, Wachtel & Benirschke, 1980). In addition, we are aware of one remarkable report of a fertile woman with normal ovaries and a predominantly XY karyotype (Dumic *et al.*, 2008). As such, our observations in sex-reversed XY (*Dax1-/Y*) mice support the notion that XY sex-reversal is not formally incompatible with reproduction. However, our data also suggest that the inter-individual milieu of mechanical and development complications caused by the presence of the Y-chromosome makes successful reproduction highly unlikely.

5.4 Summary of Findings

- C57BL/6J background is highly sensitive to male-to-female sex-reversal in the absence of the nuclear receptor Dax1.

- A minority of sex-reversed XY (*Dax1-/Y*) mice have markers of fertility.

- A minority of sex-reversed XY (*Dax1-/Y*) mice can produce live offspring without any assisted fertility treatment.

General Conclusion and Future Perspectives

6 General Conclusion and Future Perspectives

Reproduction in mammals is initiated at puberty through pulsatile release of gonadotropin releasing hormone from the gonadotropin releasing hormone neurons of the hypothalamus (Yen, 1977). Gonadotropin releasing hormone travels to the anterior pituitary through the hypophyseal circulation, where it acts to stimulate synthesis and release of gonadotropin hormones, luteinising hormone and follicle stimulating hormone. Gonadotropin hormones enter the peripheral circulation and act on the gonads to stimulate gametogenesis (oogenesis in females and spermatogenesis in males) and sexual differentiation. In response to the action of gonadotropin hormones the gonads produce estrogen (Yen, 1977; Coss, 2018; Stamatiades & Kaiser, 2018; Schally *et al.*, 1971).

Estrogen feedbacks to the hypothalamus in order to regulate gonadotropin releasing hormone release and thus regulating the levels of luteinising hormone and follicle stimulating hormone (Channing & Tsafriri, 1977; Richards, 1980; Pinilla *et al.*, 2012). Although gonadotropin releasing hormone neurons are an essential components of the reproductive axis, kisspeptins emerged as upstream regulators of GnRH neurons.

In rodents, kisspeptin neurons have been mapped to two main areas of the hypothalamus, the arcuate nucleus and the anteroventral periventricular nucleus (Tng, 2015; Dungan, Clifton & Steiner, 2006; Clarkson *et al.*, 2009; Clarkson & Herbison, 2006). As mentioned previously, sex steroids released by the gonads feedback to the hypothalamus in order to regulate gonadotropin releasing hormone release and in this way regulating the reproductive axis. However, the effects of estrogen on gonadotropin releasing hormones is not direct as these neurons do not express estrogen receptors (Wintermantel *et al.*, 2006; Herbison & Pape, 2001).

It is now known that kisspeptin play a crucial role in reproduction as kisspeptin neurons mediate the effects of estrogen on gonadotropin releasing hormone neurons. Indeed, the vast majority of kisspeptin neurons express receptors for sex steroids: the estrogen receptor alpha (approximately 90%) (Kumar *et al.*, 2015; Smith *et al.*, 2005a). Thus, highlighting kisspeptin neurons as the mediators of estrogen feedback on the reproductive axis.

In rodents, estrogen has differential effects on *Kiss1* gene expression in the two female hypothalamic nuclei. Estrogen increases expression of kisspeptin in the anteroventral periventricular nucleus, whereas it represses *Kiss1* gene expression in the arcuate nucleus (Popa, Clifton & Steiner, 2008; Oakley, Clifton & Steiner, 2009; Roa *et al.*, 2008). The

mechanism by which estrogen differentially regulates *Kiss1* gene expression in the arcuate nucleus and anteroventral periventricular nucleus of the hypothalamus remain elusive. Therefore, the aim of this project was to demystify the mechanism underlying the differential effects of estrogen in *Kiss1* gene expression in the female hypothalamic nuclei. Our hypothesis was that the mechanisms underlying the differential effects of estrogen in kisspeptin expression were analogous of the mechanisms that mediate cell- and tissue-specific actions of selective estrogen receptor modulators.

Selective estrogen receptor modulators are receptor ligands that exhibit agonistic or antagonistic effects in tissue-, cell-, and gene context-dependent manner (e.g. tamoxifen). It is now known that differences in relative expression of coactivators and corepressors accounts for the tissue-specific antagonistic versus agonistic action of selective estrogen receptor modulators (Arnal *et al.*, 2017; Smith & O'Malley, 2004; Smith, Nawaz & O'Malley, 1997). For this reason, the arcuate nucleus and anteroventral periventricular nucleus were submitted to a study comparing the expression of genes involved in estrogen receptor signalling including genes encoding for nuclear receptors and their coregulators was investigated.

We identified the *Nr0b1* gene, which encodes the corepressor Dax1, as the most differently expressed gene between the two female hypothalamic nuclei. Indeed we show that the corepressor Dax1 was highly enriched in the arcuate nucleus, where estrogen represses *Kiss1* expression. We therefore believe that Dax1 is the differentiating component between the anteroventral periventricular and the arcuate nuclei of the hypothalamus. Therefore Dax1, likely, mediates the differential effects of estrogen in kisspeptin expression in the arcuate nucleus and the anteroventral periventricular nucleus.

While the *in vitro* and *ex-vivo* methods currently available to study estrogen-mediated *Kiss1* gene expression in the female hypothalamic nuclei have been shown, here, to be unreliable and inconsistent, we have, successfully, generated mice with conditional knockout of Dax1 in kisspeptin cells. This not only enabled us to decipher the role of Dax1 in estrogen-mediated regulation of *Kiss1* but also to understand the role of Dax1 in reproduction in the female adult, something that has been overlooked over the years.

We found that Dax1, a potent corepressor, is a crucial component in the estrogen-mediated repression kisspeptin expression in the arcuate nucleus. In the absence of Dax1, female mice

with conditional knockout of Dax1 in kisspeptin cells presented with the hallmarks of perturbed estrogen-negative feedback. The animals failed to repress *Kiss1* gene expression in the arcuate nucleus which prevented the gonadotropin releasing hormone-mediated decrease in the levels of follicle stimulating hormone. As a consequence animals with conditional knockout of Dax1 in kisspeptin cells presented with high levels of estrogen and follicle stimulating hormone in their plasma. Their ovaries were also characterised by increased number of follicles. Further to this, estrogen negative feedback in the arcuate nucleus is also known to regulate estrous cyclicity therefore, unsurprisingly, knocking down Dax1 in kisspeptin cells resulted in animals presenting with estrous cycle disturbances (i.e. longer estrous cycles due to these mice spending more time in the estrous stage of the cycle).

Further to this, we also explored the role of Dax1 in sex determination. Dax1 is important for sex determination, during development, *Dax1* is a testes-determining gene (Ludbrook & Harley, 2004; Meeks, Weiss & Jameson, 2003). Studies have shown that Dax1-deficient male mice display a spectrum of sex-reversal phenotypes (from XY animals to phenotypic females). The phenotypic spectrum obtained has been linked to (i) the background of the strain in which the experiment was conducted (humans with dosage-sensitive sex reversal also present with a phenotypic spectrum) and (ii) with the relative 'strength' of the sex-determining gene, *Sry* (Bouma, 2005). We show here that both background and intra-strain variability accounts for the spectrum of sex-reversal phenotypes. While most sex-reversed XY (*Dax1-/Y*) mice presented with apparent hypothalamic hypogonadism (low plasma gonadotropins and low estrogen levels) and are infertile, this work also shows that a minority of sex-reversed XY (*Dax1-/Y*) mice resemble control animals and can produce live offspring without any assisted fertility treatment. Which adds to the small to number of reports of live-birth from sex-reversed XY mice.

This work demonstrates the importance of Dax1 in sex determination and reproduction. We show here for the first time that estrogen negative-feedback is mediated by Dax1.

Looking ahead it would be interesting to understand if a knockdown model or acute knockout of Dax1 in kisspeptin cells would have resulted in an even more striking reproductive. There is also the potential to understand if estrogen negative-feedback, in the male, is mediated by Dax1.

References

7 References

Aranda, A. & Pascual, A. (2001) Nuclear Hormone Receptors and Gene Expression. *Physiological Reviews*. [Online] Available from: doi:10.1152/physrev.2001.81.3.1269.

Arnal, J.-F., Lenfant, F., Metivier, R., Flouriot, G., et al. (2017) Membrane and Nuclear Estrogen Receptor Alpha Actions: From Tissue Specificity to Medical Implications. *Physiological Reviews*. [Online] 97 (3), 1045–1087. Available from: doi:10.1152/physrev.00024.2016.

Bae, D.S., Schaefer, M.L., Partan, B.W. & Muglia, L. (1996) Characterization of the mouse DAX-1 gene reveals evolutionary conservation of a unique amino-terminal motif and widespread expression in mouse tissue. *Endocrinology*. 137 (9).

Bateman, H.L. & Patisaul, H.B. (2008) Disrupted female reproductive physiology following neonatal exposure to phytoestrogens or estrogen specific ligands is associated with decreased GnRH activation and kisspeptin fiber density in the hypothalamus. *Neurotoxicology*. [Online] 29 (6), 988–997. Available from: doi:10.1016/j.neuro.2008.06.008.DISRUPTED.

Bauer, U., Daujat, S., Nielsen, S.J., Nightingale, K., et al. (2002) *Methylation at arginine 17 of histone H3 is linked*. 3 (1), 39–44.

Bjornstrom, L. & Sjoberg, M. (2005) Mechanisms of Estrogen Receptor Signaling: Convergence of Genomic and Nongenomic Actions on Target Genes. *Molecular Endocrinology*. [Online] 19 (4), 833–842. Available from: doi:10.1210/me.2004-0486.

Bouma, G.J. (2005) Gonadal sex reversal in mutant Dax1 XY mice: a failure to upregulate Sox9 in pre-Sertoli cells. *Development*. [Online] Available from: doi:10.1002/jlcr.2580220511.

Brzozowski, A.M., Pike, A.C.W., Dauter, Z., Hubbard, R.E., et al. (1997) Molecular basis of agonism and antagonism in the oestrogen receptor. *Nature*. [Online] 389 (6652), 753–758. Available from: doi:10.1038/39645 [Accessed: 21 May 2019].

Burris, T.P., Guo, W. & McCabe, E.R. (1996) The gene responsible for adrenal hypoplasia congenita, DAX-1, encodes a nuclear hormone receptor that defines a new class within the superfamily. *Recent progress in hormone research*. [Online] 51, 241-59; discussion 259-60. Available from: http://www.ncbi.nlm.nih.gov/pubmed/8701082 [Accessed: 29 April 2019].

Caligioni, C.S. (2009) Assessing reproductive status/stages in mice. *Current Protocols in Neuroscience*. [Online] Available from: doi:10.1002/0471142301.nsa04is48.

Castellano, J.M., Gaytan, M., Roa, J., Vigo, E., et al. (2006) Expression of KiSS-1 in Rat Ovary: Putative Local Regulator of Ovulation? *Endocrinology*. [Online] 147 (10), 4852–4862. Available from: doi:10.1210/en.2006-0117 [Accessed: 22 May 2019].

Castellano, J.M., Wright, H., Ojeda, S.R. & Lomniczi, A. (2014) An alternative transcription start site yields estrogen-unresponsive kiss1 mRNA transcripts in the hypothalamus of prepubertal female rats. *Neuroendocrinology*. [Online] 99 (2), 94–107. Available from: doi:10.1159/000362280.

Channing, C.P. & Tsafriri, A. (1977) Mechanism of action of luteinizing hormone and follicle-stimulating hormone on the ovary in vitro. *Metabolism*. [Online] Available from: doi:10.1016/0026-0495(77)90108-1.

Chen, D., Ma, H., Hong, H., Koh, S.S., et al. (1999) Regulation of Transcription by a Protein Methyltransferase. *Science*. 284 (June), 2174–2177.

Cimino, I., Casoni, F., Liu, X., Messina, A., et al. (2016) Novel role for anti-Müllerian hormone in the regulation of GnRH neuron excitability and hormone secretion. *Nature Communications*. [Online] Available from: doi:10.1038/ncomms10055.

Clarkson, J., d'Anglemont de Tassigny, X., Colledge, W.H., Caraty, A., et al. (2009) Distribution of Kisspeptin Neurones in the Adult Female Mouse Brain. *Journal of Neuroendocrinology*. [Online] 21 (8), 673–682. Available from: doi:10.1111/j.1365-2826.2009.01892.x [Accessed: 2 May 2019].

Clarkson, J. & Herbison, A.E. (2006) Postnatal development of kisspeptin neurons in mouse hypothalamus; sexual dimorphism and projections to gonadotropin-releasing hormone neurons. *Endocrinology*. [Online] 147 (12), 5817–5825. Available from: doi:10.1210/en.2006-0787.

Colledge, W.H. (2009) Transgenic mouse models to study Gpr54/kisspeptin physiology. *Peptides*. [Online] Available from: doi:10.1016/j.peptides.2008.05.006.

Coss, D. (2018) Regulation of reproduction via tight control of gonadotropin hormone levels. *Molecular and Cellular Endocrinology*. [Online] 463, 116–130. Available from: doi:10.1016/j.mce.2017.03.022.

Crawford, P.A., Dorn, C., Sadovsky, Y. & Milbrandt, J. (1998) Nuclear receptor DAX-1 recruits nuclear receptor corepressor N-CoR to steroidogenic factor 1. *Molecular and cellular biology*. [Online] 18 (5), 2949–2956. Available from:

http://www.ncbi.nlm.nih.gov/pubmed/9566914 [Accessed: 29 April 2019].

Crawford, P.A., Dorn, C., Sadovsky, Y. & Milbrandt, J. (2015) Nuclear Receptor DAX-1 Recruits Nuclear Receptor Corepressor N-CoR to Steroidogenic Factor 1. *Molecular and Cellular Biology*. [Online] 18 (5), 2949–2956. Available from: doi:10.1128/mcb.18.5.2949.

d'Anglemont de Tassigny, X. & Colledge, W.H. (2010) The Role of Kisspeptin Signaling in Reproduction. *Physiology*. [Online] 25 (4), 207–217. Available from: doi:10.1152/physiol.00009.2010.

d'Anglemont de Tassigny, X., Fagg, L.A., Dixon, J.P.C., Day, K., et al. (2007) Hypogonadotropic hypogonadism in mice lacking a functional Kiss1 gene. *Proceedings of the National Academy of Sciences*. [Online] Available from: doi:10.1073/pnas.0704114104.

Dhillo, W.S., Chaudhri, O.B., Patterson, M., Thompson, E.L., et al. (2005) Kisspeptin-54 stimulates the hypothalamic-pituitary gonadal axis in human males. *Journal of Clinical Endocrinology and Metabolism*. [Online] 90 (12), 6609–6615. Available from: doi:10.1210/jc.2005-1468.

Dhillo, W.S., Chaudhri, O.B., Thompson, E.L., Murphy, K.G., et al. (2007) Kisspeptin-54 stimulates gonadotropin release most potently during the preovulatory phase of the menstrual cycle in women. *Journal of Clinical Endocrinology and Metabolism*. [Online] 92 (10), 3958–3966. Available from: doi:10.1210/jc.2007-1116.

Dubois, S.L., Acosta-Martínez, M., Dejoseph, M.R., Wolfe, A., et al. (2015) Positive, But Not Negative Feedback Actions of Estradiol in Adult Female Mice Require Estrogen Receptor Alpha in Kisspeptin Neurons. *Neuroendocrinology*. [Online] 156 (March), 1111–1120. Available from: doi:10.1210/en.2014-1851.

Dumic, M., Lin-Su, K., Leibel, N.I., Ciglar, S., et al. (2008) Report of fertility in woman with predominantly 46,XY karyotype in family with multiple disorders of sexual development: Review of Prismatic Case. *Mount Sinai Journal of Medicine: A Journal of Translational and Personalized Medicine*. [Online] 75 (2), 168–169. Available from: doi:10.1002/msj.20046 [Accessed: 5 May 2019].

Dungan, H.M., Clifton, D.K. & Steiner, R.A. (2006) Minireview: Kisspeptin neurons as central processors in the regulation of gonadotropin-releasing hormone secretion. *Endocrinology*. [Online]. Available from: doi:10.1210/en.2005-1282.

Eddy, E.M., Washburn, T.F., Bunch, D., Gladen, B.C., et al. (1996) Targeted disruption of

the estrogen receptor gene in male mice causes alteration of spermatogenesis and infertility. *Society*. [Online] 137 (10), 4796–4805. Available from: doi:10.1210/en.137.11.4796.

Eicher, E.M., Washburn, L.L., Wihitney, J.B. & Morrow, K.E. (1982) *Mus poschiavinus Y Chromosome in the C57BL/6J Murine Genome Causes Sex Reversal*. 29 (1981), 535–538.

El-Brolosy, M.A., Kontarakis, Z., Rossi, A., Kuenne, C., et al. (2019) Genetic compensation triggered by mutant mRNA degradation. *Nature*. [Online] 568 (7751), 193–197. Available from: doi:10.1038/s41586-019-1064-z.

El-Brolosy, M.A. & Stainier, D.Y.R. (2017) Genetic compensation: A phenomenon in search of mechanisms. *PLoS Genetics*. [Online] 13 (7), 1–17. Available from: doi:10.1371/journal.pgen.1006780.

Enmark, E., Enmark, E., Pelto-Huikko, M., Pelto-Huikko, M., et al. (1997) Human estrogen receptor beta-gene structure, chromosomal localization, and expression pattern. *Journal of Clinical Endocrinology and Metabolism*. 82 (12), 4258–4265.

Funes, S., Hedrick, J.A., Vassileva, G., Markowitz, L., et al. (2003) The KiSS-1 receptor GPR54 is essential for the development of the murine reproductive system. *Biochemical and Biophysical Research Communications*. [Online] Available from: doi:10.1016/j.bbrc.2003.11.066.

Gaub, M.P., Bellard, M., Scheuer, I., Chambon, P., et al. (1990) Activation of the ovalbumin gene by the estrogen receptor involves the fos-jun complex. *Cell*. [Online] 63 (6), 1267–1276. Available from: http://www.ncbi.nlm.nih.gov/pubmed/2124518 [Accessed: 21 May 2019].

Girault, I., Bièche, I. & Lidereau, R. (2006) Role of estrogen receptor α transcriptional coregulators in tamoxifen resistance in breast cancer. *Maturitas*. [Online] 54 (4), 342–351. Available from: doi:10.1016/j.maturitas.2006.06.003.

Goodman, R.L., Lehman, M.N., Smith, J.T., Coolen, L.M., et al. (2007) Kisspeptin Neurons in the Arcuate Nucleus of the Ewe Express Both Dynorphin A and Neurokinin B. *Endocrinology*. [Online] 148 (12), 5752–5760. Available from: doi:10.1210/en.2007-0961.

Gottsch, M.L., Cunningham, M.J., Smith, J.T., Popa, S.M., et al. (2004) A role for kisspeptins in the regulation of gonadotropin secretion in the mouse. *Endocrinology*. [Online] 145 (9), 4073–4077. Available from: doi:10.1210/en.2004-0431.

Gottsch, M.L., Popa, S.M., Lawhorn, J.K., Qiu, J., et al. (2011) Molecular properties of kiss1 neurons in the arcuate nucleus of the mouse. *Endocrinology*. [Online] Available from: doi:10.1210/en.2011-1521.

Gronemeyer, H., Gustafsson, J.Å. & Laudet, V. (2004) Principles for modulation of the nuclear receptor superfamily. *Nature Reviews Drug Discovery*. [Online]. Available from: doi:10.1038/nrd1551.

Gruber, C.J., Tschugguel, W., Schneeberger, C. & Huber, J.C. (2002) Production and Action of Estrogens. *The New England Journal of Medicine Review*. [Online] 346 (5), 340–352. Available from: doi:10.1016/S0960-0760(01)00184-4.

Habiby, R.L., Boepple, P., Nachtigall, L., Sluss, P.M., et al. (1996) Adrenal hypoplasia congenita with hypogonadotropic hypogonadism: Evidence that DAX-1 mutations lead to combined hypothalamic and pituitary defects in gonadotropin production. *Journal of Clinical Investigation*. [Online] 98 (4), 1055–1062. Available from: doi:10.1172/JCI118866.

Harris, G.C. & Levine, J.E. (2003) Pubertal Acceleration of Pulsatile Gonadotropin-Releasing Hormone Release in Male Rats as Revealed by Microdialysis. *Endocrinology*. [Online] 144 (1), 163–171. Available from: doi:10.1210/en.2002-220767 [Accessed: 21 May 2019].

Heery, D.M., Kalkhoven, E., Hoare, S. & Parker, M.G. (1997) *A signature motif in transcriptional co-activators mediates binding to nuclear receptors*. [Online]. Available from: https://www.nature.com/articles/42750.pdf [Accessed: 25 April 2019].

Heldring, N., Pike, A., Andersson, S., Matthews, J., et al. (2007) Estrogen Receptors: How Do They Signal and What Are Their Targets. *Physiological Reviews*. [Online] Available from: doi:10.1152/physrev.00026.2006.

Herbison, A.E. & Pape, J.R. (2001) New evidence for estrogen receptors in gonadotropin-releasing hormone neurons. *Frontiers in Neuroendocrinology*. [Online]. Available from: doi:10.1006/frne.2001.0219.

Herbison, A.E., De Tassigny, X.D.A., Doran, J. & Colledge, W.H. (2010) Distribution and postnatal development of Gpr54 gene expression in mouse brain and gonadotropin-releasing hormone neurons. *Endocrinology*. [Online] 151 (1), 312–321. Available from: doi:10.1210/en.2009-0552.

Hillier, S.G. (2001) Gonadotropic control of ovarian follicular growth and development.

Molecular and Cellular Endocrinology. [Online]. Available from: doi:10.1016/S0303-7207(01)00469-5.

Hu, M.H., Li, X.F., McCausland, B., Li, S.Y., et al. (2015) Relative importance of the arcuate and anteroventral periventricular kisspeptin neurons in control of puberty and reproductive function in female rats. *Endocrinology*. [Online] Available from: doi:10.1210/en.2014-1655.

Hu, X. & Lazar, M.A. (1999) *The CoRNR motif controls the recruitment of corepressors by nuclear hormone receptors*. 562 (1994), 93–96.

Huang, H.-J., Norris, J.D. & McDonnell, D.P. (2002) Identification of a Negative Regulatory Surface within Estrogen Receptor α Provides Evidence in Support of a Role for Corepressors in Regulating Cellular Responses to Agonists and Antagonists. *Molecular Endocrinology*. [Online] 16 (8), 1778–1792. Available from: doi:10.1210/me.2002-0089.

Huhtaniemi, I. (2006) Mutations along the pituitary-gonadal axis affecting sexual maturation: Novel information from transgenic and knockout mice. *Molecular and Cellular Endocrinology*. [Online] 254–255, 84–90. Available from: doi:10.1016/j.mce.2006.04.015.

Huijbregts, L. & De Roux, N. (2010) KISS1 is down-regulated by 17β-estradiol in MDA-MB-231 cells through a nonclassical mechanism and loss of ribonucleic acid polymerase ii binding at the proximal promoter. *Endocrinology*. [Online] 151 (8), 3764–3772. Available from: doi:10.1210/en.2010-0260.

Ikeda, Y., Takeda, Y., Shikayama, T., Mukai, T., et al. (2001) Comparative localization of Dax-1 and Ad4BP/SF-1 during development of the hypothalamic-pituitary-gonadal axis suggests their closely related and distinct functions. *Developmental Dynamics*. [Online] Available from: doi:10.1002/dvdy.1116.

Irwig, M.S., Fraley, G.S., Smith, J.T., Acohido, B. V., et al. (2004) Kisspeptin activation of gonadotropin releasing hormone neurons and regulation of KiSS-1 mRNA in the male rat. *Neuroendocrinology*. [Online] Available from: doi:10.1159/000083140.

Ito, M., Yu, R. & Jameson, J.L. (1997) DAX-1 inhibits SF-1-mediated transactivation via a carboxy-terminal domain that is deleted in adrenal hypoplasia congenita. *Molecular and cellular biology*. [Online] 17 (3), 1476–1483. Available from: doi:10.1128/MCB.17.3.1476 [Accessed: 30 April 2019].

Iyer, A.K. & McCabe, E.R.B. (2004) Molecular mechanisms of DAX1 action. *Molecular*

Genetics and Metabolism. [Online]. Available from: doi:10.1016/j.ymgme.2004.07.018.

Jadhav, U., Harris, R.M. & Jameson, J.L. (2011) Hypogonadotropic Hypogonadism in Subjects with DAX1 Mutations. *Molecular Cell Endocrinology*. [Online] 5 (3), 379–390. Available from: doi:10.2217/FON.09.6.Dendritic.

Kaprara, A. & Huhtaniemi, I.T. (2018) The hypothalamus-pituitary-gonad axis: Tales of mice and men. *Metabolism: Clinical and Experimental*. [Online] 86, 3–17. Available from: doi:10.1016/j.metabol.2017.11.018.

Katzenellenbogen, J.A., O'Malley, B.W. & Katzenellenbogen, B.S. (1996) Tripartite steroid hormone receptor pharmacology: interaction with multiple effector sites as a basis for the cell- and promoter-specific action of these hormones. *Molecular Endocrinology*. [Online] 10 (2), 119–131. Available from: doi:10.1210/mend.10.2.8825552.

Kauffman, A.S. (2013) Coming of Age in the Kisspeptin Era: Sex differences, Development, and Puberty. *Molecular Cell Endocrinology*. [Online] 324, 51–63. Available from: doi:10.1038/mp.2011.182.doi.

Kauffman, A.S., Clifton, D.K. & Steiner, R.A. (2007) Emerging ideas about kisspeptin-GPR54 signaling in the neuroendocrine regulation of reproduction. *Trends in Neurosciences*. [Online] 30 (10), 504–511. Available from: doi:10.1016/j.tins.2007.08.001.

Kauffman, A.S., Gottsch, M.L., Roa, J., Byquist, A.C., et al. (2007) Sexual differentiation of Kiss1 gene expression in the brain of the rat. *Endocrinology*. [Online] 148 (4), 1774–1783. Available from: doi:10.1210/en.2006-1540.

Kok, F.O., Shin, M., Ni, C.-W., Gupta, A., et al. (2015) Reverse Genetic Screening Reveals Poor Correlation between Morpholino-Induced and Mutant Phenotypes in Zebrafish. *Developmental Cell*. [Online] 32 (1), 97–108. Available from: doi:10.1016/J.DEVCEL.2014.11.018 [Accessed: 18 May 2019].

Kotani, M., Detheux, M., Vandenbogaerde, A., Communi, D., et al. (2001) The Metastasis Suppressor Gene KiSS-1 Encodes Kisspeptins, the Natural Ligands of the Orphan G Protein-coupled Receptor GPR54. *Journal of Biological Chemistry*. [Online] Available from: doi:10.1016/j.econlet.2011.05.013.

Krust, A., Green, S., Argos, P., Kumar, V., et al. (1986) The chicken oestrogen receptor sequence: homology with v-erbA and the human oestrogen and glucocorticoid

receptors. *The EMBO Journal*. [Online] 5 (5), 891–897. Available from: doi:10.1002/j.1460-2075.1986.tb04300.x [Accessed: 21 May 2019].

Kumar, D., Candlish, M., Periasamy, V., Avcu, N., et al. (2015) Specialized subpopulations of kisspeptin neurons communicate with gnrh neurons in female mice. *Endocrinology*. [Online] Available from: doi:10.1210/en.2014-1671.

Kumar, T.R., Wang, Y., Lu, N. & Matzuk, M.M. (1997) Follicle stimulating hormone is required for ovarian follicle maturation but not male fertility. *Nature Genetics*. 15 (february), 201–204.

Kumar, V., Green, S., Stack, G., Berry, M., et al. (1987) Functional domains of the human estrogen receptor. *Cell*. [Online] 51 (6), 941–951. Available from: doi:10.1016/0092-8674(87)90581-2 [Accessed: 21 May 2019].

Kuno, J., Poueymirou, W.T., Gong, G., Siao, C.-J., et al. (n.d.) *Generation of fertile and fecund F0 XY female mice from XY ES cells*. [Online] Available from: doi:10.1007/s11248-014-9815-y [Accessed: 5 May 2019].

Kushner, P.J., Agard, D.A., Greene, G.L., Scanlan, T.S., et al. (2000) *Estrogen receptor pathways to AP-1*. 74, 311–317.

Lalli, E. & Sassone-Corsi, P. (2003) DAX-1, an Unusual Orphan Receptor at the Crossroads of Steroidogenic Function and Sexual Differentiation. *Molecular Endocrinology*. [Online] 17 (8), 1445–1453. Available from: doi:10.1210/me.2003-0159.

Lamminen, T., Jokinen, P., Jiang, M., Pakarinen, P., et al. (2005) Human FSHβ subunit gene is highly conserved. *Molecular Human Reproduction*. [Online] 11 (8), 601–605. Available from: doi:10.1093/molehr/gah198.

Laudet, V. (1997) Evolution of the nuclear receptor superfamily: Early diversification from an ancestral orphan receptor. *Journal of Molecular Endocrinology*. [Online] 19 (3), 207–226. Available from: doi:10.1677/jme.0.0190207.

Lee, D.K., Nguyen, T., O'Neill, G.P., Cheng, R., et al. (1999a) Discovery of a receptor related to the galanin receptors. *FEBS Letters*. [Online] 446 (1), 103–107. Available from: doi:10.1016/S0014-5793(99)00009-5.

Lee, D.K., Tuan, N., O'Neill, G.P., Regina, C., et al. (1999b) Discovery of a receptor related to the galanin receptors. *FEBS Letters*. [Online] 446 (1), 103–107. Available from: doi:10.1016/S0014-5793(99)00009-5.

Lee, J., Miele, M.E., Hicks, D.J., Phillips, K.K., et al. (1996) KiSS-1 , a Novel Human Malignant Melanoma Metastis-Supressor Gene. *Journal of the National Cancer Institute*. 88 (23),

1731–1737.

Levine, J.E., Norman, R.L., Gliessman, P.M., Oyama, T.T., et al. (1985) In Vivo Gonadotropin-Releasing Hormone Release and Serum Luteinizing Hormone Measurements in Ovariectomized, Estrogen-Treated Rhesus Macaques*. *Endocrinology*. [Online] 117 (2), 711–721. Available from: doi:10.1210/endo-117-2-711 [Accessed: 21 May 2019].

Liu, W., Eriksson, L. & Fredga, K. (1998) XY Sex Reversal in the Wood Lemming is Associated with Deletion of Xp21–23 as Revealed by Chromosome Microdissection and Fluorescence in situ Hybridization. *Chromosome Research*. [Online] 6 (5), 379–384. Available from: doi:10.1023/A:1009273205788 [Accessed: 5 May 2019].

Ludbrook, L.M. & Harley, V.R. (2004) *Sex determination : a ' window ' of DAX1 activity*. [Online] 15 (3). Available from: doi:10.1016/j.tem.2004.02.002.

Ma, H., Baumann, C.T., Li, H., Strahl, B.D., et al. (2011) methylation of histone H3 on a steroid-regulated promoter. *Current Biology*. 11 (24), 1981–1985.

Ma, X., Dong, Y., Matzuk, M.M. & Kumar, T.R. (2004) Targeted disruption of luteinizing hormone -subunit leads to hypogonadism, defects in gonadal steroidogenesis, and infertility. *Proceedings of the National Academy of Sciences*. [Online] 101 (49), 17294–17299. Available from: doi:10.1073/pnas.0404743101.

Ma, Y.J., Kelly, M.J. & Ronneklei, O.K. (1990) Pro-Gonadotropin-Releasing Hormone (ProGnRH) and GnRH Content in the Preoptic Area and the Basal Hypothalamus of Anterior Medial Preoptic Nucleus/Suprachiasmatic Nucleus-Lesioned Persistent Estrous Rats*. *Endocrinology*. [Online] 127 (6), 2654–2664. Available from: doi:10.1210/endo-127-6-2654 [Accessed: 2 May 2019].

Ma, Z., Zhu, P., Shi, H., Guo, L., et al. (n.d.) PTC-bearing mRNA elicits a genetic compensation response via Upf3a and COMPASS components. *Nature*. [Online] Available from: doi:10.1038/s41586-019-1057-y [Accessed: 18 May 2019].

Mangelsdorf, D.J., Thummel, C., Beato, M., Herrlich, P., et al. (1995) *The Nuclear Receptor Superfamily: The Second Decade*. 83, 835–839.

Martin, R.M. & Cardoso, M.C. (2010) Chromatin condensation modulates access and binding of nuclear proteins. *The FASEB Journal*. [Online] Available from: doi:10.1096/fj.08-128959.

Matsui, H., Takatsu, Y., Kumano, S., Matsumoto, H., et al. (2004) Peripheral administration of metastin induces marked gonadotropin release and ovulation in the rat.

Biochemical and Biophysical Research Communications. [Online] 320 (2), 383–388. Available from: doi:10.1016/j.bbrc.2004.05.185.

Matthews, J. & Gustafsson, J.A. (2003) Extrogen sinaling: A subtle balance between ER ER. *Molecular Intervention*. [Online] 3 (5), 281–292. Available from: doi:10.1124/mi.3.5.281.

McCabe, E.R.. (2001) Adrenal hypoplasias and aplasias. In: C. R. Scriver, A. L. Beaudet, W S Sly, D Valle, et al. (eds.). *The Metabolic and Molecular Bases of Inherited Disease*. New York, McGraw-Hill. pp. 4263–4274.

McDevitt, M.A., Glidewell-Kenney, C., Jimenez, M.A., Ahearn, P.C., et al. (2009) *New Insights into the Classical and Non-classical Actions of Estrogen: Evidence from Estrogen Receptor Knock Out and Knock In Mice*. [Online] 290, 24–30. Available from: doi:10.1016/j.mce.2008.04.003.New.

Mckenna, N.J., Lanz, R.B. & O'Malley, B.W. (1999) *Nuclear Receptor Coregulators: Cellular and Molecular Biology**.

Meeks, J.J., Weiss, J. & Jameson, J.L. (2003) *Dax1 is required for testis determination*. [Online] 34 (April), 1–2. Available from: doi:10.1038/ng1141.

Messager, S., Chatzidaki, E.E., Ma, D., Hendrick, A.G., et al. (2005) Kisspeptin directly stimulates gonadotropin-releasing hormone release via G protein-coupled receptor 54. *Proceedings of the National Academy of Sciences*. [Online] Available from: doi:10.1073/pnas.0409330102.

Millard, C.J., Watson, P.J., Fairall, L. & Schwabe, J.W.R. (2013) An evolving understanding of nuclear receptor coregulator proteins. *Journal of Molecular Endocrinology*. [Online] 51 (3), T23–T36. Available from: doi:10.1530/jme-13-0227.

Millier, S.G., Whitelaw, P.F. & Smyth, C.D. (1994) Follicular oestrogen synthesis: the 'two-cell, two-gonadotrophin' model revisited. *Molecular and Cellular Endocrinology*. [Online] 100 (1–2), 51–54. Available from: doi:10.1016/0303-7207(94)90278-X.

Mitchell, R.G. & Rhaney, K. (1959) Congenital adrenal hypoplasia in siblings. *Lancet (London, England)*. [Online] 1 (7071), 488–492. Available from: http://www.ncbi.nlm.nih.gov/pubmed/13632060 [Accessed: 22 May 2019].

Moenter, S.M., Defazio, R.A., Straume, M. & Nunemaker, C.S. (2003) Steroid Regulation of GnRH Neurons. In: *Annals of the New York Academy of Sciences*. [Online]. 2003 p. Available from: doi:10.1196/annals.1286.014.

Monroe, D.G., Secreto, F.J., Khosla, S., Spelsberg, T.C., et al. (2006) *The Classical Estrogen*

Receptor Transcriptional Pathway Implications in Human Osteoblasts. 4 (2), 129–140.

Morris, J.A., Jordan, C.L. & Breedlove, S.M. (2004) Sexual differentiation of the vertebrate nervous system. *Nature Neuroscience*. [Online] 7 (10), 1034–1039. Available from: doi:10.1038/nn1325.

Muscatelli, F., Stromt, T.M., Walker, A.P., Zanariat, E., et al. (1994) Mutations in the DAX-1 gene give rise to both X-linked adrenal hypoplasia congenita and hypogonadotropic hypogonadism. *Nature*. 372 (December), 672–676.

Nachtigal, M.W., Hirokawa, Y., Enyeart-VanHouten, D.L., Flanagan, J.N., et al. (1998) Wilms' tumor 1 and Dax-1 modulate the orphan nuclear receptor SF-1 in sex-specific gene expression. *Cell*. [Online] 93 (3), 445–454. Available from: doi:10.1016/S0092-8674(00)81172-1.

Nagy, L., Kao, H., Love, J.D., Li, C., et al. (1999) *Mechanism of corepressor binding and release from nuclear hormone receptors*. 3209–3216.

Navarro, V.M., Castellano, J.M., Fernández-Fernández, R., Barreiro, M.L., et al. (2004a) Developmental and hormonally regulated messenger ribonucleic acid expression of KiSS-1 and its putative receptor, GPR54, in rat hypothalamus and potent luteinizing hormone-releasing activity of KiSS-1 peptide. *Endocrinology*. [Online] Available from: doi:10.1210/en.2004-0413.

Navarro, V.M., Castellano, J.M., Fernández-Fernández, R., Barreiro, M.L., et al. (2004b) Developmental and hormonally regulated messenger ribonucleic acid expression of KiSS-1 and its putative receptor, GPR54, in rat hypothalamus and potent luteinizing hormone-releasing activity of KiSS-1 peptide. *Endocrinology*. [Online] 145 (10), 4565–4574. Available from: doi:10.1210/en.2004-0413.

Navarro, V.M., Castellano, J.M., Fernández-Fernández, R., Tovar, S., et al. (2005) Characterization of the potent luteinizing hormone-releasing activity of KiSS-1 peptide, the natural ligand of GPR54. *Endocrinology*. [Online] 146 (1), 156–163. Available from: doi:10.1210/en.2004-0836.

Navarro, V.M., Castellano, J.M., McConkey, S.M., Pineda, R., et al. (2011) Interactions between kisspeptin and neurokinin B in the control of GnRH secretion in the female rat. *American Journal of Physiology-Endocrinology and Metabolism*. [Online] 300 (1), E202–E210. Available from: doi:10.1152/ajpendo.00517.2010 [Accessed: 2 May 2019].

Navarro, V.M., Fernández-Fernández, R., Castellano, J.M., Roa, J., et al. (2004c) Advanced

vaginal opening and precocious activation of the reproductive axis by KiSS-1 peptide, the endogenous ligand of GPR54. *Journal of Physiology*. [Online] 561 (2), 379–386. Available from: doi:10.1113/jphysiol.2004.072298.

Nelson, J.F., Felicio, L.S., Randall, P.K., Sims, C., et al. (1982) A longitudinal Study of Estrous Cyclicity in Aging C57BL/6J Mice: I. Cycle Frequency, Length and Vaginal Cytology. *Biology of Reproduction*. 27, 327–339.

Niakan, K.K. & McCabe, E.R.B. (2005) DAX1 origin, function, and novel role. *Molecular Genetics and Metabolism*. [Online] 86 (1–2), 70–83. Available from: doi:10.1016/j.ymgme.2005.07.019.

Nilsson, S., Ma, S., Ma, S., Treuter, E., et al. (2019) *Mechanisms of Estrogen Action*. 81 (4).

O'Lone, R., Frith, M.C., Karlsson, E.K. & Hansen, U. (2004) Genomic Targets of Nuclear Estrogen Receptors. *Molecular Endocrinology*. [Online] 18 (8), 1859–1875. Available from: doi:10.1210/me.2003-0044 [Accessed: 21 May 2019].

Oakley, A.E., Clifton, D.K. & Steiner, R.A. (2009) Kisspeptin signaling in the brain. *Endocrine Reviews*. [Online]. Available from: doi:10.1210/er.2009-0005.

Obata, Y., Villemure, M., Kono, T. & Taketo, T. (2008) *Transmission of Y chromosomes from XY female mice was made possible by the replacement of cytoplasm during oocyte maturation*.

Ohtaki, T., Shintani, Y., Honda, S., Matsumoto, H., et al. (2001) Metastasis suppressor gene KiSS-1 encodes peptide ligand of a G-protein-coupled receptor. *Nature*. 411 (6837), 613–617.

Ojeda, S.R. & Urbanski, H.F. (1994) Puberty in the Rat. In: E Knobil & J. D. Neill (eds.). *The Physiology of Reproduction*. Second. New York, Raven Press, Ltd. pp. 363–409.

Parker, K.L. (2004) Steroidogenic Factor 1: A Key Determinant of Endocrine D evelopment and Function. *Endocrine Reviews*. [Online] 18 (3), 361–377. Available from: doi:10.1210/er.18.3.361.

Petersen, K.E., Bille, T., Jacobsen, B.B. & Iversen, T. (1982) X-linked congenital adrenal hypoplasia. A study of five generations of a Greenlandic Family. *Acta paediatrica Scandinavica*. [Online] 71 (6), 947–951. Available from: http://www.ncbi.nlm.nih.gov/pubmed/6891556 [Accessed: 22 May 2019].

Pinilla, L., Aguilar, E., Dieguez, C., Millar, R.P., et al. (2012) Kisspeptins and Reproduction: Physiological Roles and Regulatory Mechanisms. *Physiological Reviews*. [Online] Available from: doi:10.1152/physrev.00037.2010.

Ponglikitmongkol, M., Green, S. & Chambon, P. (1988) Genomic organization of the human oestrogen receptor gene. *The EMBO journal*. [Online] 7 (11), 3385–3388. Available from: doi:10.1002/j.1460-2075.1988.tb03211.x.

Popa, S.M., Clifton, D.K. & Steiner, R.A. (2008) The Role of Kisspeptins and GPR54 in the Neuroendocrine Regulation of Reproduction. *Annual Review of Physiology*. [Online] Available from: doi:10.1146/annurev.physiol.70.113006.100540.

Prader, A., Zachmann, M. & Illig, R. (1975) Luteinizing hormone deficiency in hereditary congenital adrenal hypoplasia. *The Journal of pediatrics*. [Online] 86 (3), 421–422. Available from: http://www.ncbi.nlm.nih.gov/pubmed/1113233 [Accessed: 22 May 2019].

Quennell, J.H., Howell, C.S., Roa, J., Augustine, R.A., et al. (2011) Leptin deficiency and diet-induced obesity reduce hypothalamic kisspeptin expression in mice. *Endocrinology*. [Online] Available from: doi:10.1210/en.2010-1100.

Rhie, Y.-J. (2013) Kisspeptin/G protein-coupled receptor-54 system as an essential gatekeeper of pubertal development. *Annals of Pediatric Endocrinology & Metabolism*. [Online] Available from: doi:10.6065/apem.2013.18.2.55.

Richards, J.S. (1980) *Maturation of Ovarian Follicles: Actions and Interactions of Pituitary and Ovarian Hormones on Follicular Cell Differentiation*. [Online]. Available from: www.physiology.org/journal/physrev.

Roa, J., Vigo, E., Castellano, J.M., Gaytan, F., et al. (2008) Opposite roles of estrogen receptor (ER)-α and ERβ in the modulation of luteinizing hormone responses to kisspeptin in the female rat: Implications for the generation of the preovulatory surge. *Endocrinology*. [Online] 149 (4), 1627–1637. Available from: doi:10.1210/en.2007-1540.

Rodriguez, I., Araki, K., Khatib, K., Martinou, J.C., et al. (1997) Mouse vaginal opening is an apoptosis-dependent process which can be prevented by the overexpression of Bcl2. *Developmental Biology*. [Online] Available from: doi:10.1006/dbio.1997.8522.

La Rosa, P. & Acconcia, F. (2011) Signaling functions of ubiquitin in the 17β-estradiol (E2):estrogen receptor (ER) α network. *The Journal of Steroid Biochemistry and Molecular Biology*. [Online] 127 (3–5), 223–230. Available from: doi:10.1016/J.JSBMB.2011.07.008 [Accessed: 21 May 2019].

Rossi, A., Kontarakis, Z., Gerri, C., Nolte, H., et al. (2015) Genetic compensation induced by deleterious mutations but not gene knockdowns. *Nature*. [Online] 524 (7564), 230–

233. Available from: doi:10.1038/nature14580.

de Roux, N., Genin, E., Carel, J.-C., Matsuda, F., et al. (2003) Hypogonadotropic hypogonadism due to loss of function of the KiSS1-derived peptide receptor GPR54. *Proceedings of the National Academy of Sciences*. [Online] Available from: doi:10.1073/pnas.1834399100.

Sand, P., Luckhaus, C., Schlurmann, K., Götz, M., et al. (2002) Untangling the human estrogen receptor gene structure. *Journal of Neural Transmission*. [Online] 109 (5–6), 567–583. Available from: doi:10.1007/s007020200047.

Schally, A. V., Arimura, A., Kastin, A.J., Matsuo, H., et al. (1971) Gonadotropin-releasing hormone: One polypeptide regulates secretion of luteinizing and follicle-stimulating hormones. *Science*. [Online] 173 (4001), 1036–1038. Available from: doi:10.1126/science.173.4001.1036.

Seminara, S.B., Messager, S., Chatzidaki, E.E., Thresher, R.R., et al. (2004) The GPR54 Gene as a Regulator of Puberty. *Obstetrical & Gynecological Survey*. [Online] Available from: doi:10.1097/00006254-200405000-00020.

Shahab, M., Mastronardi, C., Seminara, S.B., Crowley, W.F., et al. (2005) Increased hypothalamic GPR54 signaling: A potential mechanism for initiation of puberty in primates. *Proceedings of the National Academy of Sciences*. [Online] Available from: doi:10.1073/pnas.0409822102.

Sharp, A.J., Wachtel, S.S. & Benirschke, K. (1980) H-Y antigen in a fertile XY female horse. *Journal of reproduction and fertility*. [Online] 58 (1), 157–160. Available from: http://www.ncbi.nlm.nih.gov/pubmed/7359472 [Accessed: 5 May 2019].

Sikl, H. (1948) Addison's disease due to congenital hypoplasia of the adrenals in an infant aged 33 days. *The Journal of pathology and bacteriology*. 60 (2), 323.

Smith, C.L., Nawaz, Z. & O'Malley, B.W. (1997) *Coactivator and Corepressor Regulation of the Agonist/ Antagonist Activity of the Mixed Antiestrogen, 4-Hydroxytamoxifen*. [Online]. Available from: https://academic.oup.com/mend/article-abstract/11/6/657/2754434 [Accessed: 25 April 2019].

Smith, C.L. & O'Malley, B.W. (2004) *Coregulator Function: A Key to Understanding Tissue Specificity of Selective Receptor Modulators*. [Online] 25 (1), 45–71. Available from: doi:10.1210/er.2003-0023.

Smith, J.T., Acohido, B. V., Clifton, D.K. & Steiner, R.A. (2006a) KiSS-1 neurones are direct targets for leptin in the ob/ob mouse. *Journal of Neuroendocrinology*. [Online] 18 (4),

298–303. Available from: doi:10.1111/j.1365-2826.2006.01417.x.

Smith, J.T., Cunningham, M.J., Rissman, E.F., Clifton, D.K., et al. (2005a) Regulation of Kiss1 gene expression in the brain of the female mouse. *Endocrinology*. [Online] Available from: doi:10.1210/en.2005-0488.

Smith, J.T., Dungan, H.M., Stoll, E.A., Gottsch, M.L., et al. (2005b) Differential regulation of KiSS-1 mRNA expression by sex steroids in the brain of the male mouse. *Endocrinology*. [Online] Available from: doi:10.1210/en.2005-0323.

Smith, J.T., Popa, S.M., Clifton, D.K., Hoffman, G.E., et al. (2006b) Kiss1 Neurons in the Forebrain as Central Processors for Generating the Preovulatory Luteinizing Hormone Surge. *Journal of Neuroscience*. [Online] 26 (25), 6687–6694. Available from: doi:10.1523/JNEUROSCI.1618-06.2006.

Stamatiades, G.A. & Kaiser, U.B. (2018) Gonadotropin regulation by pulsatile GnRH: Signaling and gene expression. *Molecular and Cellular Endocrinology*. [Online] 463, 131–141. Available from: doi:10.1016/j.mce.2017.10.015.

Taketo, T. (2014) The role of sex chromosomes in mammalian germ cell differentiation: Can the germ cells carrying X and Y chromosomes differentiate into fertile oocytes? *Asian Journal of Andrology*. [Online] 0 (0), 0. Available from: doi:10.4103/1008-682X.143306 [Accessed: 3 May 2019].

Teles, M.G., Bianco, S.D.C., Brito, V.N., Trarbach, E.B., et al. (2008) A GPR54 -Activating Mutation in a Patient with Central Precocious Puberty . *New England Journal of Medicine*. [Online] 358 (7), 709–715. Available from: doi:10.1056/nejmoa073443.

Thomson, E.L., Patterson, M., Murphy, K.G., Smith, K.L., et al. (2004) Central and peripheral administration of kisspeptin-10 stimulates the hypothalamic-pituitary-gonadal axis. *Journal of Neuroendocrinology*. [Online] 16 (10), 850–858. Available from: doi:10.1111/j.1365-2826.2004.01240.x.

Tng, E.L. (2015) Kisspeptin signalling and its roles in humans. *Singapore Medical Journal*. [Online]. Available from: doi:10.11622/smedj.2015183.

Tomikawa, J., Uenoyama, Y., Ozawa, M., Fukanuma, T., et al. (2012) Epigenetic regulation of Kiss1 gene expression mediating estrogen-positive feedback action in the mouse brain. *Proceedings of the National Academy of Sciences*. [Online] Available from: doi:10.1073/pnas.1114245109.

Treen, A.K., Luo, V., Chalmers, J.A., Dalvi, P.S., et al. (2016) Divergent Regulation of ER and Kiss Genes by 17β-Estradiol in Hypothalamic ARC Versus AVPV Models. *Molecular*

Endocrinology. [Online] Available from: doi:10.1210/me.2015-1189.

Tremblay, J.J. & Viger, R.S. (2005) Nuclear Receptor Dax-1 Represses the Transcriptional Cooperation Between GATA-4 and SF-1 in Sertoli Cells1. *Biology of Reproduction*. [Online] 64 (4), 1191–1199. Available from: doi:10.1095/biolreprod64.4.1191.

Turner, R.T., Wakley, G.K., Hannon, K.S. & Bell, N.H. (2009) Tamoxifen prevents the skeletal effects of ovarian hormone deficiency in rats. *Journal of Bone and Mineral Research*. [Online] 2 (5), 449–456. Available from: doi:10.1002/jbmr.5650020513 [Accessed: 22 May 2019].

Uenoyama, Y., Tomikawa, J., Inoue, N., Goto, T., et al. (2016) Molecular and Epigenetic Mechanism Regulating Hypothalamic Kiss1 Gene Expression in Mammals. *Neuroendocrinology*. [Online] 103, 640–649. Available from: doi:10.1159/000445207 [Accessed: 2 May 2019].

Verdin, E. & Ott, M. (2015) 50 years of protein acetylation: From gene regulation to epigenetics, metabolism and beyond. *Nature Reviews Molecular Cell Biology*. [Online] 16 (4), 258–264. Available from: doi:10.1038/nrm3931.

Voliotis, M., Garner, K.L., Alobaid, H., Tsaneva-Atanasova, K., et al. (2018) Gonadotropin-releasing hormone signaling: An information theoretic approach. *Molecular and Cellular Endocrinology*. [Online] 463, 106–115. Available from: doi:10.1016/j.mce.2017.07.028.

Vrtačnik, P., Ostanek, B., Mencej-Bedrač, S. & Marc, J. (2014) The many faces of estrogen signaling. *Biochemia Medica*. [Online] 24 (3), 329–342. Available from: doi:10.11613/BM.2014.035.

West, A., Vojta, P.J., Welch, D.R. & Weissman, B.E. (1998) Chromosome localization and genomic structure of the KiSS-1 metastasis suppressor gene (KISS1). *Genomics*. [Online] 54 (1), 145–148. Available from: doi:10.1006/geno.1998.5566.

White, R. & Parker, M.G. (1998) Molecular Mechanisms of Steroid Hormone Action. *Journal of Endocrinology*. [Online] 5, 1–14. Available from: doi:1351-0088/98/005-001 $08.00/0.

Wiegand, S.J., Terasawa, E., Bridson, W.E. & Goy, R.W. (2008) Effects of Discrete Lesions of Preoptic and Suprachiasmatic Structures in the Female Rat. *Neuroendocrinology*. [Online] 31 (2), 147–157. Available from: doi:10.1159/000123066.

Wilkinson, M.F. (2019) Genetic paradox explained by nonsense. *Nature*. [Online] 568 (7751), 179–180. Available from: doi:10.1038/d41586-019-00823-5 [Accessed: 18

May 2019].

Wintermantel, T.M., Campbell, R.E., Porteous, R., Bock, D., et al. (2006) Definition of Estrogen Receptor Pathway Critical for Estrogen Positive Feedback to Gonadotropin-Releasing Hormone Neurons and Fertility. *Neuron*. [Online] Available from: doi:10.1016/j.neuron.2006.07.023.

Wu, S.C. & Zhang, Y. (2009) Minireview: Role of Protein Methylation and Demethylation in Nuclear Hormone Signaling. *Molecular endocrinology (Baltimore, Md.)*. [Online] 23 (9), 1323–1334. Available from: doi:10.1210/me.2009-0131 [Accessed: 27 April 2019].

Wurtz, J.-M., Bourguet, W., Renaud, J.-P., Vivat, V., et al. (1996) A canonical structure for the ligand-binding domain of nuclear receptors. *Nature structural & molecular biology*. 3 (1), 87–94.

Xhemalce, B., Dawson, M.A. & Bannister, A.J. (2011) Histone Modifications. In: *Encyclopedia of Molecular Cell Biology and Molecular Medicine*. [Online]. Weinheim, Germany, Wiley-VCH Verlag GmbH & Co. KGaA. p. Available from: doi:10.1002/3527600906.mcb.201100004 [Accessed: 22 May 2019].

Yadav, N., Lee, J., Kim, J., Shen, J., et al. (2003) *Specific protein methylation defects and gene expression perturbations in coactivator-associated arginine methyltransferase 1-deficient mice*.

Yaşar, P., Ayaz, G., User, S.D., Güpür, G., et al. (2017) Molecular mechanism of estrogen–estrogen receptor signaling. *Reproductive Medicine and Biology*. [Online] 16 (1), 4–20. Available from: doi:10.1002/rmb2.12006.

Yen, S.S.C. (1977) Regulation of the hypothalamic-pituitary-ovarian axis in women. *Reproduction*. [Online] Available from: doi:10.1530/jrf.0.0510181.

Ylikomi, T., Bocquel, M.T., Berry, M., Gronemeyer, H., et al. (1992) Cooperation of proto-signals for nuclear accumulation of estrogen and progesterone receptors. *The EMBO journal*. [Online] 11 (10), 3681–3694. Available from: doi:10.1002/j.1460-2075.1992.tb05453.x.

Yu, R.N., Ito, M. & Jameson, J.L. (2014) The Murine Dax-1 Promoter Is Stimulated by SF-1 (Steroidogenic Factor-1) and Inhibited by COUP-TF (Chicken Ovalbumin Upstream Promoter-Transcription Factor) via a Composite Nuclear Receptor-Regulatory Element . *Molecular Endocrinology*. [Online] 12 (7), 1010–1022. Available from: doi:10.1210/mend.12.7.0131.

Yu, R.N., Ito, M., Saunders, T.L., Camper, S.A., et al. (1998) Role of Ahch in gonadal development and gametogenesis. *Nature Genetics*. [Online] 20 (4), 353–357. Available from: doi:10.1038/3822.

Zanaria, E., Muscatelllt, F., Bardonf, B., Strom, T.M., et al. (1994) An unusual member of the nuclear hormone receptor superfamily responsible for X-linked adrenal hypoplasia congenita. *Nature*. 372, 635–641.

Zárate, S. & Seilicovich, A. (2010) *Estrogen Receptors and Signaling Pathways in Lactotropes and Somatotropes*. [Online] 1121, 215–223. Available from: doi:10.1159/000321683.

Zhang, H., Thomsen, J.S., Johansson, L., Gustafsson, J.Å., et al. (2000) DAX-1 functions as an LXXLL-containing corepressor for activated estrogen receptors. *Journal of Biological Chemistry*. [Online] 275 (51), 39855–39859. Available from: doi:10.1074/jbc.C000567200.

8 Appendix 1

8.1 List of Genotyping Primers

All genotyping primers were purchased from Sigma.

Primer	Sequence
Dax1	CCTTAGAAGTGTTGCTTCTG
	ACAGCTCATTGTTCTGAGTGGCT
	GCACATTGTTCTGAGTGGCT
Kiss1	GGCAAATTTTGGTGTACGGTCAG
	GACCTAGGCTCTGGTGAAG
	GAGCCTCCAGTGCTCACAGC

Table 7: Genotyping primer sequences.

8.2 List of RT-qPCR Primers

All RT-qPCR were purchased from Sigma.

Primer	Sequence	
	Froward	**Reverse**
Dax1	TGCTGCTTCTCCTCTGT	ACCGCGATTCCTTTTCC
Kiss1	AAGGGACCGTGCTCTTTAACC	TCTCCACTGAAGACCCTCAATGT
Cyp19a1	CTTTGGAGAACAATTCGCCCTTTC	GCCCGTCAGAGCTTTCATAAAGAA
Hsd3b1	TTTGCTCTCTCAGTTGTGACCA	GCCTGCTTCGTGACCATATTTATT
Cyclo	GGAGATGGCACAGGAGGAA	GCCCGTAGTGCTTCAGCTT
Cyp17a1	GATCGGTTTATGCCTGAGCG	TCCGAAGGGCAAATAACTGG

Table 8: RT-qPCR primer sequences.

9 Appendix 2

9.1 List of Copyrights Permissions

Caligioni, C.S. (2009) Assessing reproductive status/stages in mice. *Current Protocols in Neuroscience*. Wiley.

Reprinted by permission from [Springer Nature]: [Nature Reviews Molecular Cell Biology] [Verdin, E. & Ott, M. (2015) 50 years of protein acetylation: From gene regulation to epigenetics, metabolism and beyond. *Nature Reviews Molecular Cell Biology*. [Online] 16 (4), 258–264., [4611921008643] (2015).

Reprinted by permission from [Journal of biological chemistry]: [American Society for Biochemistry and Molecular Biology] [Zhang, H., Thomsen, J.S., Johansson, L., Gustafsson, J.Å., et al. (2000) DAX-1 functions as an LXXLL-containing corepressor for activated estrogen receptors. *Journal of Biological Chemistry*. [Online] 275 (51), 39855–39859.], [4611940301695] (2000).